DEVELOPMENT OF GRANULAR SEQUENCING BATCH REACTOR FOR DENITRIFICATION

By

T.V. KRISHNA MOHAN

Enrollment Number: ENGG02200804031

Indira Gandhi Centre for Atomic Research, Kalpakkam, India

A thesis submitted to the

Board of Studies in Engineering Sciences

In partial fulfillment of requirements for the Degree of

DOCTOR OF PHILOSOPHY

of

HOMI BHABHA NATIONAL INSTITUTE

July, 2015

Homi Bhabha National Institute

Recommendations of the Viva Voce Committee

As members of the Viva Voce Committee, we certify that we have read the dissertation prepared by **T.V.Krishna Mohan** entitled " **Development of Granular Sequencing Batch Reactor for Denitrification**" and recommend that it may be accepted as fulfilling the thesis requirement for the award of Degree of Doctor of Philosophy.

m-Sai baba **Date:** 11-12-15

Chairman - Dr.M.Sai Baba

PM Satya Sai **Date:** 11/12/15

Guide / Convener - Dr.P.M.Satya Sai

Ligy Philip **Date:** 11/12/2015

Examiner Prof. Ligy Philip

Date: 11/12/2015

Member -Dr.K.Velusamy

Date: 11/12/15

Member -Dr.V.P.Venugopalan

Final approval and acceptance of this thesis is contingent upon the candidate's submission of the final copies of the thesis to HBNI.

Date: 11/12/15

Place: Kalpakkam

CERTIFICATE

I hereby certify that I have read this dissertation prepared under my direction and recommend that it may be accepted as fulfilling the dissertation requirement.

Date: 11/12/15

Place: Kalpakkam

PM Satya Sai

(P.M.Satya Sai)
Guide

STATEMENT BY AUTHOR

This dissertation has been submitted in partial fulfillment of requirements for an advanced degree at Homi Bhabha National Institute (HBNI) and is deposited in the Library to be made available to borrowers under rules of the HBNI.

Brief quotations from this dissertation are allowable without special permission, provided that accurate acknowledgement of source is made. Requests for permission for extended quotation from or reproduction of this manuscript in whole or in part may be granted by the Competent Authority of HBNI when in his or her judgment the proposed use of the material is in the interests of scholarship. In all other instances, however, permission must be obtained from the author.

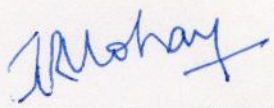

T.V. KRISHNA MOHAN

DECLARATION

I, T.V. KRISHNA MOHAN, hereby declare that the investigation presented in the thesis has been carried out by me. The work is original and has not been submitted earlier as a whole or in part for a degree / diploma at this or any other Institution / University.

T.V. KRISHNA MOHAN

Dedicated
to
My Family

ACKNOWLEDGEMENTS

Many wonderful people have influenced my personal and professional life, over the years. This acknowledgement is for all of them. I am sure, I won't be able to mention many of them even after next few paragraphs. My sincere apology to all of them.

My deepest gratitude goes first and foremost to Dr.P.M.Satya Sai, my supervisor, for his constant encouragement, unstinted inspiration, keen interest, and invaluable guidance for academic research that has greatly affected my attitude towards the acquisition of knowledge.. I am grateful to him for critically reviewing this thesis. His professional, systematic and down-to-earth approach to research, clarity of writing and presentation, are among the many things that I always proudly try to imitate. His giving of concern for my professional and personal development in these years is appreciated.

I thank Dr.M.Sai Baba, Dr.K.Velusamy and Dr.V.P.Venugopalan for being active members in my doctoral committee, and providing their inputs, encouragement and support during the regular committee meetings.

I am extremely thankful to Dr.S.Velmurugan, Head, Water and Steam Chemistry Division, for his support and encouragement during my research work. My sincere thanks goes to him for providing excellent environment and giving a free hand to carry out my research work. It gives me immense pleasure to acknowledge to my senior mentor Dr.S.V.Narasimhan, Ex. Associate Director, Chemistry Group and Ex. Head, Water and Steam Chemistry Division for his encouragement, moral support and valuable guidance, inspired me to do my best. It is also my great pleasure to thank Dr.B.N.Jagatap, Director, Chemistry Group, BARC for his encouragement and support in carrying out the research work.

I have been fortunate to have an opportunity to work closely with Dr.Y.V.Nancharaiah. I learned a lot from his wealth of experience, in terms of experimental ideas and approach to research life. Thank you, for all the conversations we had. I would like to acknowledge the support and company of my colleagues of tea group, Dr.M.P.Srinivasan, Dr.A.L.Rufus, Dr.H.Subramanian, Dr.B.Anupkumar, Shri.V.S.Sathyaseelan, Dr.Rajesh Kumar, Dr.Chandramohan, and Dr.Hiren Joshi for their moral support, diversified help and several funs, precious moments we shared, which will always be remembered.

I express my sincere thanks to Shri M.Mukunthan and Shri G.Suneel, for their useful discussions during COMSOL modeling. I convey special acknowledgements to Shri N.Jayaram, Shri Amit Kamle, Shri A.Kumaresan (Retd.), M.Sivagnanam and Jagadish for their indispensable help during my research work. I convey my sincere thanks to Shri M.Murgan, Shri M.Santha Kumar, Shri S.Marudhu Pandia Raja, S.Dharuman, Santhosh Mangle, G.L.Mohan Rao and A.George Fernandez, for fabricating the bioreactors and providing experimental help time to time.

I would also like to thank Dr.T.Subbarao, my lunch partner, who made my life cheerful during lunch time hours. I also wish Dr.S.Rangarajan for useful discussions on various topics. I would also like to thank Dr.Pushpalatha Rajesh, Dr.P.S.Murthy, Shri. K.Kiran Kumar Reddy and Mrs.Suja Girijan, who helped me in carrying out the instrumental analysis.

I am also thankful to my ESSS colleagues Shri Y.V.Harinath, Shri P.Madasamy, Shri P.J.George, T.Selvam, A.Kaikondan for their support at different times. I also thank WSCD office staff Mrs.Janaki, Mrs.Rajeshwari, Ms.Anitha and Mrs. Shanthi members for timely help during my thesis writing.

I wish to express my sincere gratitude and indebtedness to my parents, parents-in-law for their blessings, and other family members for their love and support to me. Finally, and most

importantly, thank you, Laxmi, my wife, for being very supportive, giving me all freedom to work and sparing me from some of the responsibilities by managing them so well! I thank my daughter, Sahithi for keeping my interests alive. Nothing would have been possible without their love and continuous support. I realize, I haven't been able to enjoy some of the precious days with them. I love you all and this thesis is for you.

SYNOPSIS

Introduction

Nitrate is one of the most common contaminants in surface and ground waters. High nitrate levels are reported in various water sources across the world. Nitrates are difficult to remove by conventional water treatment techniques. Improper treatment of sewage and industrial effluents, prior to discharge into the environment, is one of the main reasons for nitrate contamination of surface and ground waters. Nitrate contamination of water sources is a serious health hazard for human beings. High levels of nitrate in water can cause blue-baby syndrome in infants. Moreover, high levels of nitrates in water bodies contributes to eutrophication. In view of the significant impact on human health and environment, stringent guidelines have been laid down to regulate the discharge of nitrate into water bodies. Limit for discharge of nitrate nitrogen into inland surface waters is 10 mg L^{-1} and for marine discharge is 20 mg L^{-1}.

Nitrate bearing wastes can be of domestic or industrial origin. Domestic wastewaters are low-strength (<500 mg L^{-1} NO_3) and are typically treated via biological denitrification in a wastewater treatment plant. High strength nitrate bearing wastes containing nitrate in excess of 1000 mg L^{-1}, are generated in fertilizer, explosives, pharmaceutical, metal finishing and nuclear industries. Nitrate wastes containing 50,000 – 1,50,000 mg L^{-1} of nitrate in the form of ammonium nitrate, sodium nitrate and magnesium nitrate are generated during nuclear fuel cycle operations.

Biological denitrification is a process in which, nitrate is converted to N_2 gas by microbial reduction. The process has been successfully implemented for removing nitrogenous compounds from sewage as well as industrial wastewaters. However, there are limited studies on denitrification of wastewater with high concentration of nitrate. In the absence of a viable

treatment scheme, high strength nitrate wastes are diluted to suitable levels before subjecting to biological treatment processes. In view of the large quantities high strength nitrate bearing wastes generated, development of a process for their effective treatment is necessary. Further, treatment processes reported in the literature are limited to effluents at near neutral pH range. Biological denitrification is generally ineffective in acidic pH range. Considering the above facts, a work programme was evolved to develop a process for biological denitrification of high strength nitrate waste having acidic pH. Granular biomass was used for biological denitrification because of the specific advantages (compact biomass, rapid sedimentation, resistance to shock loading, small footprint) offered by granular biomass based sequencing batch reactors. The specific objectives of the study were:

Objectives

- Cultivation of denitrifying granular biomass under anoxic conditions using sequencing batch reactors.
- Treatment of high strength nitrate wastes using sequencing batch reactors (SBR) as well as expanded granular sludge bed reactors (EGSBR).
- Optimization of C/N ratio for efficient and complete denitrification.
- Study the effect of temperature and pH on denitrification rates
- Development of a CFD based model for the biological reactor and validation of the model with experimental results.

Thesis organization

The thesis is organized into six chapters, viz. introduction, review of the literature, materials and methods, results & discussion and modeling. A general introduction to denitrification and whole of the thesis is given in Chapter 1. Chapter 2 gives an overview of the available literature in biological denitrification of high strength nitrate wastewater. Details of setting up of sequencing batch reactors, their operation, experimental strategies, and analytical methods are given in Chapter 3. Results obtained from the experimental investigations, analysis and

discussion of results in the context of literature are given in Chapter 4. The fifth chapter gives the details of modeling. The last chapter summarizes the overall conclusions and salient findings of the entire study. The contents of the individual chapters are given below.

Chapter 1: Introduction

This chapter gives a brief description of the sources of the nitrate pollution in general. Sources of nitrate bearing effluent streams from the nuclear fuel cycle are discussed with respect to concentrations and quantities. It explains in detail about the environmental and health concerns associated with nitrate pollution. Options available for treating nitrate bearing wastes are briefly addressed. Discharge limits for nitrates in industrial effluents in different countries are also presented. The aim and scope of the study are detailed.

Chapter 2: Review of literature

This chapter presents a review of literature on denitrification, with major emphasis on biological treatment processes. Missing links in the literature are identified particularly with regard to high strength nitrate wastes. Biological denitrification methods reported in the literature are reviewed and their advantages and disadvantages are listed. Different biological denitrification processes are explained in detail with stoichiometric equations. The chapter also explains the factors controlling biological denitrification. Attached and suspended growth systems are explained. Denitrification kinetics and modeling are also discussed. Research gaps are identified and the need for further studies in the field of biological denitrification is highlighted.

Chapter 3: Materials and Methods

This chapter gives details about the experimental procedures adopted in the study. Fabrication details of the reactors used for different experiments were explained. Operation of different bioreactors for denitrification is explained in detail. This chapter also presents details of the source of the seed material used for the granulation and the feed composition

used in the experiments. Details of characterization of granular biomass by optical microscopy and scanning electron microscopy (SEM) are presented. Analytical techniques employed for analyses of nitrate, nitrite, acetate, biomass concentrations (MLSS, MLVSS), dissolved oxygen, oxidation reduction potential, total organic carbon and pH are presented. This chapter also describes the methodology followed for determining the rate kinetics of denitrification reactions.

Chapter 4: Results and Discussions

In this chapter, results of the experiments are presented and discussed in the context of the relevant literature. For all C/N ratios studied, steady increase in the biomass concentration was observed, as the number of days of operation increased. It was found that MLSS and MLVSS increased as the C/N ratio increased. Nitrate and nitrite reduction times, as well as peak nitrite concentration were found to increase as the C/N ratio increased. Complete denitrification was observed for all the nitrate concentrations and C/N ratios studied. Organic carbon content in the effluents was observed to go up as the C/N ratio increased, indicating that the acetate was not being utilized fully during denitrification. The specific denitrification rates for C/N of 1.5 were higher than the specific denitrification rates for C/N of 2 and 3. This could be because of lower MLSS concentrations at C/N of 1.5 than that at 2 and 3. The denitrification rate constants estimated in this study and specific denitrification rate constants were found to be higher than the values reported in the literature for other biological systems.

Experiments were carried out at different temperatures using a jacketed glass tank to determine the effect of temperature on denitrification rate. The results showed that specific denitrification rates increased as the operating temperature in the reactor increased.

At a C/N ratio of 1.5, the nitrate and nitrite reduction times and the peak nitrite concentrations increased as the nitrate concentrations increased. It was seen that denitrification was complete for all the nitrate concentrations. In the present study, the highest nitrate concentration used in

the feed was 42,000 mg L^{-1} at a C/N of 1.5. The highest concentration of nitrate reported in the literature till date at similar operating conditions is 40,000 mg L^{-1}. The specific denitrification rates in the present work are several fold higher than the values reported in the literature. It is concluded that the microbial consortium in the form of granular biomass can achieve high rates of denitrification compared to any other biological method reported in the literature.

Further, experiments were carried out to accomplish treatment of acidic wastes with nitrate in excess of 3000 mg L^{-1}. After establishing stable denitrification at pH 7, the feed pH was adjusted to 5.0 with HCl. Initially, denitrification was delayed at the low pH, but after acclimatization, complete denitrification was observed within 2 h. Subsequently the reactor was fed with waste of pH 4.0 and denitrification was achieved in about 24 h. With further acclimatization, the denitrification time got reduced to about 2 h.

A semi-pilot scale 24 L water volume, expanded granular sludge bed reactor (EGSBR) was designed, fabricated and set up to evaluate formation of denitrifying granular biomass and subsequently denitrification. The reactor was operated in SBR mode with 24 h cycle time and 50% VER. The SBR was inoculated with activated sludge and fed with simulated nitrate wastewater. The nitrate in the feed was increased in steps from 6 g/L through 12 and 18 to 24 g L^{-1}. Aggregation, densification and selection led to formation of compact and dense denitrifying granules in the reactor. Complete denitrification of nitrate was observed and the nitrate and nitrite levels in the effluent were below 10 mg L^{-1}. The reactor was operated for more than 3 months, thereby demonstrating efficient and stable denitrification.

Further experiments were carried out to develop continuous process for biological denitrification. A continuous stirred tank reactor (CSTR) was set up and operated with constant influent flow rate of 400 mL h^{-1} and acetate-carbon to nitrate-nitrogen ratio of 2. The CSTR was operated in batch mode for 5 days at each concentration in order to acclimatize the

biomass to higher nitrate concentration and to ensure complete denitrification in CSTR mode. The reactor was later operated in CSTR mode for about 2-weeks at each feed nitrate concentration. The feed nitrate was increased in steps to 3000, 6000, 9000, and 12000 mg L^{-1}. Complete and stable denitrification was observed at all the concentrations tested. However, accumulation of acetate was evident in the reactor, indicating incomplete utilization of carbon. Subsequently, the acetate-carbon to nitrate-nitrogen ratio in the feed was decreased to 1.5. At this C/N ratio, denitrification was complete, with no carbon accumulation in the effluent. The reactor could be operated successfully for 10 days in this condition.

Chapter 5: Modeling

Need for modeling, assumptions made, and development of the model are presented in this chapter. The list of input parameters to the model and their values are tabulated. Domain and meshing details are listed and governing equations are presented. The software used for the modeling is also explained. The model generates nitrate and nitrite profiles for a given initial nitrate concentration. Reaction rates are calculated from the experimental data. It estimates the temperature during denitrification process and plots the heat flux and temperature profiles in the radial direction from heat transfer calculations. Thermo-physical properties at transient condition are calculated. In situ temperature of the fluid is estimated.

CHAPTER 6 Conclusions

Important conclusions drawn based on the observations are presented. Scope for further investigations in this field of research is outlined.

Salient Observation and conclusions from this study

1. Denitrifying granular biomass with excellent settling characteristics was cultivated. The biomass was characterized by concentration of MLSS, MLVSS and SEM.

2. Complete denitrification was observed at C/N ratios of 1.5, 2 and 3. C/N ratio of 1.5 was found to be optimum for efficient denitrification, as denitrification times and peak nitrite concentrations were the lowest for C/N ratio of 1.5.

3. Denitrification rate constants were found to be slightly higher for the bioreactor system studied than the data available in the literature and specific denitrification rates were several folds higher than the reported data.

4. Complete denitrification was observed up to feed concentrations of 42,000 mg L^{-1} nitrate at C/N ratio of 1.5. The denitrification process was demonstrated to be stable, with the treated effluent showing nitrate of less than 10 mg L^{-1} consistently for 15 days.

5. Complete denitrification was observed at temperatures of 20, 25, 30, 35 and 40 ^{o}C. Specific denitrification rates increased with increase in reactor temperature.

6. Stable denitrification was demonstrated in a CSTR for nitrate concentrations up to 12,000 mg L^{-1} for a flow rate of 400 mL h^{-1} at C/N ratio of 1.5.

7. Rise in the reactor temperature could be used as a process parameter for monitoring of completion of denitrification of high strength nitrate bearing wastes in SBRs.

8. A process based on acclimatization of the granular sludge to acidic medium was developed. By this method, effective denitrification of high strength nitrate waste with low pH (4.0) could be achieved.

9. Complete denitrification up to 21,000 mg L^{-1} nitrate was achieved in EGSBR with a hydraulic residence time of 16 h.

10. Denitrification up to 12,000 mg L^{-1} nitrate was achieved in a Semi Pilot Scale SBR, with a throughput of 24 L day^{-1}.

11. A CFD based model was developed for the bioreactor and nitrate and nitrite profiles were generated for a given initial nitrate concentration. Reaction rates were estimated from the experimental data. Temperatures during the denitrification process were estimated and heat flux and temperature profiles in the radial direction were generated.

12. The model is validated with experimental data and it can be used for scaling up of the bioreactor.

CONTENTS

LIST OF FIGURES

LIST OF TABLES

Abstract

This study was conducted to investigate biological denitrification of high strength nitrate wastewaters. Studies were carried out with the objective of optimizing electron donor requirement, in terms of acetate-carbon to nitrate-nitrogen (C/N) ratio, for treating high strength nitrate wastewater in granular sludge sequencing batch reactors (SBRs). Three SBRs of each 6 L working volume were inoculated with activated sludge and operated in parallel at C/N ratios of 1.5, 2 and 3. Formation of denitrifying granular sludge was observed in all three SBRs. Complete and stable denitrification of feed containing nitrate up to 24 g L^{-1} was achieved in 24 h cycle period. No significant improvement in performance of high strength nitrate denitrification in terms of nitrite build-up and total time taken for complete denitrification was observed at higher C/N ratios. On the whole, C/N ratio of 1.5, as compared to 2 and 3, was found to be optimum for denitrification of high strength nitrate wastewaters. The study helps in developing high rate denitrification desired for treatment of high strength wastewaters of industrial origin.

To investigate the effect of sudden change C/N ratio on denitrification, a 6 L sequencing batch reactor (SBR) was operated for development of granular sludge capable of denitrification of high strength nitrates. Complete and stable denitrification of up to 5420 mg L^{-1} nitrate-N (2710 mg L^{-1} nitrate-N in reactor) was achieved by feeding simulated nitrate waste at a C/N ratio of 3. Compact and dense denitrifying granular sludge with relatively stable microbial community was developed during reactor operation. Accumulation of large amounts of nitrite due to incomplete denitrification occurred, when the SBR was fed 5420 mg L^{-1} NO_3-N at a C/N ratio of 2. Complete denitrification could not be achieved at this C/N ratio, even after one week of reactor operation as the nitrite levels continued to accumulate. In order to improve denitrification performance, the reactor was fed with nitrate concentrations of 1355 mg L^{-1},

while keeping C/N ratio at 2. Subsequently, nitrate concentration in the feed was increased in a step-wise manner to establish complete denitrification of 5420 mg L^{-1} NO_3-N at a C/N ratio of 2. The study shows that substrate concentration plays an important role in denitrification of high strength nitrate by influencing nitrite accumulation. Complete denitrification of high strength nitrates can be achieved at lower substrate concentrations, by an appropriate acclimatization strategy.

Denitrification of acidic nitrate wastes by granular sludge was investigated in batch assays and sequencing batch reactors (SBR) with an objective to treat nuclear fuel cycle effluents, which are acidic nature. In order to cultivate granular sludge, two 3 L SBRs were inoculated with activated sludge and fed with wastewater containing 1355 mg L^{-1} NO_3-N at pH 7.5. After formation of denitrifying granular sludge, one of the SBRs was fed with nitrate wastewater at pH 5 and 4. Though batch experiments showed pH 4 and 5 to be inhibitory to denitrification, adaptation of granular sludge in the SBR led to denitrification of nitrate at feed pH of 4 and 5, using acetate as electron donor. Nitrate was denitrified and generated alkalinity within the first few hours of SBR cycle. The pH of acidic nitrate wastewater increased from 5 to 8.7 and 4 to 6.2 in the reactor by the internal recycling of denitrification generated alkalinity. Scanning electron microscopy showed the presence of rod- and cocci-shaped microorganisms on the surface of denitrifying granular sludge collected from the reactors supplied with feed at pH 7.5 and 4, respectively.

After the optimizing C/N ratio, studies were carried out in a 6 L SBR to know the maximum nitrate concentration that can be treated. Establishment of denitrifying microbial community in the form of compact granular sludge was evident within two weeks of SBR start-up. Denitrification of 1355 mg L^{-1} NO_3-N was comparable at acetate -C to nitrate -N ratios of 1.5, 2 and 3. The influent nitrate concentrations were increased up to 42,000 mg L^{-1} i.e. 9484 mg L^{-1} NO_3-N at a fixed C/N ratio of 1.5. At steady state, complete denitrification was

observed within 20 h. Kinetic analysis revealed high rate constants for denitrification up to 2032 mg L^{-1} NO_3-N. But a decrease in rate constants was observed for nitrate-N concentrations of 2710 mg L^{-1} and above. Scanning electron microscopy of the granular sludge showed the presence of both cocci and rod shaped cells enmeshed in an extracellular polymeric substance (EPS) matrix. Establishment of denitrification in the granular sludge was associated with a major shift in its microbial community. This study shows that sequencing batch reactors using granular sludge could be effectively employed for treatment of high strength nitrate wastes of industrial origin, at low C/N ratios, with fast kinetics.

Effect of temperature on biological denitrification in treating high strength nitrate waste waters was investigated. 500 mL sequencing batch reactor (SBR) was operated for development of granular sludge capable of denitrification of high strength nitrates at a C/N ratio of 1.5. Complete and stable denitrification was observed for temperatures from 20-40 ^{o}C. Denitrification coefficients were found to be increasing with increase in temperature.

1 INTRODUCTION

Water is a major constituent of human body, approximately 65% of the body weight being due to the fluid. Over 70% of the Earth's surface is covered by water, mostly in the form of saline sea waters. Fresh water from bore wells or surface water bodies constitutes only 2.5% of total water available and about 1.7% of total water is locked up in ice caps, glaciers, & permanent snow [1]. In view of population growth, global demand for water of high quality for domestic and economic activities is on the increase. To ensure supply of good quality water for such needs, pollution of the water bodies should be prevented.

Water pollution is a major global issue of concern, which needs to be addressed by a concerted effort from the international community of scientists and policy makers [2]. Domestic/municipal wastewater and industrial wastewater are the major sources of water pollution, since they are discharged into water bodies without proper treatment. Surface waters get contaminated either from point or non-point sources. In point sources, the contaminants enter from a single, identifiable source such as discharges from a sewage treatment plant, or a factory, whereas, in the case of non-point sources, the contaminants do not originate from a single discrete source. Example of non-point source is water pollution by nitrates due to leaching of nitrogen compounds from fertilized agricultural lands and nutrient runoff in storm water from "sheet flow" over an agricultural field or a forest [3].

Consumption of polluted water by human beings can result in acute illnesses, such as respiratory problems, cardiovascular disease, cancers and neuro-developmental and hormonal disorders, and in extreme cases, can also lead to death [4]. Polluted water is unacceptable for other uses such as bathing, amusement, agriculture and industry.

Pollution reduces the tasteful nature of water in lakes and waterways. Further, polluted water wrecks amphibian life and lessens its conceptive capacity [5].

Water pollution can be highly detrimental to a nation's economy, in terms of ecological imbalances and health of the residents. Water pollution is the leading cause of deaths and diseases worldwide, it accounts for the deaths of more than 14,000 people daily [2]. An estimated 580 people in India die of water pollution related illness every day [6]. It was reported that about 90% the water in the cities of China is polluted, and as of 2007, half a billion Chinese had no access to safe drinking water [7]. The problem of water pollution is ubiquitous in nature and is not restricted to developing countries. In the United States, 45% of assessed stream miles, 47% of assessed lake acres, and 32% of assessed bays and estuarine square miles were classified as polluted [8]. In terms of health and ecological issues, one of the major causes for concern is nitrate pollution of water, as this has far reaching consequences.

1.1 Nitrates

Nitrate, expressed as either NO_3 (nitrate) or NO_3-N (nitrate-nitrogen), is a naturally occurring form of nitrogen, a part of nitrogen cycle and commonly found in soil. Nitrogen is essential to all life. Nitrate ion is the stable form of combined nitrogen for oxygenated systems [9]. Nitrate is a colorless, odorless, tasteless and stable compound [10]; which can be reduced by microbial action. Nitrates are used by the plants to fulfill the nutrient requirements and in the process, get accumulated in their leaves and stems. Nitrate is highly soluble in water and mobile in soil, thus making its presence as probably the most pervasive chemical contaminant in groundwater. Nitrate concentrations are steadily increasing in the aquatic environment (i.e. surface, ground and coastal waters) in many parts of the world because of anthropogenic activities.

Nitrogen exists in nature in all redox states from +5, the most oxidized nitrate, to -3, the most reduced ammonia as shown in Table 1.1 [9].

Table 1.1 Oxidation states of Nitrogen

Oxidation State	Common Forms
+5	NO_3^-
+3	NO_2^-
+1	N_2O
0	N_2
-3	NH_3, NH_4

1.2 Sources of Nitrates

Microorganisms in the soil break down the composts, rotting plants, fertilizers or other natural deposits and produce nitrates. Nitrates are also formed when gaseous forms of nitrogen react with rainwater. Although nitrate occurs naturally in some groundwater, in most cases higher levels are result from anthropogenic activities. Most of the nitrates originate from one of the following sources: nitrogenous fertilizers, livestock manures, agricultural irrigation, septic tanks, cesspools, pit latrines, atmospheric nitrogen deposition, domestic wastewater and wastewater from certain industries: slaughter houses, distilleries, sugar factories, textile industries, explosives, pharmaceutical, metal finishing and nuclear industries [11-14].

Nitrates in the form of ammonium nitrate, potassium nitrate, calcium nitrate and urea become major part of inorganic fertilizers. These fertilizers contain high levels of nitrogen, one of the most vital nutrients for plant growth. Nitrates emanating from the difference between the crop requirement and actual amount applied for food production get leached into groundwater because of high mobility and pollute aquatic

system via surface run off [15]. Nitrate in the form of ammonium nitrate is used as a strong oxidizing agent for making an explosive mixture with a fuel such as a hydrocarbon, usually diesel fuel (oil) or, sometimes, kerosene. Daisy cutter bomb and amatol, military explosives, use ammonium nitrate. Moreover, ammonium nitrate is also an explosive in its purest form although it is not very sensitive. **P**otassium nitrate is used in glass manufacturing, explosives for mining and civil works, metal treatment and fireworks. As calcium nitrate is easy to dissolve and has a high mixing ability, it is used in emulsions and emulsion explosives. Food industry also employs potassium nitrate to cure and preserve meats against microbial agents and also to maintain the desirable color of meats and hard cheeses. Power plants use eutectic mixture of 60% sodium nitrate and 40% potassium nitrate, which can be used as liquid between 260-550 °C. This mixture has high latent heat capacity, storing thermal energy. Potassium nitrate also finds its place in pharmaceutical industry in treatment of sensitive teeth.

In view of the wide ranging applications of nitrates, nitrate bearing wastes are generated from many industries, some generating nitrates in high concentrations. The wastes generated in fertilizer, explosives, pharmaceutical, metal finishing and nuclear industries contain high concentrations (>1000 mg L^{-1}) of nitrate [11-14]. These waste streams should be treated adequately to ensure that nitrates don't find their way into the water bodies.

1.3 Nitrates in nuclear fuel cycle operations

Nitric acid is used extensively in the nuclear fuel cycle and nitrate-bearing wastes are generated at various phases of nuclear fuel cycle. In nuclear fuel (UO_2) fabrication process, magnesium di-uranate is dissolved in nitric acid, purified by solvent extraction with Tri-Butyl Phosphate (TBP) + n-dodecane, stripped with demineralised (DM) water and precipitated by ammonia. Liquid wastes bearing ammonium nitrate,

sodium nitrate and magnesium nitrate are generated during fuel fabrication. During fuel reprocessing, irradiated UO_2 is dissolved in nitric acid, yielding aqueous solution of uranyl, plutonium, and fission-product nitrates. This is separated into streams of Plutonium, uranium and fission products by solvent extraction using Tri-Butyl Phosphate (TBP) + n-dodecane as solvent. Wastes generated during fuel reprocessing are ammonium nitrate bearing waste, $NaNO_3$ loaded declad waste, neutralized evaporator condensate and acidic HLW, which contains nitrates of fission products. In these processes nitrates are only intermediate products and not final products. Nitric acid cannot be recovered and recycled effectively, due to problems of product contamination. Consequently, high strength nitrate bearing effluents are generated in these nuclear fuel cycle (Fig. 1) operations. The concentration of nitrate in these streams ranges from 50,000 to 1,50,000 mg L^{-1} [16-18] and the nitrates are present as calcium or sodium salt. Certain high strength nitrate effluents, acidic at source of generation, are neutralized prior to storage in underground carbon steel tanks. Nitrate streams generated by the nuclear fuel cycle are shown in Fig. 2. [19].

In addition to high strength effluents, low strength nitrates are also generated in the fuel cycle operations. These effluents are generated in high volume and both nitrate and radioactive elements must be removed prior to discharge into water bodies meeting the stringent regulatory requirements.

1.4 Biological effects of nitrates

Nitrate in essence is generally nontoxic to human beings. The health risks connected with nitrates are mostly due to the bacterial transformation of ingested nitrate to nitrite. Infants under 6 months, have little acid in their digestive tract for digestion and depend on the bacteria instead for digestion. The prevailing pH condition in the gut of

infants causes a reduction of nitrate to nitrite by nitrate reducing bacteria. These bacteria get killed by the hydrochloric acid generated when the age reaches 6 months. The nitrite thus formed enters the blood stream and binds with hemoglobin, which is an oxygen carrying molecule, forming methamoglobin., which is a non-oxygen-carrying enzyme. This results in a reduction in the oxygen-carrying capacity of blood leading to fatal methemoglobinemia, or "blue baby syndrome" in infants. Severe methemoglobinemia can result in brain damage and death. In adults, the bacterial reduction of nitrate to nitrite is not favored due to prevailing acidic pH. Also, fetal hemoglobin Severe methemoglobinemia can result in brain damage and death. In adults, the bacterial reduction of nitrate to nitrite is not favored due to prevailing acidic pH. Also, fetal hemoglobin is more prone to oxidation reaction catalyzed by nitrite to form methemoglobin than adult hemoglobin [9,20-21].

$$Haemoglobin\ (Fe^{2+}) \xrightarrow{NO_2^-} Methamoglobin \qquad 1.1$$

(can combine with oxygen) (cannot combine with oxygen)

Nitrosamines and nitrosamides, which are potent carcinogens are formed as a result of nitrite reaction with secondary amines or amides. These primarily affect the esophagus and pharynx (gastrointestinal tract) [21,23].

$$H_3C - NH - CH_3 + HNO_2 \rightarrow H_3C - N - N - O + H_2O \qquad 1.2$$

Dimethyl amine Dimethyl nitrosamine (carcinogen)

High nitrate levels in water bodies can lead to enhanced growth of phytoplankton called eutrophication or hypertrophication, which is a major environmental problem. Eutrophication is also a culprit in toxic red tides in seaside waters and cyanobacterial blossoms in lakes and waterways. The undesirable consequences of eutrophication are

1. Formation of algae mats reduces passage of light into water and results in a decline in productivity of plants living in the deeper waters, thus decreasing their generation of oxygen.
2. Oxygen gets depleted when algae die and decompose, resulting in fish-kill due hypoxia. Primary production of oxygen is brought down because in deeper waters primary production is lowered.
3. Water becomes unpalatable because of the toxins produced by algal species.

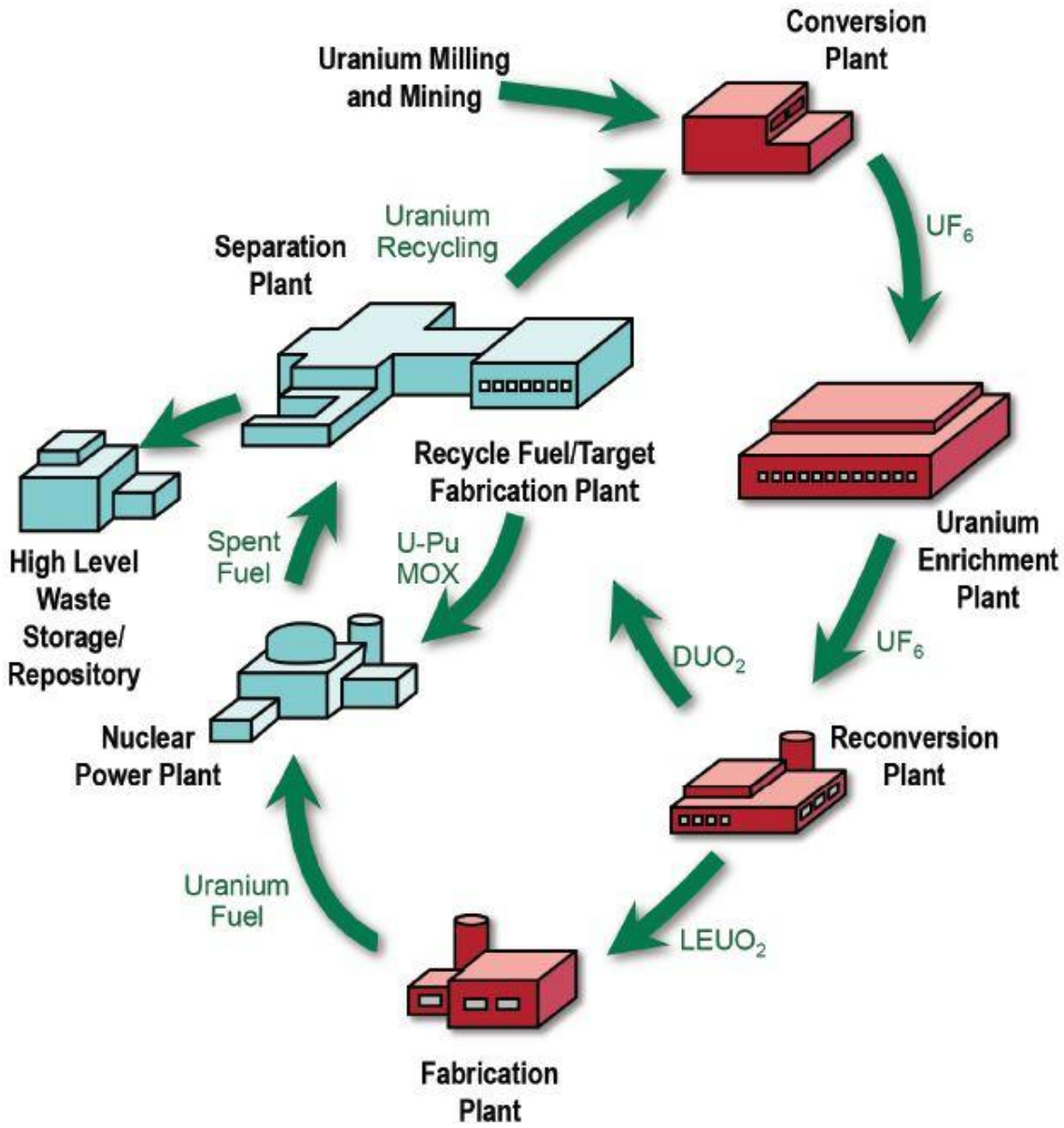

Fig. 1.1 Nuclear fuel Cycle
[22]

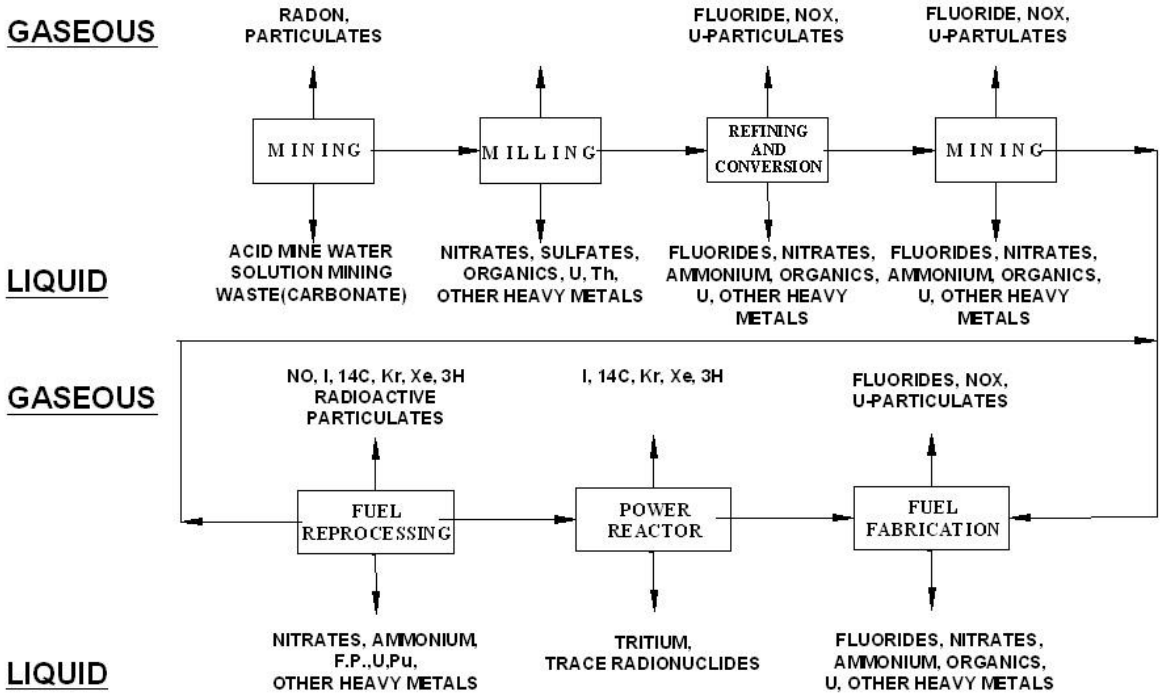

Fig. 1.2 Effluent waste streams in the uranium fuel cycle

[19]

In view of the problems associated with the nitrates, stringent limits were enforced on nitrates by the regulating agencies in different countries, as shown in Table 1.2.

1.5 Biological nitrogen cycle

Nitrogen is the building block of proteins and nucleic acids and is essential for growth and reproduction in both plants and animals. Nitrogen exists in various forms, viz., Particulate Organic-N, Soluble Organic – N, Ammonia – N, Nitrite - N Nitrate - N. Nitrogen gas (N_2) is a major constituent, about 78%, of the earth's atmosphere. Nitrogen in this form cannot be used by many organisms. It can be made available for plants by getting it incorporated into the compounds such as nitrate ions (NO_3^-), ammonium ions (NH_4^+) and urea $(NH_2)_2CO$, the process being known as fixing. Nitrogen exists in various chemical forms and gets converted from one form to another through biological and physical processes. This transformation is called

nitrogen cycle. Fixation, ammonification, nitrification, and denitrification are the important processes in the nitrogen cycle. Microbes carry out many of these processes

1.6 Treatment options

Various physical and chemical treatment processes such as reverse osmosis, ion exchange, thermal degradation, electro dialysis, chemical reduction, catalysis and electrochemical reduction are available for denitrification of water and wastewaters. However, these methods are expensive and generate secondary wastes that require additional post-treatment. Biological denitrification is a widely used process for removing nitrate from surface waters and municipal wastewaters. A comprehensive review evaluating the advantages and disadvantages of nitrate treatment/destruction is presented in Chapter -2.

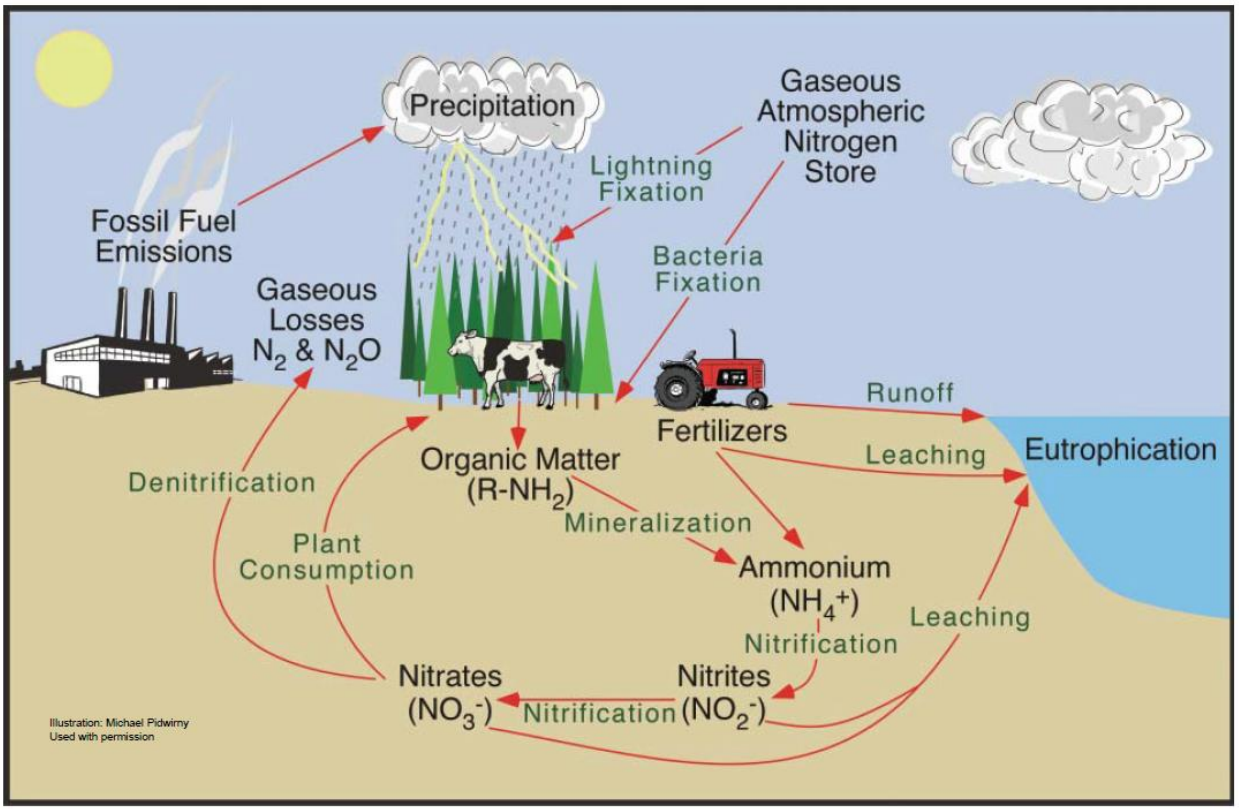

Fig. 1.3 Nitrogen Cycle
[24]

Table 1.2 Limits for Nitrate and Nitrite in drinking water

	Nitrate (NO_3^-)	Nitrite (NO_2^-)
WHO (2008)	50 mg L^{-1}	3 mg L^{-1} for short-term exposure 0.2 mg L^{-1} for long-term exposure
U.S.EPA (2012	10 (as N) MCLG (mg L^{-1})	1 (as N) MCLG (mg L^{-1})
EEC	50 (mg L^{-1})	0.5 (mg L^{-1})
Australia (2011)	50 (mg L^{-1})	3 (mg L^{-1})
Canada (2012)	45 (mg L^{-1})	3.2 (mg L^{-1})
New Zealand (2012)	50 (mg L^{-1})	3 (mg L^{-1})
India (IS:10500)	45 (mg L^{-1})	-
Nigeria (2007) NIS 554: 2007	50 (mg L^{-1})	0.2 (mg L^{-1})
Malaysia (2000)	10 (as N) (mg L^{-1})	_
Pakistan (2008)	50 (mg L^{-1})	3 (mg L^{-1})
IBWA (2012)	10 (as N) (mg L^{-1})	1 (as N) (mg L^{-1})
Japan	10 (as N) (mg L^{-1})	
Korea	10 (as N) (mg L^{-1})	-
Argentina	45 (mg L^{-1})	0.1 (mg L^{-1})

1.7 Objectives

In view of the limited literature available for treating high strength nitrates effectively,

this study is planned with the following objectives:

- Cultivation of denitrifying granular biomass under anoxic conditions using sequencing batch reactors.
- Treatment of high strength nitrate wastes using sequencing batch reactors (SBR) as well as expanded granular sludge bed reactors (EGSBR).
- Optimization of C/N ratio for efficient and complete denitrification.
- Study the effect of temperature and pH on denitrification rates
- Development of a CFD based model for the biological reactor and validation of the model with experimental results.

1.8 Thesis organization

The thesis is organized into six chapters, viz. introduction, review of the literature, materials and methods, results & discussion and modeling. A general introduction to denitrification and whole of the thesis is given in Chapter 1. Chapter 2 gives an overview of the available literature in biological denitrification of high strength nitrate wastewater. Details of setting up of sequencing batch reactors, their operation, experimental strategies, and analytical methods are given in Chapter 3. Results obtained from the experimental investigations, analysis and discussion of results in the context of literature are given in Chapter 4. The fifth chapter gives the details of modeling. The last chapter summarizes the overall conclusions and salient findings of the entire study.

2 REVIEW OF LITERATURE

2.1 Introduction

Nitrogen and nitrogen compounds from water and wastewater can either be removed by physical and chemical methods or be reduced by microbially facilitated processes in natural or engineered systems. Natural denitrification can remove small quantities of nitrates from aquifers, when sufficient electron donor is available. In artificial denitrification, suitable nutrients are injected into the groundwater to stimulate denitrification [25].

2.2 Physical and Chemical Nitrate Removal Methods

Physical and chemical methods meant for nitrate removal include ion exchange, reverse osmosis, electro dialysis, chemical denitrification and catalytic denitrification. A brief review of these conventional methods used for nitrate removal, along with their advantages and disadvantages, is presented.

2.2.1 Ion Exchange (IX)

Ion exchange is one of the most commonly used methods for removing nitrates from water and wastewater. Water/wastewaters containing nitrates is passed through a chloride form of strong base anion resin bed (SBA). The resin bed exchanges chloride ions for nitrates and other anions present in the contaminated water, thus retaining the nitrates in the ion exchanger. Conventional anion exchange resins of trimethylamine functional group have affinity in the following order $SO_4^{2-} > NO_3^- > Cl^- > HCO_3^-$ i.e. the affinity for sulfate (SO_4^{2-}) is higher than nitrate (NO_3^-). Consequently, denitrifying capacity of the resin bed decreases, if the contaminated water contains sulfate in addition to nitrate. It, therefore, becomes mandatory to look for nitrate-selective resins, which have higher affinity for nitrate than sulfate [26-29]. Exhausted

resins are regenerated with concentrated sodium chloride solution or sodium bicarbonate. Alternatively, seawater may also be used for regeneration of the exhausted resins [30]. Resin selection depends on exchange capacity, selectivity and kinetics. The process and reactions involved in the regeneration of the IX resin bed are as below:

$$R - Cl + NO_3^- \rightarrow R - NO_3 + Cl^- \quad \text{(Nitrate getting loaded on IX)} \qquad 2.1$$

$$R - NO_3^- + Cl^- \rightarrow R - Cl + NO_3^- \quad \text{(IX regeneration)} \qquad 2.2$$

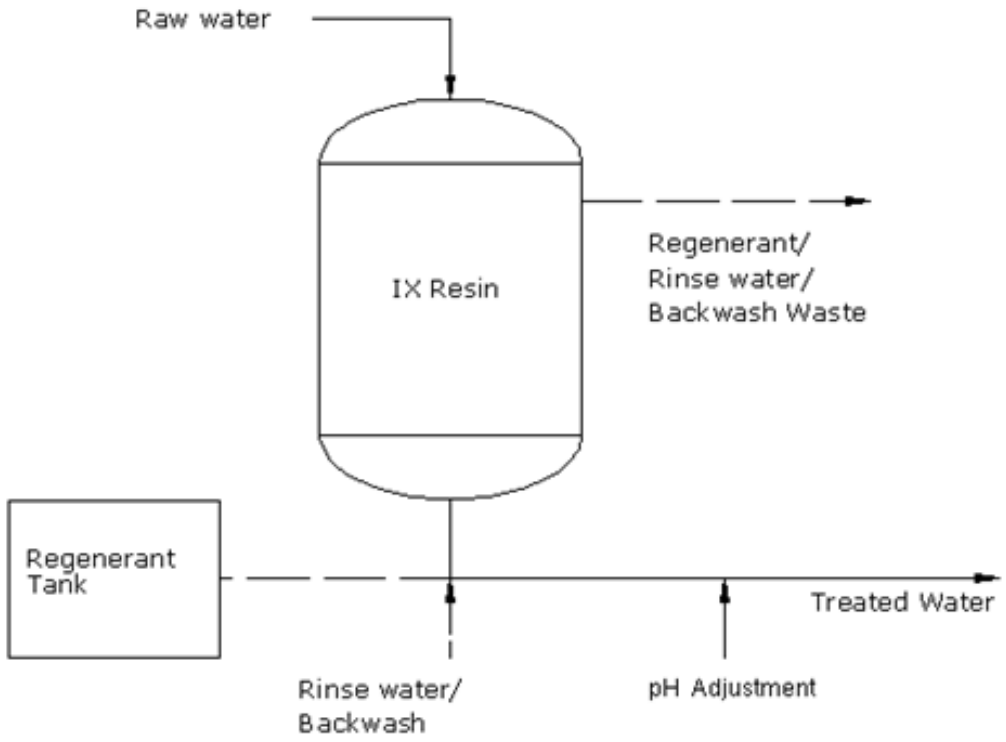

Fig. 2.1 Schematic of ion exchange process

Ion-Exchange (IX) technologies for denitrification are easy to design, simple in operation, and are independent of variations in operating temperature. The limitations of IX are [31]:

i) Economical only for small volume treatment systems

ii) Suitable for low nitrate concentrations

iii) Efficiency high only when other ions are absent

iv) Disposal of waste brines that may contain high concentrations of sodium chloride, nitrate, sulfate, and arsenate

v) Influent needs to be pre-treated for avoiding resin fouling.

vi) Effluent needs to be post treated as it is corrosive in nature, due to high chloride concentrations.

Van der Hoek and Klapwijk [32] demonstrated nitrate removal from ground water at pilot scale using macro porous (Duolite A 161, 162, 165, Bayer Lewatit MP 500, 600) and gel (Bayer Lewatit M 500, 600) type resins by ion exchange. The raw water contained 19.2 mg L^{-1} NO_3, 29.5 mg L^{-1} sulfate, and 26.1 mg L^{-1} chloride. The effluent nitrate-N levels were below 5 mg L^{-1}.

Van der Hoek et al. [33] carried out pilot plant studies for nitrate removal from ground water under different process conditions using sulfate selective resin (Duolite A 165) and a nitrate selective resin (Amberlite IRA 996). Sodium chloride and sodium bicarbonate solutions were used for regeneration. The raw water contained 19-23 mg L^{-1} NO_3, 31-181 mg L^{-1} sulfate and 28-92 mg L^{-1} chloride. The effluent nitrate levels were below 50 mg L^{-1}. Results concluded that Amberlite resins did not offer any advantage over the Duolite resins, when sulfate concentrations were low but effluent chloride concentrations were lower in case of Amberlite resins.

Clifford and Liu [34] carried out bench scale studies using standard and nitrate selective resins for nitrate removal from drinking water by ion exchange. The raw water contained 20 ± 0.5 mg L^{-1} NO_3-N, 32-56 mg L^{-1} sulfate, and 14-22 mg L^{-1} chloride. The effluent nitrate-N levels were below 10 mg L^{-1}.

Matosic et al. [35] carried out laboratory studies for nitrate removal from drinking water using strong base, sulfate selective resin (HP-441) of the gel type polystyrene

matrix with trimethyl functional group and strong base, nitrate selective macro porous resin (HP-555) with polystyrene matrix and triethyl functional group designed for nitrate removal in presence of high sulfate ion concentrations. The raw water contained 100-294 mg L^{-1} NO_3, 27-156 mg L^{-1} sulfate, and 15-18 mg L^{-1} chloride. Nitrate selective resins (HP-555) were found to be difficult to regenerate with sodium bicarbonate. The effluent nitrate-N levels were lower than10 mg L^{-1}.

Darbi et al. [36] carried out pilot scale studies for nitrate removal from ground water using standard softening resin (A554). The raw water contained 50-65 mg L^{-1} NO_3, 118-197 mg L^{-1} sulfate and 80-356 mg L^{-1} chloride. The effluent nitrate-N levels were lower than 10 mg L^{-1}.

Boumediene and Achour [37] treated underground water by a nitrate specific ionic exchange resin (Purolite A 520 E). The raw water contained 70-210 mg L^{-1} NO_3, 175 mg L^{-1} sulfate, and 200 mg L^{-1} chloride. The effluent nitrate-N levels were lower than the permissible maximum concentration (10 mg L^{-1}) for drinking water.

Samatya et al. [38] carried out laboratory studies for nitrate removal from ground water using strong base nitrate selective anion exchange resin (Purolite A 520 E) having more affinity for the nitrate ions than for the other anions. Studies include batch-mode sorption studies, batch-mode stripping studies and column-mode sorption-elution studies. Adsorption isotherm has been modeled by Langmuir and Dubinin-Radushkevich (DR) equations [31]. The raw water contained 195 mg L^{-1} NO_3, 26 mg L^{-1} sulfate, and 53 mg L^{-1} chloride. The effluent nitrate-N levels were lower than the permissible maximum concentration (10 mg L^{-1}) for drinking water.

Dördelmann et al. [39] made pilot scale investigations in Iran, using nitrate selective resins (HP 555, manufactured by Rohm and Haas Company; Ionac SR 7,

manufactured by Sybron Chemicals Inc) for nitrate removal from ground water by ion exchange. The raw water contained 105 mg L^{-1} NO_3, 140 mg L^{-1} sulfate, and 168 mg L^{-1} chloride. The effluent nitrate levels were below 40 mg L^{-1}.

Nitrate removal by ion exchange was used for treating wastewaters with lower nitrate concentrations and employed either conventional or nitrate specific ion exchange resins. Studies included influence of initial nitrate concentration, sulfate-nitrate ratio and specific flow rate on the performance of resin. The effluent nitrate-N levels were lower than the permissible maximum concentration for drinking water.

However, ion exchange may be a suitable technique for denitrification for either handling small volumes or treating feed streams low in nitrate concentrations. The main drawbacks of the technique are

(i) Processing water/wastewaters consisting of anions other than nitrates, particularly, sulphates is difficult, in view of the high affinity of the ion-exchange resins towards sulfates as compared to nitrates. In general either water or wastewater streams contain sulfates at significant levels, on par with nitrates and even more in a majority of cases. This would mean that ion-exchange resins with much higher affinity levels for nitrates as compared to sulfates are required to be employed. Or it may be required to use a two-stage process to handle sulfates and nitrates separately. Either way, it would mean higher capital and operating costs.

(ii) Higher concentrations of nitrates compound the problem with the problem of disposal of waste brines.

(iii) Requirement of pre-treatment / post-treatment of the liquid streams either to restrict fouling and/or corrosion makes the process complex and raises material and operating costs.

(iv) Much of the literature refers to laboratory or pilot scale studies on ground water, drinking water and few references on wastewater. This in itself appears to be an indicator of limitations of this technique for denitrification.

2.2.2 Reverse Osmosis (RO)

Reverse osmosis (RO) can be a feasible option for nitrate removal in both municipal and Point-of-Use applications [40-42]. RO is a physical process, wherein contaminated water is forced through the semi-permeable membrane at high operating pressures (pressure greater than the osmotic pressure). The membrane retains most of the dissolved minerals on the retentate side of the membrane and treated water comes out as permeate from the other side of the membrane. Rejection rate, extent to which the RO membrane removes constituents from the water, for sodium chloride and sodium nitrate can be as high as 98% for NaCl and 93% for $NaNO_3$, respectively [43]. Membranes are made from variety of polymers such as cellulose acetate, polyamide etc. Membranes do not show or have any preference towards the type of ions but the valence of the ions does play a role in degree of salt rejection [31]. This process removes all the contaminants and produces excellent quality of water. The process is not sensitive to minor variations in the temperature and the resulting quality of permeate or product water is such that no post treatment is required. Some of the major disadvantages of RO, are (i) the large quantities of concentrated nitrate contaminated wastewater generated, (ii) high capital investment, (iii) sensitivity to pH, (iv) variation in operating pressure due to increase is dissolved solids on the concentrate or retentate side and (v) variation in chlorine content during the process. The RO process invariably requires pre-treatment of influent water to avoid fouling. RO process, it is reported, is more suitable for treating low concentrated nitrate wastewaters [31].

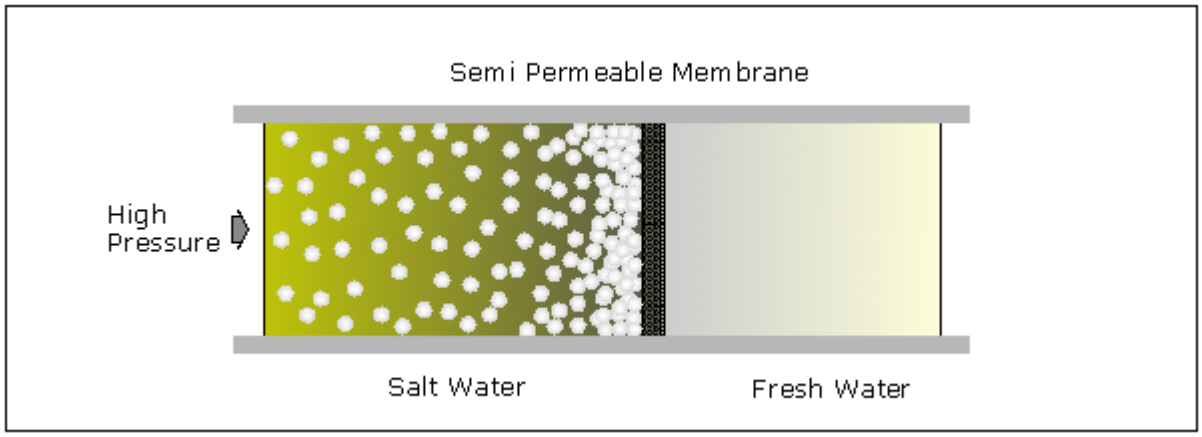

Fig. 2.2 Reverse Osmosis Process Schematic

Rautenbach et al. [44] carried out experiments using RO unit with Filmtec FT 30 spiral-wound composite membrane, with a design capacity of 2 $m^3 h^{-1}$. The unit was operated continuously for more than 20,000 h with influent nitrate concentrations of 100 mg L^{-1}. The observed nitrate rejection was 93–95%. It has been concluded that a nitrate rejection of > 90% at a recovery rate of 80% can be expected for large scale plants equipped with FT30 membranes.

Bohdziewicz et al. [45] investigated removal of nitrate ions from tap water by means of reverse osmosis. They had employed five flat acetyl cellulose osmotic membranes (type SEPA CF designated as SS10, ST10, SR10, SF, SX). Inlet water contained nitrate, 100 mg L^{-1}; magnesium ions, 19 mg L^{-1}; calcium ions, 28 mg L^{-1}; sodium ions, 52 mg L^{-1}; sulfate ions, 240 mg L^{-1}; and carbonate ions, 145 mg L^{-1}. The outlet water contained nitrate of 21 mg L^{-1}

Schoeman and Steyn, [46] carried out studies for nitrate removal from borehole waters in rural areas in South Africa using reverse osmosis. The RO plant had used Delta 10, Environmental Products USA; 4040-LHA-CPA2 membrane; membrane area of 79 m^2. The nitrate-nitrogen in the feed varied between 42 and 53 mg L^{-1}, in the RO brine (concentrate) varied between 55 and 93 mg L^{-1} and in the RO permeate was less than 5 mg L^{-1}.

Dördelmann et al. [39] made pilot scale investigations in Iran, using membrane module (type SUL-G10) for nitrate removal from ground water by reverse osmosis. The raw water contained 105 mg L^{-1} NO_3, 140 mg L^{-1} sulfate, and 168 mg L^{-1} chloride. The effluent was nitrate free.

Though Reverse Osmosis (RO) results in nitrate free water, it has several limitations for treating reasonably large quantities for extended period of time. The major drawbacks of this technique are as listed below

(i) Disposal of huge quantities of concentrated water streams high in nitrates, sulfates and other salts require additional steps and raise the operating costs.

(ii) The RO process invariably requires pre-treatment to avoid fouling of the membranes and thus adds to the operating costs

(iii) Capital towards equipment, membranes and operating costs including pre-treatment costs may not favor this technique for handling large volumes.

2.2.3 Electro dialysis (ED)

Electro dialysis (ED) is a process where, pressurized water is passed through a stack of semi permeable membranes which are connected to a direct current source. Undesirable ions are selectively removed by transferring ions from a less concentrated solution to a concentrated solution. This technology has the ability to remove nitrate ions selectively leading to better water recovery, minimal energy and chemical consumption [31, 47-52]. ED of a wastewater stream leads to nitrates getting rejected by the anion-impermeable cation-exchange membrane while moving towards the anode. Similarly, cations get rejected at the cation-impermeable anion exchange membrane while migrating towards the cathode [31].

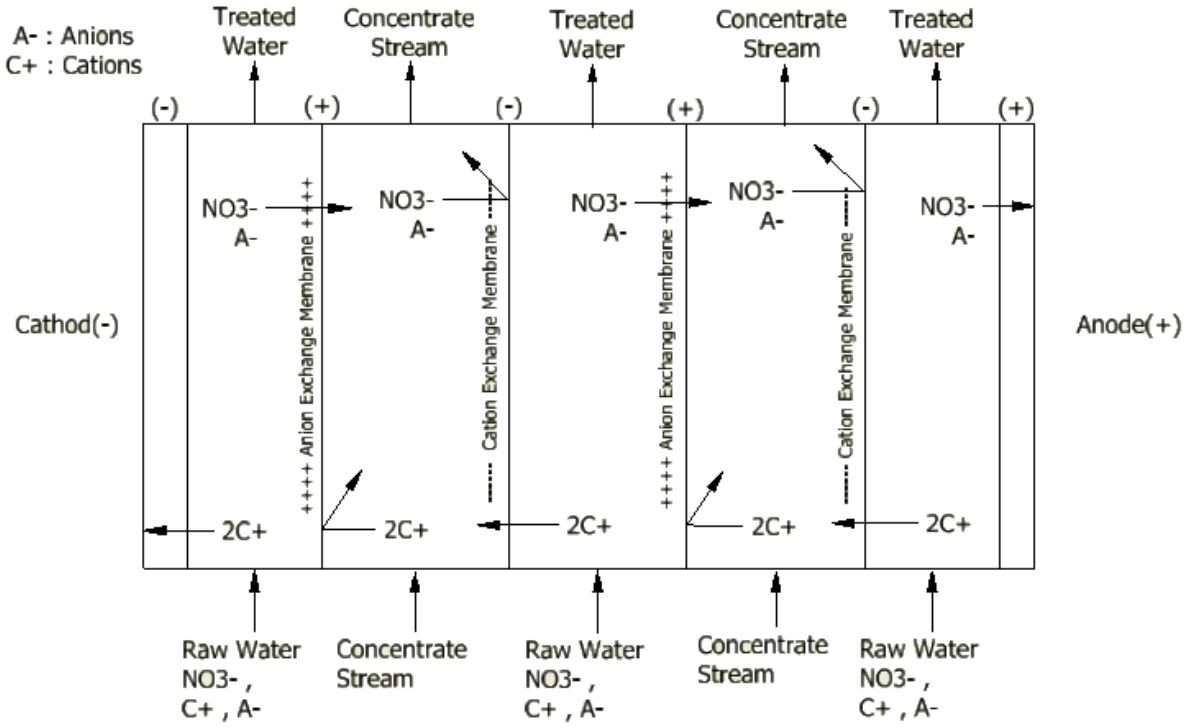

Fig. 2.3 Electrodialysis for Nitrate removal [61]

Although ED is a low pressure process and free of operational issues such as fouling, scaling etc., it requires high capital and operational & maintenance costs are similar to RO. Additionally, similar to RO, ED has a drawback of having to dispose of huge quantities of waste concentrate. Also, Ion-exchange membranes may be sensitive to iron, manganese, hydrogen sulfide (H_2S), chlorine and hardness.

Wisniewski et al. [53] investigated denitrification of ground waters with excessive nitrate concentrations by electro dialysis and found that nitrate concentration of the treated water remained below 25 mg L^{-1}. Nitrate in the feed varied between 90-155 mg L^{-1} and extraction ratios of nitrate were 70% to 90%.

Midaoui et al. [50] carried out electro dialysis to remove nitrate from ground water containing 800 mg L^{-1} of total dissolved solids (TDS); the treatment with 90 mg L^{-1} of nitrate in the feed resulted in 80% nitrate removal along with other ions. Sahli et al. [54] also studied removal of nitrate from groundwater in Morocco, by electro dialysis

using a pilot plant having a capacity of 24 m^3 d^{-1}. The nitrate concentration levels in the feed varied between 72-86 mg L^{-1} and sulfate varied between 176-207 mg L^{-1}. The product water met the desired water standards.

Sahli et al. [51] studied removal of nitrate from brackish underground water using electro dialysis equipped with an anion monovalent membrane. The feed water contained nitrate concentrations of 210 mg L^{-1} and sulfate 330 mg L^{-1}. The process produced product water with desired drinking water standards from brackish water. The principal disadvantage of this technology is the disposal of the concentrate high in nitrates.

Ali et al. [55] carried out studies for the removal of nitrate from brackish polluted water using electro dialysis to know the influence of flow rates, initial feed concentration, coexisting anions and initial pH on process efficiency. They found that the flow rate as well as the initial salt concentration and also the coexisting anions in the feed solution play a significant role on the denitrification efficiency and mainly on the specific power consumption, whereas denitrification process was independent of pH of feed solution. The nitrate concentrations were reduced from 225 to 25.5 mg L^{-1}. Studies have shown that the resulting product stream meets the desired water standards even when large volumes are treated. This may be attributed to the fact that the transport of the ions towards electrodes is specific. However, the use of Electro dialysis (ED) for denitrification has similar drawbacks as indicated for RO, mainly, the capital costs and the disposal of the concentrate stream.

2.2.4 Chemical Denitrification

Nitrate ion being highly stable and first-rate oxidising agent, special conditions such as high temperature, pressure and catalysts are required for reduction by suitable reducing agents [56]. In the chemical denitrification process (also known as nitrate to

ammonia and ceramic NAC process), Nitrate ions get reduced to ammonia by powdered aluminum and aluminum in turn gets converted to aluminum hydroxide and sodium aluminate [57].

$$3NaNO_3 + 8Al + 12H_2O \rightarrow 3NH_3 \uparrow + 5Al(OH)_3 + 3NaAlO_2 \quad 2.3$$

$$3NaNO_3 + 8.8Al + 14.4H_2O \rightarrow 3NH_3 \uparrow + 5.8Al(OH)_3 + 3NaAlO_2 + 1.2H_2 \uparrow \quad 2.4$$

Ammonia is the principal reaction product (60-95%) in the chemical denitrification and it can be removed by air stripping. This process takes place in alkaline solutions and nitrate removal is reported to be optimum at pH 12.25 and temperatures > 50 ^{o}C. Nitrates can be selectively reduced relative to sulfate. Cooling is required during the process since it is highly exothermic (-381 kcal/mole of $NaNO_3$). Inert atmosphere is required, since off-gases are flammable. The main advantage of this process is that it can be carried out at atmospheric pressure, relatively low temperatures and produces lesser solid waste. The disadvantage however, is that nitrate conversion results in ammonia instead of nitrogen gas and hence off-gas treatment becomes mandatory. Maintenance of inert atmosphere is essential, since ammonia and hydrogen gases produced are potentially exothermic [18,31].

Sabzali et al. [58] carried out studies for nitrate removal from groundwater via sulfamic acid and zinc metal and optimized process parameters like pH, sulfamic acid concentration, Zn concentration, temperature and reaction time governing the process. The feed contained nitrate 145 mg L^{-1}, sulfate 75 mg L^{-1} and chloride 45 mg L^{-1}. Near 100% nitrate removal was achieved.

Chemical denitrification can be considered as a probable nitrate treatment option. However, to achieve the desired levels of denitrification, it may require huge quantities of chemical addition,

2.2.5 Catalytic Denitrification

Catalytic denitrification (CD) is one of the promising technologies used for removing the nitrate from water without generating secondary wastes. Either formic acid or hydrogen may be used for reduction of nitrate; the latter is preferred over formic acid. Hydrogen reduction of nitrate is a multi step process as shown in the scheme below:

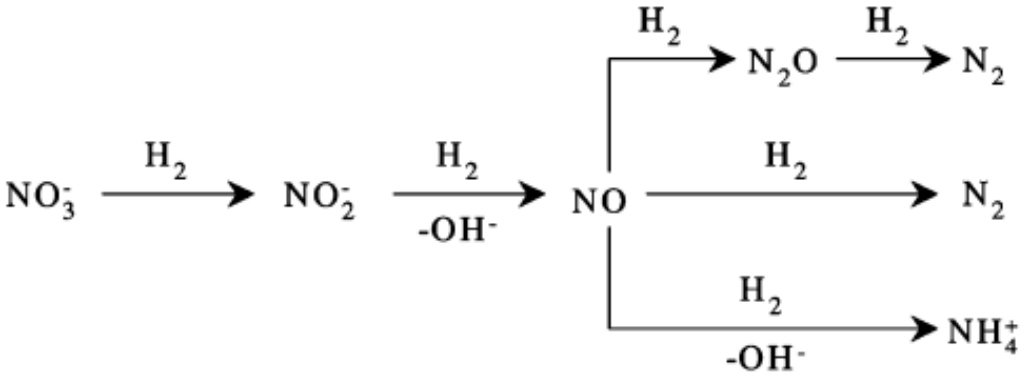

Many catalysts such as Pd, Pt, Pt-Cu, Pd-Sn, Pd-In, Pd-Cu etc. were tried for nitrate reduction. In comparison to other catalysts, Pd-Cu catalyst was studied extensively. Support materials used for these catalysts included alumina, titania, niobia, zirconia, and activated carbon. In view of the ease in modifying the surface chemistry as per the requirements, activated carbon appears to be the choice, which incidentally provides high surface area making catalyst dispersion more effective.

CD is predominantly used for treating acidic effluents. The limitations with this process include cost of catalyst and its fouling, use of flammable hydrogen gas and production of ammonia in the reaction. No full scale process is implemented employing CD [31,59-61].

Pintar et al. [60] developed a bench scale process for removal of nitrates from potable water using Pd–Cu/γ-Al_2O_3 bimetallic catalyst. This process is employed mainly for regeneration of strong base anion based resin, which was used for removal nitrates. Lemaignen et al. [59] investigated nitrate reduction using Pd bimetallic catalysts (Pd–

In and Pd–Sn) for a range of nitrate concentrations up to 1000 mg L^{-1} in acidic and close to neutral pH. In addition, Pd–Cu was also studied at pH 5. Nitrate reduction was inhibited strongly by nitrite and moderately by sulfate. Activated carbon catalysts are comparable to metal oxide supported bimetallic catalysts.

Palomares et al. [62] investigated catalytic hydrogenation of nitrates in liquid phase using Pd/Cu supported on hydrotalcite and Pd/Cu supported on alumina. Nitrate concentrations were 80-90 mg L^{-1}. Meytal and Sheintuch [63] tested Pd–Cu catalysts supported on woven fibrous cloths for continuous nitrate hydrogenation in water and found that Pd–Cu/ACC is more active and selective than Pd–Cu supported on glass fibers cloth (GFC) and on GFCs coated with Al_2O_3 or SnO_2.

In View of the disadvantages of the physical and chemical methods with respect to cost and disposal of secondary wastes, biological methods are studied extensively for denitrification of groundwater as well as wastewaters.

2.3 Biological Denitrification

Bacteria found in the activated sludge process comprise mostly of facultative anaerobes. These organisms are capable of degrading carbonaceous biochemical oxygen demand (cBOD) by using free molecular oxygen, nitrite ions or nitrate ions. Different species of bacteria can grow anaerobically by reducing the ionic nitrogenous oxides to gaseous products. In the absence of molecular oxygen, facultative bacteria use oxygen from nitrate and nitrite for respiration, generating ATP in the process. This process is known as dissimilatory nitrate reduction or denitrification [64].

Carbon source and electron donor are required for growth and maintenance of existing bacterial cell mass and production of new cells. Most of the denitrifying bacteria require anaerobic conditions and presence of certain specific bacteria favored denitrification in the presence of oxygen [65]. Biochemical analysis shows that nitrate

denitrification in microorganisms is a four step process. Nitrate (NO_3^-) gets reduced to nitrite (NO_2^-) by nitrate reductase, nitrite (NO_2^-) gets reduced to nitric oxide (NO) by nitrite reductase, nitric oxide (NO) gets reduced to nitrous oxide (N_2O) by nitric oxide reductase, finally nitrous oxide reductase reduces nitrous oxide (N_2O) to nitrogen gas [66-67].

$$NO_3^- \rightarrow NO_2^- \rightarrow NO \rightarrow N_2O \rightarrow N_2 \quad (2.5)$$

$$NO_3^- + 2\,e^- + 2\,H^+ = NO_2^- + H_2O \text{ Nitrate Reductase} \quad (2.6)$$

$$NO_2^- + e^- + 2\,H^+ = NO + H_2O \text{ Nitrite Reductase} \quad (2.7)$$

$$2\,NO + 2\,e^- + 2\,H^+ = N_2O + H_2O \text{ Nitric Oxide Reductase} \quad (2.8)$$

$$N_2O + 2\,e^- + 2\,H^+ = N_2 + H_2O \text{ Nitrous Oxide Reductase} \quad (2.9)$$

The overall reaction from NO_3^- to N_2 reduces the N by 5 electron equivalents per N. In practice, nitrite accumulation has been observed during nitrate denitrification by numerous microorganisms. Other intermediates i.e. NO and N_2O are not produced or released in significant amounts as compared to NO_2^-. However, there is a concern about the release of NO, N_2O from wastewater treatment plants, because of their potential harmful effects. Facultative anaerobes have enzymatic ability to use either nitrogen oxides or free molecular oxygen during cBOD degradation. During assimilatory reduction of nitrogen oxides, ammonium ions are formed by nitrate and nitrite ion reduction and nitrogen in ammonium ions is incorporated into cellular material. Nitrogen will not get incorporated into cellular material during dissimilatory reduction [64].

2.3.1 Heterotrophic Denitrification

Heterotrophs are organisms that cannot fix carbon and hence need organic carbon for growth. Heterotrophic denitrification is a microbially facilitated process of nitrate

reduction performed by a large group of heterotrophic facultative anaerobic bacteria, which ultimately produce molecular nitrogen (N_2) through a series of intermediate gaseous nitrogen oxide products. This respiratory process reduces oxidized forms of nitrogen in response to the oxidation of an electron donor such as organic matter.

A wide variety of carbon sources, either in the form of liquid or solid, can be used as electron donors by heterotrophic denitrifying bacteria. Being organic in nature these carbon sources are easily oxidized. The substrates are methanol, ethanol, propanol, butanol, pentanol, cellulose, glycol, methane, aromatic hydrocarbons, glucose, acetate, aspirate, formic acid, industrial wastes such as molasses, whey, and distillery stillage. Methanol, ethanol and acetate are most commonly used carbon sources for denitrification. Porges et al. [68] had suggested $C_5H_7NO_2$ as cell formula. The stoichiometric relationships of heterotrophic denitrification with various carbon sources are listed in Table 2.1 [65-66,69].

2.3.2 Autotrophic Denitrification

Autotroph is an organism that produces complex organic compounds (such as carbohydrates, fats, and proteins) from simple substances present in its surroundings, generally using energy from light (photosynthesis) or inorganic chemical reactions (chemosynthesis).

Autotrophic denitrification processes utilize autotrophic denitrifiers such as *Paracoccus, Thiobacillus, and Thiosphaera* for reducing nitrate to molecular nitrogen (N_2). Autotrophic denitrifiers utilize inorganic materials such as carbon dioxide or bicarbonate as electron donors and energy is derived by oxidation of inorganic sources such as hydrogen or various forms of sulfur compounds. In this process, operation costs are lower and secondary contamination risk is minimized because of avoiding the external carbon addition. In addition, it lowers cell yield of autotrophic

bacteria and therefore less sludge production, which minimizes the handling of sludge. Sulfur to nitrogen ratio plays a significant role in autotrophic denitrification. The stoichiometric relationships of autotrophic denitrification with various carbon sources are listed in Table 2.2 [65-66,69].

Table 2.1 Stoichiometry of heterotrophic denitrification with various carbon sources

Substrate	**Stoichiometric equation**
Acetic acid	$5\ CH_3COOH + 8\ NO_3^- \rightarrow 8\ HCO_3^- + 2\ CO_2 + 6\ H_2O + N_2$
Aromatic hydrocarbons	$C_{61}H_{67} + 62.2\ H^+ + 62.2\ NO_3^- \rightarrow 31.1\ N_2 + 61 CO_2 + 64.6\ H_2O$
Butanol	$0.208\ C_4H_9OH + NO_3^- \rightarrow 0.5\ N_2 + 0.833\ CO_2 + 0.542\ H_2O + OH^-$
Cellulose	$5\ (C_6H_{10}O_5)_n + 24n\ NO_3^- \rightarrow 6n\ CO_2 + 13n\ H_2O + 12n\ N_2 + 24n\ HCO_3^-$
Ethanol	$5\ C_2H_5OH + 12\ NO_3^- \rightarrow 10\ HCO_3^- + 2\ OH^- + 9\ H_2O + 6\ N_2$
Glucose	$C_6H_{12}O_6 + 2.8\ NO_3^- + 0.5\ NH_4^+ + 2.3\ H^+ \rightarrow 0.5\ C_5H_7NO_2 + 1.4\ N_2 + 3.5\ CO_2 + 6.4\ H_2O$
Glycol	$0.5\ (CH_2OH)_2 + NO_3^- \rightarrow 0.5\ N_2 + 0.833\ CO_2 + 0.5\ H_2O + OH^-$
Methane	$CH_4 + 8\ NO_3^- + 8\ H^+ \rightarrow 4\ N_2 + 5\ CO_2 + 14\ H_2O$
Methanol	$NO_3^- + 1.08\ CH_3OH + H^+ \rightarrow 0.065\ C_5H_7NO_2 + 0.467\ N_2 + 0.76\ CO_2 + 2.44\ H_2O$
Pentanol	$0.167\ C_5H_{11}OH + NO_3^- \rightarrow 0.5\ N_2 + 0.833\ CO_2 + 0.5\ H_2O + OH^-$
Propanol	$0.278\ C_3H_7OH + NO_3^- \rightarrow 0.5\ N_2 + 0.833\ CO_2 + 0.611\ H_2O + N_2$
Typical Organic matter	$C_5H_9NO + 3.36\ NO_3^- + 3.92\ H^+ \rightarrow 1.68\ N_2 + 0.36\ C_5H_7NO_2 + 3.26\ CO_2 + 3.92\ H_2O + 0.64\ NH_4^+$

Table 2.2 Stoichiometry of autotrophic denitrification with various carbon sources

Electron donor	Stoichiometric equation
Elemental sulfur	$10\ NO_3^- + 11\ S^0 + 4.1\ HCO_3^- + 0.5\ CO_2 + 1.71\ NH_4^+ + 2.54\ H_2O \rightarrow 0.92\ C_5H_7NO_2 + 11\ SO_4^{2-} + 5.4\ N_2 + 9.62\ H^+$
Ferrous iron	$NO_3^- + Fe^{2+} \rightarrow 0.5\ N_2 + 5\ Fe(OH)_2 + 9\ H^+$
Hydrogen	$2\ NO_3^- + 5\ H_2 \rightarrow N_2 + 4\ H_2O + 2\ OH^-$
Sulfide	$14\ NO_3^- + 5\ FeS_2 + 4\ H^+ \rightarrow 7\ N_2 + 10\ SO_4^{2-} + 5\ Fe^{2+} + 2\ H_2O$
Thiosulfate	$8\ NO_3^- + 5\ S_2O_3 + H_2O \rightarrow 4\ N_2 + 10\ SO_4^{2-} + 2\ H^+$ $0.141\ NO_3^- + 0.125\ S_2O_3 + 0.0643\ CO_2 + 0.1\ H_2O \rightarrow 0.0129\ C_5H_7NO_2 + 0.064\ N_2 + 0.25\ SO_4^{2-} + 0.109\ H^+$

2.3.3 Types of reactors

Biological denitrification studies were carried out using sequencing batch reactors (SBR), fluidized bed biofilm reactors (FBBR), continuous stirred tank reactors (CSTR) and anoxic/oxic membrane reactors (MBR). Sequencing batch reactors require less space since all the biological reactions and clarification take place in a single vessel. This gives the savings in cost and operational flexibility and control. However, the main disadvantage is a higher level of sophistication compared to conventional systems in terms of timing units and controls [70]. Sequencing batch reactors (SBR) were used for biological denitrification [12-13,71-77].

Fluidized bed biofilm reactors produce high concentration of microorganism since the media available for the development of microorganisms is quite large. Large concentration of microorganisms has high potential to remove BOD, COD, and

nitrogen, can handle shock loads. In addition they occupy less space and provide long SRT for microorganisms necessary to degrade the xenobiotic and toxic compounds. Main disadvantage of FBBR is the pumping power required to operate and the proper design of inlet and outlet arrangement for proper distribution of flow. Fludized bed biofilm reactors (FBBR) were employed by many researchers {78-81].

Continuous stirred tank reactors are simple in construction, versatile and low operating costs. Their well -mixed nature permits straightforward control over the temperature and pH of the reaction and the supply or removal of gases. They are easy to control and can be cleaned easily. Disadvantage is lowest conversion per unit volume and chance of by-passing and channeling because of poor agitation. Continuous stirred tank reactors were utilized for denitrification [82-85].

Anoxic/oxic membrane reactors produce cleaner effluent suitable for multiple reuse purposes and have fewer aeration basins. The disadvantages being high power and capital costs and needs chemicals for membrane cleaning. Anoxic/oxic-membrane bioreactor (A/O-MBR) were used for denitrification studies [86-87].

2.3.4 High Strength Nitrates

In spite of the extensive work carried out on biological denitrification, only limited studies were carried out with high strength nitrate wastewaters. Denitrification of high strength nitrate-nitrogen (> 1000 mg L^{-1}) wastewaters were carried out [12-14,74-77,86,88-99]. Concentrations of nitrate studied by these researchers were in the range of 100 to 14000 mg L^{-1} NO_3-N, C/N ratios of 1 to 4 were utilized and specific denitrification rates obtained were 3 to 91 mg-NO_3-N L^{-1} g-$MLSS^{-1}$ h^{-1}. As can be seen, this concentration range is less than the levels encountered in nuclear industry.

2.3.5 Factors controlling denitrification

It was reported that there are several factors influencing the denitrification. Major factors which control rates of denitrification include temperature, oxygen, organic carbon, pH, inhibitors and nitrate concentrations

Temperature

Temperature effect on denitrification process was essentially considered on the premise of favoring bacterial growth and metabolism in a fixed temperature range. Mesophiles which form a major portion of denitrifying bacteria, have an optimum temperature in the range of 20-45 ^{o}C. Fogler [100] reported that a temperature range of 35-38 ^{o}C was optimum for bacterial growth.

Microbial growth is affected by temperature in two opposing ways. Increase in temperature increases the microbial growth and product formation because rise in temperature accelerates the chemical enzymatic reactions as per Arrhenius equation $k_{d,T2} = k_{d,T1}\theta^{(T2-T1)}$, where $k_{d,T}$ is the specific rate constant at temperature T (Celsius) with units of inverse of time, and θ is dimensionless empirical constant ranging from 1.06 to 1.10. For every organism, there is an optimum temperature range for growth: Microbial growth has been reported between -12 ^{o}C and +120 ^{o}C, but there is no single microbe which can grow throughout this range. With rise in temperature, proteins, nucleic acids and other cellular components that are sensitive to temperature, i.e. temperature labile, will tend to become irreversibly deactivated and lysis, death and endogenous metabolism rates will increase. Hydrolysis rates will also increase with temperature [101].

Temperature dependence of denitrification is more pronounced in soils than in aquatic sediments. Denitrification in soils was observed even at 0 to 5 ^{o}C, but at a slower rate [66]. Delwiche and Bryan [102] reported that different organisms have different

optimum temperatures and near 30 ^{o}C is favored for denitrification by most organisms.

Optimum temperature for nitrogen and carbon removal was found to be between 22-37 ^{o}C for shrimp aquaculture. Temperature between 10-20 ^{o}C, had a greater effect on specific denitrification and carbon consumption rates, when compared to temperature between 20-30 ^{o}C. As specific growth rate of ammonia-oxidizing bacteria (AOB) is higher than that of nitrite-oxidizing bacteria (NOB), nitrogen removal was via nitrite, at higher temperatures of 28-38 ^{o}C. At lower temperatures specific growth rate of NOB is higher than that of AOB and hence nitrite accumulation was higher during winter. Inhibition of nitrification and denitrification was observed when temperature decreased to 10 ^{o}C [69,103-104]. However, denitrification can occur between 2-50 ^{o}C, though at lower rates at low temperatures [69].

Oxygen

Denitrification gets inhibited by presence of dissolved oxygen because it gets priority as an electron acceptor, when compared to nitrate and nitrite. Nitrogen oxides become terminal electron acceptors by facultative bacteria, when oxygen is absent. Organic substrate (cBOD) gets converted to carbon dioxide under aerobic and anaerobic respiration. Aerobic respiration yields higher cellular energy and higher cellular growth. Thus the bacterial cells prefer molecular oxygen to nitrogen oxides for their respiration [64,69].

$$\text{Glucose} + 6\,O_2 \xrightarrow{\text{(aerobic respiration)}} 6\,CO_2 + 6\,H_2O + 686\,\text{kCal} \quad (2.10)$$

$$\text{Glocose} + 4.8\,NO_3^- + 4.8\,H^+ \xrightarrow{\text{(anoxic respiration)}} 6\,CO_2 + 2.4\,N_2 + 8.4\,H_2O + 636\,\text{kCal} \quad (2.11)$$

DO represses the denitrifying enzyme synthesis/formation and inhibits the existing denitrifying enzyme activity. For derepression of reductive enzymes a period of 40

min to 3 h are required. Nitrite reductase takes longer derepression time than the NaR (nitrate reductase) [66,105].

Dissolved oxygen gradient exists when the floc particle size becomes greater than 100 µm, two types of respiration occurs: Aerobic respiration on the periphery of the floc particle and anaerobic respiration where nitrogen oxides used at the centre of the floc particle [64]. Many studies concluded that DO concentrations of 0.2 mg L^{-1} or less are required for denitrification to proceed.

DO inhibitory effects on denitrification depend on carbon source and microbial strains [106-107]. Presence of DO inhibited the biofilm growth and reduced the denitrifying to nitrate reducing bacteria ratio and bacterial density. [69]. This resulted in nitrogenous intermediates appearance in the effluent [106].

Higher DO concentration (2.5 mg L^{-1}) is required to inhibit /suppress nitrite reductase activity than nitrate reductase activity [106].

Nitric oxide accumulation was never seen during denitrification since NO reductase activity is 10 times higher than nitrite reductase activity. DO concentration goes higher than the threshold concentration, N_2O accumulation is seen since N_2O reductase is highly sensitive to DO [106].

During heterotrophic denitrification, oxides of nitrogen (nitrate and nitrite) get reduced to dinitrogen. Nitrogen production progressively decreased with increase in DO concentration and nitrous oxide appeared first, followed by nitrite as denitrification product at higher DO concentration [108].

Presence of DO can be tackled by addition of excess electron donor or addition of oxygen scavenging agents like Na_2SO_3, but it increases the cost of denitrification and decreases the denitrifying to nitrate reducing bacteria ratio [107].

Denitrification was observed even at DO concentration of 3 mg L^{-1} but the rates were 25% lower than those observed under anaerobic conditions [109]. Oxygen inhibition model by Eckenfelder [110] predicts that denitrification ceases when DO concentration reaches 1 mg L^{-1}.

Oh and Silverstein [109] observed that the denitrification was inhibited by the presence of DO and specific denitrification rates decreased by over 35% when the DO was 0.09 mg L^{-1}. Gaber and Joseph[69] reported that type of carbon source influences the DO effect on denitrification. Ethanol and methanol were reported to have less effect of DO on denitrification as compared to sucrose.

$$r_D = r_{D,max} \, X \, 1.09^{(T-20)} \, (1 - DO) \qquad 2.12$$

Where r_D = observed specific denitrification rate $\left(g - NO_3 - \frac{N}{g} - (g - NO_3 - N/g - MLSS/d)\right)$;

$r_{D,max}$ = anoxic specific denitrification rate $(g - NO_3 - N/g - MLSS/d)$;

T = water temperature (^oC); DO = mixed liquor dissolved oxygen concentration (mg L^{-1}).

Henze et al. [111] proposed one parameter model for oxygen-inhibition of denitrification in activated sludge

$$r_D = r_{D,max} \left(\frac{1}{1+(DO/K_{O_2})} \right) \qquad 2.13$$

Where

$r_D = observed\ specific\ denitrification\ rate\ in\ the\ presence\ of\ oxygen\ (mg - NO_x - N/g - MLSS/h)$ and

$$NO_x - N = NO_3 - N + NO_2 - N \left(mg - \frac{N}{L}\right);$$

$r_{D,max}$ = anoxic specific denitrification rate $(mg - NO_x - N/g - MLSS/h)$;

K_{O_2} is the inhibition constant where the denitrification rate is half that of the anoxic rate ($\frac{mg}{L}$ DO)

Organic Carbon/cBOD/Substrate

The carbon sources that can potentially support denitrification can be categorized as: 1) pure chemicals like methanol, ethanol, acetate, sugar, butanol etc.; 2) purified agricultural or industrial byproducts; 3) raw industrial/agricultural byproducts as corn syrup, molasses, brewery waste and other process wastes; 4) sludge fermentation products and 5) others such as hydrogen, methane and H_2S [112].

Availability of a suitable substrate is vital for biological denitrification, as this is a source of carbon and energy. The demand for electron acceptors, such as free molecular oxygen, nitrite ions, and nitrate ions (O_2, NO_2^-, NO_3^-) increases with increase in soluble cBOD. Increase in demand for electron acceptors is an indication of increase in denitrification [64]. Enzymatic activity of heterotrophs is controlled by the availability of electrons in the organic carbon [66]. Extra carbon source is required for biological denitrification, because of substrate limitation. Denitrification stability and efficiency of biological nutrient removal (BNR) can be enhanced by external carbon addition. Very low carbon limits the electron supply for reductive half-reactions to proceed further and leads to accumulation of denitrification intermediates($NO_2^-, NO\ and\ N_2O$). Excess carbon addition increases the effluent COD, necessitating secondary treatment. Biodegradability of the carbon source is an important factor in selecting the carbon source for denitrification [112-113].

When cBOD is present in higher quantities, denitrifying bacteria use nitrate/nitrite as an electron acceptor, to meet the requirement of electron acceptors beyond the available free molecular oxygen [64].

The following factors were considered in deciding the carbon source: cost, sludge production, denitrification rate, kinetics, degree of utilization, adaptation period, handling and storage safety, the content of unfavorable/toxic compounds and the potential for complete denitrification without the need for adaptation of the microflora [77]. The carbon source characteristics will have significant effects on the decisive parameters of denitrification process such as the denitrification rate, COD demand, nitrate reduction pathway, carbon utilization patterns, biomass yield and biomass composition [77,114-115].

Yang et al. [114] studied three carbon sources (glucose, acetate and citrate) and found that glucose was not the best carbon source for denitrification, though it is widely used. It was also reported that some enzymatic conversions were required for glucose to enter denitrifier metabolism, whereas acetate and citrate can be directly inserted into metabolic process.

Denitrification favored nitrate reduction pathway, when volatile fatty acids were used. Ammonium pathway dominated during dissimilatory nitrate reduction, when glycerol or glucose was employed [116].

Filippis et al. [99] investigated three carbon sources (methanol, acetic acid and sucrose) and reported that two weeks was required for steady state denitrification. Methanol gave faster acclimatization, when compared to acetic acid and sucrose. Acetic acid and methanol showed 100% nitrate removal efficiency, whereas lower removal rates were found with sucrose

Acetate was found to be the most efficient carbon source for denitrification as compared to ethanol and hydrolysed rice [117]. Methanol, ethanol and acetate were compared for their nitrate denitrifying capacity and it was found that on a molar basis

methanol>acetate>ethanol is the order for their enhancing the enzyme activity of the nitrate removal [118]. Ethanol was found to be most effective complete denitrification as compared to methanol, and methane [119]. Most of the research on the carbon sources for denitrification concluded that ethanol, methanol and acetate were most suitable and best carbon sources [113]

Onnis-Hayden and Gu [112] reported that methanol was chosen as standard carbon source for wastewater denitrification because of its low cost, favorable kinetics, and low cell yield. Acetyl Co-A, the key compound of glycolytic and tricarboxylic acid (TCA) cycle pathways, is easily formed from acetic acid, acetate or ethanol. These cycles employ organic substrate as sources of energy and carbon in most organisms. In this manner, sodium acetate and ethanol are more easily and completely metabolized than methanol or glucose. Pharmaceutical waste, rich in ethanol, can potentially provide a readily available carbon source to implement in Biological Nutrient Removal (BNR) system. [112]. Acetate, propionate, butyrate and lactate had shown higher denitrification rates than methanol or glucose [120].

Higher nitrite build-up was observed with glucose as carbon on comparison with methanol. In addition, nitrite accumulation was also observed with less labile organic compounds and true denitrifiers were driven out and favored facultative microorganism proliferation [121].

Industrial or agricultural wastes were utilized as external carbon sources for denitrification during initial days [122-124]. It was found that formaldehyde and dextrose waste were less effectively degraded than distillery oils or methanol; however most of wastes from food industry showed very high denitrification rates and/for C/N ratio from 2 up to 6. Pretreatment, viz., degreasing, pH adjustment, removal of color of industrial wastes was found to be essential before employing as

carbon source. Dairy waste is rich in readily biodegradable COD, but it produced foam and inferior effluent quality because of excess fats. MicroC™ is highly degradable and possesses complex composition, acclimated biomass consisting of heterogeneous microorganisms. Moreover this substrate was found to have high utilization rate even with non acclimated sludge. Corn syrup (CS) which contains high glucose is widely used in the food industry. Many sodas and fruit-flavored drinks use high-fructose corn syrup (HFCS) which has fructose as the major sugar [112].

Sludge-based carbon sources

Studies were carried out to decrease/minimize the cost of external carbon, by utilizing the hydrolyzed sludge (hydrolyzate) as an internal carbon source. Hydrolyzate generated through biological process gave comparable denitrification rates realized with acetate [125].

Carbon sources for which kinetic studies were carried out are: Methanol, Ethanol, Acetate, Acetic acid, Butyric acid, Citrate, Propionic acid, Propionate, Formic acid, Succinic acid, Glucose, Hydrolysed/Fermented sludge, Fermented MSW, Hydrolysed molasses, Hydrolysed rice, news paper, cotton, rice husk, Corn Syrup, Sugar solution, Olive Oil Mill, Dairy Waste, Winery waste, Distillery Fusel oils, Pea blanch water, Wines Sludge Conc., Methanol Still Bottoms, National Starch, Tomato Sludge, Distillers' Fusel Oils, Organic Acid Waste, Fibres Gicol Waste, Waste Dextrose, Formaldehyde waste, Brewery waste, Bio-Diesel, MicroC™, Beet-sugar waste, methane, saw dust [112-114].

pH

Denitrification can happen over a broad range of pH values but the rate reduces as pH decreases. pH in the range 6.5 to 8.5 suits facultative anaerobes to form flocs and same range is adequate for denitrification. The optimal pH range for denitrification is

7.0 to 7.5 based on enzymatic activity of facultative anaerobe and nitrifying bacteria [64].

Optimum pH range for denitrification is 7.0 to 8.0 for single strain (pure) cultures and natural systems. As pH decreases, overall denitrification rate decreases because of steady reduction in the nitrous oxide (N_2O) reductase activity, which increases the mole fraction of N_2O. Denitrification did not occur in acid peat whose pH was 3.5 [66].

Delwiche and Bryan [102] reported that neutral pH range suits denitrifying systems for best performance and maximum rate of denitrification is found to be between 7.0 and 8.2 of pH, though denitrification is observed between 5.8 and 9.2. Type of organism, concentration of nitrate and culture age play key roles in deciding the optimum pH for denitrification. *P aeruginosa* performed denitrification in a pH range of 5.8 to 9.2, with an optimum range of 7.0 to 8.2. When the pH goes out of range for denitrification, intermediate nitrogen gases are produced and denitrification gets hindered [102].

Heterotrophic denitrifiers prefer pH range of 5.95 to 7.9, though 7.5 to 8.5 is considered to be the optimum pH for complete denitrification without nitrite accumulation. Denitrification process gets hampered when the pH values cross these limits, but optimal pH varies from site to site because microbial ecosystem gets acclimatized and adapts to the specific site. Denitrification fails under strong acidic conditions (pH<5) because of accumulation of nitrite and N_2O. Hydroxyl ions get released and alkalinity increases during heterotrophic denitrification, whereas alkalinity is consumed during autotrophic denitrification, generating sulfate in high concentration. $NaHCO_3$ is the most generally used alkalinity source. Granular lime stone and elemental sulfur particles are cheaper and alternative sources for alkalinity.

Pyrite (FeS_2) has no toxic effect on denitrifying microorganisms, is unstable mineral under anoxic conditions used as an in situ buffering agent for hydrogenotrophic denitrification and gets converted to ferrous hydroxide [69].

Denitrification is carried out by enzymatic reactions. pH plays a major role in the enzyme kinetics of biological reactions by influencing the denitrifier growth, metabolism, denitrification gene expression and denitrification rate. Hence denitrification is pH dependent [105,125].

$$\text{(Specific growth rate) } \mu_{j,net} = \frac{\delta_j}{1+\frac{[H^+]}{K_{H1_j}}+\frac{K_{H1_j}}{[H^+]}} \quad 2.14$$

At near neutral pH, many micro-organisms become active giving the best performance of denitrifying systems [66,102]. As the pH decreases below 5, N_2O proportion in the evolved products increases and inhibits overall denitrification rate [66, 126]. During dissimilatory reduction of nitrate to nitrogen gas, pH increases since alkalinity is produced. The increase in pH reduces the microorganism activity and increases the accumulation of NO_2 subsequently decreases nitrate removal rate. Phosphate buffer addition was reported to improve denitrification by maintaining the pH near 7 [127].

Lu et al. [106] concluded that optimal pH for denitrification is 7-9 and it gets hindered when pH goes out of this range and denitrification intermediates gets accumulated. N_2O reduction rate was more dependent on pH than the nitrate and nitrite reduction rate.

Denitrification experiments at different pH were carried out and found that denitrification was completely inhibited at pH $\leq$ 7 and as the pH increased between 7.5 and 9, increase in nitrite accumulation was observed and total denitrification time for nitrate and nitrite reduction was constant for all pH ranges [12]. Denitrification

reaction progress can be monitored by monitoring the pH, though there is a negligible pH change during nitrate reduction compared nitrite reduction, where appreciable pH change can be seen. High-strength nitrate wastewater denitrification performance can be enhanced by monitoring and controlling the pH [12].

Inhibitors

Denitrification is inhibited by a variety of compounds. Table 2.3 summarizes some inhibitors reported in the literature. The mechanism of inhibition is not well understood. Sulfide inhibits specifically reduction of NO and N_2O [66].

Nitrate concentration

High nitrate concentrations inhibit the dissimilatory reduction process of denitrification. For treating such high nitrate wastewaters, acclimatization strategy is adopted for developing an appropriate consortium. The aim is to grow nitrate tolerant bacteria, which comprise true denitrifiers suited for nitrate reduction to nitrogen and nitrate respirators suited for nitrate reduction to nitrite [69,74].

2.4 Attached growth and suspended growth systems

The microorganism will be either attached as biofilms to some inert material such as rocks/ceramic/plastic materials or suspended in the medium. Trickling filters (biological tower), rotating biological contactors (RBC), packed bed reactors and fluidized bed biofilm reactors come under attached growth systems. Nitrate bearing water flows over biofilms comprising of denitrifying microorganisms and nitrate gets removed. In suspended growth systems, nitrate bearing water flows through the reactor, which is in the form of a column or a tank, where the denitrifying microorganisms grow in the forms of flocs or granules [128-129] Attached-growth systems are simple to operate, have less equipment maintenance and require less energy, than the suspended-growth systems. However, attached-growth processes

require larger land, pose odor and clogging of certain media problems, and has inability to handle high volumes of wastewater which makes them to suit small to medium-sized operations. Suspended-growth processes are opted by urban facilities [130].

2.5 Kinetics of denitrification

The rate of nitrate conversion depends on the magnitude of specific rate constant, order of reaction and growth rate of microorganisms. The conversion of nitrate to N_2 is either by direct reduction of nitrate into N_2 or through formation of nitrite intermediate.

Denitrification reaction can be written in simple form

$$NO_3^- \rightarrow NO_2^- \rightarrow N_2 \qquad 2.15$$

and

$$NO_3 \rightarrow N_2 \qquad 2.16$$

The general denitrification rate with respect to biomass growth is written by Monod's kinetic equation [101,131] and it is written as:

$$-r_{NO_3} = \left\{\frac{dC_{NO_3}}{dt}\right\} = \frac{\mu_{max}\, C_{NO_3}^{n}\, C_X^{m}}{(k_{NO_3} + C_{NO_3})\, y} \qquad 2.17$$

where

m, and n are the orders of reaction with respect biomass and nitrate concentrations

μ is growth rate (h^{-1})

y is growth rate constant

k_{NO_3} is rate constant for Nitrate concentration (mg NO_3-N L^{-1} h^{-1})

C_x is the growth of biomass (g MLSS L^{-1})

Table 2.3 Denitrification inhibitors
[66]

Inhibitor (concn)	Reaction inhibited
Acetylene (10^{-3} atm)	$N_2O \rightarrow N_2$
Azide, cyanide, DNP (2,4-Dinitrophenol) (ca. 10^{-4} M)	$NO_3^- \rightarrow N_2, N_2O \rightarrow N_2$
Nitrapyrin (nitrification inhibitor)	
14 mg L^{-1} in soil	$NO_3^- \rightarrow N_2$
50 mg L^{-1} in soil	No effect
50 mg L^{-1} in culture	$NO_3^- \rightarrow N_2$
N-serve formulation (20 mg L^{-1} in enrichment culture)	$NO_3^- \rightarrow N_2O \; and \; N_2$
Pesticide	
Vapam (20 mg L^{-1} in soil)	$NO_3^- \rightarrow N_2$
Dalapon (10 mg L^{-1} in soil)	$NO_3^- \rightarrow N_2$
Toluidine derivatives	$NO_2^-, N_2O \rightarrow N_2$
Sulfur compound	
(SO_4^{2-} 100-500 μg of S g^{-1})	NO_3^- disappearance in soil
S^{2-}	
40 mmol g^{-1}	NO_3^- gaseous products
0.3 mM	$NO \rightarrow N_2O$
0.3 mM, 8 μmol g^{-1}	$N_2O \rightarrow N_2$

C_{NO_3} is the Nitrate concentration, (mg $NO_3 - N \; L^{-1}$)

$$-r_{NO_3} = \left\{\frac{dC_{NO_3}}{dt}\right\} = \frac{K_D\, C_{NO_3}}{(k_{NO_3}+C_{NO_3})} \quad 2.18$$

where, $K_D = \frac{\mu_{max}\ C_X^m}{y}$,

Since, the $k_{NO_3} \ll C_{NO_3}$, k_{NO_3} can be neglected and for specific denitrification rate, the above equation is reduced to

$$-r_{NO_3} = \left\{\frac{dC_{NO_3}}{dt}\right\} = K_D \quad 2.19$$

showing that the Monod equation is reduced to zero order kinetics for constant bio growth.

Based on Monad kinetics model, the growth rate of granular sludge follows first order kinetics and its growth rate is insignificant as compared to the rate of denitrification, whereas the specific denitrification reaction follows zero order kinetics. This is validated by the experimental observations of many researchers [74,90,132-133].

Thus, the above equation 2.18 is deduced to general form of expressions for nitrate and nitrite decomposition respecively

$$-\left\{\frac{dC_{NO_3}}{dt}\right\} = K_{NO_3}\, C_{NO_3}^n\, C_X^m \quad 2.20$$

$where\ m = 1\ \&\ n = 0$

$$-\int_{C_{NO_3,0}}^{C_{NO_3,t}} \frac{dC_{NO_3}}{C_{NO_3}^0} = K_{NO_3}\, C_x \int_0^t dt \quad 2.21$$

since C_x is independent and taken as constant

On integration

$$\frac{[C_{NO_3,t} - C_0]}{[C_x]} = -K_{NO_3}\, t \quad 2.22$$

Similarly the rate expression for nitrite in presence and in the absence of nitrate is written as

$$\left\{\frac{dC_{NO_2}}{dt}\right\} = \left[K_{NO_3}\, C_{NO_3} - K'_{NO_2}\, C_{NO_2}\right] C_x \quad \text{(in the presence of nitrate)} \quad 2.23$$

$$\left\{\frac{dC_{NO_2}}{dt}\right\} = K_{NO_2}\ C_{NO_2}\ C_x \qquad \text{(in the absence of nitrate)} \qquad 2.24$$

and the influence of nitrite formation is estimated by the relative rate, which is a ratio of rates (RR) of decomposition of nitrate and that of nitrite in the presence of nitrate.

$$\text{Relative rate (RR)} = \frac{K_{NO_3}}{K'_{NO_2}} \qquad 2.25$$

The rate of denitrification reaction is determined from the nitrate and nitrite profiles obtained during SBR cycle period. The rate constant of the denitrification reaction is calculated by graphical analysis from the experimental data. The specific rate constant is calculated by dividing the rate constant with MLSS values.

Cavari and Phelps [134] reported that denitrification was strongly influenced by, and directly proportional to nitrate concentrations when *Pseudomonas aeruginosa* 2 Kin was employed. Grady et al. [135] correlated the denitrification rates with nitrate concentrations using Michelis-Menten-type-kinetics.

$$V = \tilde{V}\ \frac{[NO_3^-]}{K_s + [NO_3^-]} \qquad 2.26$$

Where V = Denitrification rate, $Time^{-1}$

$\tilde{V}$ = Maximum denitrification rate, $Time^{-1}$

$[NO_3^-]$ = Nitrate concentration, Mass/Volume

K_s = Half-saturation coefficient, mass/Volume

Messer and Brezonik [136] stated that when nitrate concentrations are much lower than K_s, the kinetics may be approximated by a first-order relationship, where the denitrification rate is linearly related to nitrate concentrations:

$$V = k_d[NO_3^-] \qquad 2.27$$

Where k_d = denitrification rate constant, $Time^{-1}$

Filippis [99] reported from the results of their batch tests that denitrification pathway depends on the nitrate concentrations when nitrite accumulation took place and reached maximum concentration.

for first order kinetics,

$$\int_{C_o}^{C_{NO_3,t}} \frac{dC_{NO_3}}{C^1_{NO_3}} = -k \int_0^t dt \qquad 2.28$$

$$\ln \left[C_{NO_3,t} - C_0 \right] = -k\,[t - 0] \qquad 2.29$$

$$\ln \left[C_{NO_3,t} - C_0 \right] = -k\,t \qquad 2.30$$

$$\left[C_{NO_3,t} - C_0 \right] = e^{-kt} \qquad 2.31$$

Or

$$\ln C_{NO_3,t} = \ln C_{0,t} - kt \qquad 2.32$$

The rate kinetic is written as $[y] = m\,X + C$

$$\ln C_{NO_3,t} = -kt + \ln C_{0,t} \qquad 2.33$$

The rate constant is calculated from the slope of the semilog curve between concentration and time. The instantanous time and its rate constant is determined by the following equation for first order kinetics.

$$\left\{ \begin{array}{c} \text{Time required at any} \\ \text{instant of concentration, } C_{NO_3,t} \end{array} \right\} = t = \left\{ \frac{-[C_{NO_3,t} - C_0]}{k} \right\} \text{sec} \qquad 2.34$$

$$\left[\begin{array}{c} \text{concentration at} \\ \text{any instant} \end{array} \right] = C_{NO_3,t} = C_0 + e^{-kt} \quad \frac{\text{mol}}{\text{lit}} \qquad 2.35$$

For nitrite concentration, C_{NO_2}

$$C_{NO_2} = \frac{K_{NO_3} C_{NO_{3,0}}}{K_{NO_2} - K_{NO_3}} \left[e^{(-K_{NO_3} t)} - e^{(-K_{NO_2} t)} \right] \frac{\text{mol}}{\text{lit}} \qquad 2.36$$

For Nitrogen concentration, C_{N_2}

$$C_{N_2} = C_{NO_{3,0}} - \left[1 - \frac{1}{K_{NO_2} - K_{NO_3}} \left(K_{NO_2} e^{(-K_{NO_3} t)} - K_{NO_3} e^{(-K_{NO_2} t)} \right) \right] \frac{\text{mol}}{\text{lit}} \qquad 2.37$$

It is evident for the above review that biological denitrification offers a wide range of advantages compared to the physic-chemical methods, due to ease of operation, minimum addition of chemicals and generation of small volumes of biological sludge. Studies on different reactor configurations indicate the advantages of sequential batch reactors for bio-denitrification.

3 MATERIALS AND METHODS

Details about fabrication and setting up of the experimental facilities are described in this chapter. Experimental methods, including analytical techniques employed and data analysis are detailed.

3.1 Fabrication and setting up of reactors for denitrification studies

3.1.1 Fabrication and setting up of sequencing batch reactors

Sequencing batch reactors with working volume of 6 L were used for the denitrification studies. Fig. 3.1 shows a schematic as well as a photograph of the SBR. The reactors were made from acrylic tubes having an internal diameter (ID) of 0.15 m and a height (H) of 0.6 m. The base of the reactors was made from a 10 mm thick flat acrylic sheet for providing stability without additional anchorage. The reactors were fitted with tubing connectors for feed port at 1.5 cm and effluent port at 17 cm from the bottom and a provision for inserting the RTD. The reactor was provided with baffles to prevent vortexing, settling of the solids and rotation of the liquid mass as whole. Release of carbon dioxide and nitrogen in significant amounts is expected during denitrification of high strength wastes. The gas generation and associated foaming may cause loss of solids from the reactor top. To prevent loss of biomass, the reactors were provided with an additional 4 L head space. The reactors were provided with baffles to prevent vortex formation and rotation of the liquid mass as whole.

A stirrer (ELTEK Labstir, India) with a working speed of 30 to 200 RPM was used for mixing of reactor contents. An additional paddle was fixed to the centre shaft of the reactor for preventing foam formation at the top surface. The reactors were fitted

with an RTD for temperature measurement. The reactors along with the stirrer were mounted on the working bench and drain from the reactors was connected to the sink. The reactors were covered with two halves of acrylic plates to minimize contact with atmospheric air.

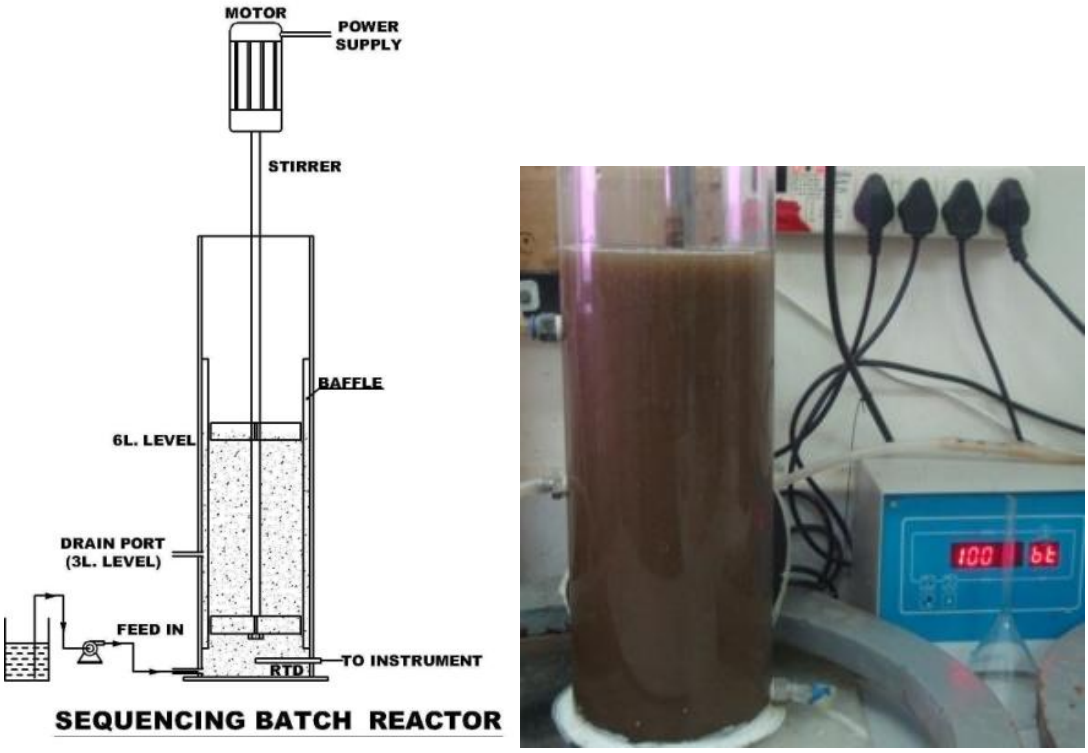

Fig. 3.1 Schematic and digital image of 6 L SBR used for denitrification experiments.

3.1.2 Fabrication and setting up of continuous stirred tank reactor (CSTR)

The reactor used for operation as a CSTR is similar in construction to the SBR. An effluent port was provided at a port situated at 34 cm from the bottom. Feed port was provided at 1.5 cm from the bottom of the reactor. The stirrer was provided with two impellers at 1/3 and 2/3 of the working liquid height. The reactor along with the stirrer was mounted on the working bench and the drain from the reactor was connected to the sink. The reactor was covered with two halves of acrylic plates to minimize contact with atmospheric air.

3.1.3 Fabrication and setting up of Expanded Granular Sludge Bed Reactor (EGSBR)

An EGSBR was designed for studying denitrification and granulation in continuous reactor conditions. The reactor was fabricated using plexiglass tube, with a total height of 1.72 m and an internal diameter of 5.4 cm, with an expanding section at the top. An inverted conical device was placed inside the enlarged portion, which to act as gas-liquid-solid separator. Fig. 3.3 shows a schematic and photography of the EGSBR. Total working volume of the reactor was 4 L.

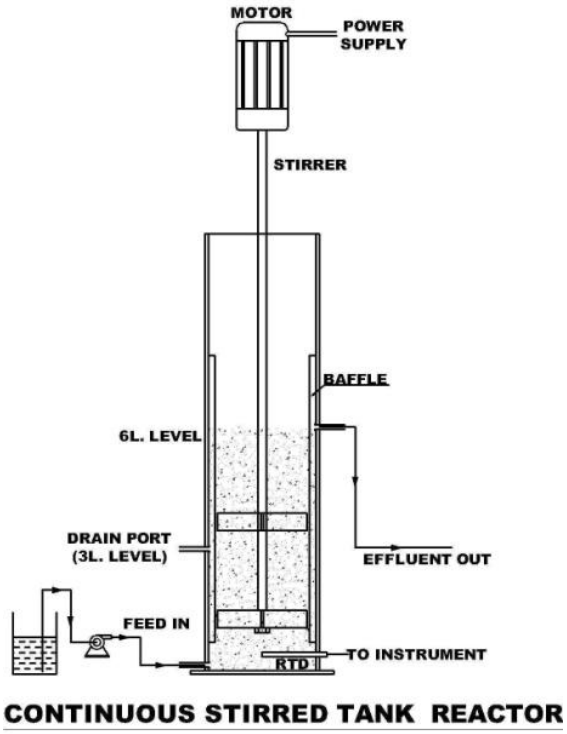

Fig. 3.2 Schematic of 6 L volume reactor operated in CSTR mode for denitrification.

The reactor was fitted to the wall with the help of a U clamp. A peristaltic pump was connected to the reactor for recirculation. The reactor was provided with RTD for temperature monitoring.

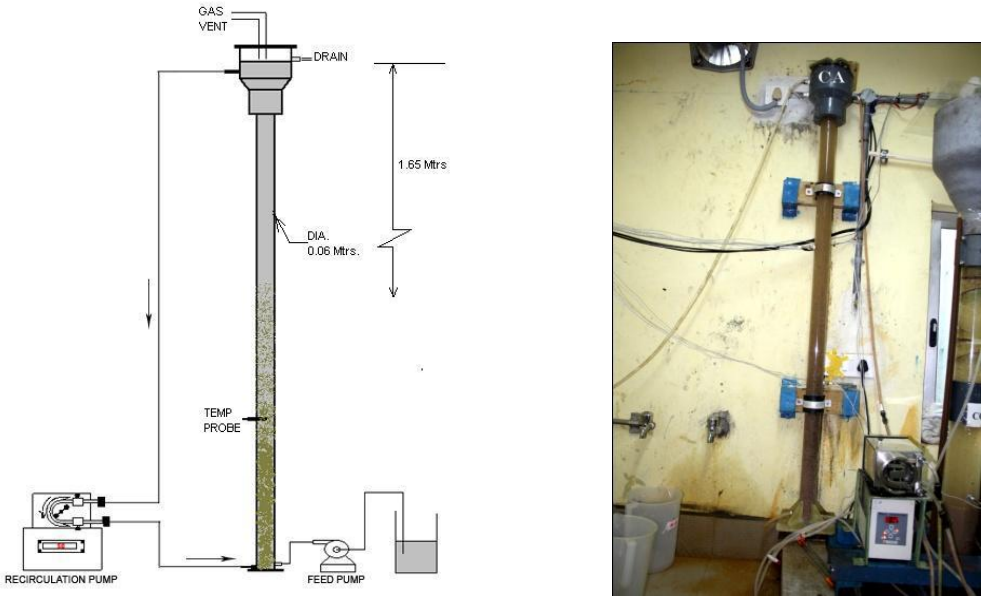

Fig. 3.3 Schematic and digital image of 4 L volume EGSBR for denitrification

3.1.4 Fabrication and setting up of semi-pilot scale SBR

A reactor with a working volume of 24 L was fabricated to check granulation and denitrification with higher volume of waste. The reactor consisted of 0.1 m inside diameter straight acrylic tube of length 1.16 m and an expander portion of 0.315 m inside diameter. Expansion from 0.11 m to o.315 m was achieved by joining two expanders. The reactor was provided with baffles on the sides for solid gas separation. The reactor was fitted with 20 mm thick flat acrylic sheet (60 cm X 60 cm) for providing stability without additional anchorage.

The reactor was mounted on the working bench in the bioreactor room and fitted with a clamp to support the expander. A peristaltic pump was connected to the reactor for recirculation of the contents. The reactor was provided with RTD for temperature monitoring.

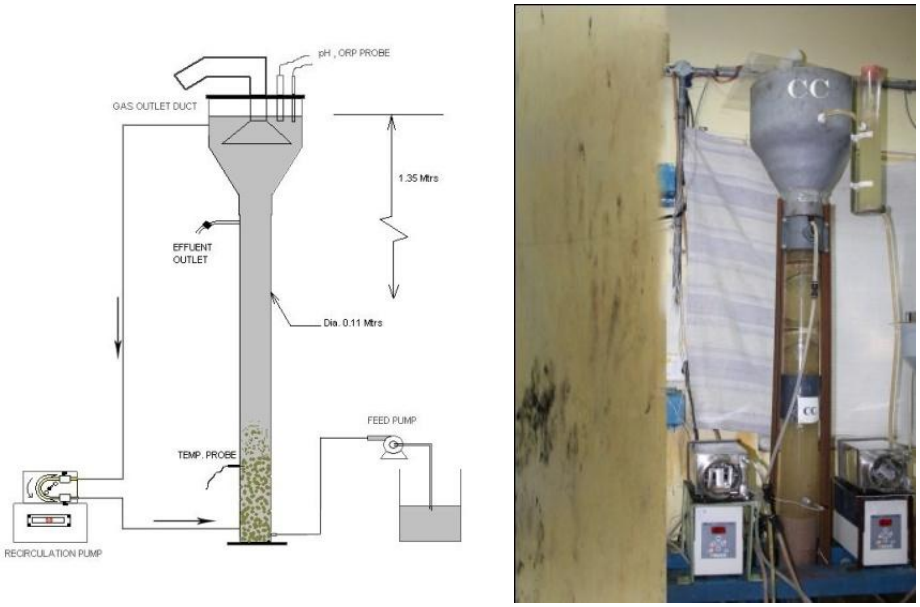

Fig. 3.4 Schematic and digital image of 24 L volume reactor operated in SBR mode

3.2 Inoculum for denitrification studies

The inoculum was collected from the outlet of aeration tank of an operating domestic-wastewater treatment plant at Kalpakkam, India, where no denitrification was carried out. The wastewater treatment plant at Kalpakkam uses an activated sludge processes for biological treatment of sewage. The activated sludge was black in color and consisted for flocculent sludge. After collection, the activated sludge was washed a few times with deionized water, filtered and stored at 4 °C in a refrigerator until further use.

3.3 Composition of simulated nitrate waste

Simulated nitrate waste (SNW) was prepared in deionized water based on typical nitrate bearing effluents of nuclear industry. Sodium acetate was chosen as the electron donor for denitrification studies. The SNW contained the following (in g L^{-1}): sodium acetate 10, sodium nitrate 5, $MgSO_4.7H_2O$ 0.08, KCl 0.035, K_2HPO4 0.06, KH_2PO_4 0.028, pH 7.43 and trace elements 0.1 mL L^{-1}. The pH of the SNW was observed to be ~7.4. The acetate - carbon to nitrate-nitrogen mass ratio was

maintained by varying sodium acetate and sodium nitrate quantities and keeping other components of the medium constant.

3.4 Operation of bioreactors for denitrification

3.4.1 Operation of SBRs

The reactor was operated in sequencing batch mode with a cycle time of 24 h. The cycle period consisted of 5 min filling, 23 hour reaction, 5 min settling, 10 min effluent decant period and 40 min of idling. Mixing was provided by means of an impeller stirred at 50 rpm. Each reactor was inoculated with 1 L of activated sludge and SNW. The reactors were either filled at the bottom using a peristaltic pump or dump filled by manual addition. At the end of cycle period, effluent was drawn from a port situated at a height of 17 cm from the bottom using a peristaltic pump. Typically, the SBRs were operated with 24 h cycle period and 50% volume exchange ratio (VER) for convenience.

3.4.2 Operation of CSTR

The reactor was inoculated with 1 L of activated sludge and operated in CSTR mode. The rector was fed with SNW at a feed rate of 400 mL h^{-1} from bottom of the reactor using a peristaltic pump. A hydraulic retention time of 15 h was maintained throughout the experimental period. The reactor was mixed at 100 rpm to maintain homogeneity and to avoid damage to the granules. The effluent was removed from the effluent port, which is located at 6 L position, ensuring a hold up of 6 L liquid in the reactor at any time.

3.4.3 Operation of EGSBR

The EGSBR was inoculated with 1 L of activated sludge and operated in SBR mode during initial start-up. After establishing denitrification and cultivating biomass with good settling abilities, the reactor was turned to continuous mode. Feeding at the bottom and removal of treated effluent from the top of the reactor was carried out

using peristaltic pumps. The reactor was operated with a hydraulic retention time of 16 h. Mixing was provided via recirculation, the treated liquid was collected from a port at the top of reactor and pumped to the reactor at the bottom. Recirculation velocity of 3 m h^{-1} was used. The reactor was fed with a feed containing 3 g L^{-1} nitrate at a fixed C/N ratio of 1.5.

3.5 Experiments

3.5.1 Denitrification at different C/N ratios

Three 6 L SBRs (RA, RB and RC) were inoculated with 1 L activated sludge (MLSS 2.5 g L^{-1}) and fed with SNW containing sodium nitrate and sodium acetate at C/N ratios of 1.5, 2 and 3 as given in the Table 3.1. The reactors were inoculated with 1 L activated sludge and fed with SNW containing an initial nitrate concentration of 3 g L^{-1} and initial pH 7. The SBRs were operated at room temperature (~30 °C) with 50 % VER in SBR mode with 24 h cycle period. Effluent was drawn from a port situated at 34 cm height from the bottom of the SBR.

Table 3.1 Constituents for SNW with different C/N ratios and with different initial nitrate concentrations

Constituants	NO_3 in reactor (mg L^{-1})			
	3000	**6000**	**9000**	**12000**
$NaNO_3$ (g L^{-1})	4.11	8.23	12.34	16.45
CH_3COONa (g L^{-1}) (1.5)*	2.79	5.59	8.38	11.18
CH_3COONa (g L^{-1}) (2)*	3.73	7.45	11.18	14.90
CH_3COONa (g L^{-1}) (3)*	5.59	11.18	16.77	22.35

*Sodium acetate was added to give a C/N mass ratio of 1.5, 2 and 3 i.e. 3, 2, 1.5 g of carbon for every g of nitrogen.

Fig. 3.5 Digital image of 6 L volume reactors operated in SBR mode for denitrification at different C/N ratios.

All the reactors were equipped with DO, pH and RTD probes for online monitoring of dissolved oxygen, pH and temperature profiles during cycle period. Liquid samples were collected periodically for monitoring denitrifying (nitrate, nitrite) profiles. Biomass samples were collected to determine MLSS.

3.5.2 Denitrification at different initial pH

In order to determine the optimum pH for denitrification, batch experiments were carried out in 125 mL (working volume = 100 mL) serum bottles. SNW containing different pH (4,5,6,7,8, and 9) was used in denitrification experiments. The SNW and serum bottles were autoclaved separately. Aliquots of 100 mL media were dispensed

into 125 mL serum bottles containing 4 g (wet weight) of acetate-fed anoxic granular biomass (equivalent to 0.094±0.002 g dry biomass). The serum bottles were sealed with butyl rubber stoppers, and purged with ultra high purity nitrogen gas for 10 min. The serum bottles were incubated at 30 °C on an orbital shaker set at 100 rpm. At periodic time intervals, 4 ml of media was removed and pH, nitrate and nitrite were analyzed. The pH of the SNW media was varied from 4 to 9. The pH was adjusted using 0.1 N HCl or NaOH. All the experiments were performed in duplicate. Liquid samples were collected at regular time intervals for monitoring pH, nitrate and nitrite.

3.5.3 Denitrification in CSTR

A 6 L CSTR (ID 0.15 m and 0.6 m H) was inoculated with 1 L of activated sludge. SNW with 3 g L^{-1} of nitrate and acetate-C to nitrate-N ratio of 2:1, at 400 mL h^{-1} was added. Stirring was provided by means of impeller set at 100 rpm. At each concentration, the reactor was operated in batch mode for 5 days to acclimatize biomass to higher concentrations and subsequently for two weeks in CSTR mode to ensure complete denitrification. Effluent samples were collected for monitoring nitrate, nitrite, pH, total organic carbon and biomass concentration.

a) Denitrification at C/N ratio of 2

In CSTR, the influent nitrate was increased in steps to 3, 6, 9, and 12 g L^{-1}. After achieving complete and stable denitrification, the influent nitrate concentration was increased to the next level.

b) Denitrification at C/N ratio of 1.5

A CSTR containing denitrifying consortium treating 12 g L^{-1} nitrate at a C/N ratio of 2 was fed with SNW with a C/N ratio of 1.5. The CSTR was operated to determine denitrification efficiency.

3.5.4 Denitrification of acidic nitrate effluents

Denitrification efficiency of acidic effluents was studied by operating two numbers of 3 L volume SBRs. The reactors were made of 3 mm thick acrylic tubes. The total height of the reactor was 0.855 m, consisting of 0.735 m long expander of 5.4 cm ID and enlarged portion of 0.160 m ID. The reactors were operated with 50 % VER with a 24 h cycle. Mixing was provided via recirculation of media from top to bottom using a peristaltic pump set at a liquid up flow velocity (V_{up}) of 3 m h^{-1}. It was reported that at the V_{up} of 3 m h^{-1} nitrite nitrogen concentration in the effluent reached below 0.1 mg L^{-1} and average MLSS and MLVSS reached maximum of 58.84 g L^{-1} and 38.23 g L^{-1} [14]. The reactors were inoculated with activated sludge and operated for 2 weeks with the same SNW (pH 7.5) for cultivation of denitrifying granular biomass. Subsequently, SNW with pH of 5 was added to one reactor (BR-1). After achieving complete and stable denitrification, the pH of the SNW feed was adjusted to 4.0. The other parallel SBR (BR-2) was fed with SNW with a pH of 7.5 throughout experiment. The pH of the SNW was adjusted using concentrated HCl. The reactors were operated for 75 days. The reactors were equipped with online monitoring of DO, pH and temperature. Liquid samples were collected during cycle time and analyzed for nitrate and nitrite. The effluent samples were analyzed for TOC and alkalinity.

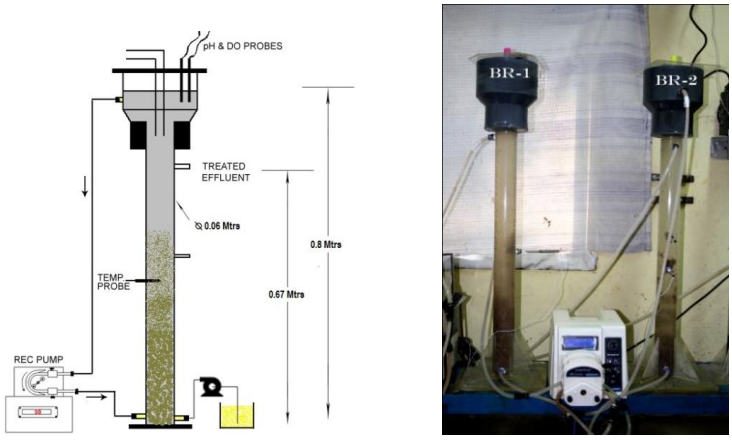

Fig. 3.6 Schematic and digital image of 3 L volume reactor operated in SBR mode for denitrification of acidic effluents.

3.5.5 Denitrification at different temperatures

Experiments were carried out to determine the effect of the temperature on denitrification rate. The experiments were carried out in a jacketed glass tank. The temperature in the reactor was maintained by passing hot/cold water through the jacket using NESLAB endocal refrigerated circulation bath (range: -30 ^{o}C to +100 ^{o}C and accuracy of ±0.01 ^{o}C). The reactor was cylindrical in shape, made of glass and had 750 mL volume. The reactor was operated with a working volume of 500 mL and a magnetic stirrer set at 100 rpm was used for mixing. The reactor was fitted with rubber cork for inserting a temperature probe and one outlet for escape of gases generated during denitrification. The reactor was seeded with denitrifying granular biomass. The reactor was fed with SNW with 6 g L^{-1} at a C/N ratio of 1.5. The pH of the SNW was not adjusted and found to be 7.5. The reactor was operated at different temperatures as described in Table 3.2. The solution temperature in the reactor was monitored online using RTD probe and recorded in the Eurotherm 12 channel paperless recorder. Liquid samples were collected at regular time interview during cycle period for nitrate and nitrite.

Table 3.2 Experimentation strategy used for denitrification studies of 3 g L^{-1} nitrate at different temperatures.

Set	Temperature	Nitrate Conc.	No. of Cycles
1	20 ± 0.5 ^{o}C	3000 mg L^{-1}	5
2	25 ± 0.5 ^{o}C	3000 mg L^{-1}	5
3	30 ± 0.5 ^{o}C	3000 mg L^{-1}	5
4	35 ± 0.5 ^{o}C	3000 mg L^{-1}	5
5	40 ± 0.5 ^{o}C	3000 mg L^{-1}	5

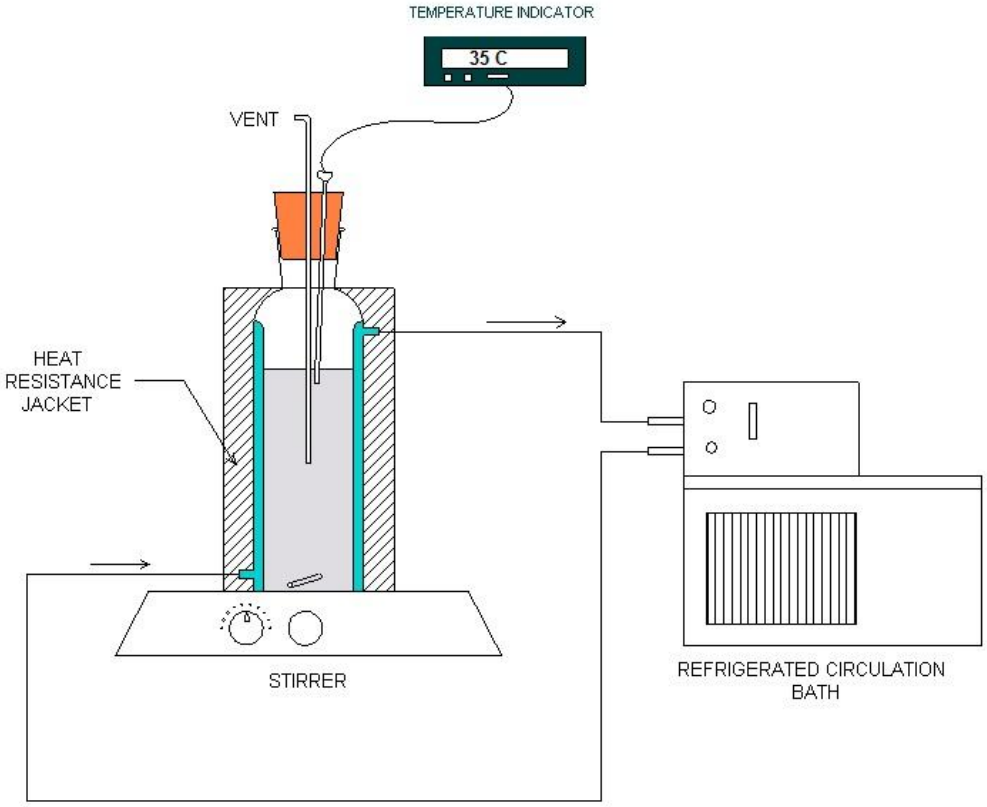

Fig. 3.7 Schematic 0.5 L volume reactor operated in SBR mode for denitrification at different temperatures

3.6 Microscopy of biomass

3.6.1 Optical Microscopy

Morphology of the microbial granules was documented with an Olympus DP70 camera connected to a SMZ1000 stereo zoom microscope (Nikon, Japan). Particle size and circularity of the aerobic microbial granules were determined by using the freeware *ImageJ* v1.43 as described by Nancharaiah et al. [137]. Microstructure of microbial granules was determined by confocal laser scanning microscopy (CLSM) and scanning electron microscopy (SEM). For CLSM imaging, the microbial granules were stained with LIVE/DEAD® *Bac*Light™ bacterial viability kit (Molecular Probes, USA) according to the manufacturer's instructions. A 200 µL of *Bac*Light™ stain mixture was transferred to 1.5 mL Eppendorf tube containing a few microbial granules and incubated on an orbital shaker set at 100 rpm. After 15 min of

incubation, the microbial granules were washed twice with ultrapure water. Stained granules were placed directly on top of a glass cover-slip and imaged using a confocal laser scanning microscope TCS SP2 AOBS (Leica Microsystems, Germany) equipped with an inverted microscope (Leica DMIRE2). A 63x 1.2 NA water immersion objective lens was used for imaging. Argon laser (488 nm line) was used for excitation and emission was collected between 500 and 520 nm for SYTO 9 and between 600 and 680 nm for propidium iodide.

3.6.2 Scanning electron microscopy (SEM) of denitrifying granular biomass

Denitrifying granular biomass was collected from different reactors for observing microstructure. For SEM imaging, the denitrifying granular biomass was fixed overnight with 2.5% glutaraldehyde in phosphate buffered saline. The fixed denitrifying granules were subjected to dehydration for 3 min each in a graded ethanol series (50%, 70%, 90% and 100%). The dehydrated denitrifying granules were sputter-coated with gold-palladium and imaged using a scanning electron microscope (Philips XL30 ESEM).

3.7 Analytical measurements

3.7.1 Nitrate, nitrite, acetate (HPLC/IC)

The samples collected at periodic time intervals were centrifuged at 12000 rpm for five minutes and filtered through a 0.45 μm Millex filter, and nitrate and nitrite in the filtrate were analyzed by high pressure liquid chromatography (Dionex Ultimate 3000) fitted with Acclaim OA column. The mobile phase was 0.003 N H_2SO_4 at a flow rate of 0.7 mL min^{-1}. Nitrate was determined using a UV-Vis detector set at 210 nm.

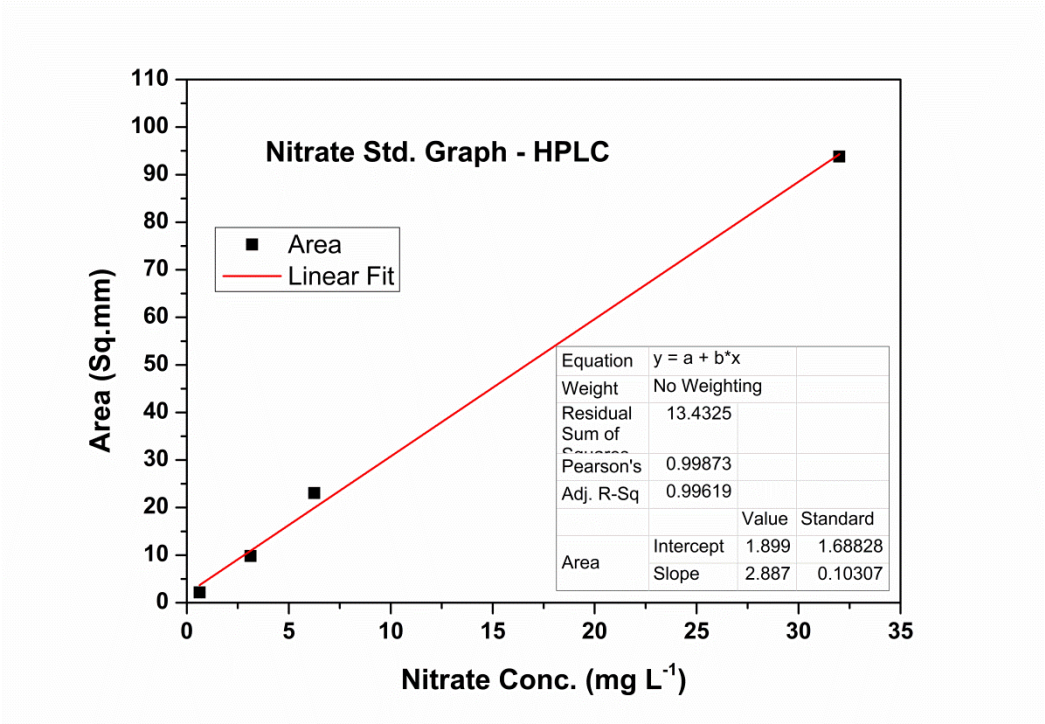

Fig. 3.8 Calibration curve for determination of nitrate using HPLC with UV detector at 210 nm.

Measurement of acetate nitrite and nitrate was carried out using Dionex ion chromatograph, ICS – 2100, USA having a 25 µL sample loop. The ions were analyzed using 25 mM KOH eluant with a flow rate 1 mL min^{-1}, Ion pac AS 18 (4 mm x 250 mm) analytical column, IonPac AG18 guard column (4 mm x 50 mm), Anion Self-Regenerating Suppressor (ASRS -300), suppressed conductivity detector, and a Dionex AS-DV automated sampler. A suppressor current of 67 mA was applied to the auto suppressor. Remote operation of the instrument and data analysis was carried out using commercial software (Chromeleon Version: 7). Under these conditions the retention times for acetate, nitrite and nitrate were 3.28, 5.257 and 8.457 min, respectively.

3.7.2 UV-Vis spec for nitrite

Nitrite was also determined by NED (Napthylene diamine dihydrochloride) method [138] using spectrophotometer by measuring absorbance at 540 nm. Reagent A: 1%

(w/v) sulfanilic acid in 1M HCl. Reagent B: 0.1% (w/V) Napthylene diamine dihydrochloride (NED).

3.7.3 Biomass analysis

Mixed liquor suspended solids (MLSS) and Mixed liquor volatile suspended solids (MLVSS) were measured according to standard methods [138]. Whatman glass microfibre filter (GF/C) 47 mm in diameter, was used for carrying out the MLSS and MLVSS analyses.

3.7.4 pH, DO and ORP measurements

The pH and DO in the reactors were measured online using HACH Probes. The data were logged into the HACH HQ40D PORTABLE METER. The pH probe (Intellical Probe pH probe, Model PHC10101), is a gel-filled probe with double junction reference with built-in temperature sensor. The probe has resolution of 0.01 pH units, with operating temperature range of 0 – 50 ^{o}C and in built Ag/AgCl is used as reference electrode. The pH probe was calibrated with standard buffers of pH 4.01, 7.00 and 10.00 buffers. The slope was found to be within 90 to 110 % of -59 mV/pH unit. The DO probe (Intellical LDO Probe Model LDO10101), is a luminescent based dissolved oxygen (LDO) probe with a range of 0.1 to 20.0 mg L^{-1} and with accuracy of ±0.1 mg L^{-1} for 0 to 8 mg L^{-1}. The probe has resolution of 0.01 mg L^{-1} with operating temperature range of 0-50 ^{o}C. The dissolved oxygen probe was calibrated against water saturated air at 25 ^{o}C. A redox probe was made by attaching a platinum gauze to a Saturated calomel reference electrode. The potential difference between the reference and platinum gauze in the test solution was measured and reported as redox potential using a high impedance voltmeter. The ORP probes were calibrated using pH 4 and pH 7 buffer in saturated Quinhydrone.

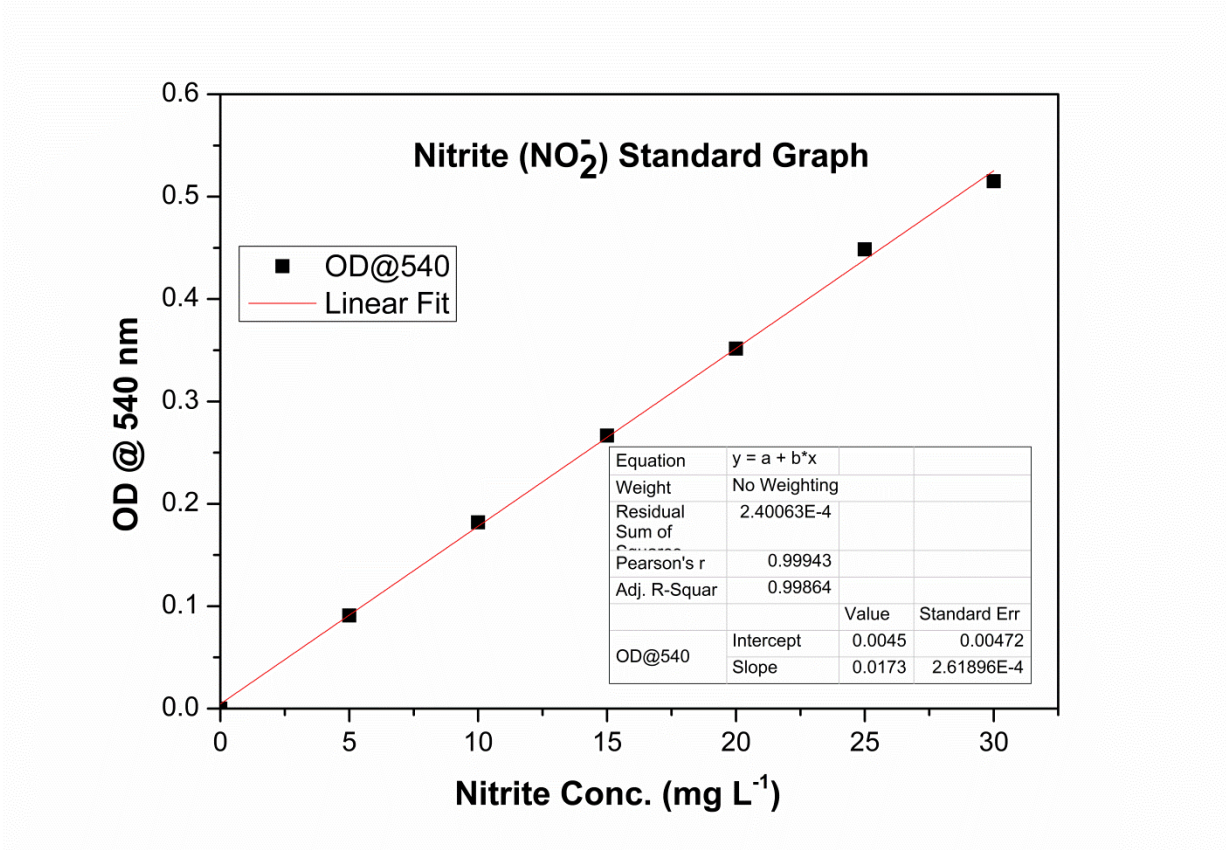

Fig. 3.9 Calibration curve for determination of nitrite using UV-Vis spectrophotometer.

3.7.5 Total Organic Carbon Analysis

Organic carbon is a major constituent in water and wastewater and is composed of a variety of organic compounds. There are several methods for measurement of TOC like a) High temperature combustion method, b) Persulfate ultraviolet or heated Persulfate oxidation method and c) Wet oxidation method. In the present study high temperature combustion method was used for estimation of total dissolved organic carbon in water using a TOC analyser (Shimadzu Model TOC V series). The sample is injected into a heated reaction chamber packed with an oxidative catalyst (Platinum). The aqueous sample is vaporized and the organic carbon is oxidized to carbon dioxide (CO_2) and water (H_2O). The carbon dioxide (CO_2) from produced from the oxidation of organic and inorganic carbon is transported by a carrier gas in the stream phase and is measured by means of non-dispersive infrared analyzer. The

instrument measures both total carbon and inorganic carbon (after acidification) and the total organic carbon is calculated by subtracting the inorganic carbon from total carbon. Minimum detectable concentration of TOC is 10 µg C L^{-1}.

3.7.6 Genomic DNA Isolation and Bacterial Phylogeny

For microbial population analysis, total DNA was extracted from 0.5 g biomass taken from reactors, using QIAGEN DNA extraction kit (Germany) as per the manufactures instructions. The V3 region of the bacterial 16S rRNA gene was PCR-amplified using the primers PRBA338f (5'CGC CCG CCG CGC GCG GCG GGC GGG GCG GGG GCA CGG GGG GACT CCT ACG GGA GGC AGC AG3') containing 40 bp of GC clamp and PRUN518r (5' ATT ACC GCG GCT GCT GG 3') in a thermocycler (Eppendorf AG, Germany). The following were used: 50 µL reaction mixture containing 0.5 U of Taq polymerase (Promega), 5 µL of 10× reaction buffer, 1 µL of each deoxynucleotide triphosphate (dNTP), 1.25 µL of each primer, and 1 µL of DNA template (20 µg μL^{-1}). An initial denaturation was carried out at 94°C for 2 min, followed by 30 cycles of 94 °C for 1 min, 55°C for 1 min and 72 °C for 1 min and a final extension of 72 °C for 2 min. The size of amplified DNA was confirmed by electrophoresis (Life Technologies HORIZON 11.14) on 0.8% agarose gel with 1× Tris-acetate-EDTA (TAE) buffer using GeneRuler DNA Ladder mix (#SM0331, Fermentas LifeScience) prior to denaturing gradient gel electrophoresis (DGGE) analysis .

DGGE was performed using INGENY phor U-2. The PCR products were loaded onto vertical polyacrylamide gel [acrylamide solution (40% acrylamide and bisacrylamide in 37.5:1 ratio)] 8% (w/v) with urea-formamide as denaturant ranging from 30% to 80% in 0.5×TAE buffer [40 mM Tris base, 20 mM acetic acid, 1 mM EDTA, pH 8.0] , 100 µL of ammonium persulphate (10%) and 5 µL of N,N,N',N'-tetramethylethylenediamine.

The denaturant gradient gel was covered by a 6 mL of acrylamide stacking gel (8%) without denaturant. Electrophoresis was run overnight at a voltage of 90 V and a temperature of 60°C. The electrophoretogram was then incubated for 15 min in 0.5×TAE buffer containing ethidium bromide (0.5 mg L^{-1}) and observed with a UV transilluminator (Vilber Lourmat, France) and photographed using INFINITY gel documentation system. Dendrogram was generated using SPSS 20 statistics software (IBM) according to jaccards coefficient.

For the denitrification experiments carried out at very high nitrate concentrations, the biomass samples were taken at nitrate loading conditions (3000 mg L^{-1}, 6000 mg L^{-1}, 9000 mg L^{-1}, 12000 mg L^{-1},15000 mg L^{-1}) from the reactor at the end of cycle. DNA was extracted from biomass using QIAGEN DNA extraction kit (Germany) as per the manufactures instructions. 16S rRNA primers were used to amplify V3 region followed by denaturing gradient gel electrophoresis (DGGE) analysis as explained earlier. Dendrogram was generated using SPSS 20 statistics software (IBM) according to jaccards coefficient.

For the denitrification experiments carried out at different temperatures, the biomass samples were taken at different temperature operating conditions from the reactor at the end of cycle. DNA was extracted from biomass using QIAGEN DNA extraction kit (Germany) as per the manufactures instructions. 16S rRNA primers were used to amplify V3 region followed by denaturing gradient gel electrophoresis (DGGE) analysis as explained earlier. Dendrogram was generated using SPSS 20 statistics software (IBM) according to jaccards coefficient.

For the denitrification experiments carried out at different C/N ratios, the biomass samples were taken at different concentrations from the reactor at the end of cycle. DNA was extracted from biomass using QIAGEN DNA extraction kit (Germany) as per

the manufactures instructions. 16S rRNA primers were used to amplify V3 region followed by denaturing gradient gel electrophoresis (DGGE) analysis as explained earlier. Dendrogram was generated using SPSS 20 statistics software (IBM) according to jaccards coefficient.

3.8 Methodology to determine the rate kinetics of denitrification reactions

3.8.1 Introduction

Kinetics of biodenitrification reaction is a complex one. It involves the decomposition of complex nitrate in the waste into simple nitrite compounds and its derivatives such as nitrogen di oxide, nitrous oxide and etc., then into elemental nitrogen gas. The degradation of the nitrate group in the reactor will take place in series as well as in the parallel reaction. Nitrate is being converted into nitrogen through the intermediate product is nitrite group by series chemical reaction and few quantity is directly converted into nitrogen. This reaction is taking place in the presence of specific nitrogen bearing bacteria in the reactor which is available in the waste. Hence, it is called as bio-denitrification. So, cultured bacterial loaded waste is called as biomass. Biomass growth is increases in the reactor as long as bio-denitrification happening in the reactor. The biodegradation of nitrate in the bioreactor is mainly depends on the concentration of nitrate in waste, biomass concentration, oxygen level in the fluid medium and initial temperature & ambient temperature condition. Understanding the rate kinetics of bio-denitrification in the presence of biomass is essential for bioengineering for scaling up the process in the industrial scale.

3.8.2 Determination of rate law for bio-denitrification reaction for various C/N ratios

The concentrations profiles from the experiments were used to determine the kinetics of bio-denitrification. The reaction rate of bio-denitrification is mainly depending on

the quantity of electron donor present in the waste. The kinetics study have been carried out in the lab scale with simulated waste.

Nitrate in the feed is being converting into nitrite and then into elemental nitrogen gas. This is ensured by the generation of the nitrogen gas during the denitrification reaction and it is escaped from the reactor as bubbles and similarly, acetate in the reactor is converted into carbon-di-oxide gas.

Decomposition to nitrate, nitrite and acetate is written as

$$NO_3 \rightarrow NO_2 \rightarrow N_2 \quad (3.1)$$

$$NO_3 \rightarrow N_2 \quad (3.2)$$

and

$$CH_3COONa \rightarrow CO_2 + H_2O + NaOH \quad (3.3)$$

and its rate is written as

$$-r_A = K_{NO_3} C_{NO_3}^n C_X^m \quad (3.4)$$

Where m and n are the order of the reaction

$C_{NO_3} - - > Concentration\ of\ Nitrate$

$C_x - - > Concentration\ of\ Bio - mass$

$$\text{Differential rate of reaction for Nitrate reduction} = \frac{-dC_{NO_3}}{dt} = \left[K_{NO_3} C_{NO_3}^n C_X^m \right] \quad (3.5)$$

Since, the rate of decomposition of nitrate is faster than the rate of growth of biomass hence, for determining the denitrification rate, the reaction rate depends on the biomass (C_X^m) is neglected. But, the denitrification rate depends on the biomass presence in the reactor, so, the specific denitrification rate was calculated for fixed C/N ratio. This is estimated by dividing the reaction rate of nitrate and nitrite with total biomass measured at the end of the experiment. The above differential rate equation for denitrification reaction is reduced into the following equation

Rate of nitrate decomposition is written as:-

$$\left[\begin{array}{c}\text{Differential rate}\\ \text{of reaction for Nitrate reduction}\end{array}\right] \frac{-dC_{NO_3}}{dt} = \left[K_{NO_3} C_{NO_3}^{n}\right] \quad 3.6$$

similarly,

Rate expression for nitrite decomposition in the absence of nitrate is written as

$$\left\{\begin{array}{c}\text{Rate of decomposition}\\ \text{of nitrite in the absence of nitrate}\end{array}\right\} \frac{dC_{NO_2}}{dt} = -K_{NO_2} C_{NO_2}^{n} \quad 3.7$$

Rate expression for nitrite decomposition in the presence of nitrate:-

$$\left\{\begin{array}{c}\text{Rate of decomposition of}\\ \text{nitrite in the presence of nitrate}\end{array}\right\} \frac{dC_{NO_2}}{dt} = K_{NO_3} C_{NO_3}^{n} - K'_{NO_2} C_{NO_2}^{n} \quad 3.8$$

From the experimental analysis, concentration of nitrate and nitrite were plotted w.r.t. time for fixed C/N ratio. This procedure is followed for various initial nitrate concentrations in SBR. The mean value of each concentration for every time step is plotted against the time. The slope of the concentration curve gives the overall rate of the bio-denitrification for the given C/N ratio. The graphical method of determining the reaction rate is shown in the Fig. 3.10 and it is written as

$$\left\{\begin{array}{c}\text{Rate of}\\ \text{decomposition of nitrite}\end{array}\right\} = \{-r'_{NO2}\} = \left\{\frac{\Delta C_{NO_2}}{\Delta t}\right\} \quad 3.9$$

$$= \left\{\frac{-\text{ change in concentration}}{\text{Time}}\right\} \frac{\text{mg}}{\text{L}-\text{h}} \quad 3.10$$

The negative sign indicating that the concentration of reactant decreases with time.

3.8.3 Determination of Rate constant for specific denitrification reaction:

The rate constants for biodenitrification reaction are estimated by plotting the reaction rate vs concentration of reactant for every time step. The general rate expression for the above equation is plotted against concentration for each nitrate and nitrite group. The linear equation is arrived by taking the log scale on both side of the expression and its parameters are plotted with log concentration on X-axis and Log rate on Y-axis.

$$\ln(-r_A) = \ln K_{NO_3} + n \ln C_{NO_3} \quad 3.11$$

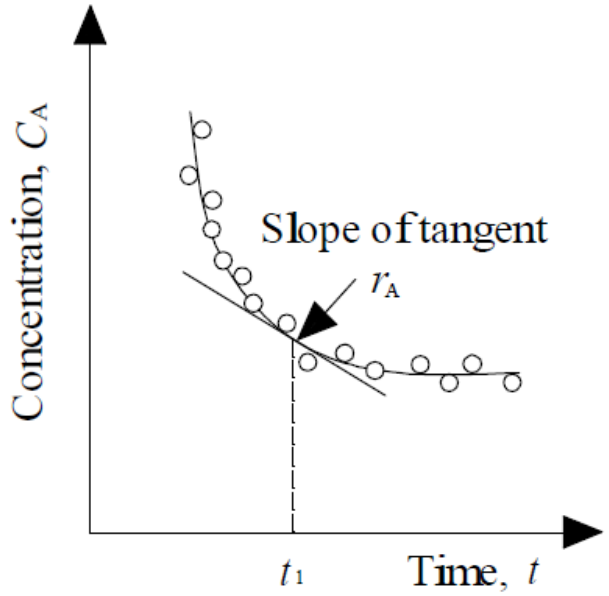

Fig. 3.10 Concentration of nitrate, nitrite w.r.t.time

Order is calculated from the slope of the plot and its rate constant is determined from the Y-intercept. The resultant specific denitrification rate was determined by taking into the accounting of biomass measured during the denitrification reaction (mg NO_3-N L^{-1} h^{-1} g X^{-1}).

From graphical result, it was found that order of the reaction for biodenitrification is zero order hence, its rate is independent of the initial concentration of the reactant. It is useful for designing the bioreactor for higher initial nitrate waste. The mathematical expression for the above said method is explained in the following procedure.

The rate is generally expressed as

$$\text{Differential rate of reaction for Nitrate reduction} \Big] \quad \frac{-dC_{NO_3}}{dt} = \left[K_{NO_3} C_{NO_3}^{n} \right] \quad 3.12$$

$$-dC_{NO_3} = \left[K_{NO_3} C_{NO_3}^{n} \right] dt \quad 3.13$$

Rearranging the equation,

$$\left[\frac{-dC_{NO_3}}{C_{NO_3}^n} = K_{NO_3} \; dt \right] \tag{3.14}$$

on integrating the above equation, we get

$$\int_{C0}^{C} \frac{-dC_{NO_3}}{C_{NO_3}^n} = K_{NO_3} \int_0^t dt \tag{3.15}$$

From the graph, it was observed that, the order of the reaction is ZERO hence,

$$\int_{C0}^{C} \frac{-dC_{NO_3}}{C_{NO_3}^0} = K_{NO_3} \int_0^t dt \tag{3.16}$$

$$\int_{c0}^{c} -dC_{NO_3} = K_{NO_3} \int_0^t dt \tag{3.17}$$

The concentration profile of bio-denitrification at any time is

$$C_{NO_3} = C_{NO_{3,0}} - K_{NO_3} t \tag{3.18}$$

Similarly, Nitrite decomposition takes place both in the presence of nitrate and absence of nitrate. The rate of reaction of nitrite is represented by the following equations.

$$\left\{ \begin{matrix} \text{Rate of decomposition} \\ \text{of nitrite in the absence of nitrate} \end{matrix} \right\} \frac{dC_{NO_2}}{dt} = - K_{NO_2} \; C_{NO_2} \tag{3.19}$$

and

$$\left\{ \begin{matrix} \text{Rate of decomposition of} \\ \text{nitrite in the presence of nitrate} \end{matrix} \right\} \frac{dC_{NO_2}}{dt} = K_{NO_3} \, C_{NO_3} - K'_{NO_2} \; C_{NO_2} \tag{3.20}$$

The rate of conversion of denitrification reaction is dependent on the initial concentration of nitrate and temperature of the reacting species in the reactor. Rate of conversion increases as the biomass concentration in the reactor increases. The specific rate conversion was determined by accounting the biomass for the corresponding batch operation.

$$C_{NO_3} = \frac{\frac{C_0 \left(1 - X_{C_{NO_3}}\right)}{1 + \varepsilon X_{C_{NO_3}}}}{X} \tag{3.21}$$

For homogeneous and constant volume reactor system $\varepsilon = 0$

$$\text{The rate of conversion, } X_{C_{NO_3}} = \frac{\left\{\frac{C_0 - C_{NO_3,t}}{C_0}\right\}}{X} \qquad 3.22$$

4 RESULTS AND DISCUSSIONS

Experimental results from the study of denitrification in SBRs are presented in this chapter and are discussed. The results presented to discuss the effects of C/N ratios, sudden change in C/N ratio, initial pH, temperature and initial nitrate concentrations. Also the results from different reactor configurations, viz. CSTR and EGSBR are presented. Methodology developed for denitrification of high strength nitrates, based on acclimatization of the bacteria, is presented in details.

4.1 Denitrification at different C/N ratios

Experiments were carried out to study the effect C/N ratios on denitrification as described in section 3.5.1. The experiments were carried out in a column reactor operated in sequencing batch mode. Mixing was provided by means of an impeller stirred at 100 rpm. Typically, the SBRs were operated with 24 h cycle period and 50% volume exchange ratio (VER). The results are presented and discussed in the following section.

Table 4.1 Biomass (MLSS, MLVSS) concentrations in the SBRs operated at different C/N ratios and initial nitrate concentrations.
The biomass concentrations shown are obtained after attaining steady state in the SBRs in terms of minimum time for complete and stable denitrification.

Nitrate Conc. (mg L^{-1})	C/N = 1.5		C/N = 2		C/N = 3	
	MLSS (g L^{-1})	MLVSS (g L^{-1})	MLSS (g L^{-1})	MLVSS (g L^{-1})	MLSS (g L^{-1})	MLVSS (g L^{-1})
677	3.42	2.08	3.66	2.5	4.14	2.3
1355	6.34	3.89	9.4	5.56	10.94	6.2
2032	9.42	6.1	10.92	7.74	14.72	8.3
2710	11.24	7.34	12.82	10.32	17.04	11.54

4.1.1 Biomass characterization

Activated sludge used for inoculation typically consisted of flocs dominated by filamentous bacteria [105,139-140]. Within two weeks of reactor start-up, the activated sludge slowly evolved into compact and dense granular sludge under the prevailing anoxic conditions (Fig. 4.1A and B). Rod shaped cells enmeshed in an extracellular polymeric substances matrix were evident in scanning electron microscope images (Fig. 4.1C and D).

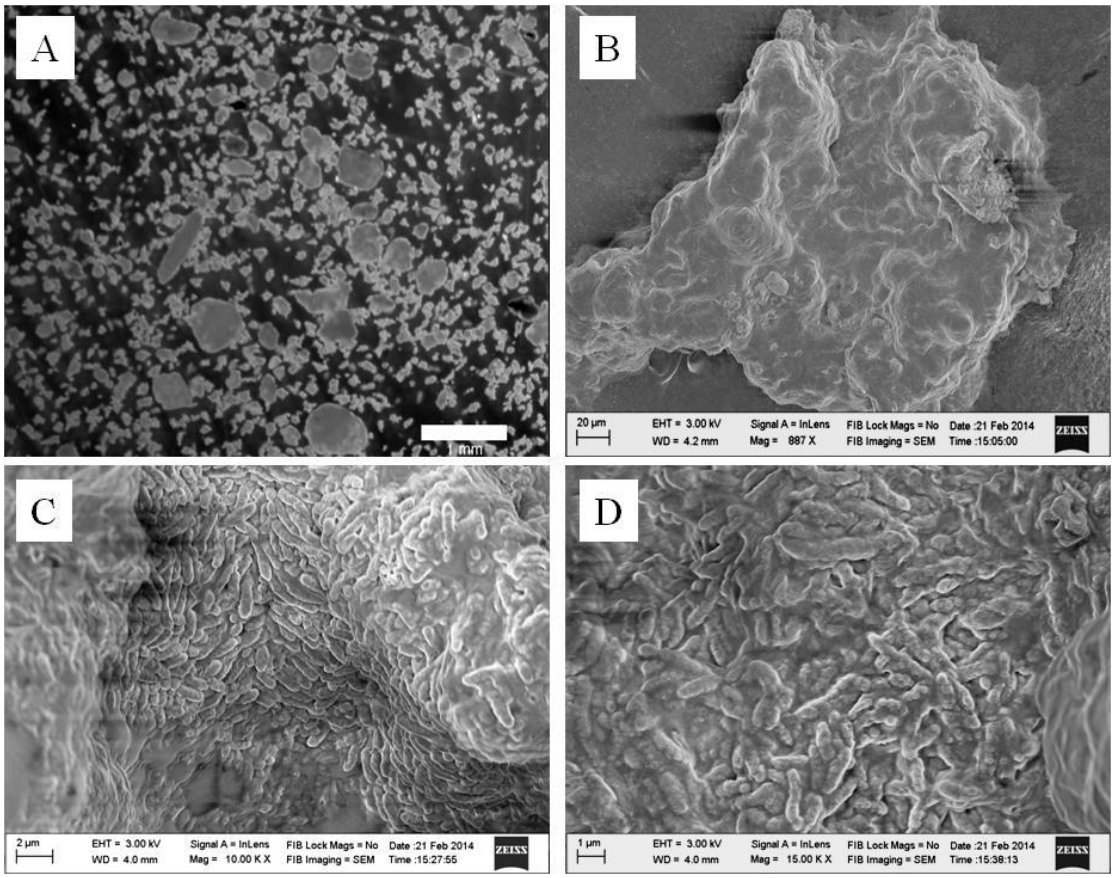

Fig. 4.1 Morphology (A, B) and microstructure (C, D) of denitrifying granular sludge formed in 6 L volume SBR.

For A, Bar = 1 mm. B, C and D are scanning electron microscope images of denitrifying granular sludge. Bar = 0.1 mm (B), 2 µm (C, D). Shape of microorganisms and their appearance on the surface of granular sludge is shown in C and D.

The SBRs were inoculated with 2.5 g L^{-1} of MLSS at startup. The MLSS and MLVSS levels observed at different reactor nitrate concentrations are given in Table 4.1. For

all C/N ratios (1.5, 2 and 3) studied, a steady increase in the biomass concentration was observed with reactor operation time in the SBRs. It was found that MLSS and MLVSS increased as the C/N ratio increased. High biomass growth at high C/N ratios indicates utilization of excess carbon in other metabolic reactions (i.e. aerobic metabolism).

Table 4.2 Nitrate and nitrite reduction times determined in SBRs operated at different C/N ratios and initial nitrate concentrations.
The given values are obtained after attaining steady state in terms of minimum time for complete and stable denitrification.

Nitrate (mg L^{-1})	Component	Time taken for complete reduction (h)		
		C/N = 1.5	C/N = 2	C/N = 3
3000	NO_3^-	1.00	1.00	1.25
	NO_2^-	1.25	1.25	1.75
6000	NO_3^-	2.50	2.50	3.00
	NO_2^-	3.00	3.00	3.50
9000	NO_3^-	5.00	4.50	6.50
	NO_2^-	6.00	5.50	6.50
12000	NO_3^-	6.50	7.00	7.80
	NO_2^-	7.50	8.00	8.00

4.1.2 Denitrification performance

In the SBRs, the pH increased from initial 7.5 to above 9 during the first cycle and stabilized close to 9.5 during subsequent cycles of denitrification [141]. The DO of feed decreased from 6 mg $L^{-1}$to below 0.08 mg L^{-1} within a few minutes of filling in the SBRs. The rapid decrease in DO was apparently caused by the intense microbial respiration. The DO present in the feed was consumed by the microbial activity during the short dump fill period. The alkaline pH (≥7.5) and the low DO (<0.08 mg L^{-1}) conditions favored denitrification without any lag phase in the SBRs.

These observations are in agreement with earlier studies on high strength denitrification in SBRs and MBRs [12,109142]. Moreover, denitrification was effective from the first cycle onwards, as evident from complete denitrification of 1355 mg $L^{-1}NO_3$-N by the end of 24 h cycle period. The NO_3^- concentration in the SBRs decreased to <10 mg L^{-1} by the end of the first cycle. During subsequent cycles, the time taken for complete denitrification decreased significantly due to adaptation and growth of denitrifying microorganisms. After a few cycles of reactor operation, steady state was reached in terms of minimum time needed for complete reduction of nitrate. The time taken for complete denitrification of different nitrate concentrations at three C/N ratios at steady state is given in Table 4.2.

The time taken for nitrate concentration to reach <10 mg L^{-1} from the initial concentration is taken as nitrate reduction time. For nitrite, cumulative time taken to reach maximum concentration and to reduce it to < 1 mg L^{-1} from the maximum concentration is taken as nitrite reduction time. Table 4.2 depicts the nitrate and nitrite reduction times for different C/N ratios, at different initial nitrate concentrations. Initially, SBR with activated sludge was acclimatized to 1355 mg $L^{-1}NO_3$-N for two weeks. The reduction times for nitrate and nitrite (1 h and 1.25 h) at 677 mg $L^{-1}NO_3$-N (in the reactor) were almost the same for C/N ratios of 1.5 and 2, whereas at C/N ratio of 3, nitrate was completely reduced in 1.25 h and nitrite in 1.75 h. In the second stage, the nitrate concentration in the reactor was increased from 677 mg L^{-1} to 1355 mg $L^{-1}NO_3$-N. The times taken for complete reduction of nitrate and nitrite at C/N ratios 1.5 and 2 were observed to be the same (2.5 h and 3 h) but lower than those observed at C/N ratio of 3 (3 h and 3.5 h). In the third stage, the nitrate concentration in the reactor was increased from 1355 mg L^{-1} to 2032 mg $L^{-1}NO_3$-N. The nitrate and nitrite reduction times for the C/N ratio of 1.5 were 5 h and 6 h, but

for C/N ratio 2 there was a decrease (4.5 h and 5.5 h), whereas for the C/N 3 the denitrification times increased (6.5 h and 6.5 h). In the final stage, the nitrate concentration in the reactor was increased from 2032 mg L^{-1} to 2710 mg $L^{-1}NO_3$-N. The nitrate and nitrite reduction times for the C/N ratio 1.5 were 6.5 h and 7.5 h, but for C/N ratio of 2, the times increased to 7 h and 8 h. For C/N ratio of 3 both nitrate and nitrite took 8 h for complete degradation. It clearly shows that degradation times increased with an increase in initial nitrate concentration as well as with increase in C/N ratios. Previous studies have also noted slightly lower denitrification rates at high C/N ratios in the treatment of low strength wastewaters, using acetate as carbon source [143]. Although the exact mechanisms are unknown, it was hypothesized that alternative pathways such as methanogenesis [143-144] and formation of suspended cells in biofilm reactors [145] would consume part of the electron donor. Surprisingly, this was not reported in the case of high strength nitrate wastes. The concentrations of acetate are exceptionally high in the case of high strength nitrate denitrification at higher C/N rations. High concentrations of acetate available at high C/N ratios under limited electron acceptor (i.e. NO_3^-) conditions somehow result in decreased denitrification performance; this requires further investigation.

Nitrate and nitrite profiles at different C/N ratios during denitrification have been shown in Fig. 4.2 to Fig. 4.5. Complete denitrification was observed for all the nitrate concentrations tested at all three C/N ratios. Steady decrease in nitrate concentration was observed for all initial nitrate concentrations at the three C/N ratios without any accumulation of nitrate. No lag phase was observed in nitrate removal profiles. Nitrate removal profiles were corroborated with the formation of nitrite in the reactors. Nitrite concentrations passed through a maximum for all the nitrate concentrations and all C/N ratios. The accumulated nitrite was subsequently reduced, leading to complete

denitrification. Effluent nitrite level of less than 1 mg L^{-1} was invariably achieved at the end of cycle time.

The peak nitrite concentration as a function of initial nitrate concentration is shown in Fig. 4.6. At C/N ratio of 1.5, peak nitrite concentration in the SBRs was found to increase from 402 (±64) mg L^{-1} at 677 mg $L^{-1}NO_3$-N to 2657 (±120) mg L^{-1} at 2710 mg $L^{-1}NO_3$-N, at C/N ratio 2.The peak nitrite concentration in the SBRs was found to increase from 416 (±64) mg L^{-1} at 677 mg L^{-1} of NO_3-N to 2694 (±71) mg L^{-1} at 2710 mg $L^{-1}NO_3$-N and at C/N ratio 3; the nitrite peak nitrite concentration in the SBRs was found to increase from 396 (±55) mg L^{-1} at 677 mg L^{-1} of NO_3-N to 2808 (±143) mg L^{-1} at 2710 mg $L^{-1}NO_3$-N. Thus, as expected, the peak nitrite concentrations increased with increase in nitrate concentrations from 677 mg $L^{-1}$to 2710 mg $L^{-1}NO_3$-N. The peak nitrite concentrations were found to increase across C/N ratios for a given nitrate concentration. It was reported that as C/N ratio increased, the nitrite accumulation would also increase [143]. In the present study, there is a decrease in denitrification performance in terms of increase in denitrification time and increase in nitrite built up as C/N ratios increased. The reason for this observation is not clearly understood and requires further investigation.

Organic carbon concentrations in the effluents were observed to increase with increase in nitrate concentrations in the feed.TOC concentrations were found to increase with increase in C/N ratio for a constant nitrate concentration (Table 4.3).

Table 4.3 Total organic carbon in the effluents of SBRs operated at different C/N ratios and initial nitrate concentrations.
The presented TOC values are obtained after attaining steady state in terms of minimum time for complete and stable denitrification in SBRs.

Initial nitrate concentration in the SBR (mg L^{-1})	Effluent TOC (mg L^{-1})		
	C/N = 1.5	C/N = 2	C/N = 3
3000	300	400	1200
6000	500	600	2500
9000	800	900	3600
12000	1000	2000	5800

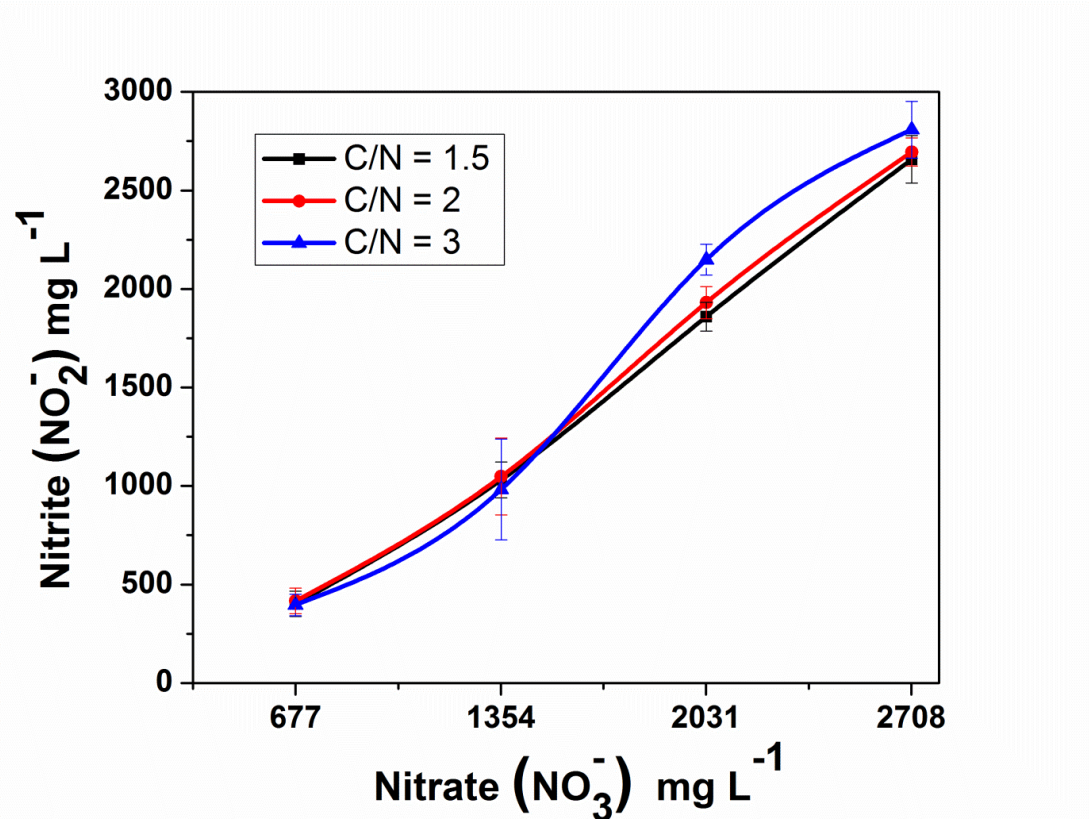

Fig. 4.2 Maximum nitrite accumulation observed for different C/N ratios during denitrification of different initial nitrate concentration.
The denitrification experiments were carried in a sequencing batch reactor at fixed C/N ratio of 1.5, 2 and 3. Error bars represent ± 1 SD.

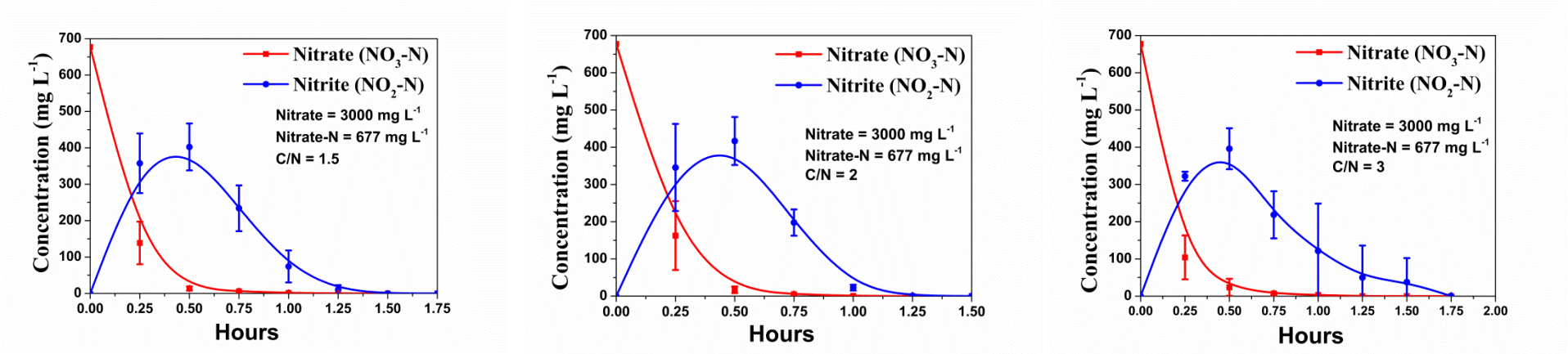

Fig. 4.3 Concentration profiles of nitrate and nitrite during denitrification of 677 mg L^{-1} NO_3-N at different C/N ratios

Three SBRs operated at different C/N ratios of 1.5, 2 and 3. The denitrification profiles presented are obtained after attaining steady state in the SBRs in terms of minimum time for complete and stable denitrification. The MLSS (MLVSS) values (g L^{-1}) were 3.4 (2.1), 3.7 (2.5) and 4.1 (2.3) for C/N ratios of 1.5, 2 and 3 respectively.

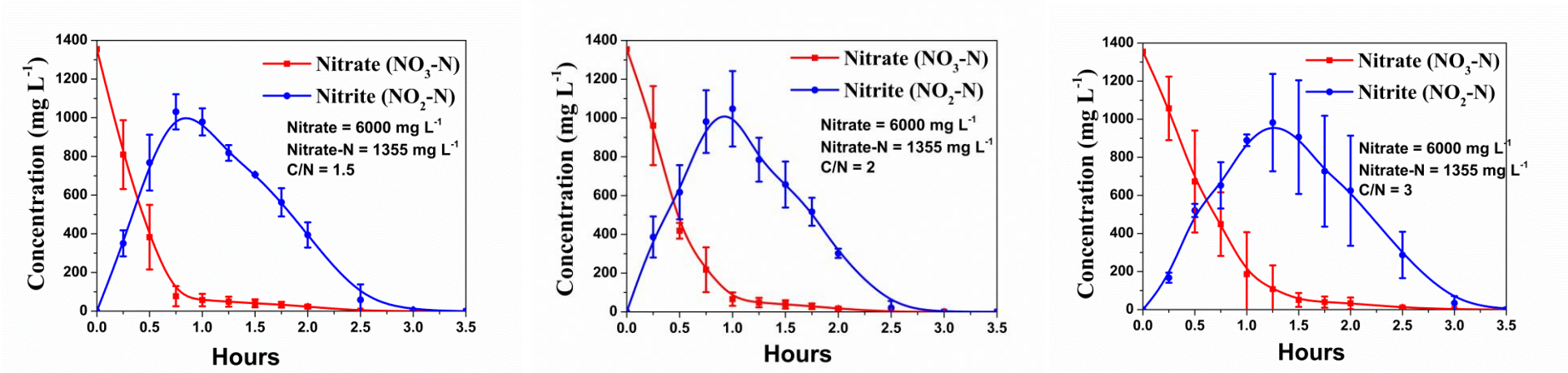

Fig. 4.4 Concentration profiles of nitrate and nitrite during denitrification of 1355 mg L^{-1} NO_3-N at different C/N ratios

Three SBRs operated at different C/N ratios of 1.5, 2 and 3. The denitrification profiles presented are obtained after attaining steady state in the SBRs in terms of minimum time for complete and stable denitrification. The MLSS (MLVSS) values (g L^{-1}) were 6.3 (3.9), 9.4 (5.6) and 10.9 (6.2) for C/N ratios of 1.5, 2 and 3 respectively.

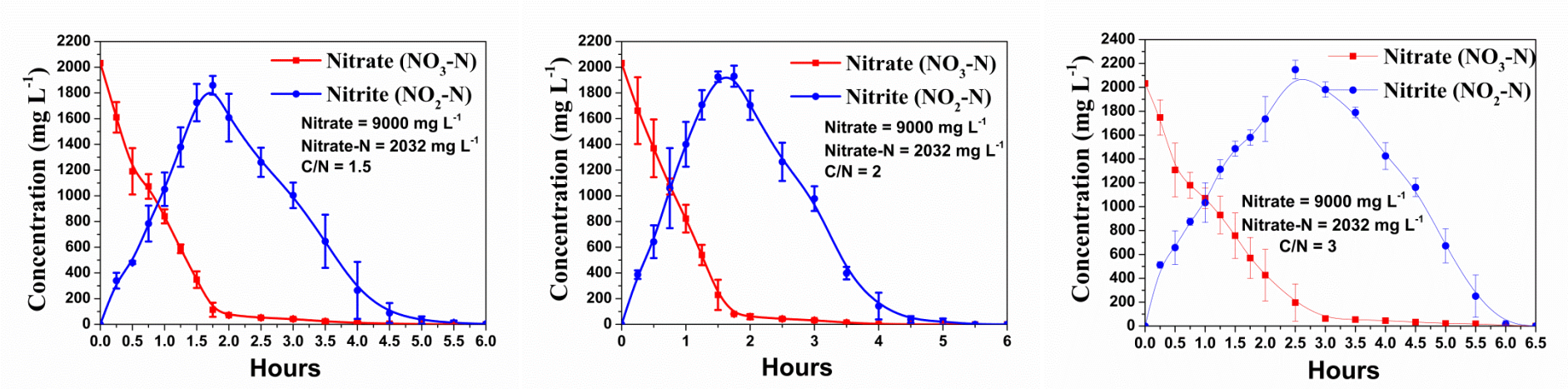

Fig. 4.5 Concentration profiles of nitrate and nitrite during denitrification of 2032 mg L^{-1} NO_3-N at different C/N ratios

Three SBRs operated at different C/N ratios of 1.5, 2 and 3. The denitrification profiles presented are obtained after attaining steady state in the SBRs in terms of minimum time for complete and stable denitrification. The MLSS (MLVSS) values (g L^{-1}) were 9.4 (6.1), 10.9 (7.7) and 14.7 (8.3) for C/N ratios of 1.5, 2 and 3 respectively.

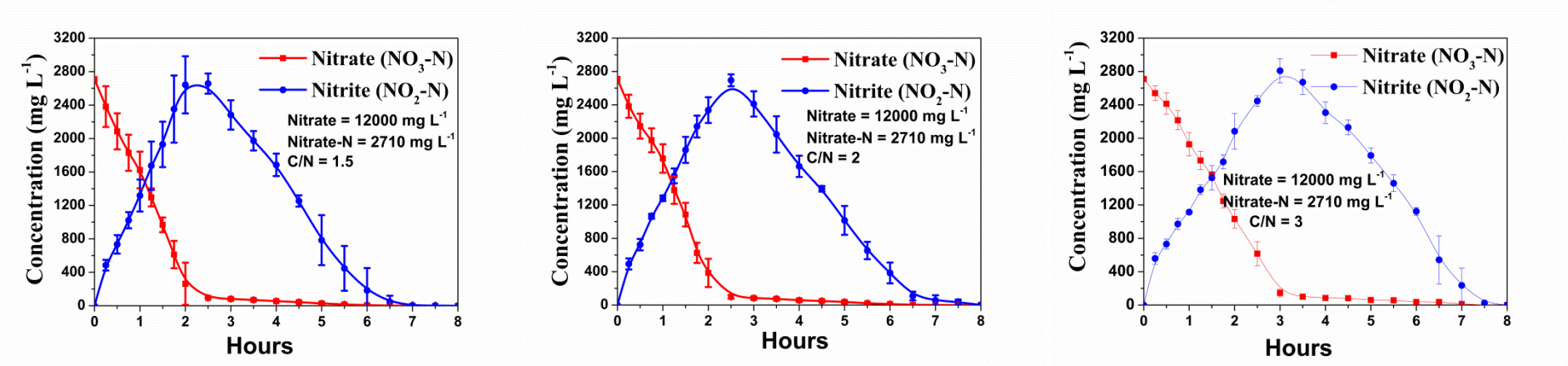

Fig. 4.6 Concentration profiles of nitrate and nitrite during denitrification of 2710 mg L^{-1} NO_3-N at different C/N ratios

Three SBRs operated at different C/N ratios of 1.5, 2 and 3. The denitrification profiles presented are obtained after attaining steady state in the SBRs in terms of minimum time for complete and stable denitrification. The MLSS (MLVSS) values (g L^{-1}) were 11.2 (7.3), 12.8 (10.3) and 17.0 (11.5) for C/N ratios of 1.5, 2 and 3, respectively.

4.1.3 Reaction kinetics

Table 4.4 shows the nitrate reduction rate and nitrite accumulation rate in the presence of nitrate, nitrite reduction rate in the absence of nitrate and their respective specific reduction rates and relative rate for different C/N ratios at different nitrate concentrations. Nitrate and nitrite reduction rates were calculated from the slopes of the nitrate and nitrite decay profiles, respectively. Nitrite accumulation rate is calculated from nitrite build up profile. Specific denitrification rates were calculated by dividing the nitrate and nitrite decay slopes by the MLVSS concentrations. Specific nitrate reduction rates decreased from 827 mg NO_3-N L^{-1} h^{-1} g-$MLVSS^{-1}$ at 677 mg L^{-1} of NO_3-N to 98.97 mg NO_3-N L^{-1} h^{-1} g-$MLVSS^{-1}$ at 2710 mg NO_3-N for C/N ratio of 1.5. For C/N ratio 2 the specific nitrate reduction rates decreased from 373 mg NO_3-N L^{-1} h^{-1} g-$MLVSS^{-1}$ at 677 mg $L^{-1}NO_3$-Nto 94.8 mg NO_3-N L^{-1} h^{-1} g-$MLVSS^{-1}$ at 2710 mg $L^{-1}NO_3$-N and for C/N ratio 3, the specific nitrate reduction rates decreased from 353 mg NO_3-N L^{-1} h^{-1} g-$MLVSS^{-1}$ at 677 mg $L^{-1}NO_3$-N to 47.98 mg NO_3-N L^{-1} h^{-1} g-$MLVSS^{-1}$ at 2710 mg $L^{-1}NO_3$-N. The maximum temperature reached during denitrification of 677-1355 mg NO_3-N L^{-1} was less than 40 °C for all C/N ratios but for concentrations 2032-2710 mg $L^{-1}NO_3$-N, the maximum temperature was in the range of 40-48 ^oC. Increase in temperature above 40 ^oC could be the reason for decrease in the rate constants, since proteins and other cellular components are sensitive to temperature [101]. The optimum temperature for denitrification by mesophilic microbial communities was reported to be between 30 and 37 ^oC [75,157]. The specific denitrification rates achieved in our study were considerably higher than those reported in the literature [12-13,74,90,147-150]. Steady decrease in specific nitrate reduction rates with increase in the nitrate concentration and decrease in specific nitrate reduction rates were observed across C/N ratios for a given nitrate

concentration (Fig. 4.7). Specific nitrite accumulation rates in the presence of nitrate and specific nitrite reduction rate in the absence of nitrate also were found to decrease with increase in nitrate concentrations and with increase in C/N ratio for a given nitrate concentration. Relative rates (RR) were found to increase with increased nitrate concentrations and with increase in C/N ratio for a constant nitrate concentration. This can be correlated with nitrite built up rates.

Glass and Silverstein [12] reported that nitrite build-up in high strength denitrification reactors could occur because of oxygen presence, insufficient electron donor supply and absence of true denitrifiers, which convert nitrate to nitrogen gas, in the consortium. In our study, the measured DO was less than 80 ppb and acetate was not fully utilized at the end of the cycle, ruling out two of the proposed reasons. Thus, the decrease in population of true denitrifiers and increase in nitrate respiring organisms which reduce nitrate to nitrite, could be reason for nitrite build-up in the present study. However, microbial community analysis is required to infer population level differences on reactor performance. The relative rates (RR) were always more than one during whole study at all three C/N ratios, implying that nitrite reduction is the controlling reaction and nitrite build-up will be observed [74]. Nitrate reduction rates were greater than nitrite reduction rates (Table 4.4). Moreover, nitrite reduction rate in the absence of the nitrate was always greater than the nitrite reduction rate in the presence of nitrate. It can be deduced that nitrite reductase activity was inhibited in the presence of nitrate because competition for the flow of electrons to nitrate reductase. In other words, nitrate is preferred as an electron acceptor over nitrite when both nitrate and nitrite were available for microorganisms. Additional fundamental studies are required to infer the effect of nitrate

on nitrite reductase activity, particularly under high strength conditions. Nevertheless, this study shows that high strength denitrification is best achieved at a C/N ratio of 1.5. The study demonstrates that C/N ratio of 1.5 is optimum with acetate as carbon source, for complete and stable denitrification of high strength nitrate wastewaters, in anoxic granular sludge sequencing batch reactors.

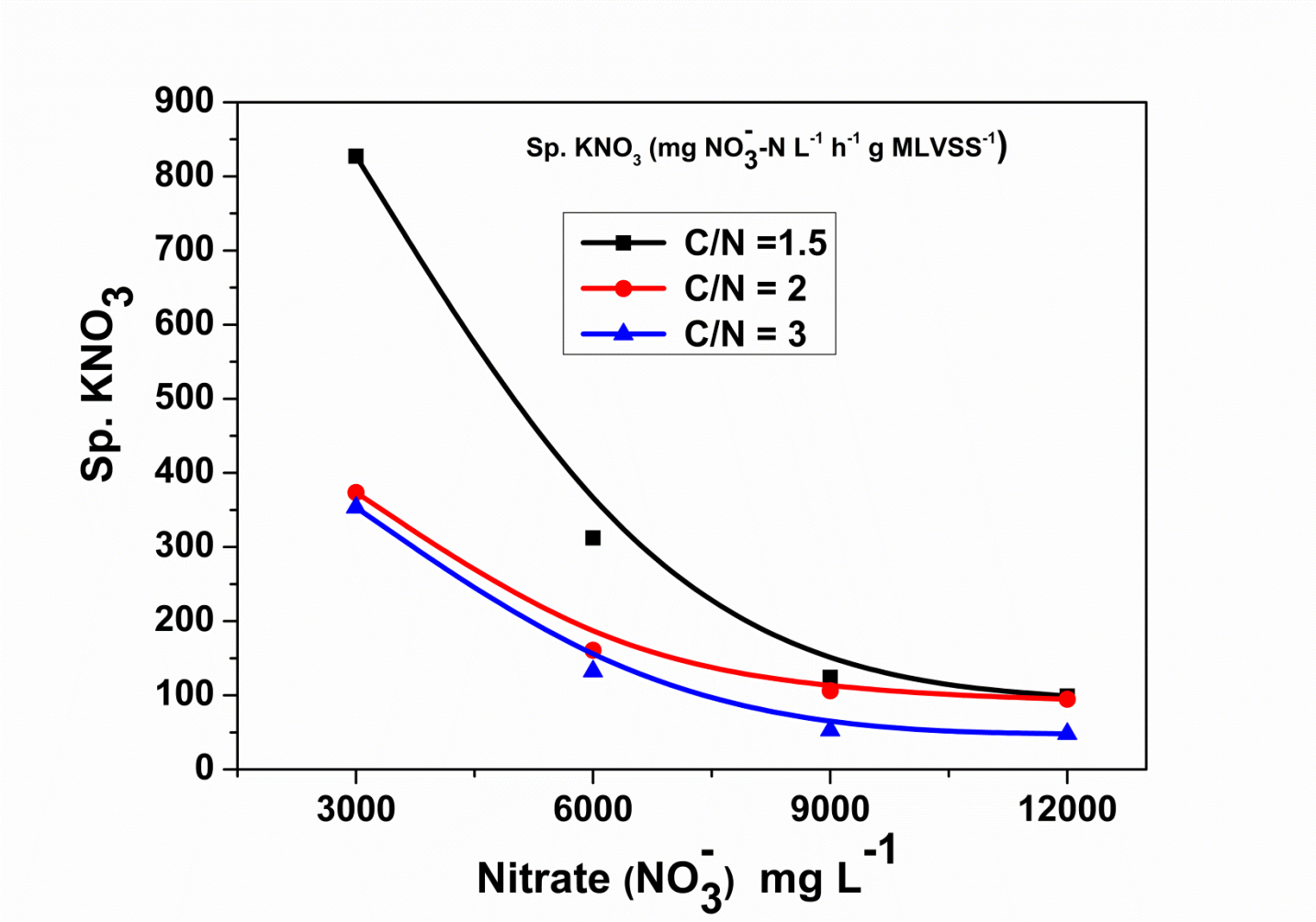

Fig. 4.7 Sp. Nitrate reduction rates for different C/N ratios during denitrification of different initial nitrate concentration.

Table 4.4 Nitrate and nitrite denitrification rates and specific denitrification rates for different C/N ratios

For zero order kinetics at different initial nitrate concentrations

Initial nitrate in the SBR (mg L^{-1})	$K_{NO_3^-}$ (mg NO_3-N $L^{-1}h^{-1}$)	$K_{NO_2^-}$ (mg NO_2-- N $L^{-1}h^{-1}$) Nitrate is absent	$K'_{NO_2^-}$ (mg NO_2-- N $L^{-1}h^{-1}$) Nitrate is present	$\frac{K_{NO_3^-}}{X}$ (mg NO_3-- N $L^{-1}h^{-1}g$ $MLVSS^{-1}$)	$\frac{K_{NO_2^-}}{X}$ (mg NO_2- N $L^{-1}h^{-1}g$ $MLVSS^{-1}$) Nitrate is absent	$\frac{K'_{NO_2^-}}{X}$ (mg NO_2- N $L^{-1}h^{-1}g$ $MLVSS^{-1}$) Nitrate is present	RR
C/N = 1.5							
3000	1472.76	650.16	644.00	827.39	365.26	361.00	2.29
6000	1980.00	451.08	489.33	312.30	71.15	77.18	4.05
9000	1170.11	511.49	165.14	124.22	54.30	17.53	7.09
12000	1112.40	782.21	72.80	98.97	69.59	6.48	15.28
C/N = 2							
3000	1366.92	815.76	480.00	373.48	222.89	131.15	2.85
6000	1510.92	461.20	510.67	160.74	49.06	54.33	2.96
9000	1158.77	689.98	65.14	106.11	63.18	5.97	17.79
12000	1215.90	620.06	61.20	94.84	48.37	4.77	19.87
C/N = 3							
3000	1463.18	326.52	454.00	353.43	78.87	109.66	3.22
6000	1447.20	419.36	670.67	132.29	38.33	61.30	2.16
9000	778.14	597.56	46.86	52.86	40.60	3.18	16.61
12000	817.63	590.87	10.00	47.98	34.68	0.59	81.76

4.1.4 Conclusion

Compact denitrifying granular sludge capable of denitrification of up to 2710 mg $L^{-1}NO_3$-N at different C/N ratios was developed in sequencing batch reactor, using acetate as carbon source. Complete denitrification was observed at C/N ratios of 1.5, 2 and 3. Nitrite accumulation was observed at all three C/N ratios tested. The specific denitrification rates observed were 2 - 3 times higher than those reported for similar studies on high strength denitrification. Kinetic study revealed that nitrate and nitrite denitrification rates were of zero order. The study shows that C/N ratio of 1.5 is optimum for efficient and stable denitrification, as denitrification times and peak nitrite concentrations were lowest for this C/N ratio. As this is low compared to the optimum C/N ratios reported by many other researchers, the treatment scheme investigated in the present study, using granular biomass in SBRs is highly cost effective.

4.2 Effect of sudden change in C/N on nitrate removal from high strength nitrate-bearing wastes

Experiments were carried out to study the effect of sudden change in C/N on nitrate removal from high strength nitrate-bearing wastes in a glass tank with 6 L working volume which was operated in a sequencing batch mode. Mixing was provided by means of an impeller stirred at 100 rpm.

4.2.1 Denitrification performance

The SBR was inoculated with activated sludge and fed with simulated waste containing 1354 mg L^{-1} NO_3-N at a C/N ratio of 3. It may be noted that the starting concentration in the reactor would be 677 mg L^{-1} NO_3-N, because the SBR retains 50% of waste from the previous batch (50% VER), with < 10 mg L^{-1} nitrates in it. The pH of simulated nitrate waste was 7.5 before feeding to the reactor. The pH observed in the reactor at the end of

cycle was 9.5, the increase being due to denitrification. In subsequent cycles of operation, the pH in the reactor stabilized at ~9.5 (Fig. 4.8). The simulated waste prepared in deionized water and the dissolved oxygen (DO) content before feeding was noted to be 6.0 mg L^{-1}. The DO rapidly decreased to below 0.08 mg L^{-1} within a few minutes of addition to the reactor, due to respiration by the aerobic microbial population. The reactor tank was open to atmosphere and the mixing was provided by means of bottom stirring at 100 rpm. Under these conditions, the DO in the SBR cycle period was always below 0.08 mg L^{-1}.

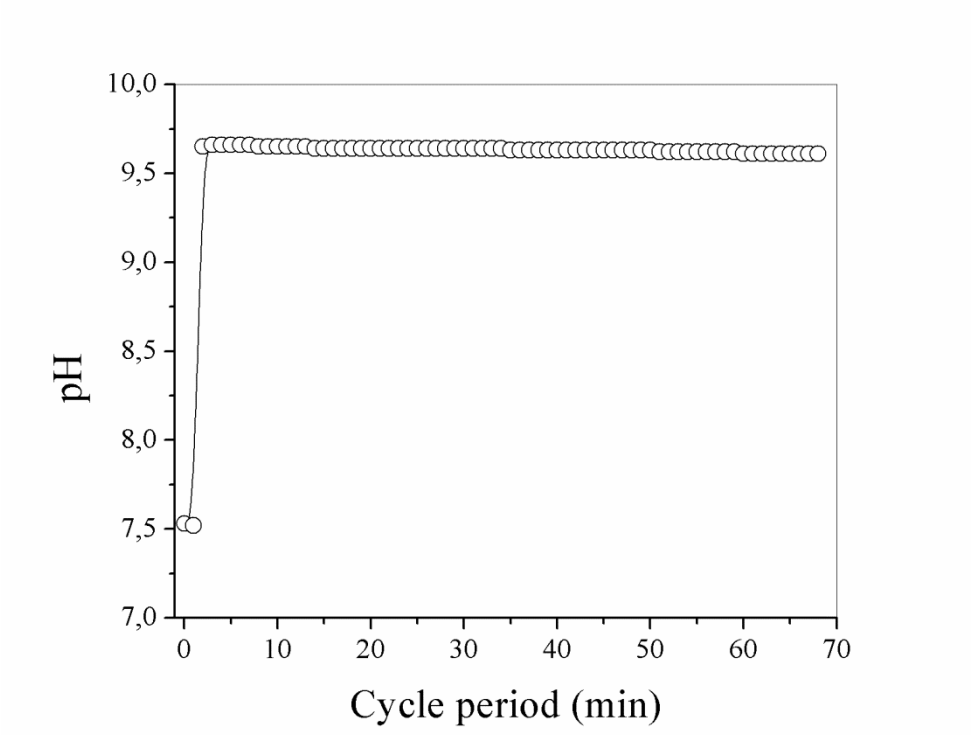

Fig. 4.8 Profile of pH during the first one hour of cycle period in 6 L SBR.
The reactor was fed with simulated nitrate waste with a pH of 7.5. The sequencing batch reactor was operated with 24 h cycle period and 50% volume exchange ratio.

The reactor operating conditions were conducive for heterotrophic denitrification, observed from cycle 1 onwards (Fig. 4.9). By keeping the C/N ratio constant at 3, feed

nitrate-N was increased to 2710 and then to 5420 mg L^{-1}. Complete denitrification was observed at the increased feed nitrate concentrations of 2710 and 5420 mg L^{-1} NO_3-N. The effluent nitrate and nitrite concentrations were invariably less than 10 mg L^{-1} during long term operation of the SBR, except during a few occasions (Fig. 4.9).

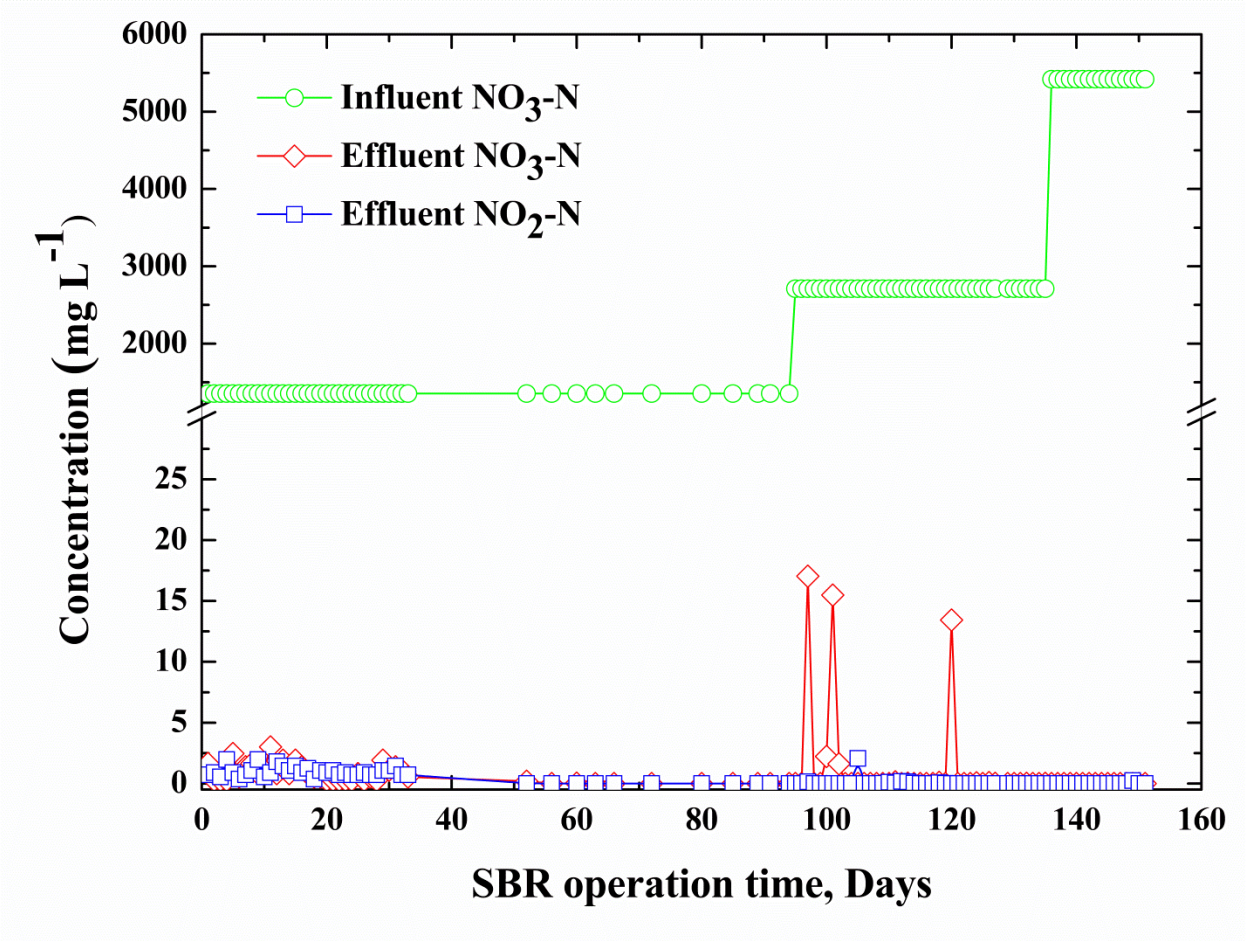

Fig. 4.9 Effluent nitrate and nitrite levels during 150 days of operation denitrifying SBR.
The reactor was fed with simulated nitrate waste containing 1350, 2710, 4060 and 5420 mg L^{-1} NO_3-N at a C/N ratio of 3.

Denitrification of feed NO_3-N concentrations of 1354, 2710 and 5420 mg L^{-1} was completed within the first 4, 6 and 8 hours, respectively. Typical denitrification profiles consisted of nitrate removal, accumulation of nitrite and nitrite removal. Nitrite

accumulation reached a maximum value of approximately 250 mg L^{-1} NO_2-N at 1354 mg L^{-1} nitrate-N in the feed.

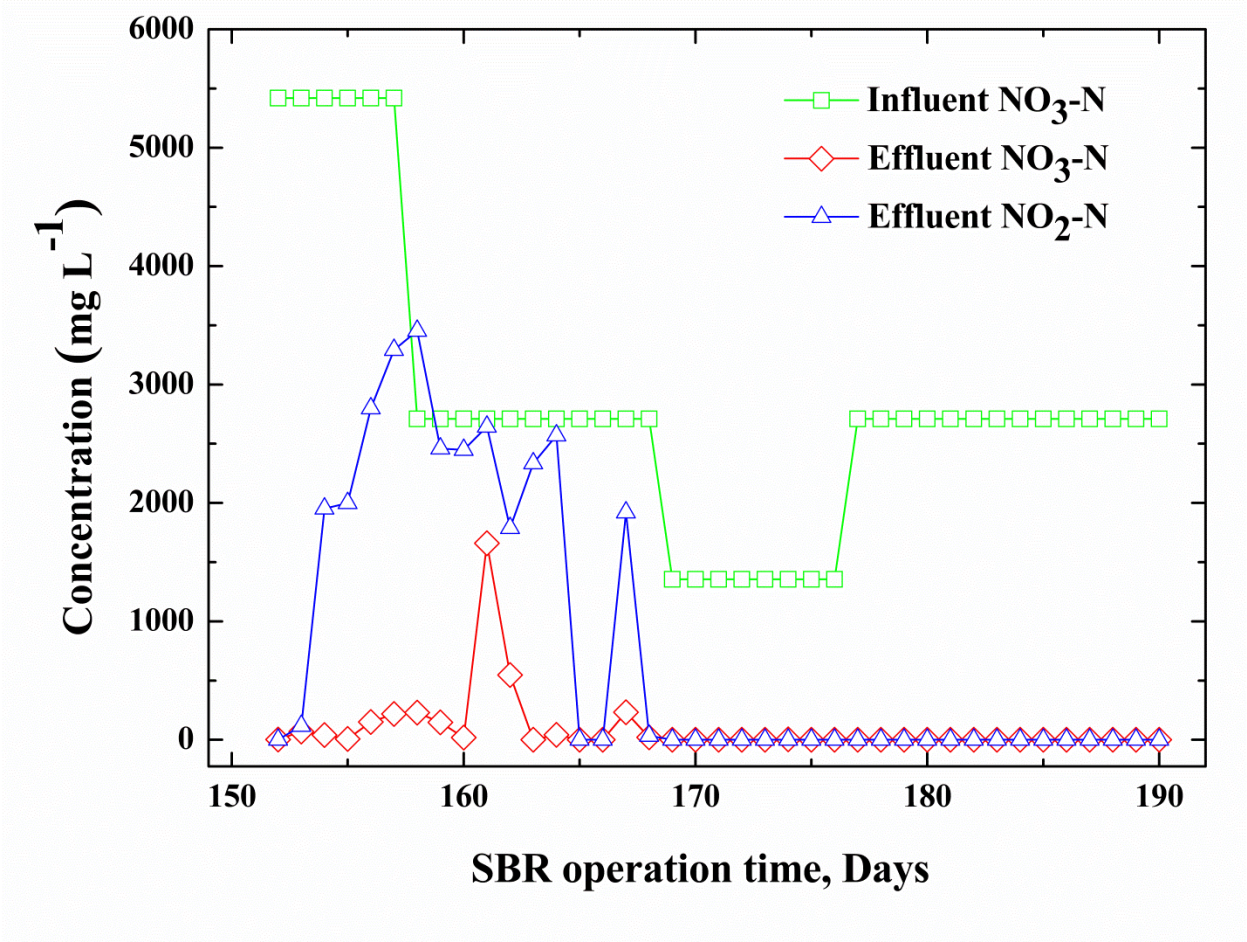

Fig. 4.10 Nitrate and nitrite levels in the effluent during break period and post-break period.
Denitrifying granular sludge capable of high strength denitrification of up to 5420 mg L^{-1} at C/N ratio of 3 was achieved. Denitrification was severely inhibited when the reactor was fed with 5420 mg L^{-1} NO_3^{-1} at C/N ratio of 2 due to accumulation of high concentrations of nitrite. A step-down procedure was adopted for decreasing feed nitrate concentration up to 1350 mg L^{-1} for re-establishing high strength denitrification.

In order to study the denitrification at reduced substrate concentration, the reactor was subsequently fed with 5420 mg L^{-1} NO_3-N at a C/N ratio of 2. The change in C/N ratio caused inhibition of denitrification, resulting in incomplete denitrification and accumulation of nitrite-N as high as 3500 mg L^{-1} (Fig. 4.10). SBR operation in the

subsequent cycles consistently showed the buildup of the high concentrations of nitrite and nitrate. Inhibition of the denitrification process was probably due to the toxicity caused by high nitrite levels.

In order to improve the denitrification performance, the feed C/N ratio was reverted to 3. However, high nitrite levels continued to accumulate in the SBR, in spite of the presence of surplus electron donor in the reactor. Oh and Siverstein [109] reported accumulation of significant amount of nitrite during low strength denitrification, when the C/N ratio was decreased from 2 to 1. In the present case, complete denitrification of low strength denitrification was restored only 3 weeks after reverting the C/N ratio to 2. Complete denitrification could not be restored in spite of operating the SBR for two weeks at C/N of 3, and the nitrite accumulation continued to be exceptionally high. High strength denitrification cannot be directly compared with low strength denitrification as the nitrite levels in the former case reach very high concentrations even in the presence of excess electron donor. TOC measurements showed that the effluent still contained about 2000 mg L^{-1} for feed with 5420 mg L^{-1} nitrate at C/N ratio 2. Some unutilized organic carbon was found in the treated water leaving the reactor at the lowest C/N ratio of 1.2 tested. This indicates that even though some electron donor is still available at C/N ratio 2, the nitrite levels formed are relatively higher due to stiff competition for electrons between nitrate and nitrite. Thus, it is likely that high nitrite levels inhibited high strength denitrification.

To re-establish denitrification, a step-down procedure was adopted and the feed nitrate concentration was decreased to 1355 mg L^{-1} NO_3-N. At this concentration of nitrate, complete denitrification was established within a few days. Subsequently, the feed nitrate

level was increased in a step-wise manner (1355, 2710, 4065 and 5420 mg L^{-1}) at C/N ratio 2. After 10 days of operation, stable denitrification could be re-established for all the concentrations of nitrate studied (Fig. 4.11). At this stage, the microorganisms were acclimatized to high levels of nitrate as well as nitrite. Therefore, the reactor was fed with various nitrate concentrations, increasing in steps, but at a reduced substrate concentration, viz., C/N ratio of 2. By this strategy, complete and stable denitrification was achieved at C/N ratio of 2 for feed NO_3-N concentrations of 1355, 2710, 4065 and 5420 mg L^{-1} (Fig. 4.11).

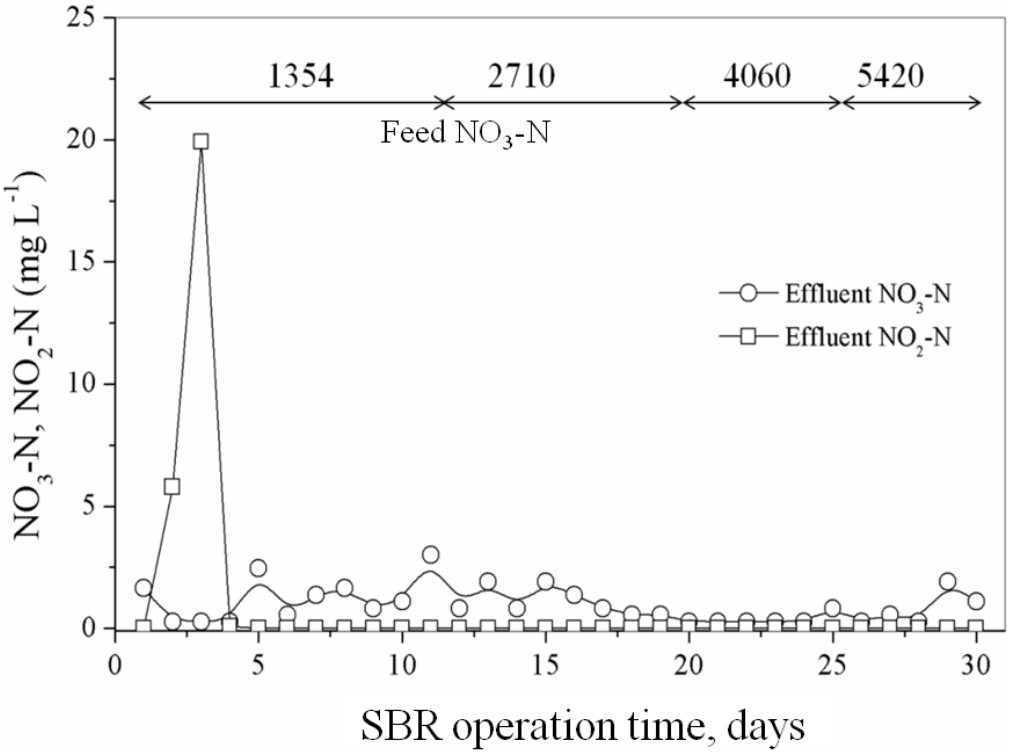

Fig. 4.11 Nitrate and nitrite concentrations in the sequencing batch reactor outlet. Treating simulated nitrate waste containing 1354, 2710, 4065 and 5420 mg L^{-1} NO_3-N at a C/N ratio of 2. Reactor was seeded with denitrifying granular sludge developed on feed with C/N ratio of 3.

4.2.2 Denitrifying granular sludge

During the startup, the SBR was operated with 10 min settling time to minimize biomass loss from the system. After one week of operation, the settling time was reduced to 5 min to select granular sludge with good settling characteristics. Formation of tiny, irregularly shaped and well settling granules was apparent within two weeks of operation. The morphology of granules, which evolved in the reactor during high strength denitrification, is shown in Fig. 4.12. The sludge predominantly consisted of granules as evident from visual observations, microscopy and settling characteristics. Long rod-shaped microorganisms were evident on the surface of granules (Fig. 4.12).

PCR-DGGE revealed clear shifts in the total bacterial community during the course of reactor operation. Some bands were found to be stable throughout the reactor operation, while some new bands became dominant towards the later period of reactor operation (Fig. 4.13). Certain bands became more intense than the others, possibly due to the enrichment of specific denitrifying strains. Apart from selection pressure imposed for enrichment, nitrite accumulation during high strength denitrification may strongly influence development of microbial community, as depicted by the appearance and disappearance of bands. In spite of the break in the denitrification process due to change in C/N ratio (day 153 through 174), the microbial community was found to be resilient to the operational perturbations.

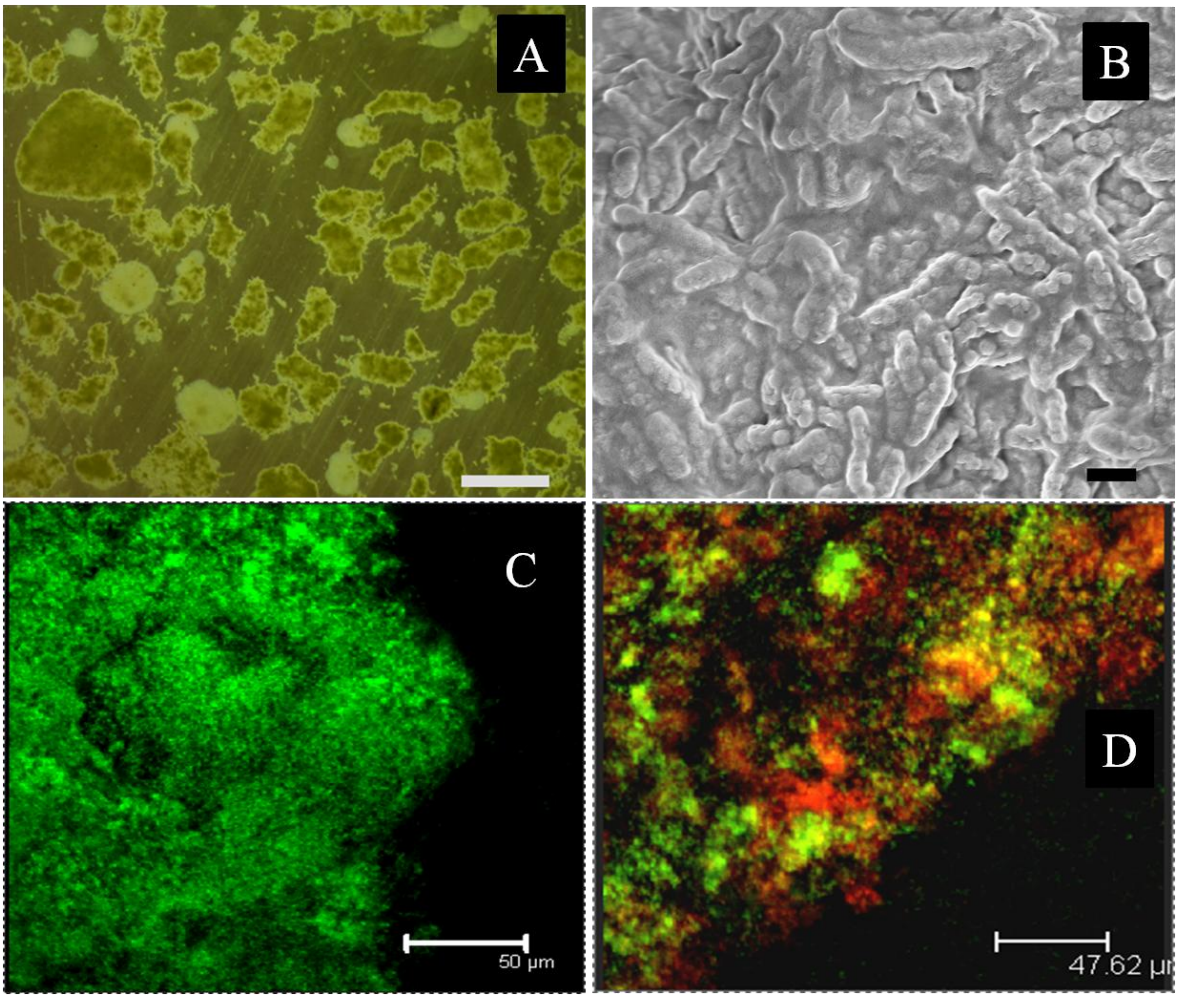

Fig. 4.12 Micrographs showing the morphology and microstructure of denitrifying granular sludge developed in the sequencing batch reactor.

A) Morphology of denitrifying granules collected on day 30 of SBR operation. Bar = 1 mm. B) Scanning electron microscope (SEM) image showing morphology of microorganisms on the surface of denitrifying granule. Scale bar = 1 µm. C, D are confocal images. C) maximum intensity project of xy-images obtained from acridine orange stained denitrifying granule. D) Maximum intensity project of an overlay green and red channel of multiple xy-images obtained from denitrifying granule stained with BacLight™ viability stain. Green = SYTO 9 signal, Red = propidium iodide signal.

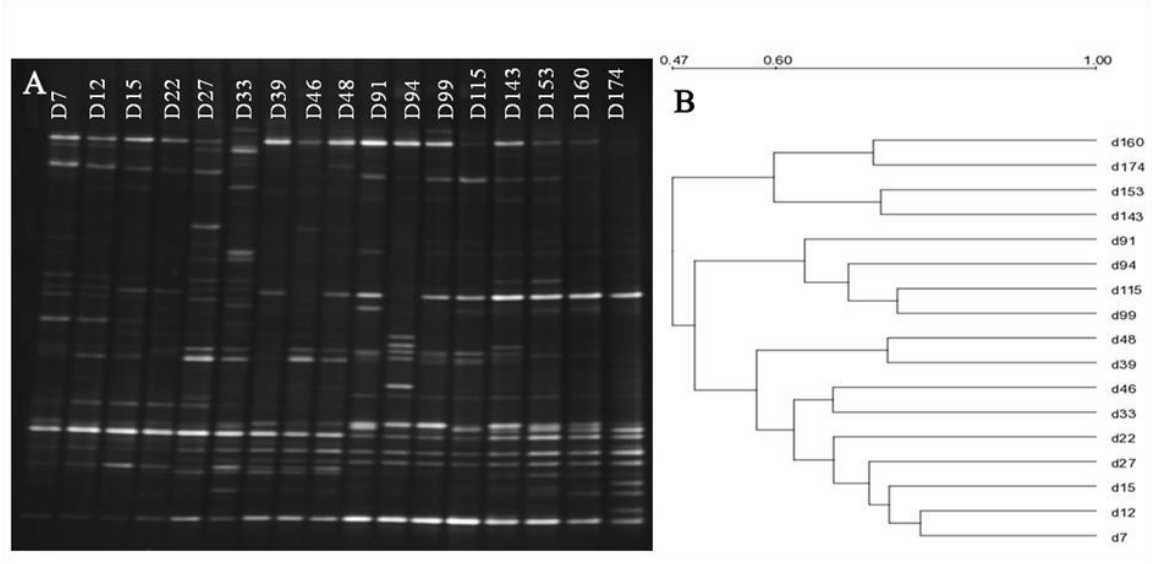

Fig. 4.13 (A) Ethidium bromide stained DGGE gel, B) dendrogram prepared using UPGAMA clustering method.

DGGE analysis of PCR amplified 16S rRNA gene of bacteria from denitrifying sludge collected from the reactor during six months of operation. The reactor was inoculated with activated sludge and fed with simulated nitrate waste. Feed nitrate was increased in a step wise manner to achieve denitrification of 5420 mg L^{-1} NO_3-N at C/N ratio of 3. Lane labels refer to day of sample collection after reactor startup.

Several researchers have reported accumulation of nitrite during denitrification of high strength nitrates [12,141,74-75,141,151-152]. Nitrite accumulation during denitrification by mixed liquor activated sludge was explained on the basis of differences in the rates of reduction of nitrate and nitrite at cellular and population level. Nitrate reduction rates are much higher than nitrite reduction rates, causing accumulation of nitrites. Nitrite and nitrate reductases use protons for reduction reactions from periplasm and cytoplasm, respectively. Thus it results in nitrite accumulation in periplasmic space of denitrifying bacteria. Further, at alkaline pH, concentration of protons in the periplasmic space may be limited, leading to inhibition of nitrite reduction [12]. Dhamole et al.[74] also stated

that competition for electrons between nitrate and nitrite reductases can lead to nitrite accumulation.

At population level, nitrite accumulation has been explained on the basis of relative distribution of nitrate-respiring bacteria and true denitrifying bacteria [12,74]. Nitrate respiring bacteria can use only nitrate as electron acceptor, leaving nitrite as the end product. In the present study, only 4 out of 14 isolates obtained from the denitrifying granular sludge were able to completely reduce nitrate to N_2 gas, while all the remaining isolates could only reduce nitrate to nitrite and no further. These results point to the possibility that nitrite accumulation could be also be due to differences in the populations of nitrate-respiring and true denitrifying bacteria that co-existed in the granular sludge.

4.2.3 Conclusions

Denitrifying granular sludge cultivated in SBR exhibited efficient and stable denitrification during long-term operation. Complete denitrification of feed nitrate-N up to 5420 mg L^{-1} was achieved, with effluent nitrate-N and nitrite-N levels of below 10 mg L^{-1}. The granular sludge formed under denitrifying conditions possessed compact microstructure and diverse microbial community. When the denitrifying granular sludge, cultivated with a C/N ratio of 3, was abruptly fed with high strength nitrate at a lower C/N ratio of 2, complete denitrification could not be achieved. Acclimatization of the granular sludge by increasing the feed nitrate concentration in steps, at a given C/N ratio, appears to be essential to achieve complete and stable denitrification of high strength nitrates. High strength denitrification involves nitrite accumulation and therefore, selection of nitrite tolerant strains through adaptation and enrichment of the denitrifying community is a prerequisite.

4.2.4 Practical implications

Transient accumulation of nitrite depends on initial nitrate, electron donor concentrations as well as on microbial community composition. Exposure of microbial community to transient nitrite accumulation is inevitable during high strength nitrate denitrification in sequencing batch reactors. Since nitrite is inhibitory to microorganisms, enrichment of nitrite tolerant denitrifying bacteria is desirable. A step-wise increase in initial nitrate concentration at a fixed C/N ratio allows enrichment of nitrite tolerant microbial community. It is evident that an abrupt decrease in electron donor supply will lead to accumulation of higher nitrite levels to which microbial community has not been exposed thus far and can decrease nitrite reduction and then nitrate reduction by inhibiting the denitrifying microorganisms. Therefore, proper electron donor dosing of nitrate contaminated water along with enrichment strategy needs to be adopted in order to protect denitrifying community by avoiding inadvertent exposure to high nitrite levels.

4.3 Denitrification at different initial pH

Experiments were carried out in two 3 L volume SBRs to study denitrification of acidic wastewater, having pH 7.5, 5 and 4. The results are presented below and discussed in the light of available literature on the treatment of acidic nitrate wastewaters and effect of pH on denitrification.

4.3.1 Biomass growth and characterization

Evolution of granular sludge was observed in both the reactors within two weeks. Granular sludge formed under anoxic conditions allowed easy separation of biomass. Denitrifying biomass was predominantly in the form of distinct, compact and fast settling granules (Fig. 4.14a,b). The granular sludge was stable during several months of reactor operation. Scanning electron microscope showed the presence of rod shaped

microorganisms on the surface of granular sludge, when fed with simulated nitrate waste at pH 7.5 (Fig. 4.14c). In contrast, the surface of granular sludge developed when the SBR was fed with nitrate waste at pH 4.0 was mostly colonized by cocci shaped microorganisms (Fig. 4.14d).

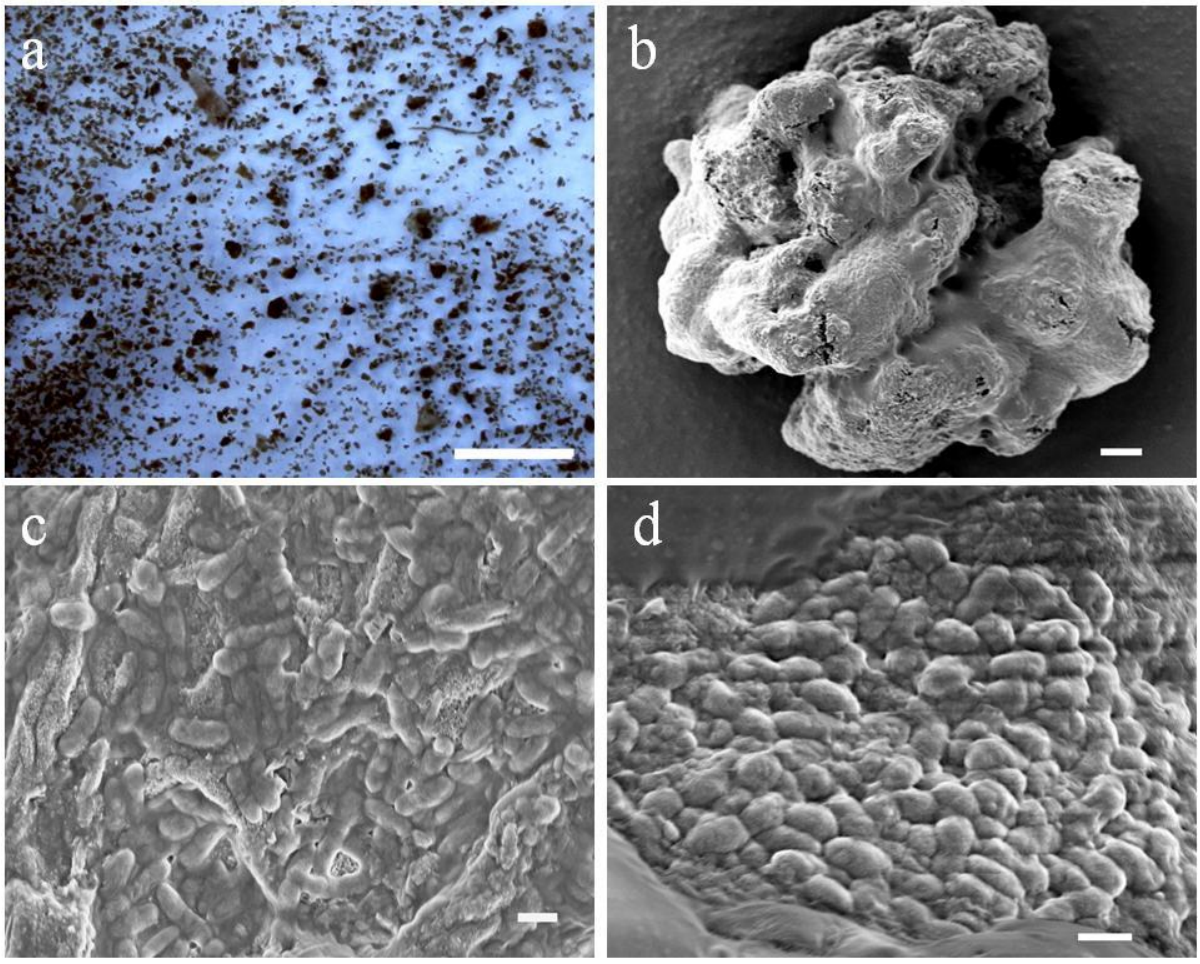

Fig. 4.14 Morphology of denitrifying granular biomass collected from the reactor fed with simulated nitrate waste at pH 7.5 and 4.

a) Digital image showing the morphology of granular sludge, scale bar = 10 mm. b) SEM image of individual denitrifying granule, scale bar = 10 µm. c) SEM image of granule formed at feed pH of 7.5. d) SEM of granule formed at feed pH of 4. Scale bar for c and d = 1 µm.

4.3.2 Denitrification at different initial pH in batch experiments

In batch experiments, denitrification of 677 mg $L^{-1}NO_3$-N was carried out at different pH of 4, 5, 6 and 7.5. Denitrification was observed at initial pH of 6 and 7.5. No significant denitrification activity was observed at initial pH of 4 and 5. This was evident from the negligible nitrate removal and associated changes in solution pH (Fig. 4.15). No significant change in pH was evident for initial pH of 4 and 5. But, a small decrease in nitrate concentration was observed at pH 4 and 5. In contrast, the medium pH increased from 6 and 7.5 to 8.7 and 9.5, respectively, due to denitrification activity. When denitrified medium titrated with fresh nitrate feed of pH 4 and 5 showed the possibility of achieving pH above 6. Therefore, this strategy was used for treatment of acidic nitrate waste by feeding into sequencing batch reactor with 50% volume exchange ratio.

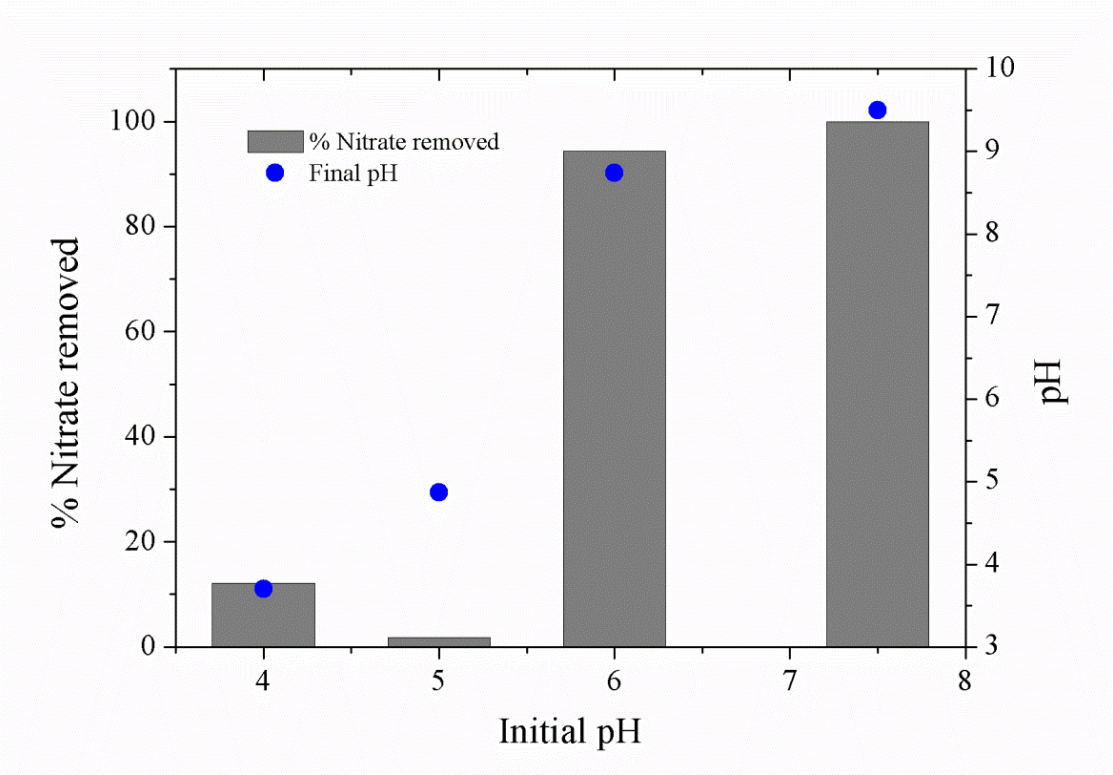

Fig. 4.15 Nitrate removal and associated changes in the medium pH through denitrification by unacclimated granular sludge.

Simulated nitrate waste with 677 mg $L^{-1}NO_3$-N was prepared with different initial pH, inoculated with granular sludge and incubated under anoxic conditions in serum bottles. Nitrate removal and final pH were determined after 48 h of incubation.

4.3.3 Denitrification of simulated nitrate wastewater with different initial pH

Complete reduction of 677 mg L^{-1} NO_3-N (1355 mg L^{-1} NO_3-N in feed) was observed from cycle 1 onwards indicating the presence of denitrifying organisms and conditions in the reactor. Due to acclimatization and enrichment of denitrifying bacteria, the time needed for complete denitrification decreased progressively and stabilized within two weeks of startup. At steady state, reduction of nitrate was complete within the first ~3 h of cycle period. The denitrification profiles observed during the cycle period in R1, fed with simulated nitrate waste at pH 7.5 are shown in Fig. 4.16. Typically, denitrification profile consisted of a rapid nitrate removal pattern, accumulation of nitrite and nitrite removal phase. Denitrification profiles and performance were almost similar in both the SBRs operated under similar conditions (Fig. 4.17). Although SBRs were fed with nitrate waste of pH 7.5, the pH in the reactor increased to 9.5 soon after filling. At the end of denitrification, the pH in the reactor was stabilized at 9.6 (Fig. 4.18).

Denitrification profiles determined during 4 representative cycles at steady-state are presented. Steady state in terms of minimum period for complete denitrification was attached within 2 weeks of startup. The MLSS was 3.4 g L^{-1}.

Denitrification profiles determined during 4 representative cycles at steady-state are presented. Steady state in terms of minimum period for complete denitrification was attached within 2 weeks of startup.

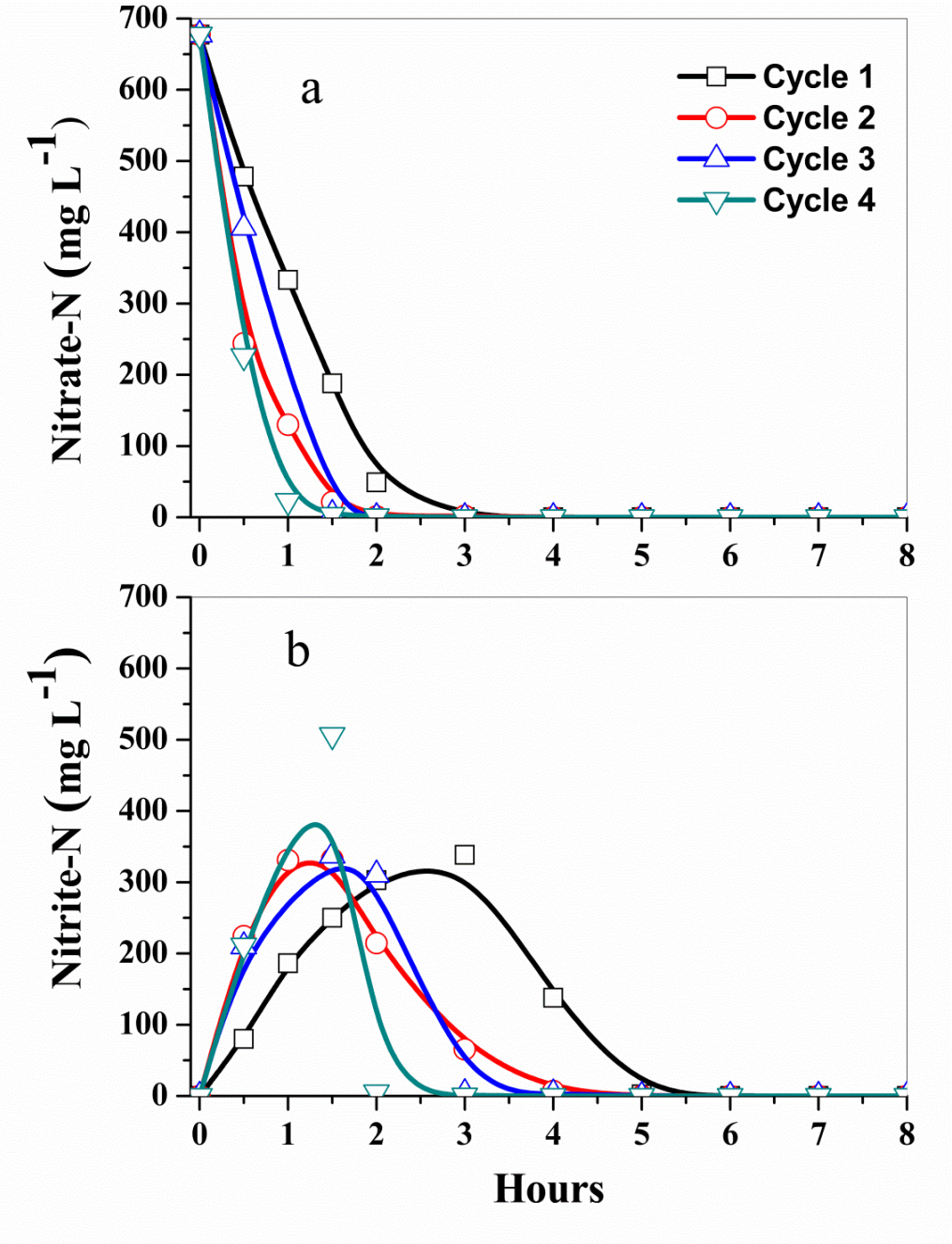

Fig. 4.16 Nitrate and Nitrite concentration profiles during cycle period of R1, fed with simulated nitrate waste containing 1355 mg L^{-1} NO_3-N in the feed at pH 7.5.

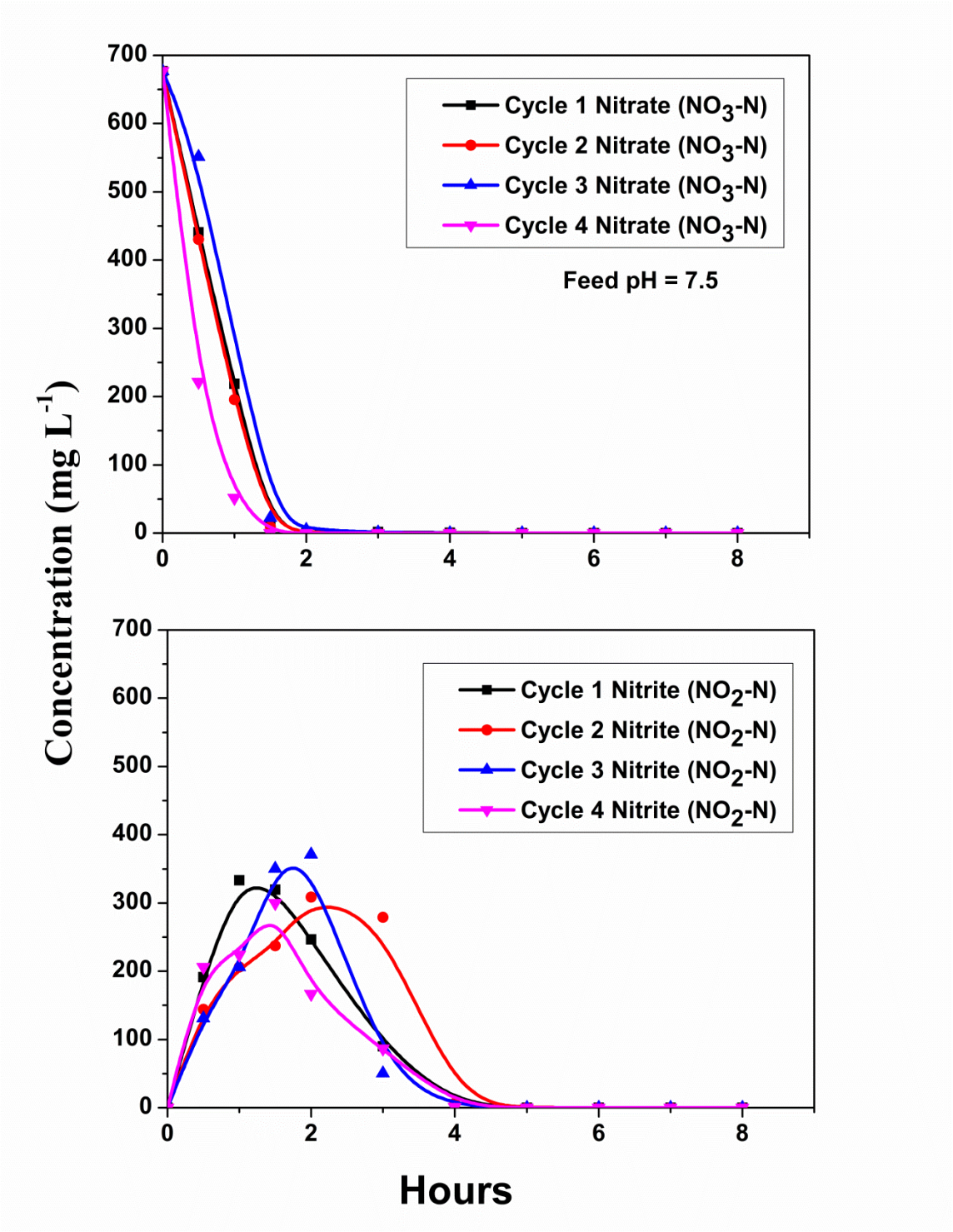

Fig. 4.17 Nitrate and Nitrite concentration profiles during cycle period of R2, fed with simulated nitrate waste containing 1355 mg L^{-1} NO_3-N at pH 7.5.

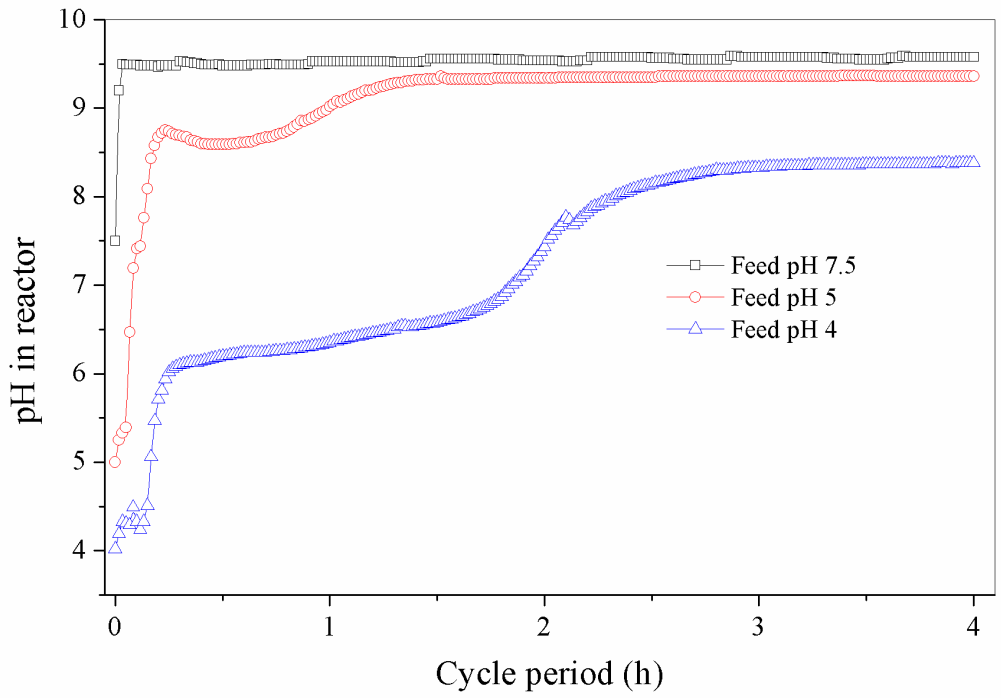

Fig. 4.18 pH profiles of during the cycle period of R1, fed with simulated nitrate waste containing 1355 mg L^{-1} NO_3-N at 7.5, 5 and 4.

After two weeks, R1 was fed with nitrate waste of pH 5. Immediately after filling, the pH in the reactor was determined to be 8.7, which stabilized at 9.4 at the end of denitrification phase (Fig. 4.12). The time taken for complete denitrification of 677 mg L^{-1} NO_3-N increased from 3 to 8 h in the 1st cycle after adjustment of feed pH to 5. After a few cycles of R1 operation with feed pH 5, the time needed for complete denitrification decreased and stabilized at 3 h. This could have been due to adaptation of the denitrifying microorganisms (Fig. 4.19). Subsequently, R1 was fed with nitrate waste of Ph 4. After filling, the pH in the reactor was found to be 6.2. Denitrification was complete during the cycle period, although it took almost 20 h. At the end of denitrification, the pH in the reactor was stabilized at 8.2 (Fig. 4.18). The time needed for complete denitrification gradually decreased and stabilized at 3 h, again through a

process of adaptation of the microbial community (Fig. 4.20). However, the adaptation of microbial community took almost one month for achieving steady-state in denitrification of feed with pH 4.

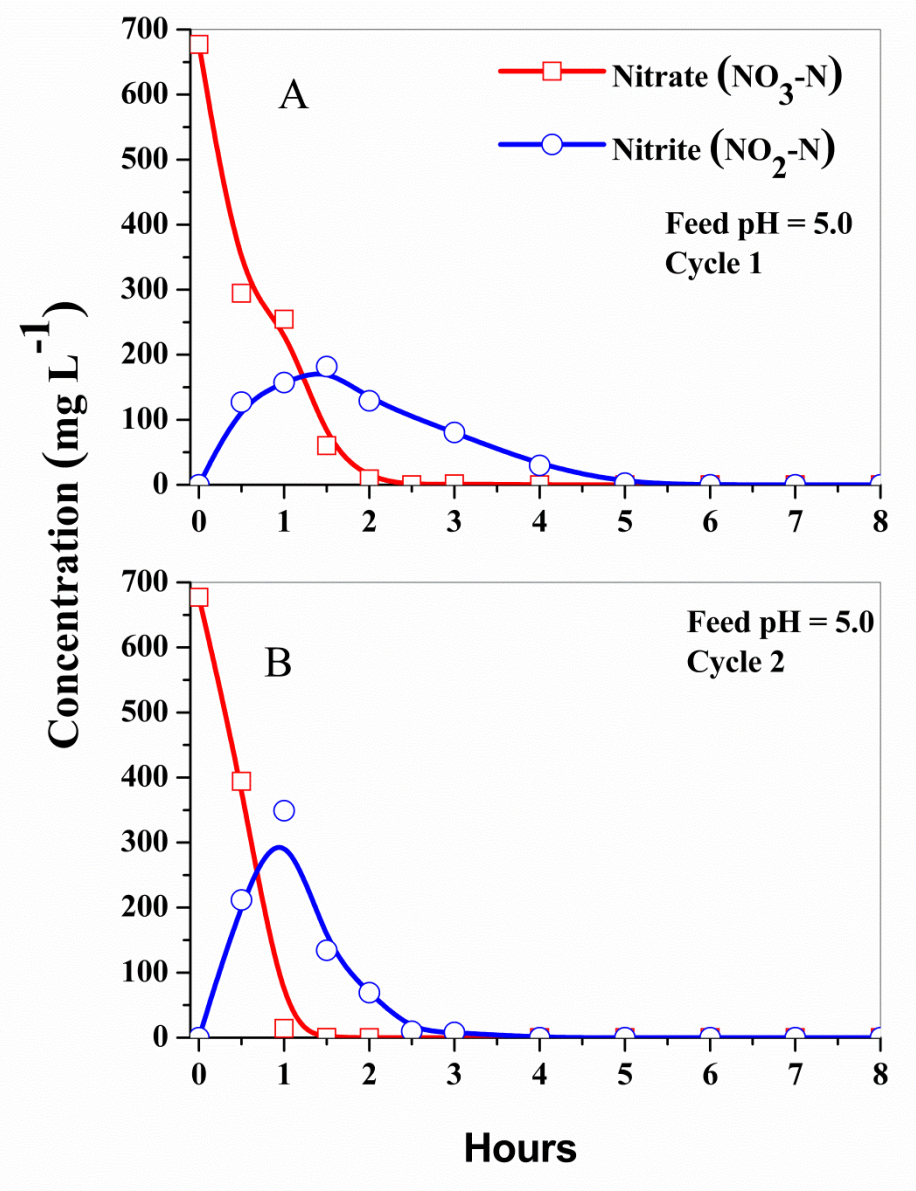

Fig. 4.19 Denitrification profiles of nitrate during the cycle period of R1, fed with simulated nitrate waste containing 1355 mg L^{-1} NO_3-N at pH 5.
Denitrification data for two representative cycles showing denitrification before (A) and after (B) attaining steady-state is presented. The minimum time needed for complete denitrification was stabilized within two weeks of reactor operation with feed at pH 5. The MLSS was 3.4 g L^{-1}.

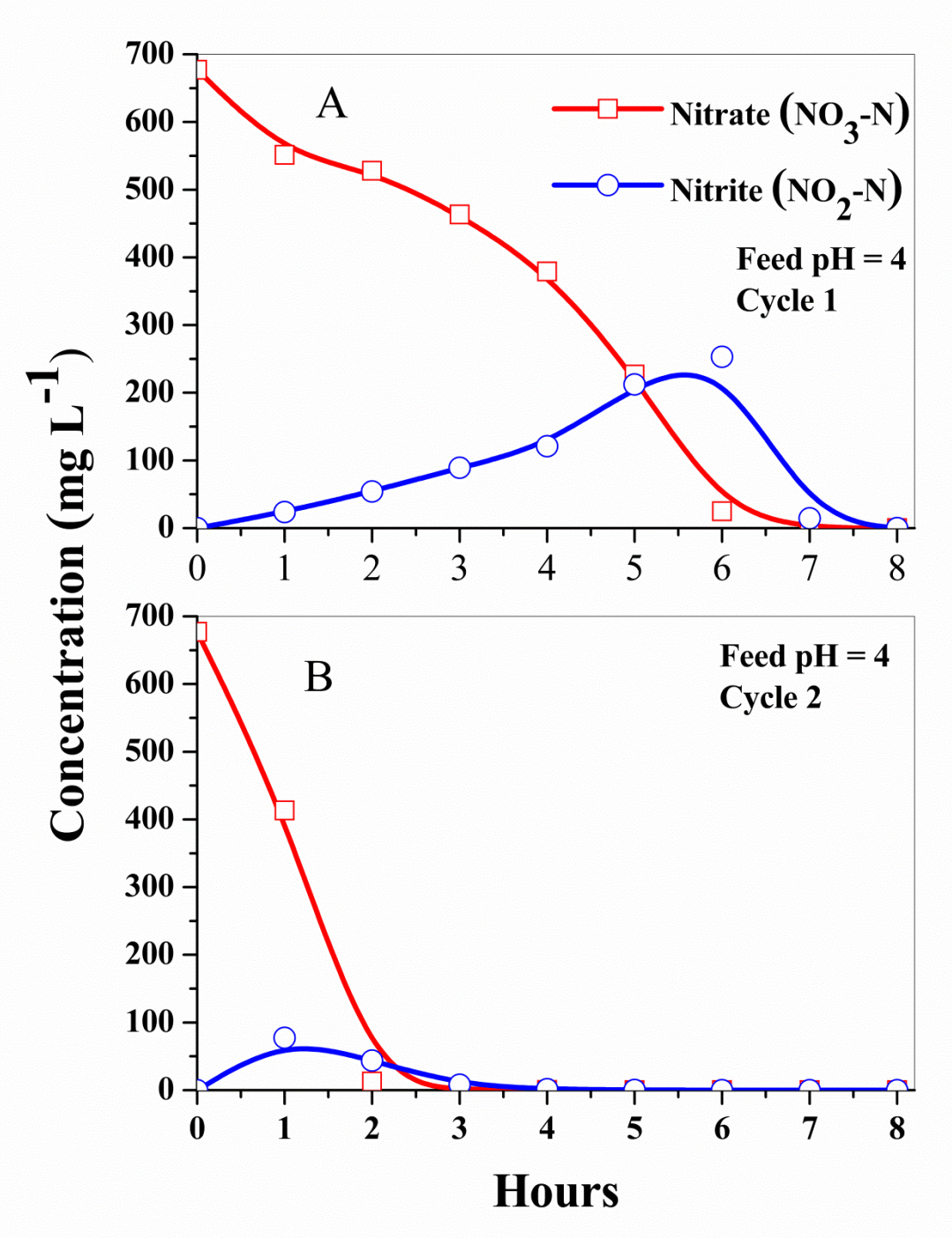

Fig. 4.20 Denitrification profiles of nitrate during the cycle period of R1, fed with simulated nitrate waste containing 1355 mg L^{-1} NO_3-N at pH 4.
Denitrification data for two representative cycles showing denitrification before (A) and after (B) attaining steady-state is presented. The minimum time needed for complete denitrification was stabilized (B) after one month of reactor operation with feed at pH 4. The MLSS was 3.4 g L^{-1}.

4.3.4 Denitrification of acidic wastewater

Heterotrophic denitrification consists of four sequential reduction reactions from nitrate to nitrite (NO_2^-), nitric oxide (NO), nitrous oxide (N_2O) and finally to dinitrogen (N_2). These reactions are catalyzed by distinct reductases [67]. Denitrifying microorganisms efficiently reduce nitrate to N_2, provided the necessary conditions, viz., electron donor supply and oxygen limiting conditions are available. Other parameters such as solution pH and temperature strongly influence denitrification performance. The rate of production and accumulation of denitrification intermediates are strongly influenced at pH below 7 [153]. Complete inhibition of denitrification was observed in batch assays carried out at pH 4 and 5. Inhibition of high strength denitrification at pH below 7 was observed in activated sludge systems [12]. The denitrification reaction coupled to acetate oxidation generates alkalinity, as given by:

$$CH_3COOH + \frac{8}{5}NO_3^- + \frac{4}{5}H_2O \rightarrow \frac{4}{5}N_2 + 2H_2CO_3 + \frac{8}{5}OH^- \quad (4.1)$$

The alkalinity generated in the above reaction has the potential to neutralize the pH of acidic wastewater fed to the SBR. Internal recycling of denitrification generated alkalinity led to neutralization of nitrate wastewaters with pH 4 and 5 (Fig. 4.15). The pH of acidic wastewater increased from 5 to 8.7 and 4 to 6.2 in the reactor. Thus, establishment of steady state denitrification was relatively fast with feed pH of 5 compared to 4. The longer time for complete denitrification and adaptation of denitrifying community at pH 4 was because the pH in the reactor was below 7, even after neutralization. pH between 6 and 7 has been reported to affect denitrification and contribute to N_2O accumulation in wastewater treatment plants [153]. In addition, adaptation of microbial community and possible enrichment of acid tolerant strains have

led to steady state denitrification of feed at pH 4. In a recent work, Papirio et al. [154] employed internal recycling of biologically produced alkalinity in fluidized bed reactor for neutralization of low strength nitrate and sulfate acidic wastewaters. The nitrate containing effluents produced in nuclear industry are inadequately buffered and the biologically produced alkalinity could be beneficially used for the neutralization and treatment of nitrate rich acidic waters. In addition, the biologically produced alkalinity has the potential to cause precipitation of co-contaminants (i.e. metals, radionuclides) of low level radioactive wastes as hydroxides or carbonates, which would be an added advantage.

4.3.5 Reaction kinetics

Table 4.5 shows the nitrate reduction rate and nitrite accumulation rate in the presence of nitrate, nitrite reduction rate in the absence of nitrate and their respective specific reduction rates and relative rate for different pH at 677 mg L^{-1} of NO_3-N. Nitrate and nitrite reduction rates were calculated from the slopes of the nitrate and nitrite decay profiles, respectively. Nitrite accumulation rate was calculated from nitrite build up profile. Nitrate reduction rates varied between 307-336 mg L^{-1} h^{-1} at different pH for 677 mg L^{-1} of NO_3-N. Nitrite reduction rates in the presence of nitrate and in the absence of nitrate decreased with a decrease in feed pH. Relative rates (RR) were found to increase with a decrease in feed pH. This can be correlated with nitrite build up rates.

The optimum pH for most heterotrophic denitrifying bacteria was reported to be between 7 and 8 [105]. pH control in denitrifying reactors showed that the rate of denitrification was same in pH range between 7.5 and 9.5. Denitrification rates decreased significantly at pH values below 7 [12].

Table 4.5 Nitrate and nitrite denitrification rates for Zero order at different feed pH

Initial Feed pH	$K_{NO_3^-}$ (mg NO_3-N L^{-1} h^{-1})	$K_{NO_2^-}$ (mg NO_2- N L^{-1} h^{-1}) Nitrate is absent	$K'_{NO_2^-}$ (mg NO_2- N L^{-1} h^{-1}) Nitrate is present	RR
4.0	318	76	34	9.35
5.0	336	165	154	2.18
7.5	307	175	246	1.25

4.3.6 Conclusion

Denitrifying granules capable of complete denitrification of 1355 mg $L^{-1}NO_3$-N in the feed at pH 4 and 5 were cultivated in a three litre SBR. Complete denitrification of feed with pH 4 and 5 was successfully achieved by *in situ* neutralization caused by the biologically generated alkalinity and adaptation of microbial community. Denitrifying granules were colonized by rod and coccus shaped microorganisms when fed with nitrate waste at pH 7.5 and 4, respectively. The denitrification performance in bench scale SBR shows the practical utility of internal recycling of biologically generated alkalinity for neutralization and treatment of acidic nitrate waters.

- Batch experiments showed that pH 4 and 5 were inhibitory to denitrification of high strength nitrate.

- Compact denitrifying granular sludge capable of efficient denitrification was cultivated in 6 L volume SBR. Complete denitrification of 1355 mg L^{-1} NO_3-N in the feed at pH 4 and 5 could be successfully achieved in sequencing batch reactor.
- Denitrification of low pH high strength nitrate was possible because of internal recycling of denitrification generated alkalinity and adaptation of microbial community.
- The denitrification performance in bench scale SBR shows the practical utility of internal recycling of biologically generated alkalinity for neutralization and treatment of acidic nitrate waters.

4.4 Denitrification in continuous reactor

4.4.1 Operation of reactor

The continuous stirred tank reactor (CSTR) was operated, with a constant feed flow rate of 400 mL h^{-1} at an acetate-carbon to nitrate-nitrogen (C/N) ratio of 2. Stirring was provided by means of a bottom impeller set at 100 rpm. In most of the CSTRs, the feed will be at the top and stirred at high rpm for uniform concentration. Since high rpm is harmful to biomass, the feed was introduced at bottom to enhance mixing. The CSTR was operated in batch mode for 5 days at each concentration in order to acclimatize the biomass to high nitrate concentration and subsequently operated in CSTR mode for about 2 weeks at each influent nitrate concentration. Effluent samples were collected for monitoring nitrate, nitrite, pH, total organic carbon and biomass.

4.4.2 Biomass characterization

The reactor was inoculated with 1 g L^{-1} of MLSS initially. Steady increase in MLSS was observed as the number of days of operation increased. The reactor stability got

disturbed when the C/N ratio was decreased from 2 to 1.5 and the MLSS values also decreased.

4.4.3 Denitrification performance

a. Denitrification at C/N ratio of 2

In CSTR, the influent nitrate was increased in steps to 677, 1355, 2032 and 2710 mg L^{-1} NO_3-N shown in Fig. 4.15. Complete and stable denitrification was observed at all the initial nitrate concentrations in CSTR mode. Accumulation of neither nitrate nor nitrite was observed in the CSTR. However, accumulation of acetate was evident in the reactor indicating incomplete utilization. Subsequently, the acetate-carbon to nitrate-nitrogen ratio was decreased to 1.5 in the influent. .

Table 4.6 Biomass (MLSS, MLVSS) concentrations in the SBRs operated at different initial nitrate concentrations.
The biomass concentrations shown are obtained after attaining steady state in the CSTRs in terms of complete and stable denitrification.

Day	Nitrate Conc. (NO_3-N) mg L^{-1})	C/N	MLSS (g)	MLVSS (g)
8	677	2	1.40	0.94
25	1355	2	2.80	1.55
32	2032	2	2.96	1.55
90	2710	2	6.48	4.6
110	2710	1.5	3.76	2.36

b. Denitrification at C/N ratio of 1.5

CSTR containing denitrifying consortium was fed with synthetic waste with 2710 mg L^{-1} NO_3-N at C/N ratio of 1.5. At this C/N ratio, denitrification was complete. Accumulation of nitrate or nitrite was not observed during 10 days of operation.

c. Denitrification in Continuous EGSBR

Expanded Granular Sludge Bed Reactor (EGSBR) of 4 L volume containing denitrifying consortium was fed with synthetic waste with C/N ratio of 1.5. The feed concentration to the reactor was increased from 677 mg L^{-1} NO_3-N to 4742 mg L^{-1} NO_3-N. Denitrification was complete at the concentrations from 677 mg L^{-1} NO_3-N to 4742 mg L^{-1} NO_3-N. Accumulation of nitrate or nitrite was not observed during 90 days of operation.

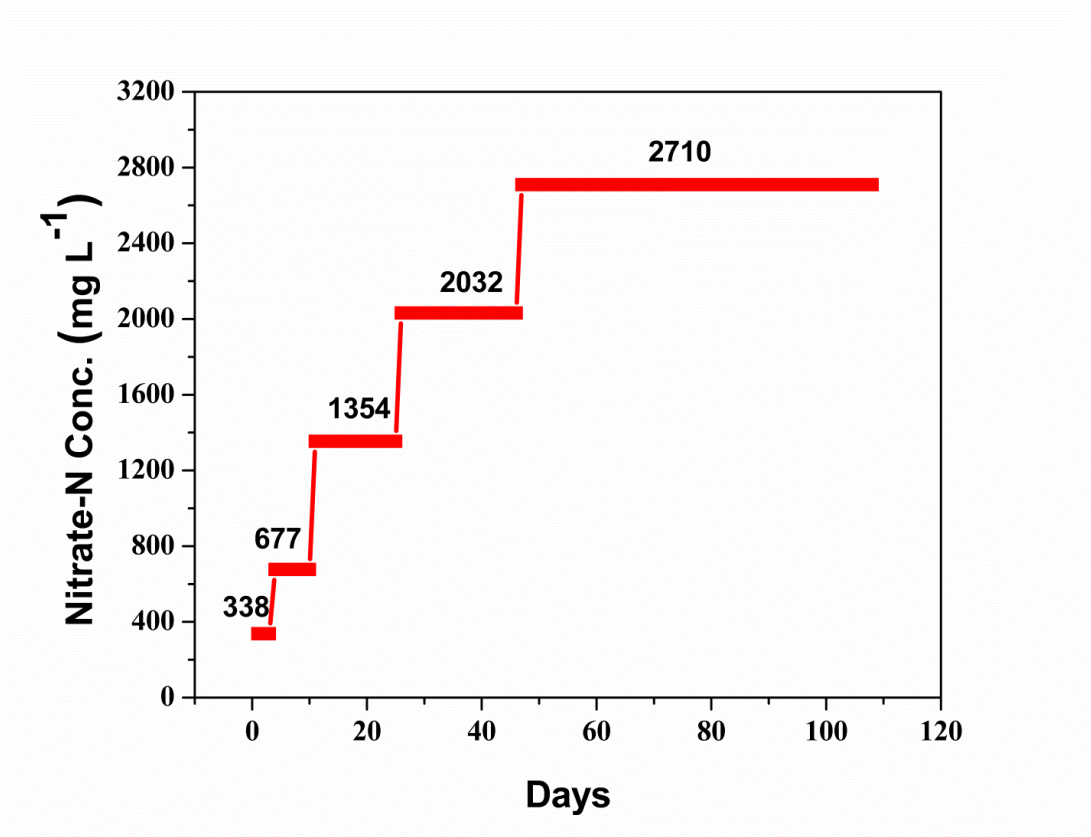

Fig. 4.21 Stepwise increase in nitrate concentration from 338 mg L^{-1} to 2710 mg L^{-1} NO_3-N in CSTR.

4.4.4 Conclusion

Compact denitrifying granular biomass capable of denitrification of up to 2710 mg L^{-1} NO_3-N at both C/N ratios was developed in a continuous stirred tank reactor. The denitrification was complete and stable during long term operation for both C/N ratios without any accumulation of nitrite. The study shows that C/N ratio of 1.5 is optimum for efficient and stable denitrification, as complete utilization of acetate was observed and further treatment of effluent for removal of excess carbon is not required. Complete denitrification up to 4742 mg L^{-1} NO_3-N was achieved in EGSBR with a hydraulic residence time of 16 h.

4.5 Denitrification at different temperatures

4.5.1 Reactor operation

Experiments were carried out at different temperatures using a jacketed glass tank to determine the effect of temperature on denitrification rate. The temperature in the reactor was maintained by allowing hot/cold water through the jacket.

4.5.2 Biomass characterization

Table 4.7 Biomass concentrations in the SBR operated at different temperatures.

The biomass concentrations shown are obtained after attaining steady state in the SBRs in terms of minimum time for complete and stable denitrification.

Nitrate Conc. (NO_3-N) mg L^{-1}	C/N	Temp	MLSS
677	1.5	20 ± 0.5 ^oC	6.0 ± 0.1
677	1.5	25 ± 0.5 ^oC	6.0± 0.2
677	1.5	30 ± 0.5 ^oC	6.0± 0.2
677	1.5	35 ± 0.5 ^oC	6.0± 0.1
677	1.5	40 ± 0.5 ^oC	6.0± 0.1

4.5.3 Denitrification at different temperatures

Nitrate and nitrite profiles at different temperatures during denitrification were shown in the Fig. 4.22 to Fig. 4.26. It was found that complete denitrification was observed at all temperatures. Steady decrease in nitrate concentration was observed for all initial nitrate concentrations at all temperatures without any accumulation. Slower removal of nitrate was observed at lower temperatures because lower bacterial activity. Nitrate removal rate increased with increase in temperature. Nitrite concentrations increased from zero to a peak value and subsequently the concentration steadily decreased at all temperatures. The time for nitrite peak corresponds to the time for complete conversion of nitrate, as shown in Fig. 4.22 to Fig. 4.26. Nitrite peak was about 300-350 mg L^{-1} for the temperatures 20-30 ^{o}C. Nitrite peak concentrations increased to 450 mg L^{-1} at 35 ^{o}C because of sudden decrease in nitrate reduction time but nitrite peak concentration reduced to 300 mg L^{-1} at 40 ^{o}C could be because of higher biological activity. Time required for complete denitrification reduced with increase in temperature due to faster kinetics.

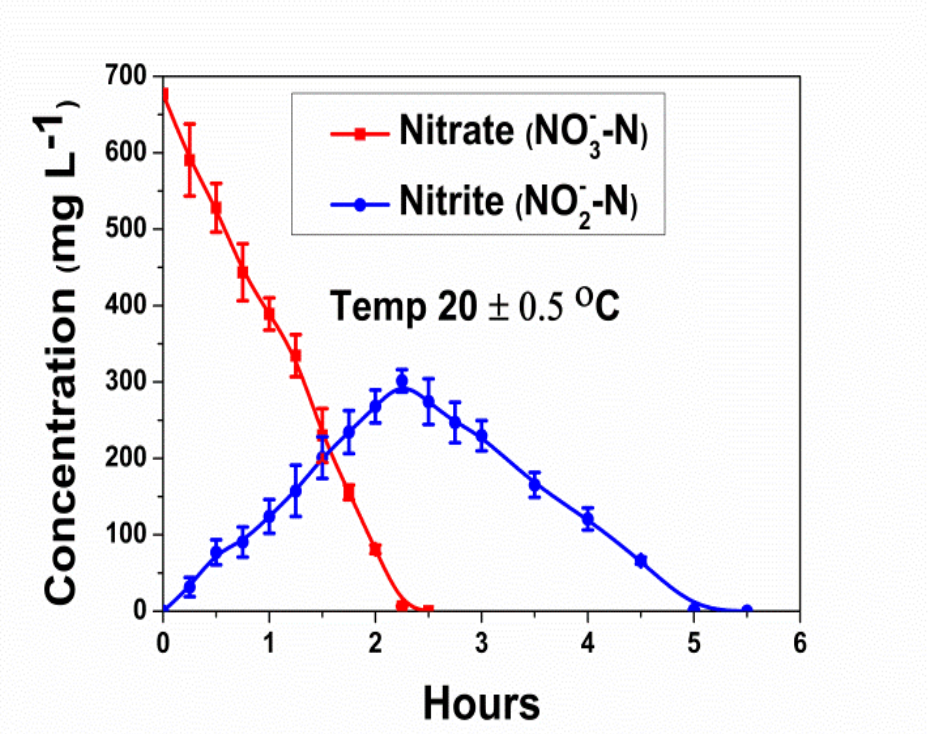

Fig. 4.22 Concentration profile of nitrate and nitrite during denitrification at 20 ± 0.5 °C.

Initial nitrate concentration 677 mg L^{-1}, $pH_{initial}$ = 7.5, MLSS = 6± 0.1 g L^{-1}.

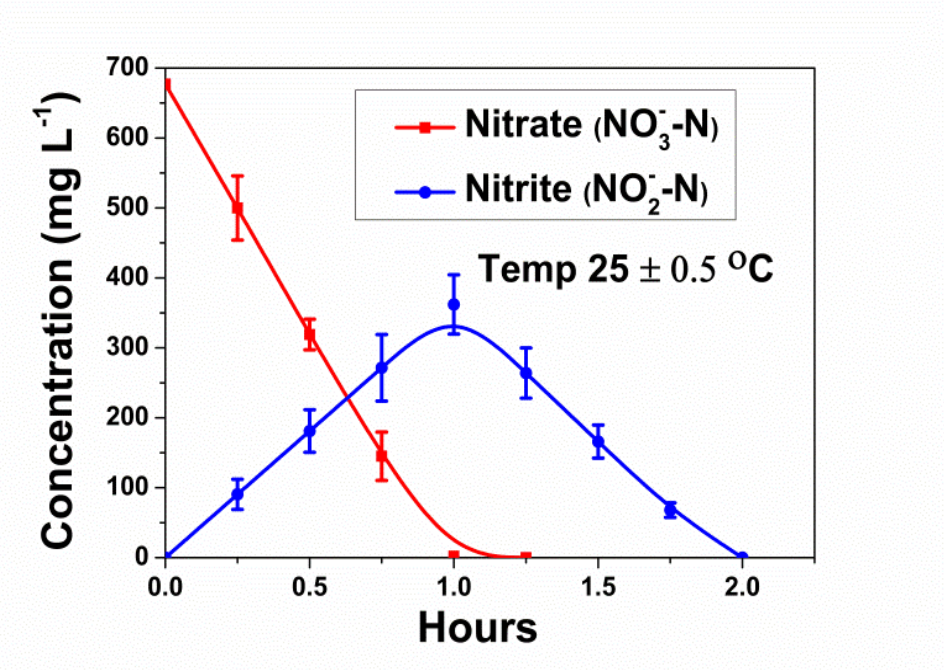

Fig. 4.23 Concentration profile of nitrate and nitrite during denitrification at 25 ± 0.5 °C.

Initial nitrate concentration 677 mg L^{-1}, $pH_{initial}$ = 7.5, MLSS = 6± 0.2 g L^{-1}

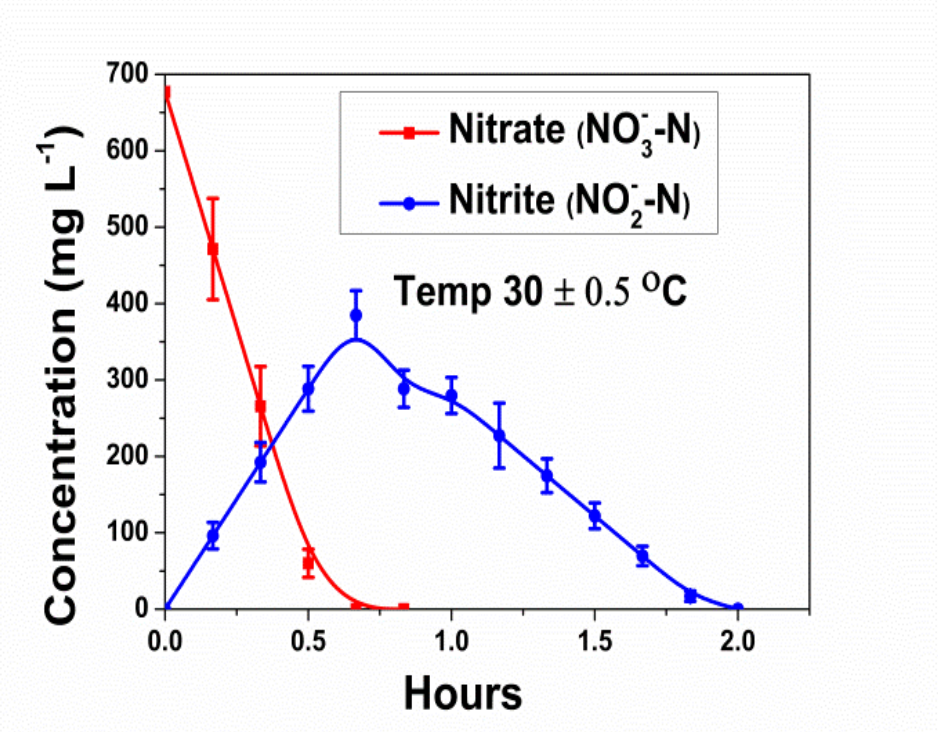

Fig. 4.24 Concentration profile of nitrate and nitrite during denitrification at 30 ± 0.5 °C.

Initial nitrate concentration 677 mg L^{-1}, $pH_{initial}$ = 7.5, MLSS = 6± 0.2 g L^{-1}.

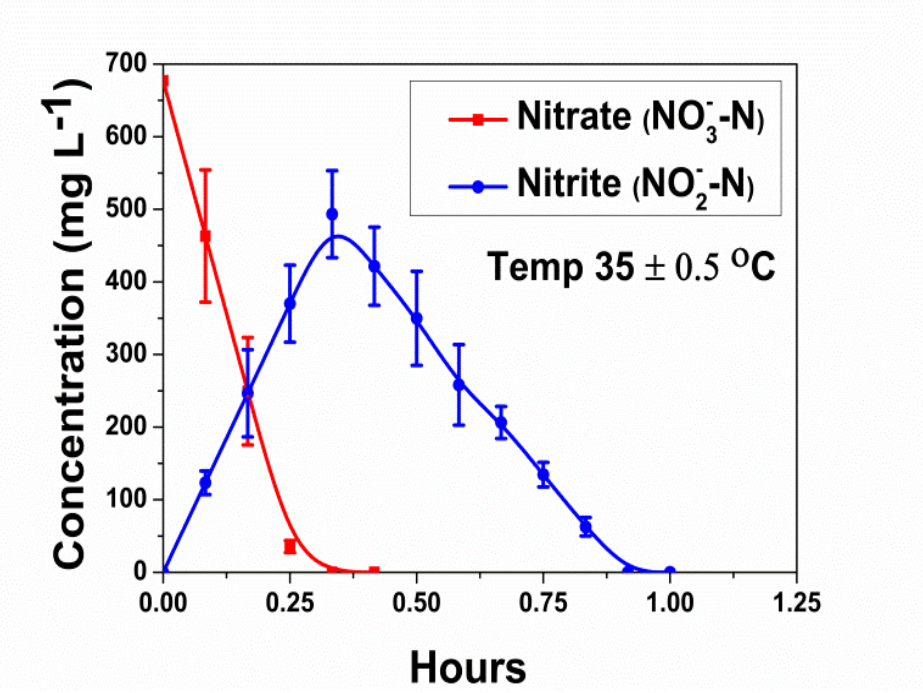

Fig. 4.25 Concentration profile of nitrate and nitrite during denitrification at 35 ± 0.5 °C.

Initial nitrate concentration 677 mg L^{-1}, $pH_{initial}$ = 7.5, MLSS = 6± 0.1 g L^{-1}

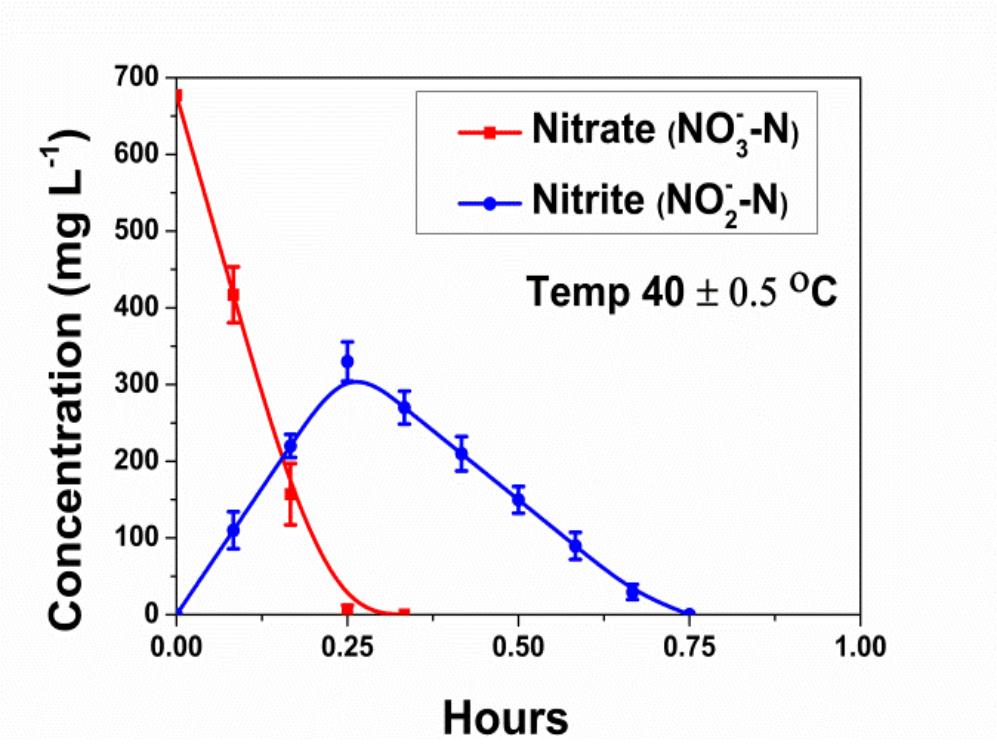

Fig. 4.26 Concentration profile of nitrate and nitrite during denitrification at 40 ± 0.5 °C.

Initial nitrate concentration 677 mg L^{-1}, $pH_{initial}$ = 7.5, MLSS = 6± 0.1 g L^{-1}

4.5.4 Reaction kinetics

Table 4.8 Nitrate and Nitrite denitrification rates at different temperatures

Initial Nitrate in the SBR (mg L^{-1})	$K_{NO_3^-}$ (mg NO_3- N L^{-1} h^{-1})	$K_{NO_2^-}$ (mg NO_2-N L^{-1} h^{-1}) Nitrate is absent	$K'_{NO_2^-}$ (mg NO_2-N L^{-1} h^{-1}) Nitrate is present	RR
20 ± 0.5 °C	1319.36	358.34	440.68	2.73
25± 0.5 °C	3080.16	1289.38	1191.4	1.77
30 ± 0.5 °C	5467.16	1037.3	1896.58	2.14
35± 0.5 °C	11363.98	2830.38	4864.5	2.97
40± 0.5 °C	13820.42	2372.22	4339.64	4.32

The nitrate reduction rate, nitrite accumulation rate in the presence of nitrate, nitrite reduction rate in the absence of nitrate and relative rate for different at different temperatures are tabulated in Table 4.7. Nitrate reduction rates increased from 1319 mg NO_3-N L^{-1} h^{-1} at 20 ^oC to 13820 mg NO_3-N L^{-1} h^{-1} at 40 ^oC. The nitrite reduction rates in the presence of nitrate and in the absence of nitrate also increased with increase in temperature.

Temperature influences the biological denitrification significantly. Fig. 4.27 shows the Arrhenius plot for K_{NO_3}. The obtained line with linear fit (y= -11.044 x + 45.007) had a high degree of linearity (R^2 = 0.956). The obtained activation energy, 91.81 kJ/mol, which is higher than the reported in literature [90,133]. Higher values for activation energy clearly reflected on decrease in time for nitrate reduction.

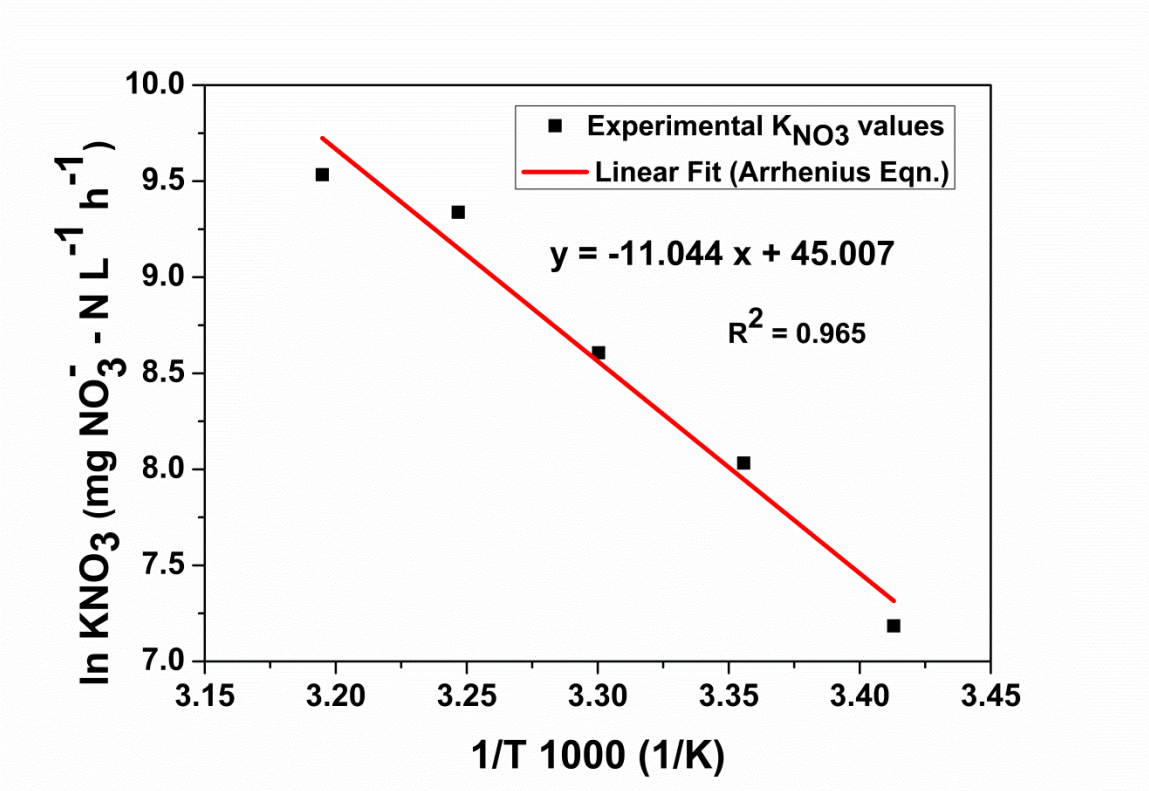

Fig. 4.27 Graphic plot of ln K_{NO3} w.r.t. 1/T

The magnitude of temperature influence can be expressed by an Arrhenius-type function of the form:

$$k_T = k_{20}\,\theta^{(T-20)} \qquad 4.2$$

Where k_T is the denitrification rate at temperature T

Fig. 4.28 shows the influence of temperature on the denitrification rates and the calculated θ is 1.15 for the temperature range 20-35 ^{o}C, which is slightly higher than reported values 1.02-1.08 [156] and 1.06 to 1.13 [146].

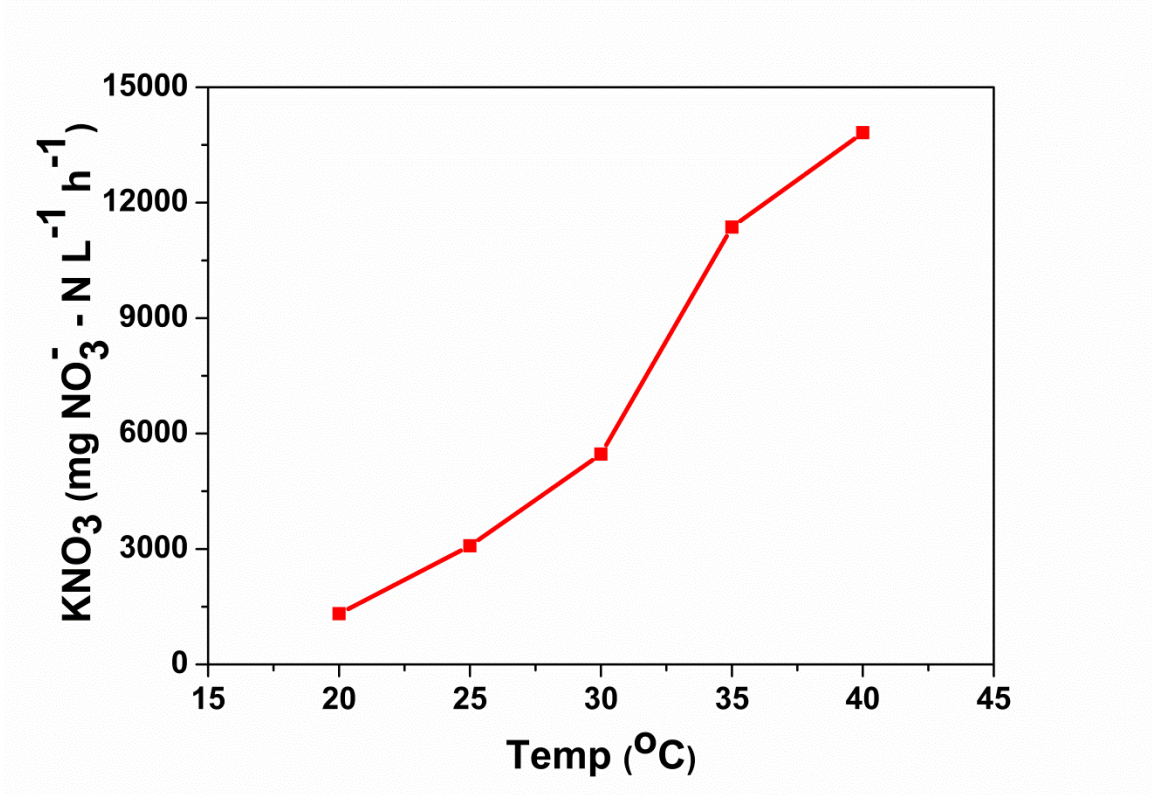

Fig. 4.28 Effect of temperature on denitrification rate

4.5.5 Conclusion

Complete denitrification of SNW for nitrate concentration of 1355 mg L^{-1} NO_3-N was observed at all temperatures studied. Nitrite accumulation for all C/N ratios at all temperatures was observed. Denitrification rates were found to increase with increase in

temperature. Kinetic study revealed that nitrate and nitrite denitrification rates were found to be zero order. The study shows that 35-40 ^{o}C was found to be optimum for efficient denitrification.

4.6 Denitrification at very high nitrate concentrations

4.6.1 Reactor Operation

The reactor was operated in sequencing batch mode with a cycle time of 24 h. The cycle period consists of 5 min filling, 23 hour reaction, 5 min settling, 10 min effluent decant period and 40 min idle period. Nitrate concentration in the reactor increased in steps from 677 mg L^{-1} NO3-N to 4742 mg L^{-1} NO_3-N with an objective to develop compact denitrifying granular biomass capable of denitrification of highest possible nitrate concentrations. Mixing was provided by means of an impeller stirred at 100 rpm. Each reactor was inoculated with 1 L of activated sludge and SNW. The reactors were either filled at the bottom using a peristaltic pump or dump filled by manual addition. At the end of cycle period, effluent was drawn from port situated at a height of 17 cm from the bottom using a peristaltic pump. The reactor was operated at C/N of 1.5. Typically, the SBRs were operated with 24 h cycle period and 50% volume exchange ratio for convenience.

4.6.2 Biomass characterization

Formation of granular sludge (Fig. 4.29 A) with good settling characteristics was observed within two weeks of reactor start-up. The granular sludge formed under anoxic conditions was compact, dense and allowed easy biomass - liquid separation in the reactor. Average particle size was determined to be 0.68 mm (Fig. 4.30). The biomass concentration in the SBR increased from 2.5 to 29.5 g L^{-1} MLSS during reactor operation up to 9484 mg L^{-1} NO_3-N feed concentration. Up to 50% of the MLSS was constituted by

inorganic solids as shown in Table 4.8. The denitrifying granular sludge was stable during several months of SBR operation. Scanning electron microscope showed the presence of both cocci and rod shaped cells enmeshed in an EPS matrix (Fig.4.29 B, C, D). Microbial community analysis by PCR-DGGE revealed a major shift in the microbial population of denitrifying granular sludge during its transformation from floccular activated sludge to compact granular sludge (Fig. 4.30). As can be seen from Fig. 4.31A, the DGGE pattern showed a major shift in microbial community reflected in terms of number and intensity of bands. There were changes in the intensity of the bands and also appearance of new bands during the course of reactor operation as the nitrate concentration increased. However, establishment of a stable microbial community is seen at each initial nitrate concentration. The DGGE banding pattern was clustered into three major groups (Fig. 4.31B). Group I contained activated sludge, which was used for cultivation of denitrifying granular sludge. Groups II and III contained banding patterns associated with establishment of denitrifying granular sludge, with a major shift in microbial community of activated sludge. The band patterns of microbial community denitrifying up to 1355 mg $L^{-1}NO_3$-N were clustered into group II, while the band patterns obtained from microbial community, treating from 2710 to 4065 mg $L^{-1}NO_3$-N clustered into to group III.

Table 4.9 Biomass (MLSS, MLVSS) concentrations in the SBRs operated at different initial nitrate concentrations.

The biomass concentrations shown are obtained after attaining steady state in the SBRs in terms of minimum time for complete and stable denitrification.

Nitrate Concentrations (mg L^{-1})	**Initial Nitrate-Nitrogen in the SBR (mg L^{-1} NO_3-N)**	**MLSS (g L^{-1})**	**MLVSS (g L^{-1})**
3000	677	5.05	2.40
6000	1355	6.82	2.92
9000	2032	9.70	4.74
12000	2710	15.88	7.96
15000	3387	18.30	8.77
18000	4065	22.32	9.16
21000	4742	25.90	11.69

4.6.3 Denitrification performance

The pH of Simulated nitrate waste (SNW) prior to addition to the SBR was 7.5. In the SBR, the pH increased to above 9 during the first cycle and stabilized close to 9.5 during subsequent cycles of denitrification (Fig. 4.32). The DO in the feed was 6 mg L^{-1}, which after addition to the SBR dropped to below 0.08 mg L^{-1}. This drop was apparently caused by intense microbial activity. It has been reported that denitrification at these pH and DO conditions is significant [12,109,142]. It was observed in the present work that denitrification was effective from the first cycle onwards. Further, the time required for

complete denitrification decreased significantly during the first few cycles and stabilized at the lower value thereafter.

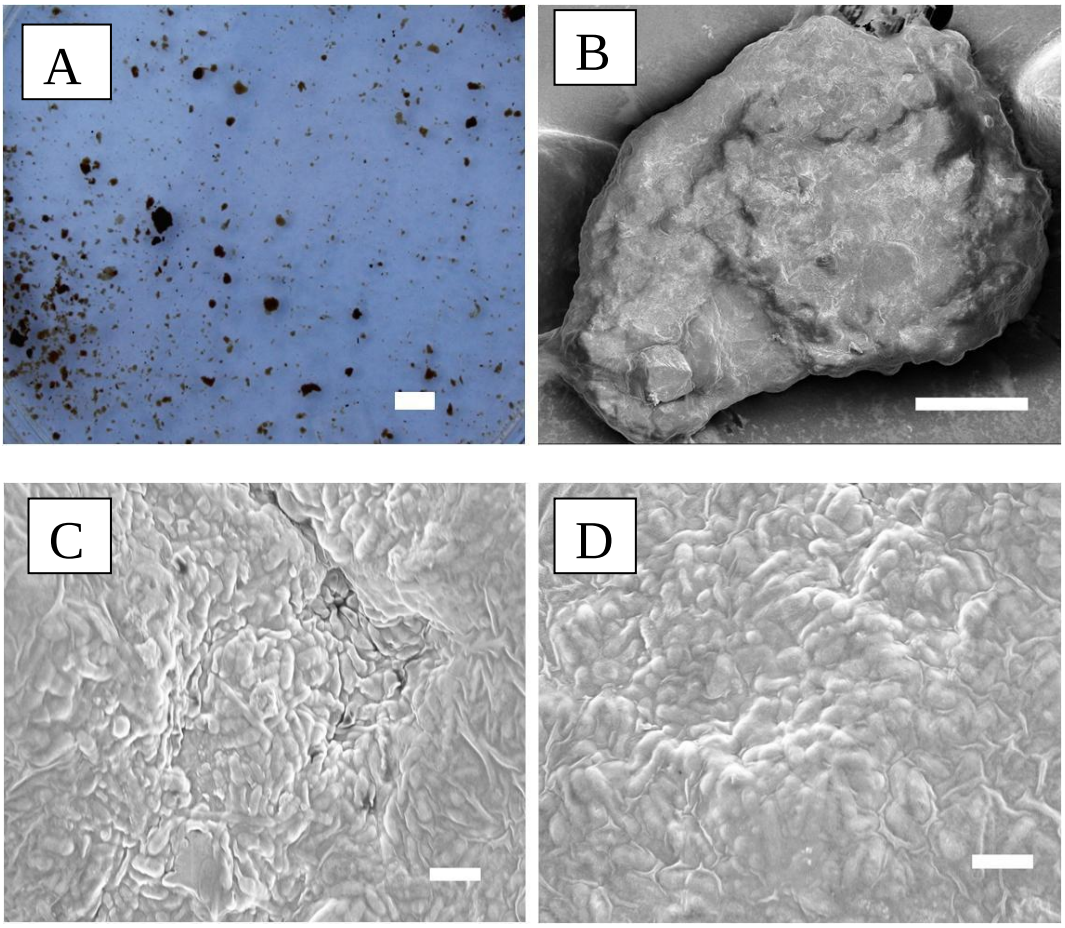

Fig. 4.29 Morphology (A, B) and microstructure (C, D) of denitrifying granular sludge formed in 6 L volume SBR.
For A, Bar = 5 mm. B, C and D are scanning electron microscope images of denitrifying granular sludge. Bar = 0.1 mm (B), 2 µm (C, D). Shape of bacteria and slimy appearance on the surface of granular sludge is shown in C and D.

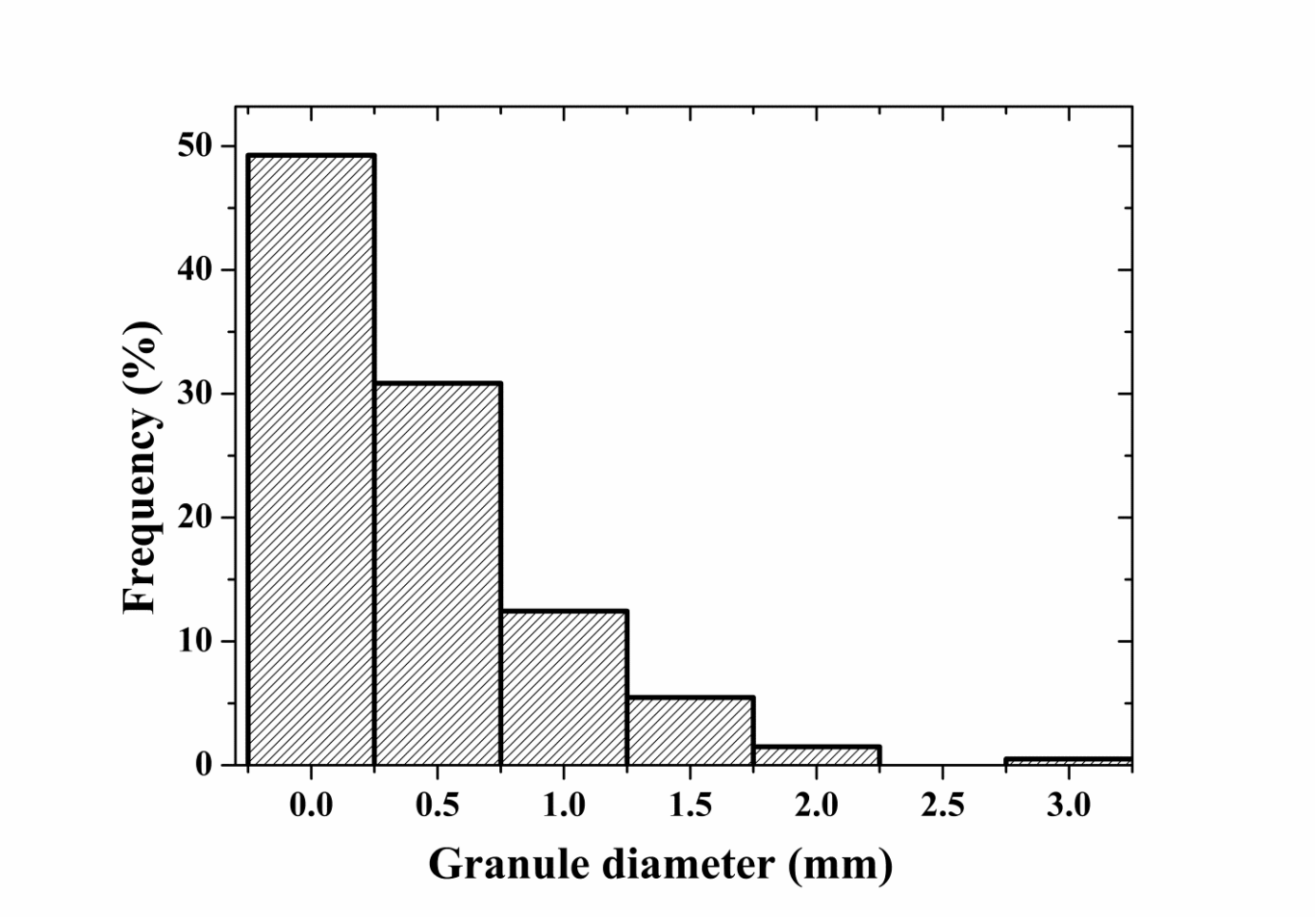

Fig. 4.30 Particle size distribution of denitrifying granular sludge cultivated in a 6 L volume SBR

SBR inoculated with activated sludge and fed with simulated nitrate waste. The average particle size was found to be 0.68 mm.

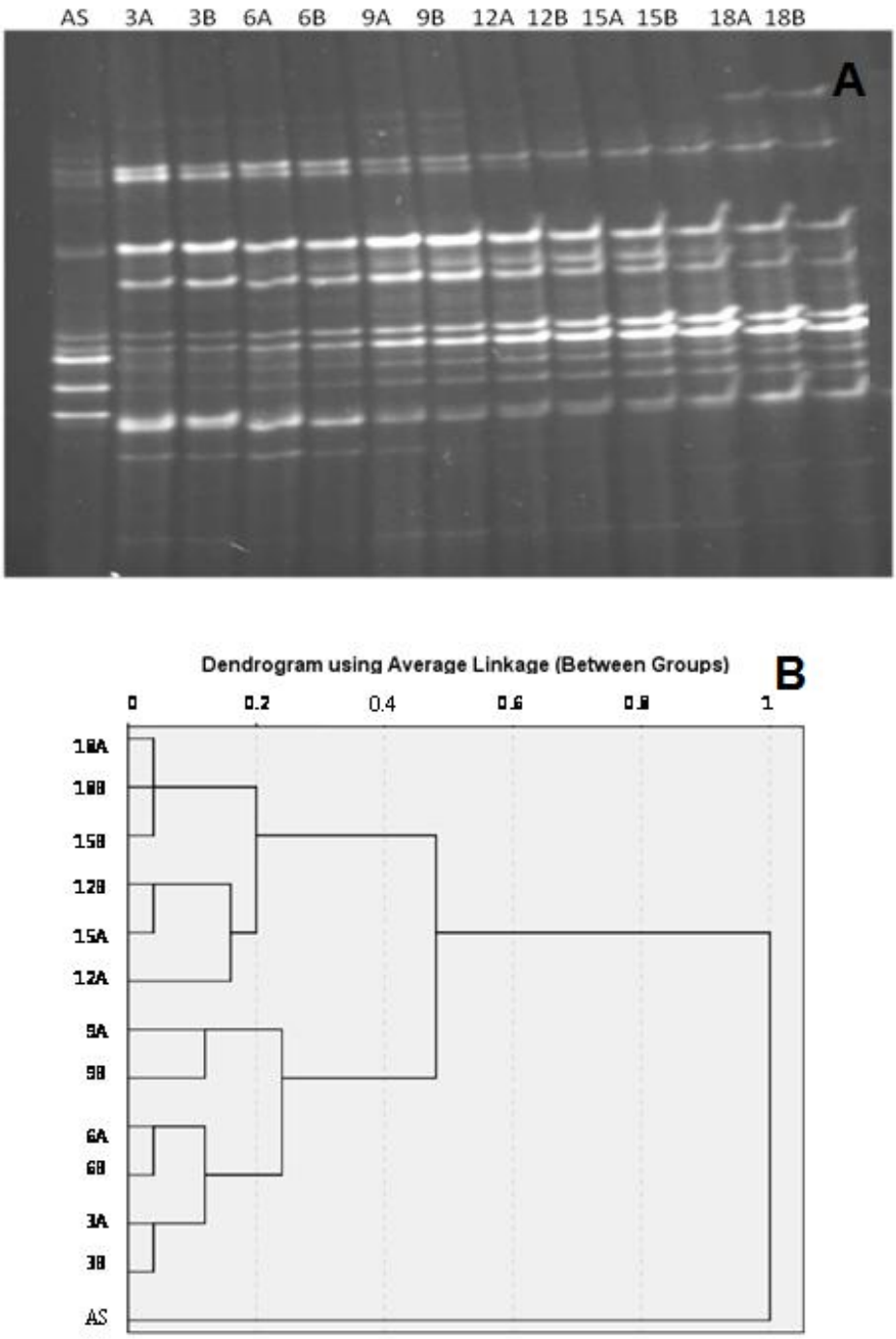

Fig. 4.31 PCR-DGGE analysis of denitrifying granular sludge at different initial nitrate concentrations.

A) DGGE gel shows the number of bands in the denitrifying consortium obtained from SBR. B) Dendrogram shows the relation between different lanes of DGGE gel.

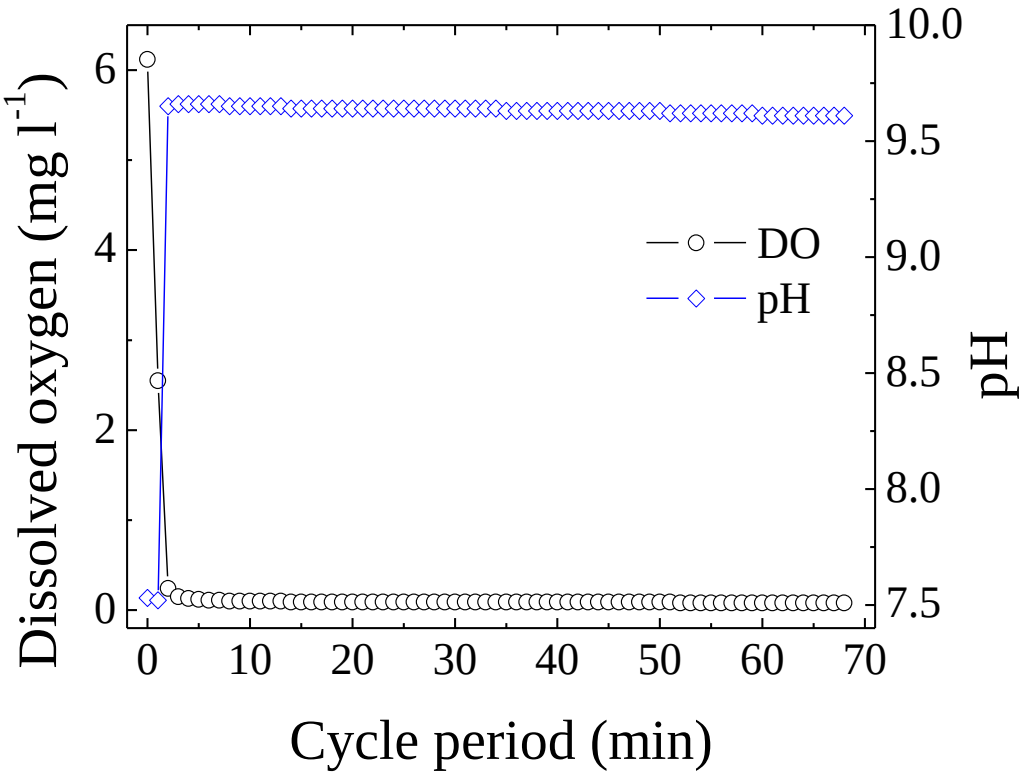

Fig. 4.32 pH and dissolved oxygen profiles during SBR cycle period.
The reactor was fed with SNW containing 1355 mg L^{-1} NO_3-N. Before adding to the SBR, the pH and DO were 7.5 and 6.0 mg L^{-1} respectively.

In order to optimize the C/N ratio, denitrification of 1355 mg L^{-1} NO_3-N was studied at acetate-C to nitrate-N ratios of 1.5, 2 and 3. Complete denitrification was observed within 2 h at all the tested C/N ratios. Hence, a fixed C/N ratio of 1.5 was chosen for denitrification of higher initial concentrations of nitrate. Fig. 4.33 to Fig. 4.39 show denitrification profiles during the SBR cycle period, in terms of nitrate removal, and build-up and subsequent removal of nitrite. The total time required for complete denitrification increased with increase in the initial nitrate concentration. At steady state, complete denitrification of 9484 mg L^{-1} NO_3-N was achieved in 20 h. By the time the nitrite concentration reached the maximum, more than 95% nitrate was reduced.

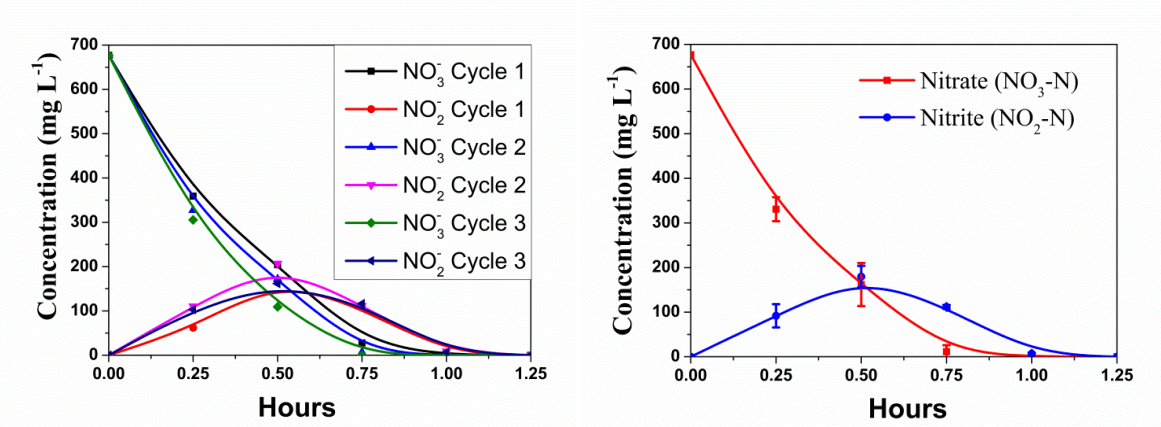

Fig. 4.33 Nitrate and nitrite concentration profiles during denitrification of 677 mg L^{-1} NO_3-N

SNW with initial pH of 7.5 and MLSS 5.05 g L^{-1}. Error bars are ± one standard deviation.

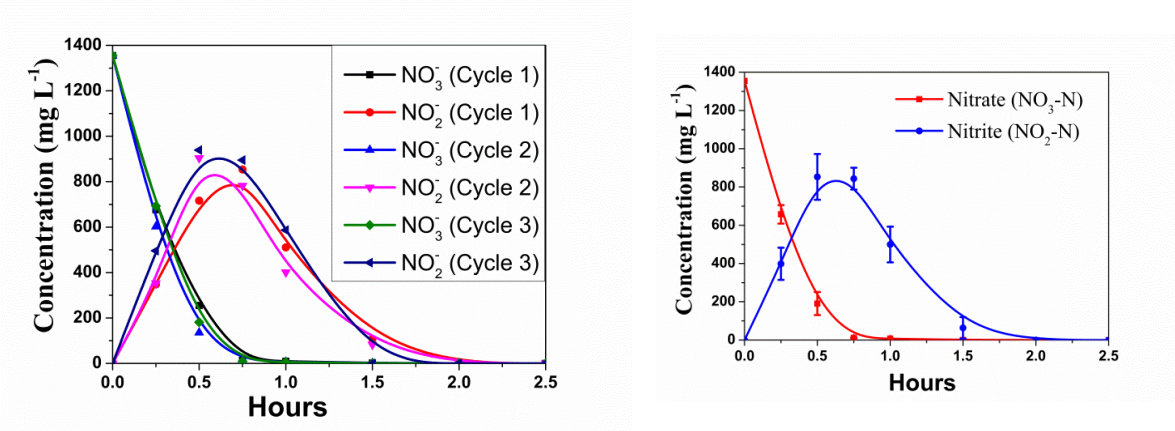

Fig. 4.34 Nitrate and nitrite concentration profiles during denitrification of 1355 mg L^{-1} NO_3-N

SNW with initial pH of 7.5 and MLSS 6. g L^{-1}. Error bars are ± one standard deviation.

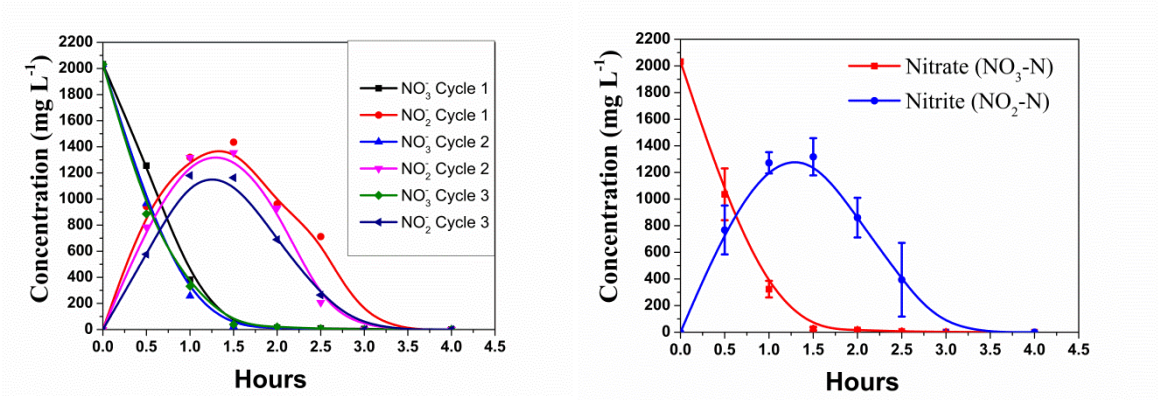

Fig. 4.35 Nitrate and nitrite concentration profiles during denitrification of 2032 mg L^{-1} NO_3-N

SNW with initial pH of 7.5 and MLSS 9.70 g L-1. Error bars are ± one standard deviation.

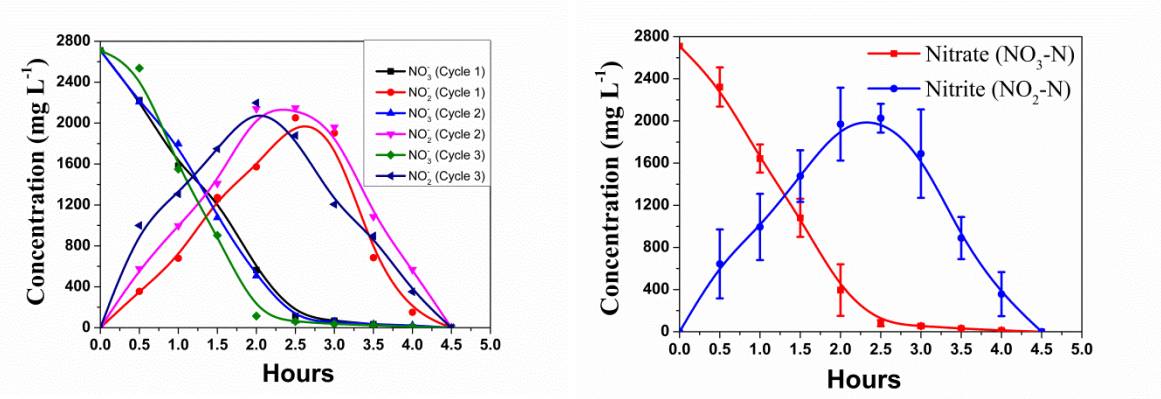

Fig. 4.36 Nitrate and nitrite concentration profiles during denitrification of 2710 mg L^{-1} NO_3-N

SNW with initial pH of 7.5 and MLSS 15.88 g L^{-1}. Error bars are ± one standard deviation**.**

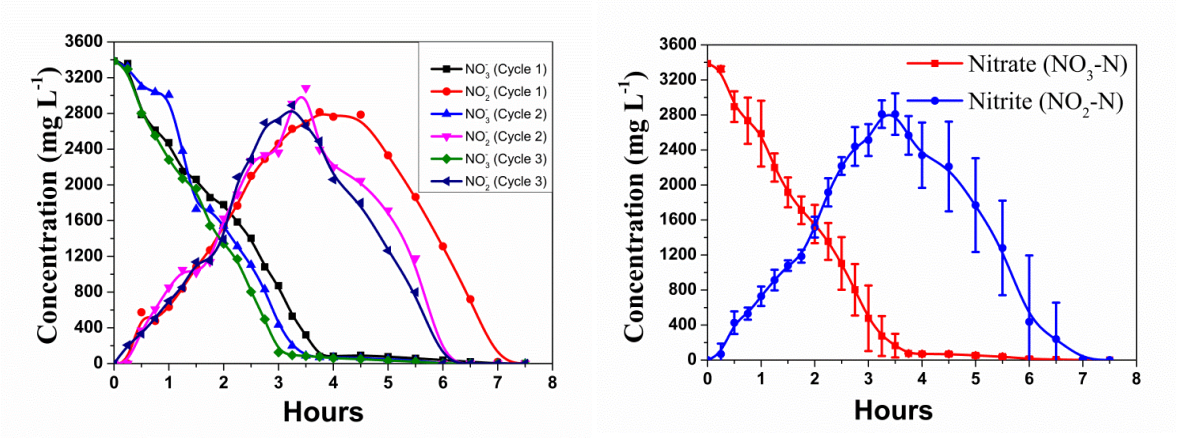

Fig. 4.37 Nitrate and nitrite concentration profiles during denitrification of 3387 mg L^{-1} NO_3-N

SNW containing with initial pH of 7.5 and MLSS 18.30 g L^{-1}. Error bars are ± one standard deviation.

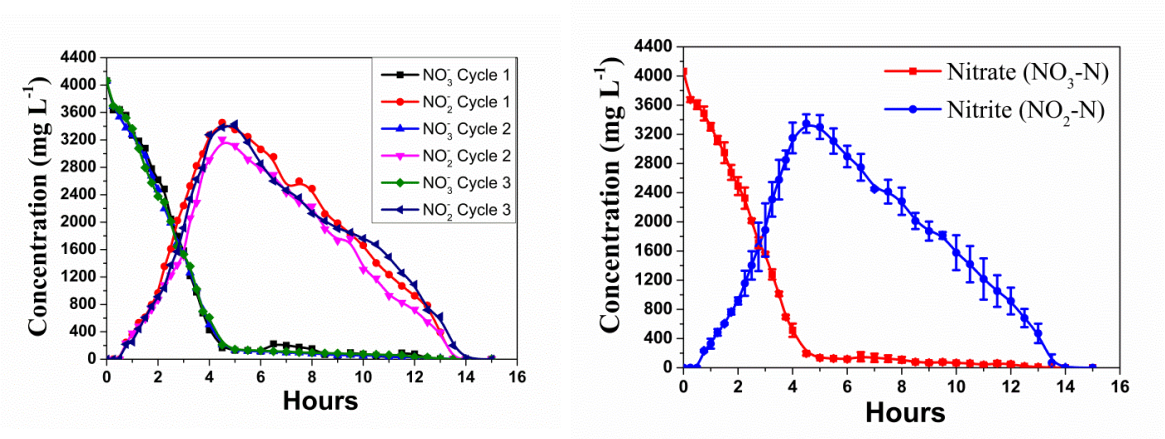

Fig. 4.38 Nitrate and nitrite concentration profiles during denitrification of 4064 mg L^{-1} NO_3-N

SNW containing with initial pH of 7.5 and MLSS 22.32 g L^{-1}. Error bars are ± one standard deviation

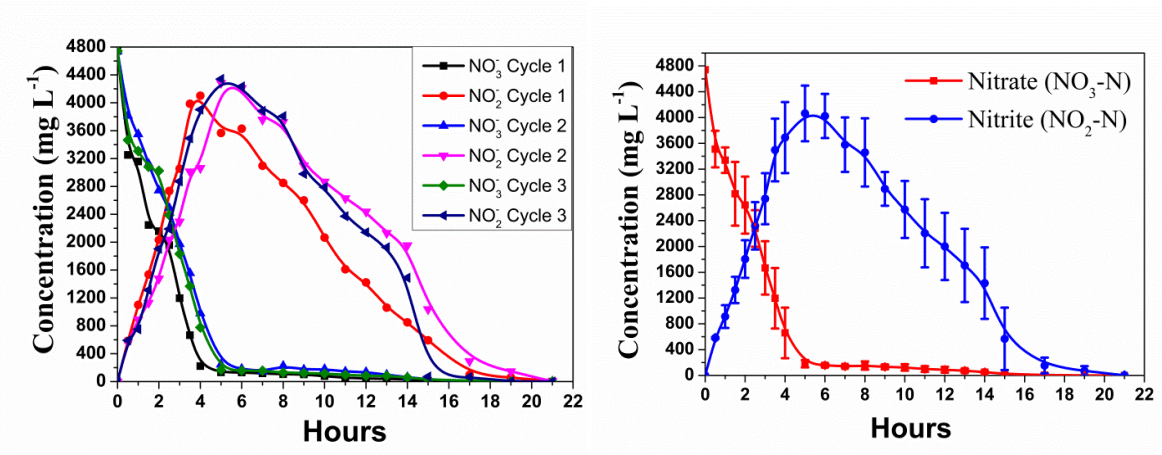

Fig. 4.39 Nitrate and nitrite concentration profiles during denitrification of 4742 mg L^{-1} NO_3-N

SNW containing with initial pH of 7.5 and MLSS 25.90 g L^{-1}. Error bars are ± one standard deviation.

Nitrite accumulation was observed at all the nitrate concentrations studied and this is presented in Fig. 4.40, both in terms of absolute values and as % of maximum nitrite that would have been accumulated, if there was no nitrite reduction. NO_2-N build up was only 26% for denitrification of 1355 mg L^{-1} NO_3-N in the influent, but increased to almost 85% for denitrification of 9484 mg L^{-1} NO_3-N. Glass and Silverstein [12] reported nitrate accumulation of 3778 mg L^{-1} NO_2-N (85%) for influent nitrate concentration of 2710 mg L^{-1} NO_3-N, whereas 2803 mg L^{-1} NO_2-N (62%) was observed in the present work. Dhamole et al.[74] reported accumulation of 5907 mg L^{-1} NO_2-N (98%) for influent nitrate concentration of 9032 mg L^{-1} NO_3-N, whereas accumulation of 4064 mg L^{-1} NO_2-N (85%) was observed in the present work for influent nitrate concentration of 9484 mg L^{-1} NO_3-N. Activated sludge is reported to contain true denitrifiers, which reduce nitrate to nitrogen gas and nitrate respirers, which reduce nitrate to nitrite. Nitrite is further reduced to nitrogen gas by nitrite reductase. Presence of

true denitrifiers in more proportion in the activated sludge may be responsible for less nitrite build up in the present work.

Temperature has been monitored during the denitrification cycle for all the initial nitrate concentrations. Maximum temperature reached during denitrification increased with increase in the initial concentration of nitrate, because of the exothermic reactions. Temperature rise was 7 ^{o}C – 16 ^{o}C for the concentrations studied.

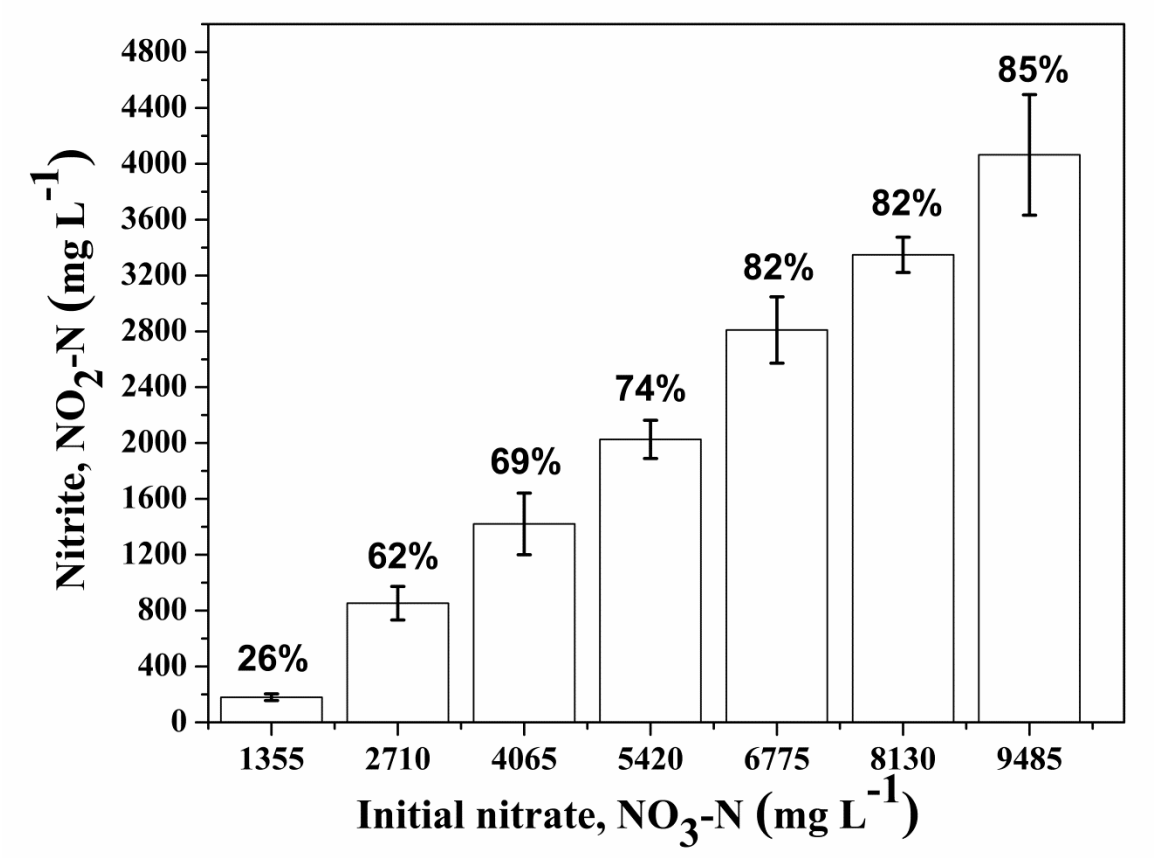

Fig. 4.40 Maximum nitrite concentration at different initial nitrate concentrations
Given as absolute values and as percentage of initial nitrate concentration. The denitrification experiments were carried in a sequencing batch reactor at fixed C/N ratio of 1.5. The data points represent average of three consecutive cycles and error bars represent standard deviation.

4.6.4 Denitrification kinetics

Nitrate and nitrite reduction rates were calculated from the slopes of the nitrate and nitrite decay profiles, respectively. Nitrite accumulation rate is calculated from nitrite build up profile. The change of MLSS from 2.5 to 29.5 g L^{-1}, indicated in section 4.5.2, is over a time period of 100 days. As the denitrification cycle is only one day, the MLSS is taken to be constant in this period. Specific denitrification rates were calculated by dividing the nitrate and nitrite decay slopes by the MLSS concentrations. These rates are presented in Table 4.9. The rate constants for nitrate and nitrite denitrification for nitrate concentrations of 677 to 4742 mg L^{-1} NO_3-N (in the SBR) can be divided into two groups. The rate constants are in the range of 63 – 292 mg NO_3-N or NO_2-N L^{-1}g $MLSS^{-1}$ h^{-1} for initial reactor concentrations of 677 to 2032 mg L^{-1} of NO_3-N and the maximum temperature reached during denitrification was less than 40 ^oC. On the other hand for initial reactor concentrations of 2710 – 4742 mg L^{-1} of NO_3-N, rate constants of 5.2 – 68 mg NO_3-N or NO_2-N L^{-1}g $MLSS^{-1}$ h^{-1} were observed (in the SBR) and the maximum temperatures were 42-48 ^oC. The optimum temperature for denitrification was reported to be 36-37 ^oC [75,157]. With rising temperature, proteins, nucleic acids and other cellular components that are sensitive to temperature will tend to become irreversibly deactivated and lysis, death and endogenous metabolism rates will increase [101]. Increase in the temperature during denitrification at higher concentrations could be the reason for reduced denitrification rate constants. Relative rates increased with increase in the initial nitrate concentration in the reactor. This increase is associated with increase in the accumulation of nitrite due to decrease in nitrite reduction rate in the presence of nitrate.

Table 4.9 shows that there was a decrease in the rate constants during denitrification of higher initial nitrate concentrations. Similar observation was reported by Glass and

Silverstein [13]. The widely applied kinetic model of Monod [158] was originally derived for continuous–growth pure-culture systems. It must be borne in mind that biological denitrification is a complex process, compounded by the heterogeneous nature of both the substrate and microbial population [101]. The growth yield, Y is usually considered a constant during modelling but can vary, according to reaction conditions. Due to these limitations, this model is incomplete for nitrate concentrations above 400 mg L^{-1} NO_3-N [90].

Nitrite is known to exert inhibition on heterotrophic bacteria at concentrations higher than 200 mg L^{-1} [159]. It is evident that nitrite build-up prolonged the total time required for complete denitrification, probably by such inhibition [12,159]. The specific denitrification rates obtained in this study were much higher than those obtained using activated sludge [13,74,90,147]. A comparison of the specific denitrification rates reported in the literature is given in Table 4.11 [12,74,90,133,148-150]. These can be compared with the specific denitrification rates reported in the present work, which are given Table 4.10. Specific denitrification rates obtained by Dhamole et al. [74] for 4516 mg L^{-1} NO_3-N were slightly higher but were obtained at a higher C/N ratio of 2. Though nitrite build-up can be inimical in biological denitrification of high strength nitrate, the compact microbial structure of granular sludge allows denitrifying microorganisms to function despite such high nitrite concentrations. This appears to be a promising feature justifying the application of granular biomass for high strength nitrate denitrification.

4.6.5 Conclusion

Compact denitrifying granular biomass capable of efficient denitrification of up to 9484 mg L^{-1} NO_3-N was developed in SBR operated with 24 h cycle period and 50%

volumetric exchange ratio. Microscopy showed that compact granular sludge was composed of cocci and rod shaped cells enmeshed in a matrix. PCR-DGGE revealed a major shift and formation of stable microbial community during denitrification. Nitrite accumulation of up to 85% of initial nitrate was observed. High specific denitrification rates were observed which were 2 - 3 times higher than those reported for activated sludge systems. The study shows that granular sludge sequencing batch reactors could be effectively employed for treatment of high strength nitrate wastes of industrial origin, at low C/N ratios with fast kinetics and are inherently immune to the problems caused by nitrite accumulation.

Table 4.10 Nitrate and Nitrite denitrification rates and specific denitrification rates for Zero order at different nitrate concentrations.

Initial Nitrate-N in the SBR (mg L^{-1})	$K_{NO_3^-}$ (mg NO_3-N L^{-1} h^{-1})	$K_{NO_2^-}$ (mg NO_2-N L^{-1} h^{-1}) Nitrate is absent	$K'_{NO_2^-}$ (mg NO_2-N L^{-1} h^{-1}) Nitrate is present	$\frac{K_{NO_3^-}}{X}$ (mg NO_3-N L^{-1} h^{-1} g^{-1} MLSS)	$\frac{K_{NO_2^-}}{X}$ (mg NO_2-N L^{-1} h^{-1} g^{-1} MLSS) Nitrate is absent	$\frac{K'_{NO_2^-}}{X}$ (mg NO_2-N L^{-1} h^{-1} g^{-1} MLSS) Nitrate is present	RR
677	1472.8	496	995.7	291.5	98.2	197.2	1.5
1355	1656.0	486	1003.5	242.8	71.3	147.1	1.7
2032	1440.0	938.16	610.9	148.5	96.7	62.9	2.4
2700	1005.5	1077	273.4	63.3	67.8	17.2	3.7
3387	908.6	765	164.9	49.6	41.8	9.0	5.5
4064	840.2	347.4	159.2	37.6	15.6	7.1	5.3
4742	1000.1	293.8	135.6	38.6	11.3	5.2	7.4

Table 4.11 Specific denitrification rates reported in literature

Initial nitrate concentration (mg $L^{-1}NO_3$–N)	The specific denitrification rate K_{NO_3}/X	Temperature (^oC)	References
1350	23–54 mg NO_3 –N L^{-1} g^{-1} MLSS h^{-1}	25	[12]
100-500	21.0 mg NO_3 –N L^{-1} g^{-1} MLVSS h^{-1}	25	[90]
847	24 mg NO_3 –N L^{-1} g^{-1} MLSS h^{-1}	*	[74]
1694	91 mg NO_3 –N L^{-1} g^{-1} MLSS h^{-1}	*	[74]
4132	42 mg NO3 –N L^{-1} g-1 MLSS h^{-1}	*	[74]
6002	66 mg NO3 –N L^{-1} g-1 MLSS h^{-1}	*	[74]
750	56.3 mg NO_3 –N L^{-1} g^{-1} MLVSS h^{-1}	25	[133]
5	10–20 mg NO_3 –N L^{-1} g^{-1} MLVSS h^{-1}	20	[148]
550	32–111 mg NO_3 –N L^{-1} g^{-1} MLVSS h^{-1}	25	[150]
140	12–27.6 mg NO_3 –N L^{-1} g^{-1} biomass h^{-1}	30	[149]

* Not reported

4.7 Denitrification in Semi Pilot Scale reactor

4.7.1 Operation of reactors

A 24 L volume semi pilot reactor was operated in sequencing batch mode with a cycle time of 24 h and 50% VER. Mixing was provided by recirculation of the reactor fluid. Each reactor was inoculated with 1 L of activated sludge and simulated nitrate waste. The nitrate in the feed was increased step wise from 6, 12, 18 and 24 g L^{-1}.

4.7.2 Biomass Characterization

Granular sludge was observed within two weeks of semi pilot scale reactor startup. The granular sludge formed under anoxic conditions allowed easy separation of biomass from treated liquid during short settling period employed during SBR operation. Denitrifying biomass was predominantly in the form of distinct, compact and well settling particles. Scanning electron microscope showed the presence of rod shaped microorganisms enmeshed in a slimy matrix of granular sludge formed in the SBR. The surface of the granular sludge was mostly colonized by coccoid and rod shaped microorganisms in the reactor.

4.7.3 Denitrification performance

It can be clearly seen from the nitrate and nitrite profiles that reduction times for both nitrate and nitrite reduced as no. days of operation increased. Complete denitrification was observed from the first day.

The denitrification times for nitrate and nitrite increased with increase in initial nitrate concentration. Complete denitrification was observed at all nitrate concentrations. The effluent nitrate and nitrite levels were below 10 mg L^{-1}.The reactor was operated for more than 3 months, thereby demonstrating efficient and stable denitrification.

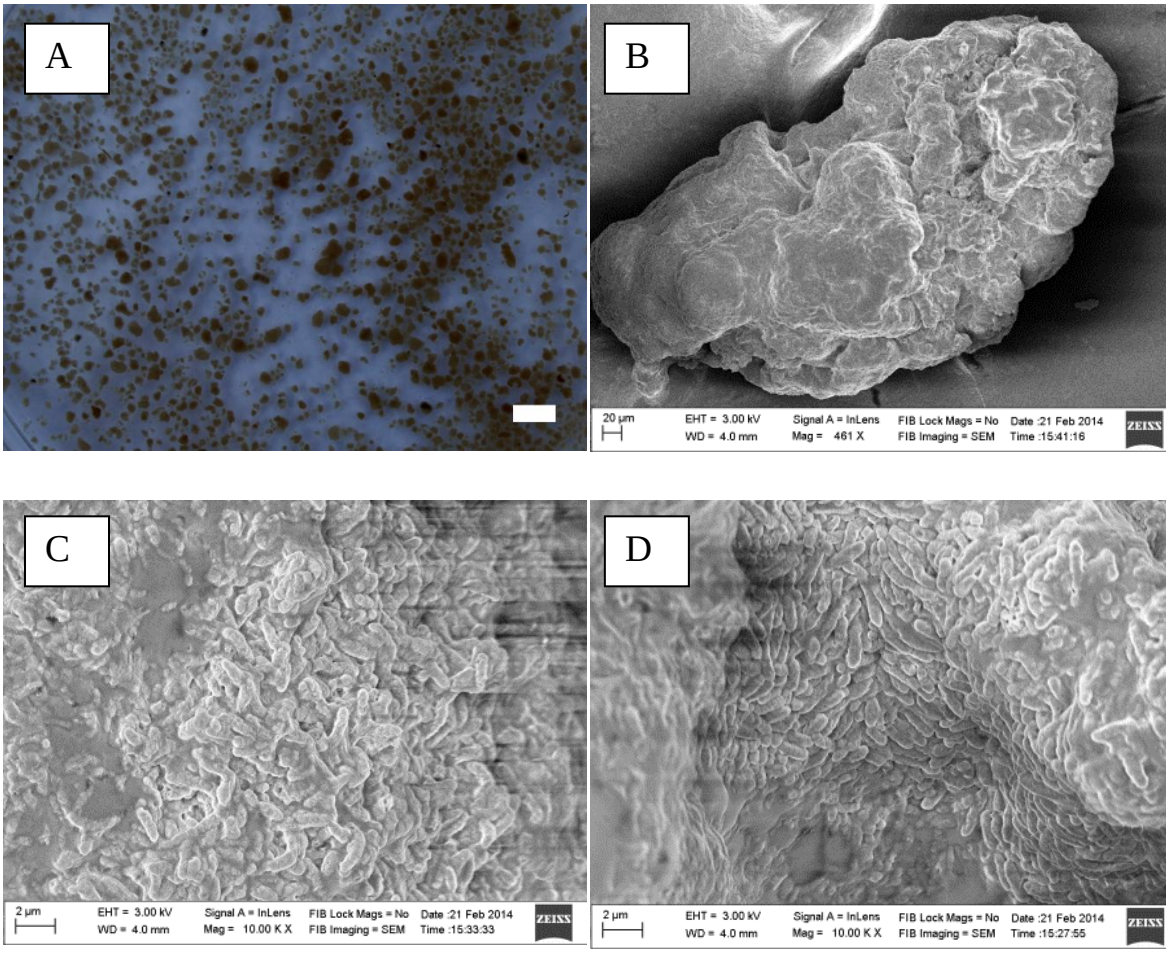

Fig. 4.41 Morphology (A, B) and microstructure (C, D) of denitrifying granular sludge formed in 24 L volume semi pilot scale reactor (EGSBR).

4.7.4 Conclusion

Formation of denitrifying granular biomass capable of complete denitrification of up to 5420 mg L^{-1} NO_3-N was demonstrated in a 24 L volume semi pilot scale sequencing batch reactor. Microscopy showed that compact denitrifying granules were colonized by cocci and rod shaped microorganisms. Successful denitrification of up to 5420 mg L^{-1} NO_3-N in the feed was achieved at C/N ratio of 1.5 in semi pilot reactor. The data obtained in this work shows possibilities for scale up of granular sludge sequencing batch reactors for treating large quantities of high strength nitrate wastewaters.

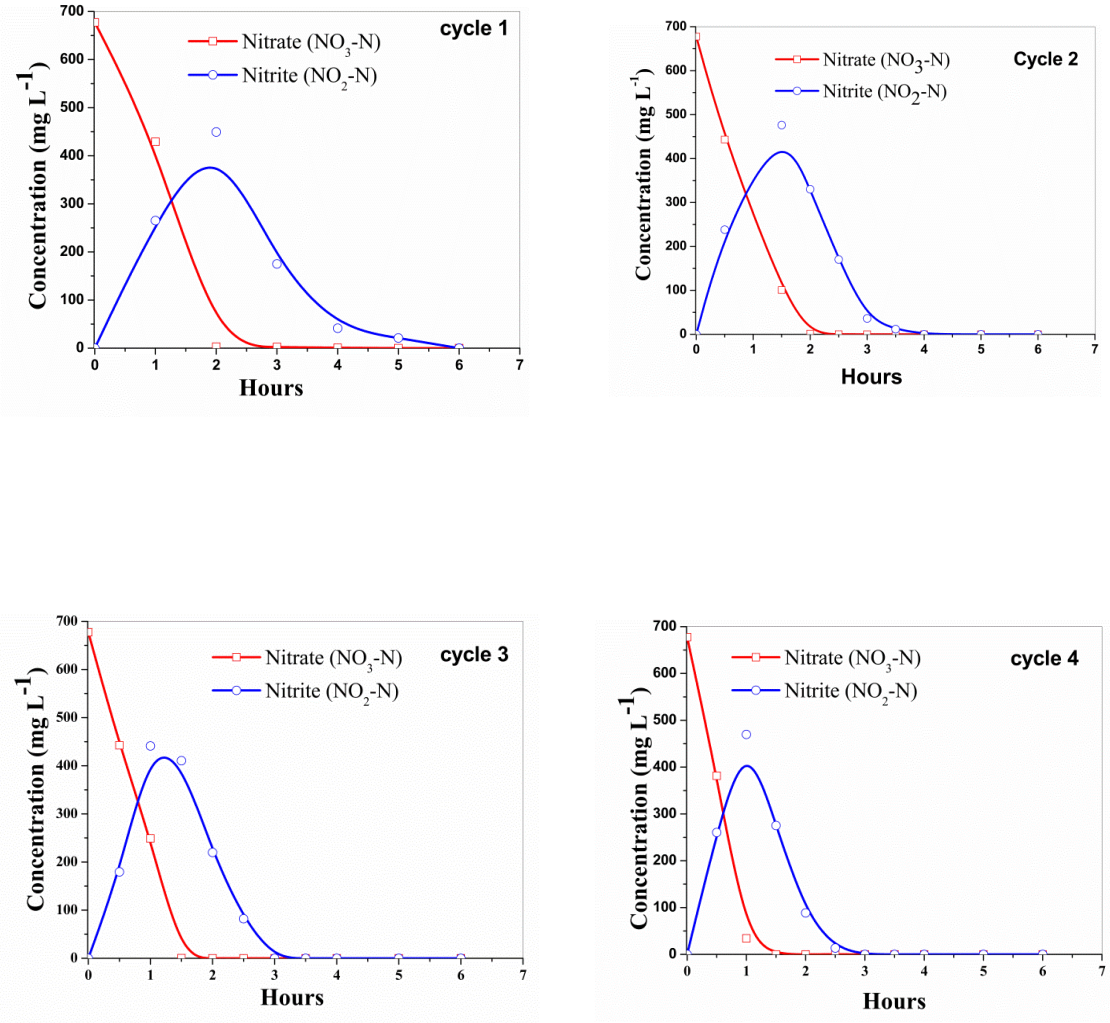

Fig. 4.42 Nitrate and nitrite concentration profiles during denitrification of SNW containing 677 mg L^1 NO_3-N during different days of operation.

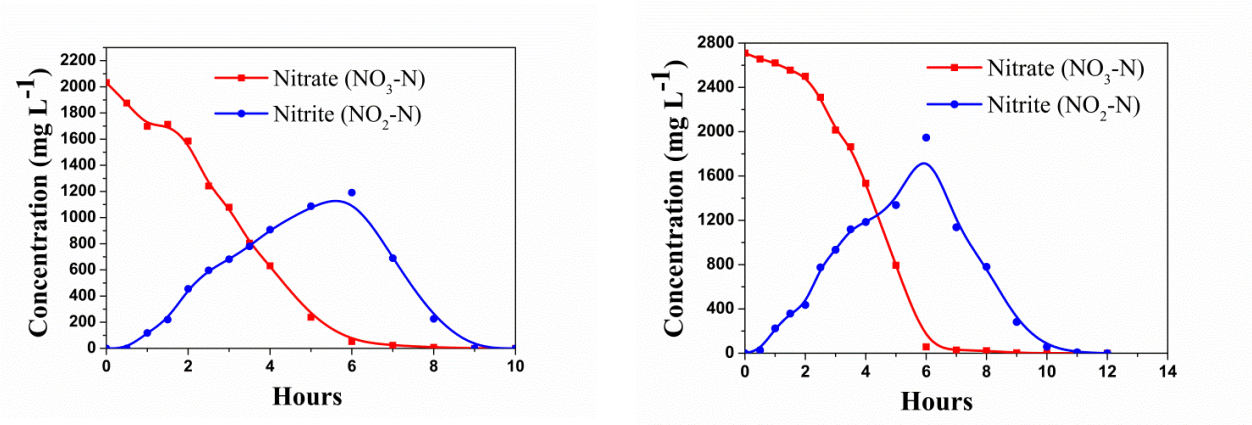

Fig. 4.43 Nitrate and nitrite concentration profiles during denitrification of SNW containing 2032 mg L^{-1} and 2710 mg L^{-1} NO_3-N.

5 MODELLING

5.1 Introduction

Biological denitrification takes place in the presence of bacteria available in the water and wastewater. Nitrogen is present in the wastewater in the form of nitrate and nitrite salts. The denitrification reaction is a very slow process in natural environmental conditions. This process is generally conducted in both modes of operation, viz. batch and continuous. Denitrification process being an exothermic reaction, temperature of the waste increases when the initial concentration of the nitrate increases. The bio-reaction rate depends on the resultant temperature in the reactant at higher concentration.

Several mathematical models were proposed for bio-denitrification reaction. Marazioti et. al. [160] explained kinetic modeling of a mixed culture (*Pseudomonas and Bacillus*) under aerobic and anoxic operating condition. Another mathematical model proposed by Monod and Michaelis-Menten explains denitrification kinetics by Pseudomonas under growth conditions limited by carbon and /or nitrate or nitrite as shown

$$\mu = \mu_{max} \frac{S}{K_s + S} \frac{N}{K_s + N} f(T) f(pH) \quad 5.1$$

where S and N are substrate and nitrate concentration,

Van-Handel model (1981) explains the temperature dependency of bio-denitrification as

$$K = 0.72\ \theta^{(T-20)} \quad 5.2$$

where θ varies from 1.08 to 1.2.

Bioreactor used in the present work is modeled in COMSOL 4.4 to predict concentration and temperature profiles in the reactor at various operating conditions. This chapter explains the construction of geometry with the in-built geometry building features of

COMSOL 4.4. It also explains the governing equations and boundary conditions such as initial and ambient conditions. Heat of reaction is taken as the heat source. Material properties used for each domain are given in detail. The model uses chemical reaction species transport and heat transfer physics using the discrete ordinates method (DOM) for evaluation of heat transfer in solid and fluid system. It employs time dependent solver for estimating heat transfer and ordinary differential equation for determining the rate kinetics of bio-denitrification process.

5.2 Estimation of Rate constants

Rate constants for denitrification of waste of 3000 mg L^{-1} NO_3 concentration were determined experimentally in a 500 mL SBR at isothermal conditions. Temperature dependence of the rate constants is determined from Arrhenius plots as shown in Fig. 5.1 to Fig. 5.3. The rate constants and Arrhenius parameters are given in Table 5.1 and Table 5.2.

Table 5.1 Denitrification rate constants at different temperature

Temp (^oC)	**KNO_3 ($mol/m^3/h$)**	**KNO_2 (p) (presence of nitrate) ($mol/m^3/h$)**	**KNO_2 (Ab) (absence of nitrite) ($mol/m^3/h$)**
20	21.28	9.58	7.79
25	49.68	25.90	28.03
30	88.18	41.23	22.55
35	183.29	105.75	61.53
40	222.91	94.34	51.57

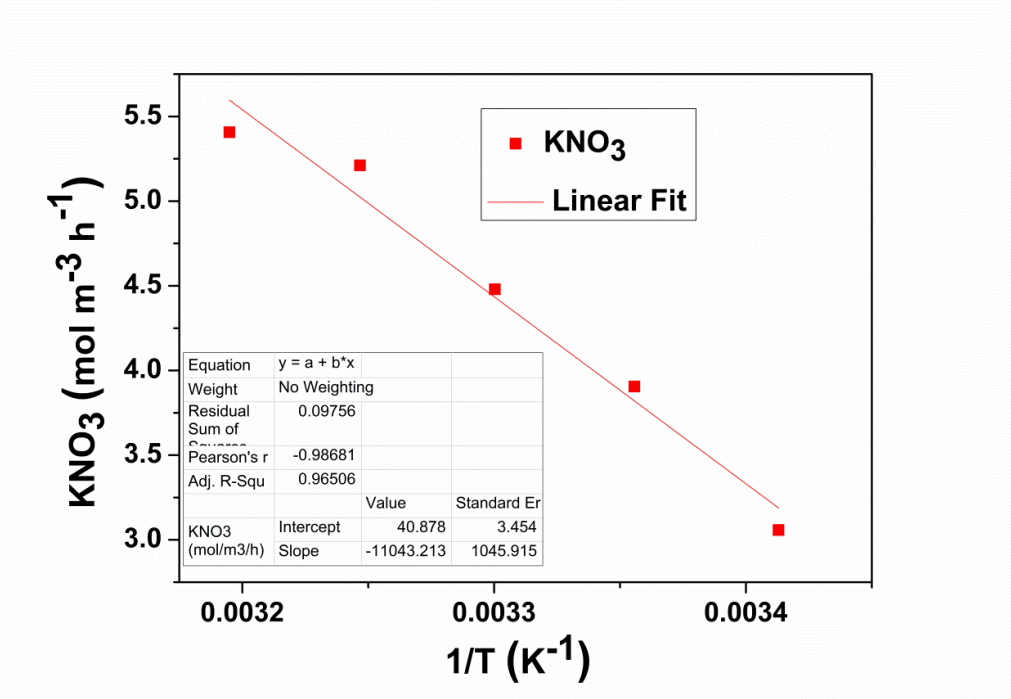

Fig. 5.1 Arrhenius plot for nitrate decomposition

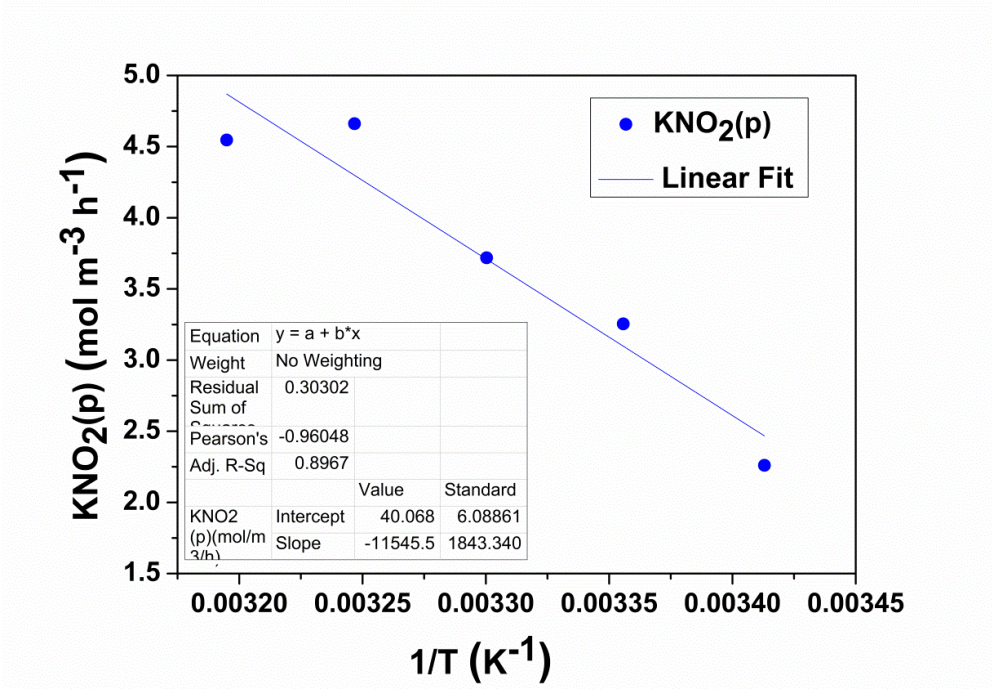

Fig. 5.2 Arrhenius plot for nitrite decomposition in the presence of nitrate

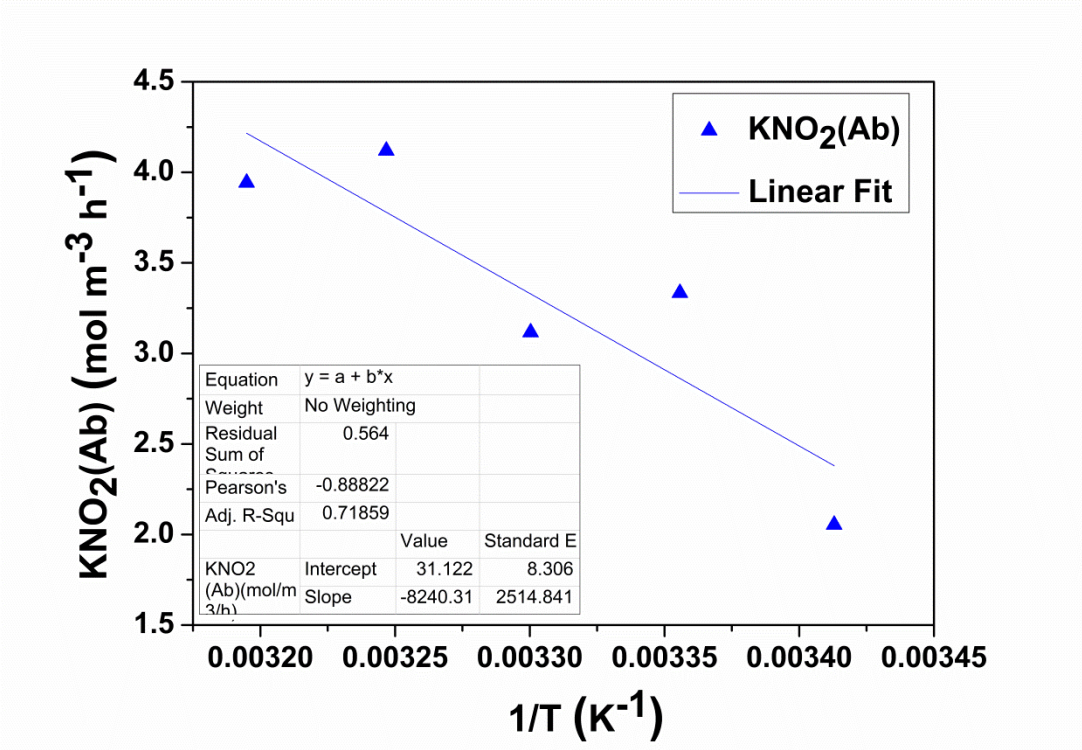

Fig. 5.3 Arrhenius plot for Nitrite decomposition in the absence of nitrate

Table 5.2 Arrhenius parameter for Denitrification

3000 (mg L^{-1})	A1 (mol/m^3/s)	1.57 x 10^{14}	E1 (kJ/mol)	91.81
	A2 (mol/m^3/s)	7 x 10^{13}	E2 (kJ/mol)	95.99
	A3 (mol/m^3/s)	9.12 x 10^9	E3(kJ/mol)	68.51

Biological denitrification takes place in the bioreactor under controlled environmental conditions in the presence of mixed cultured bacteria. During denitrification, nitrate and nitrite decompose into elemental nitrogen gas. The decomposition of nitrate to nitrogen gas is a two-step series reaction; decomposition of nitrate into nitrite and subsequently

nitrite into elemental nitrogen gas. The rate kinetics of decomposition of nitrite into nitrogen mainly depends on the nitrate decomposition. The rate kinetics of biological denitrification was adequately explained by the Monod equation [13].

$$\frac{-dc}{dt} = \frac{X\ C_{NO_3}}{K_N + \mu} \left\{\frac{mol}{m^3\ s}\right\} \quad 5.3$$

The reaction rate of biological denitrification is faster than the biomass growth in the bioreactor. Hence, the biological growth of bacteria for any batch is very small in quantity in mg L^{-1} and even it is not measurable for a complete batch of denitrification process. The growth rate of biomass is reported as first order kinetics [74]. As explained in Chapter 3, degradation of nitrate and nitrite follows zero order kinetics. Thus the Monod equation is reduced to simple zero order rate expression for nitrate and nitrite decomposition. But, nitrite degradation takes place at different rates in the presence and absence of the nitrate.

5.3 Assumptions

The following assumptions were made in the development of the model,

1. Heat transfer in axial direction is neglected.
2. The system is considered to be homogenous as the mixing was carried out with mechanical stirrer.
3. Heat generation due to mechanical stirrer is negligible due to low rpm maintained for stirring.
4. Thermal conductivity of fluid domain is considered to be constant–only single phase sludge concentrations.
5. Material properties are taken from the in-built model builder.

5.4 Geometry

The first step in creating a model is to create geometry. The 2D geometry has been constructed with the dimensions of the bioreactor as shown in Fig. 5.4. Reactors of 150 mm ID and 160 mm OD were created in the geometry model builder.

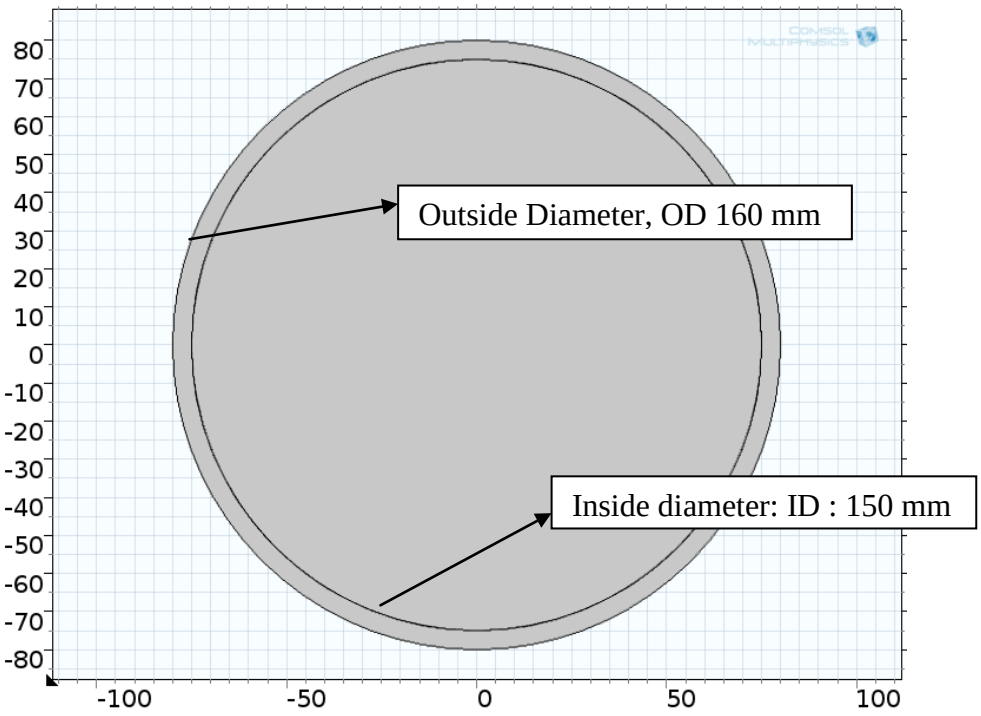

Fig. 5.4 Geometry of bioreactor

The aim of the modeling is to study the concentration profile and temperature distribution in bio reactor. The heat transfer analysis is carried out in modeling by solving energy balance equations and substituting the appropriate boundary conditions such as initial temperatures and ambient conditions.

5.5 Parameter Specification

Set of parameters are used in the model and their values are given in Table 5.3 and these values are taken as user inputs to the model.

Table 5.3 Model Parameters

S.No	Parameter	Value/ Expression	Unit	Description
1	A1	1.57×10^{14}	$mol/m^3/s$	Nitrate decomposition
2	A2	7×10^{13}	$mol/m^3/s$	Nitrite decomposition in the presence of nitrate concentration
3	A3	9.12×10^{9}	$mol/m^3/s$	Nitrite decomposition in the absence of nitrate concentration
4	E1	*91.81*	kJ/mol	Nitrate decomposition
5	E2	*95.99*	kJ/mol	Nitrite decomposition in the presence of nitrate concentration
6	E2	*68.51*	kJ/mol	Nitrite decomposition in the absence of nitrate concentration
7	X	*6*	g	MLSS value of biomass at 105^oC
8	k_{NO3}	*0.023*	$mol/m^3/s$	Rate constant of Nitrate to nitrite reaction
9	k_{NO2}	0.0149	$mol/m^3/s$	Nitrite decomposition in the presence of nitrate concentration
10	$k_{,NO2}$	0.01	$mol/m^3/s$	Nitrite decomposition in the absence of nitrate concentration
11	H1	-135	kJ/mol	Enthalpy of reaction -1 (Nitrate to Nitrite)
12	H2	-362	kJ/mol	Enthalpy of reaction -2 (Nitrite to N_2 gas)
13	V	6	L	Volume of reacting fluid (water-feed-biomass)
14	P	1	atm	Operating pressure of bioreactor
15	T_{amb}	304	K	Ambient condition
16	T1	303K	K	Initial feed temperature, (It may vary for different batch operation)
17	Ci_NO_3	48.37 93.45 143 196.15	mol/m^3	Initial Molar Concentration of Nitrate
10	Ci_NO2	0	mol/m3	Initial Molar Concentration of Nitrite
11	Ci_N2	0	mol/m3	Initial Molar Concentration of Nitrogen gas
12	A	0.155	m^2	Heat transfer area
13	h	8	W/m^2 k	Convective heat transfer coefficient

5.6 Domain Specification

Two different domains were used for modeling. Water with biomass was considered as domain-I and acrylic cylinder of the bioreactor wall was considered as domain-II. These domains were constructed as concentric cylinders in modeling software. The selected dimensions for the above geometry were similar to that of bioreactor used in the present study.

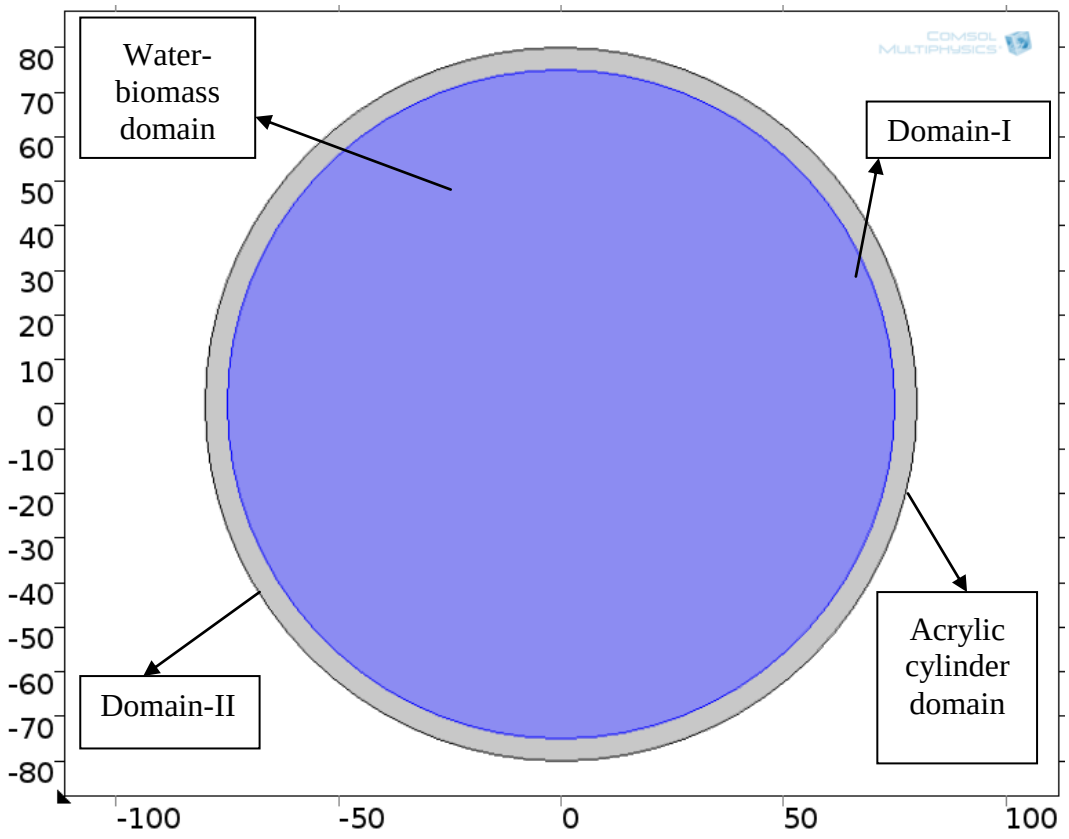

Fig. 5.5 Material properties for each domain

5.7 Material Properties

The physical properties of the air, water and acrylic sheet were taken from in built library in the COMSOL 4.4, using the option "INBUILD PROPERTIES". Material properties for different domains are given in Table 5.4.

Following are the properties of air surrounded by the reactor. The air property is assigned as default value in the model.

Table 5.4 Properties of Air

Physical Quantity	**Symbol**	**Unit**	**Value / Expression**
Density	ρ_{air}	kg/m^3	rho(p A[1/Pa],T[1/K])
Viscosity	μ_{air}	Pa S	eta(T[1/K])
Specific Heat Capacity	Cp_{air}	J/kg.K	1.005
Thermal Conductivity	k_{air}	W/m.K	k(T[1/K])
Ratio of specific heat	γ	-	1.4

Following are the properties assigned for the water-biomass domain-I as shown in Fig. 5.4 and its properties are shown in the Table 5.5.

Table 5.5 Properties of Water-biomass

Physical Quantity	**Symbol**	**Unit**	**Value / Expression**
Density	ρ_{fluid}	kg/m^3	rho(T[1/K])
Viscosity	μ_{fluid}	Pa S.	eta(T[1/K])
Specific Heat Capacity	Cp_{fluid}	J/kg.K	4200
Thermal	k_{fluid}	W/m.K	k(T[1/K])[W/(m K)]
Ratio of specific	ν_{fluid}	-	1

Following are the properties assigned for the domain-II as shown in Fig. 5.5 and its physical properties are shown in the Table 5.6

Table 5.6 Properties of Acrylic Cylinder

Physical Quantity	**Symbol**	**Unit**	**Value**
Density	ρ	kg/m^3	1190
Specific Heat Capacity	Cp	J/kg.K	1470
Thermal Conductivity	k	W/m.K	0.18
Coefficient of thermal expansion	α	1/K	$7x10^{-5}$

5.8 Boundary Conditions

The main aim of the modeling is to study the concentration and temperature profiles. The heat transfer analysis is carried out by solving energy balance equations and substituting boundary conditions such as initial temperatures at the inside and outside wall of the acrylic sheet. The boundary conditions for the above said geometry is depicted in the Fig. 5.6.

The temperature distribution in the bioreactor is derived from energy balance equation. Heat transfer analysis is carried out by considering the convective heat transfer coefficient for liquid and surrounding air. Heat transfer takes place from liquid to the surrounding air through the conduction of acrylic cylinder, followed by convection from the wall to surrounding air.

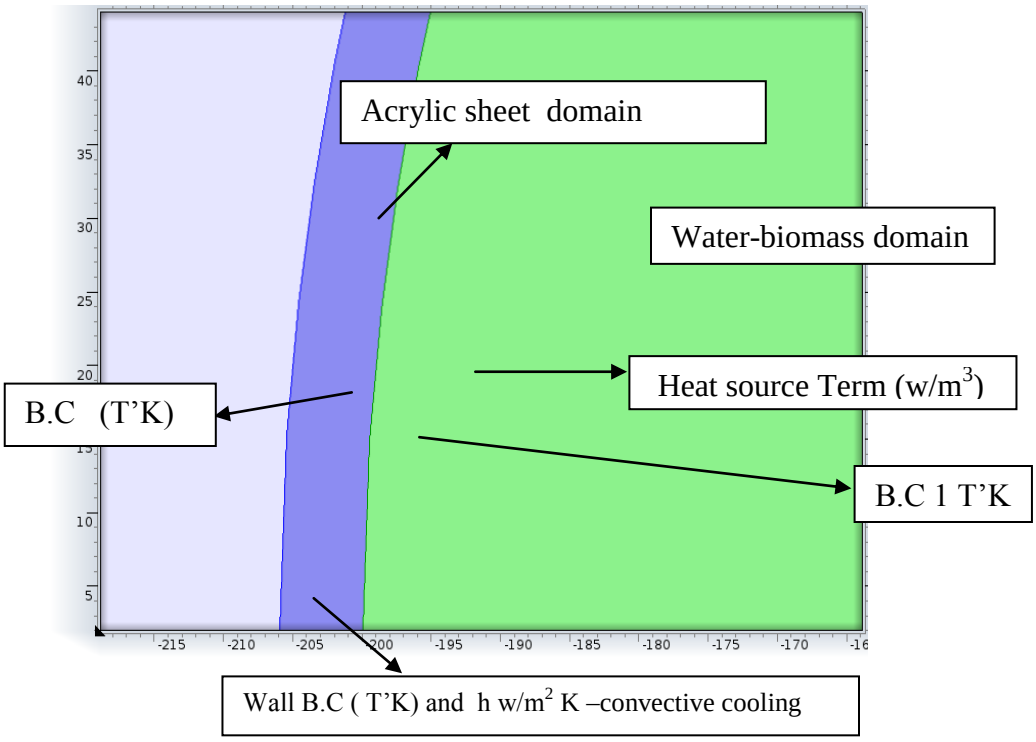

Fig. 5.6 Boundary conditions for liquid and solid domain in a bioreactor

5.9 Governing Equation:-

Energy balance equation is written as

$$\{\text{heat in}\} + \left\{\begin{matrix}\text{heat generation} \\ \text{due to reactio}\end{matrix}\right\} = \left\{\begin{matrix}\text{heat} \\ \text{out}\end{matrix}\right\} + \{\text{heat loss}\}$$

$$V_r \sum_i c_i \; C_{p,i} \frac{dT}{dt} = \cancel{W_s} + Q + Qext + V_r \frac{dp}{dt} \qquad 5.4$$

Where c_i is the concentration of the species, mol/m^3, $C_{p,i}$ molar specific heat kJ/mol K and $Qext$ external hear source W/m^3.

For Liquid phase reaction, shaft work, $W_s \; and \; \frac{dp}{dt} = 0$, as per the assumption (i) and (ii), hence, the above equation is reduced to

$$V_r \sum_i C_i \; C_{p,i} \frac{dT}{dt} = Q \qquad 5.5$$

$$V_r \sum_i C_i \; C_{p,i} \frac{dT}{dt} = V_r \sum_i H_i \; (-r_i) \qquad 5.6$$

H_i is heat of reaction kJ/mol

$$V_r \sum_i C_i \; C_{p,i} \frac{dT}{dt} = V_r \sum_i X \, \Delta H_r{}^0 \frac{dc_i}{dt} \qquad 5.7$$

X is % conversion

$$V_r \sum_i C_i \; C_{p,i} \frac{dT}{dt} = V_r \sum_i X \, \Delta H_r{}^0 \; k \, C^n \qquad 5.8$$

Since n = 0, eq.5.6 becomes

$$V_r \sum_i C_i \; C_{p,i} \frac{dT}{dt} = V_r \sum_i X \, \Delta H_r{}^0 \; k \qquad 5.9$$

$$V_r \; C_{p,i} \frac{dT}{dt} = \frac{V_r \sum_i X \, \Delta H_r{}^0 \, k}{C_i} \qquad 5.10$$

$$V_r \; C_{p,i} \frac{dT}{dt} = \frac{V_r \sum_i X \, \Delta H_r{}^0 \, k}{\sum_i C_i} \qquad 5.11$$

$$V_r \; C_{p,i} \frac{dT}{dt} = \frac{V_r \sum_i X \, \Delta H_r{}^0 \, k}{C_o \, (1-X)} \qquad 5.12$$

$$\int_{T0}^{T} V_r \; C_{p,i} \, dT = \int_0^t \frac{V_r \sum_i X \, \Delta H_r{}^0 \, k}{C_o \, (1-X)} \, dt \qquad 5.13$$

The maximum temperature (adiabatic) attained during the decomposition of nitrate and nitrite is

$$T = T_0 + \int_0^t \frac{V_r \sum_i X_{NO_3} \, \Delta H_{NO_3}{}^0 \, K_{NO_3}}{C_{NO_3} \, (1-X_{NO_3})} \, dt + \int_0^t \frac{V_r \sum_i X_{NO_2} \, \Delta H_2{}^0 \, K_{NO_2}}{C_{NO_2} \, (1-X_{NO_2})} \qquad 5.14$$

Heat loss from bioreactor to ambient through the wall of the bioreactor

$$\rho C_p \frac{dT}{dt} + \rho C_p u \frac{dT}{dx} = -k \frac{d^2T}{dx^2} + \cancel{Q_{ext}} + Q_r \qquad 5.15$$

$$\rho C_p \frac{dT}{dt} + \rho C_p u \frac{dT}{dx} = -k \frac{d^2T}{dx^2} + x \sum_i H_i \; (-r_i) \qquad 5.16$$

For individual species such as nitrate and nitrite decomposition, the above equation becomes under static conditions

$$\rho C_p \frac{dT}{dt} + \rho C_p u \frac{dT}{dx} = k \frac{d^2T}{dx^2} + X_{NO_3} \sum_i H_{NO_3} \left(-r_{NO_3}\right) + X_{NO_2} \sum_i H_{NO_2} \left(-r_{NO_3}\right) \quad 5.17$$

The heat generated during the reaction will raise the temperature of the reactor, thereby inducing a driving force as temperature gradient between the reactor and outside atmosphere.

$$q_r = x \sum_i H_{NO_3} \left(-r_{NO_3}\right) + x \sum_i H_{NO_2} \left(-r_{NO_2}\right) = k \frac{d^2T}{dx^2} + (h \, x \, (Text - T)) \quad 5.18$$

From Eq. 5.3 and Eq. 5.16 the general governing equation for heat transfer is written as

$$V_r \sum_i c_i \, C_{p,i} \frac{dT}{dt} - \nabla . (k \nabla T) = Q \quad 5.19$$

The governing equation for the heat loss is arrived by equating the conductive flux across the acrylic cylinder and of convective fluxes of liquid and surrounding air. The heat transfer coefficients for liquid and surroundings are calculated from the Nusselt correlation. The boundary conditions for heat transfer given as

$$-n . (-k \nabla T) = h . (T_{ext} - T) \quad 5.20$$

User Input, Text = Tamb

h = h_side W/m^2.K

Heat transfer from the wall of the bioreactor is by conduction and will depend upon the physical properties selected and heat flux generated for different nitrate concentration.

5.10 Creation of Mesh

Triangular size mesh was created for both the domains of the bioreactor because of the simplicity of its construction. Heat transfer analysis was carried out in radial direction across the reactor from the fluid to its surroundings. Different sizes of mesh elements

have been selected for different locations of the bioreactor. A large number of element sizes were selected near the interfaces of both domains of the bioreactor. The different mesh element size and its statistical data are represented in the following Table 5.7 and Table 5.8.

Table 5.7 Mesh elements Report

Parameters	Values
Tetrahedral element	24560
Edge element	614
Vertex element	8

Table 5.8 Mesh Statistical data

Parameters	Values
Element quality	0.81
Average element quality	0.93
Element volume ratio	0.289
Mesh area (2D)	20090 mm^2
Maximum growth rate	2.71 mm
Minimum element size	0.0032 mm

There are total number of 24560 triangular elements are created in the model. The element size near the source region is in the range of 0.0032 mm – 1.09 mm. The mesh size distribution is given in Fig. 5.7 to Fig. 5.9. The Average Mesh quality of 0.97 was achieved in water-biomass domain & acrylic sheet as shown in Fig. 5.9.

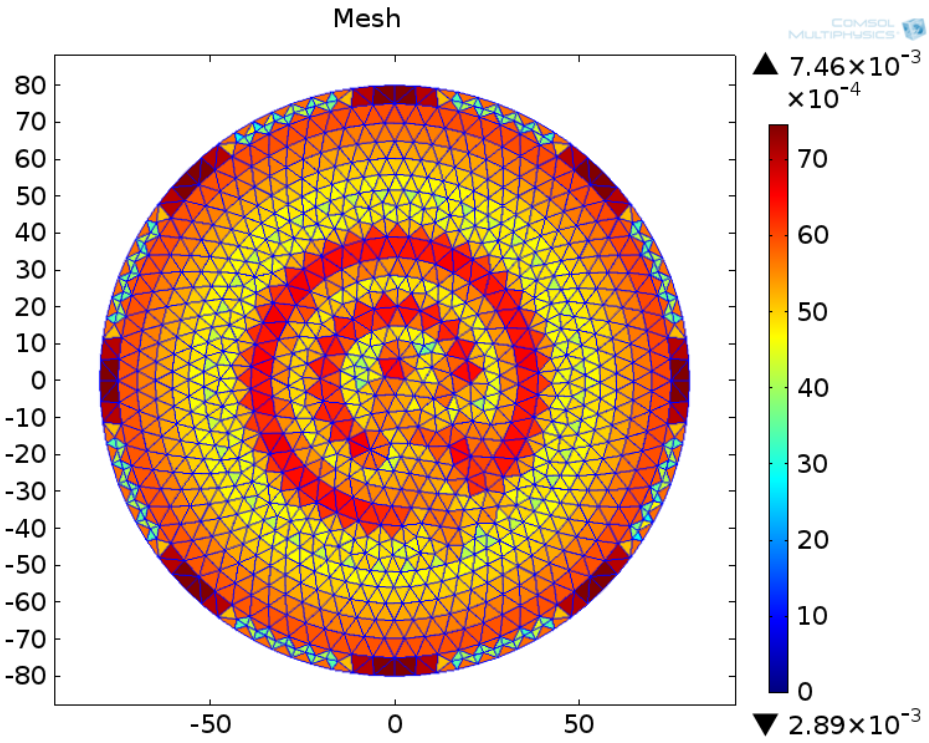

Fig. 5.7 Finer Meshed geometry of Bioreactor domain

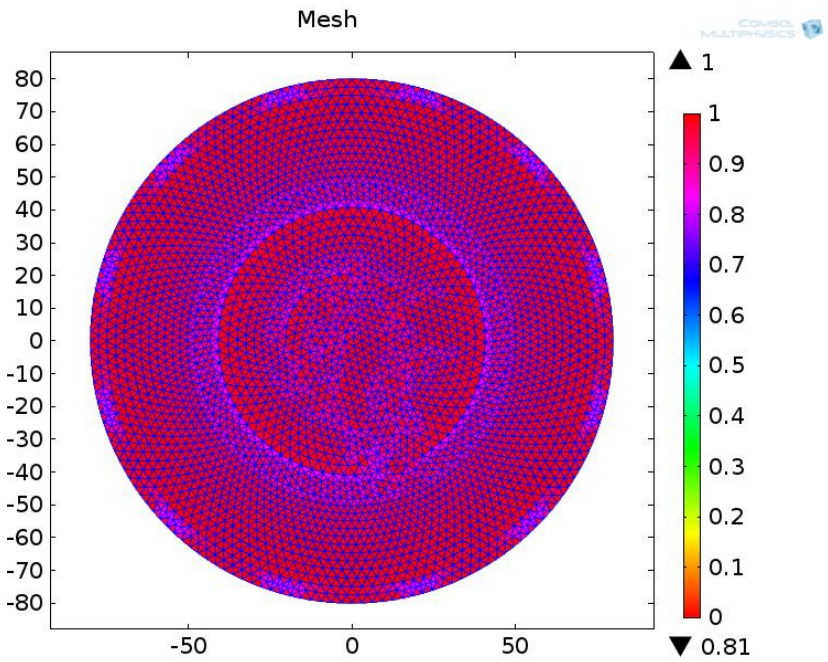

Fig. 5.8 Mesh quality report from simulation geometry

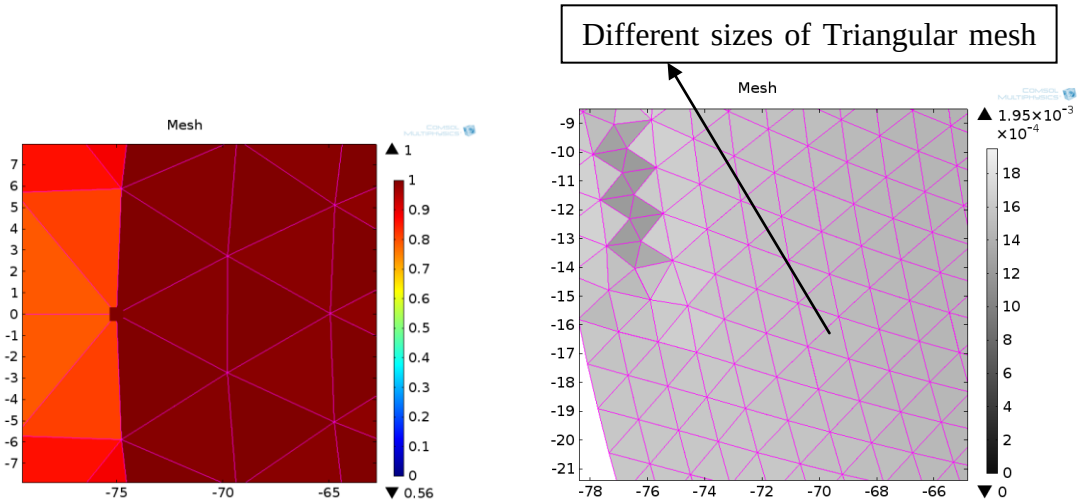

Fig. 5.9 Magnified mesh quality and size distribution in Acrylic sheet and Fluid domain.

Temperature and concentration profiles of the bioreactor for different nitrate concentrations were predicted by simulation of heat transfer and chemical reaction using

COMSOL 4.4 Multi-physics software. The model is validated by comparing simulated results with the experimental values.

5.11 Mesh Independence Test

Mesh independence test was conducted for different mesh sizes of triangular shape for both the domains of bioreactor. Different combinations were tried to get a good approximation with experimental values. The test was conducted for temperature profile of 12000 mg L^{-1} as initial nitrate in the bioreactor. Details of the mesh size are presented in the Table 5.9.

As it is 2D geometry, results obtained from the model for various mesh size did not show major difference for temperature as well as for concentrations for various initial nitrate concentrations.

The domains of fluid and reactor wall were made with triangular mesh. The resultant temperature profile from various sizes of meshes showed a similar result with minimum error. Hence, for the mesh size of maximum of 1 mm to minimum size of 0.001 mm was chosen for modeling to minimize computational time.

5.12 Model Development

The model is validated for the experimental data generated in the SBR for different initial concentrations. The rate constants determined from the laboratory experiments for initial concentration of 3000 mg L^{-1} were used for all concentrations. The validated model can be used for scaling up the reactor for denitrification of high strength nitrates or for predicting the concentration profiles.

Table 5.9 Details of different mesh sizes

S. No	Description	Coarse	Normal	Fine	Extra Fine	Extremely fine	User-defined
1	Maximum Element size(mm)	16	10.7	8.48	3.2	1.6	1
2	Minimum element size(mm)	0.32	0.048	0.048	0.012	0.003	0.001
3	Domain-1	Triangular	Triangular	Triangular		Triangular	Triangular
4	Domain-2	Triangular	Triangular	Triangular		Triangular	Triangular
5	Curvature factor	0.4	0.3	0.3	0.25	0.2	0.2
6	Resolution of narrow region	1	1	1		1	1
7	Distribution method	Geometry sequence	Geometry sequence	Geometry sequence		Geometry sequence	Geometry sequence
8	No of iteration	1000	1000	1000		1000	1000

5.13 Validation of Concentration Profile in the Bioreactor

Modeling of the bioreactor is carried with the following inputs

1. Volume of the reactor
2. Mode of operation
3. Initial condition
4. Enthalpy of reaction
5. Molar mass of different species
6. Thermo-physical properties
7. Rate constants.

Temperature profile in the reactor is modeled by Heat transfer analysis and input for this model was calculated from the result obtained from the chemical species transport model. The main input for the model is that of heat of reaction calculated from the volumetric heat source (W/m^3).

The model is also validated for various nitrate concentrations. It is compared with the experimentally measured concentrations from 3000 to 12000 mg L^{-1} nitrate and it is shown in Fig. 5.10 and Fig. 5.11 for nitrate and nitrite decomposition for various initial nitrate concentration in the bioreactor.

The predicted concentration profiles for initial nitrate concentrations of 3000 to 12000 mg L^{-1} are in good agreement with experimental results. The deviations in the results which are around 10% at higher concentration (>9000 mg L^{-1}) and 15% deviation for lower concentration (<6000 mg L^{-1}). Time duration for various initial nitrate concentrations were predicted from the modeling and it is shown in the following Table 5.10 and Table 5.11.

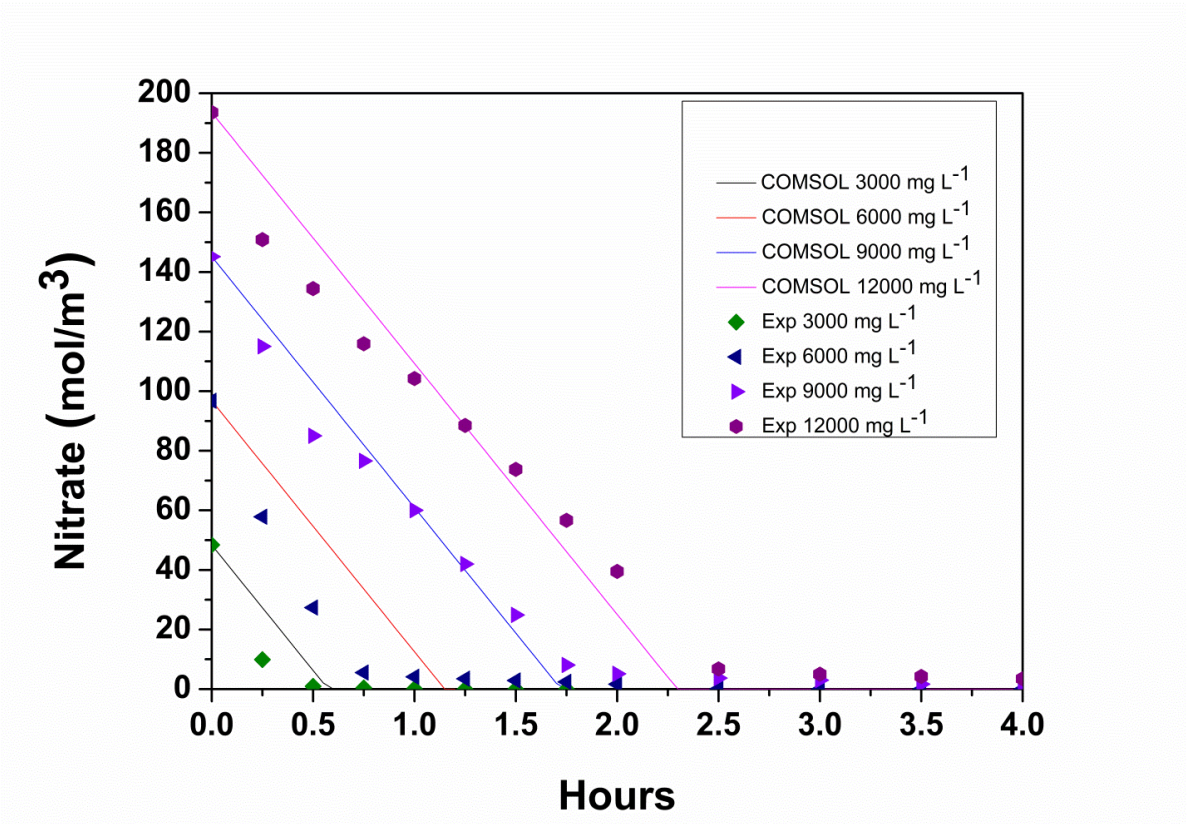

Fig. 5.10 Validation of model for Nitrate Concentration profile

Table 5.10 Time for nitrate degradation for different initial nitrate concentrations

Initial Nitrate (mg L^{-1})	Time duration by Experiments (h) (Nitrate degradation)	Time duration by model (h) (Nitrate degradation)
3000	0.5	0.7
6000	0.8	1.2
9000	2	1.8
12000	2.5	2.4

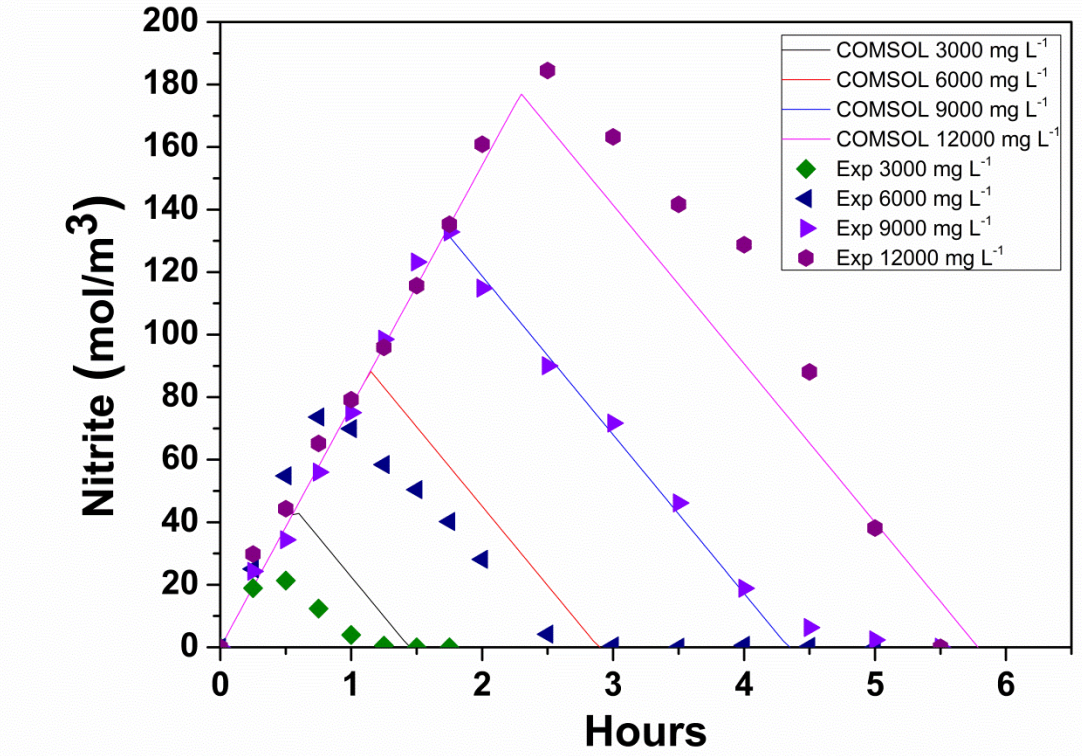

Fig. 5.11 Validation of model for Nitrite Concentration profile

Table 5.11Time for nitrite degradation for different initial nitrate concentrations

Initial Nitrate (mg L^{-1})	Time duration by Experiments (h) (Nitrite degradation)	Time duration by model (h) (Nitrite degradation)	Peak nitrite concentration (mg L^{-1}) Model and Exp	
3000	1.2	1.4	42	28
6000	2.8	2.9	90	78
9000	4.4	4.3	133	130
12000	5.5	5.7	182	190

5.14 Temperature Profile in a Bioreactor during Bio-denitrification

Temperature profile in the reactor is of main interest in modeling because bio reactions are highly sensitive to temperature. The rate of reaction of bio-denitrification falls when the temperature of the reacting species increases and the reaction may not sustain at high temperatures. The recommended temperature for bio-denitrification reaction is about 30 to 37 ^{o}C [101]. The maximum temperature achieved in the bioreactor in the present work is 45 ^{o}C for 12000 mg L^{-1}.

Temperature distribution in the bio-reactor for initial nitrate concentrations of 3000 mg L^{-1} to 12000 mg $L^{-}$was simulated at transient conditions for 8 h operation. The resultant output from the heat transfer analysis was compared with the experimentally determined temperature distribution for 3000 to 12000 mg L^{-1} in the bioreactor.

The following are the inputs for the model for heat transfer analysis

1. Outside fluid is considered as Air
2. Convective heat transfer at the surface of the reactor
3. Conduction heat transfer across the wall
4. Convective heat transfer inside the fluid
5. Convective heat transfer coefficient (8 W/m^2/K).

Temperature distribution for various concentrations was simulated in the model and shown in Fig. 5.12 to Fig. 5.15. Starting/initial temperature (304.8 K) of the bioreactor and ambient temperatures (305 K) were kept constant in the model, where as starting/initial temperature of the bioreactor is different for different days and ambient temperature also varies during the cycle. Due these reasons, there is a difference in the temperature measured by the RTD from the predicted by the model as shown in the validation.

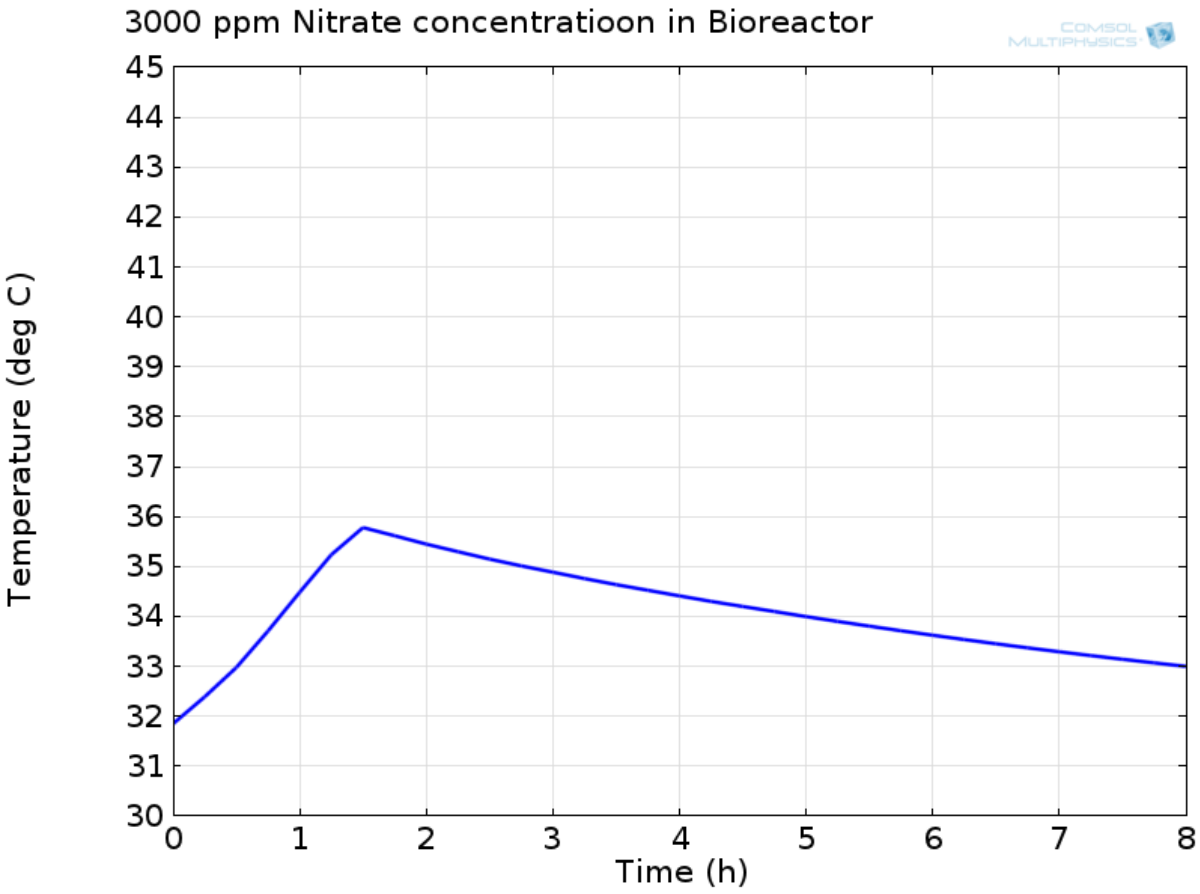

Fig. 5.12 Temperature distributions 3000 mg L^{-1} of nitrate

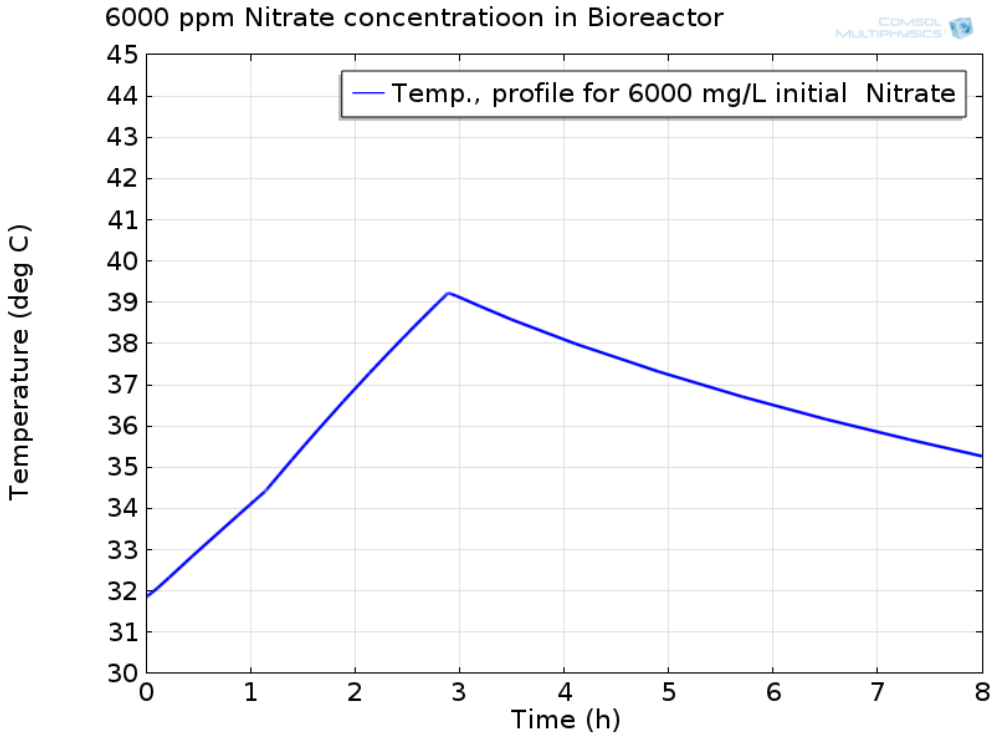

Fig. 5.13 Temperature distributions for 6000 mg L^{-1} of nitrate

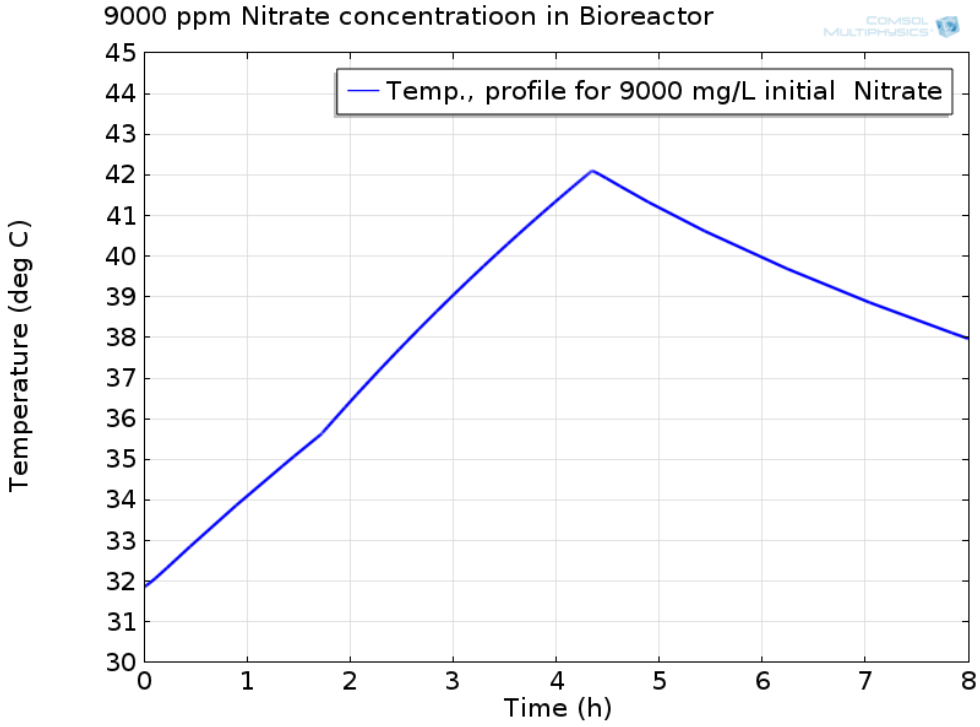

Fig. 5.14 Temperature distributions for 9000 mg L^{-1} of nitrate

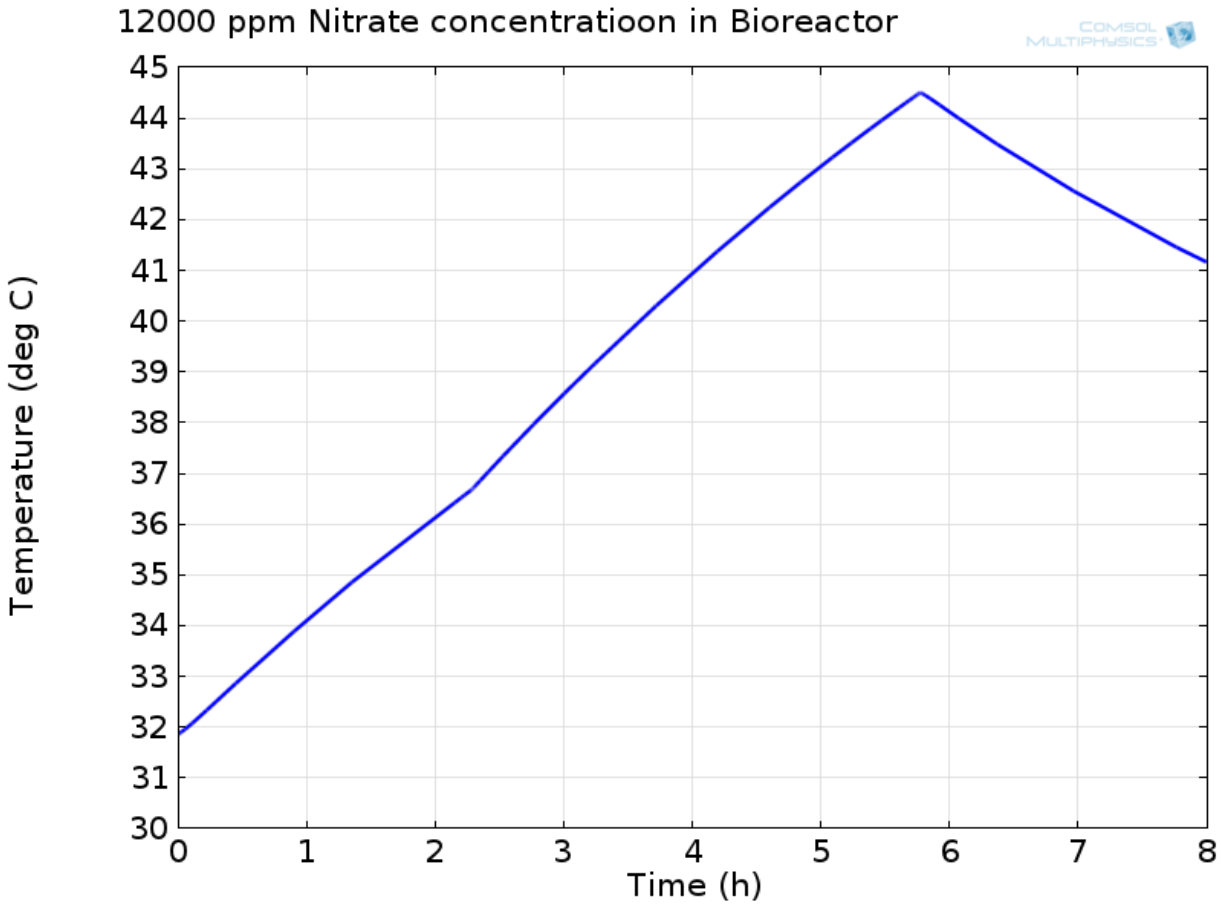

Fig. 5.15 Temperature distributions in the bioreactor for 12000 mg L^{-1} of nitrate

5.15 Temperature Profile in 2D Format

Temperature distribution in the reactor was simulated for nitrate concentration of 12000 mg L^{-1} using the heat transfer simulation option and shown in 2D format in Fig. 5.16 to Fig. 5.24.

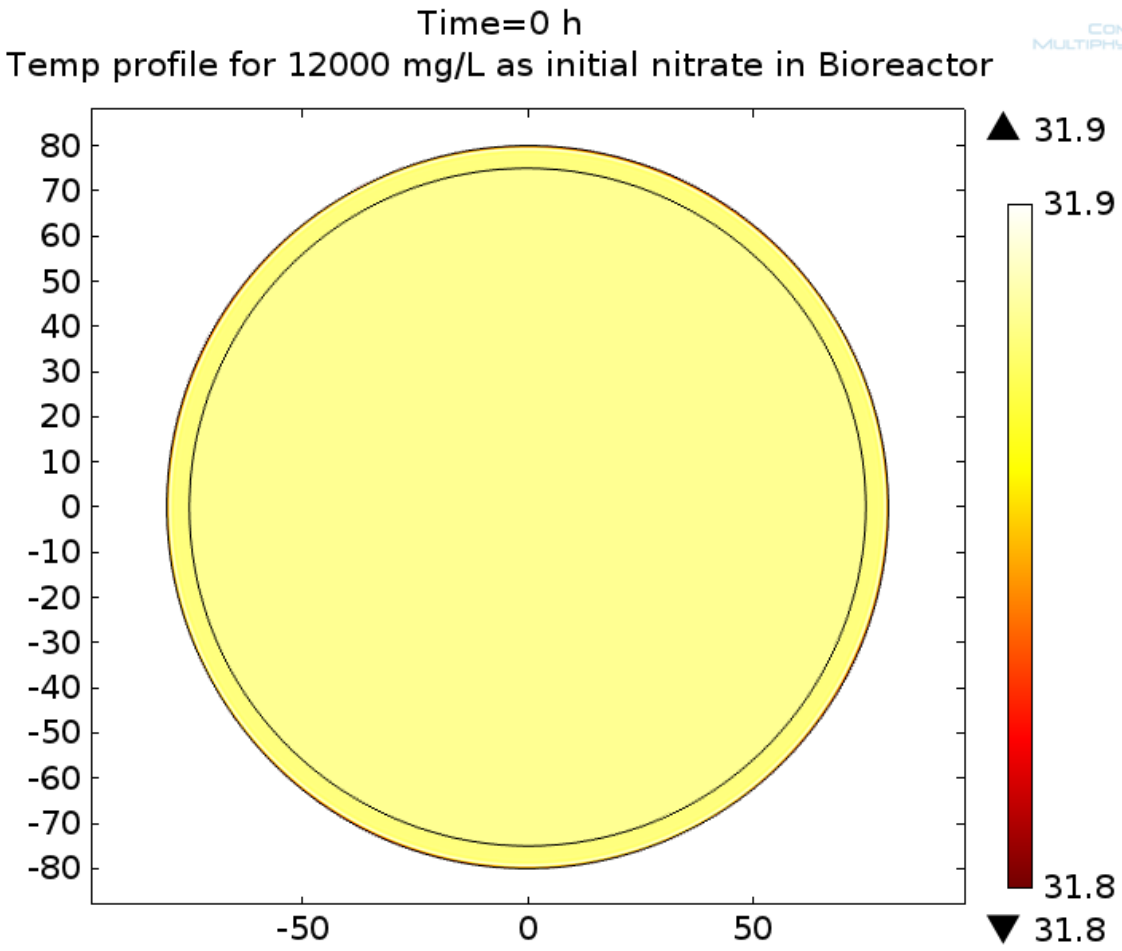

Fig. 5.16 Temperature in the bioreactor at 0 h

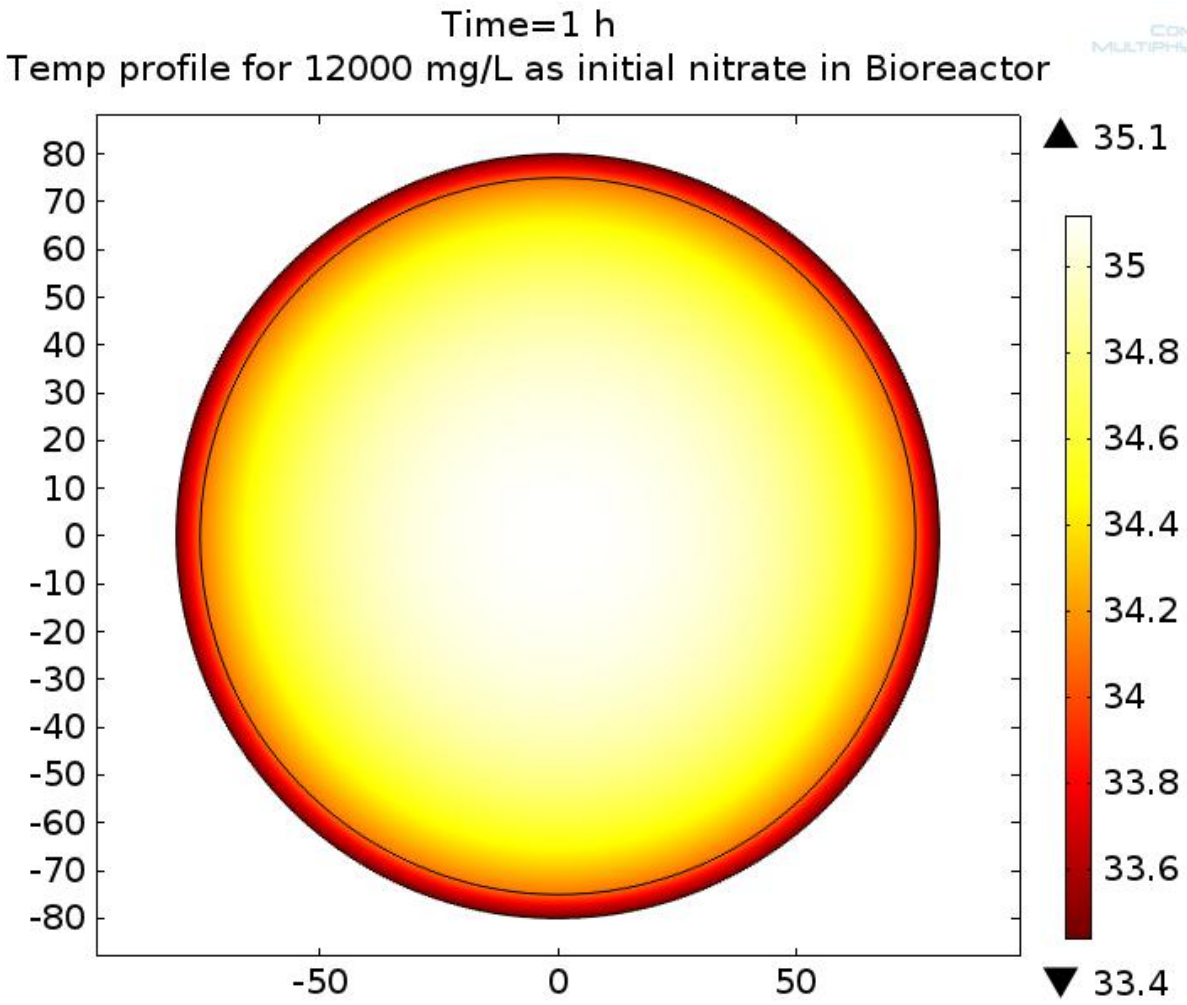

Fig. 5.17 Temperature in the bioreactor at 1 h operation

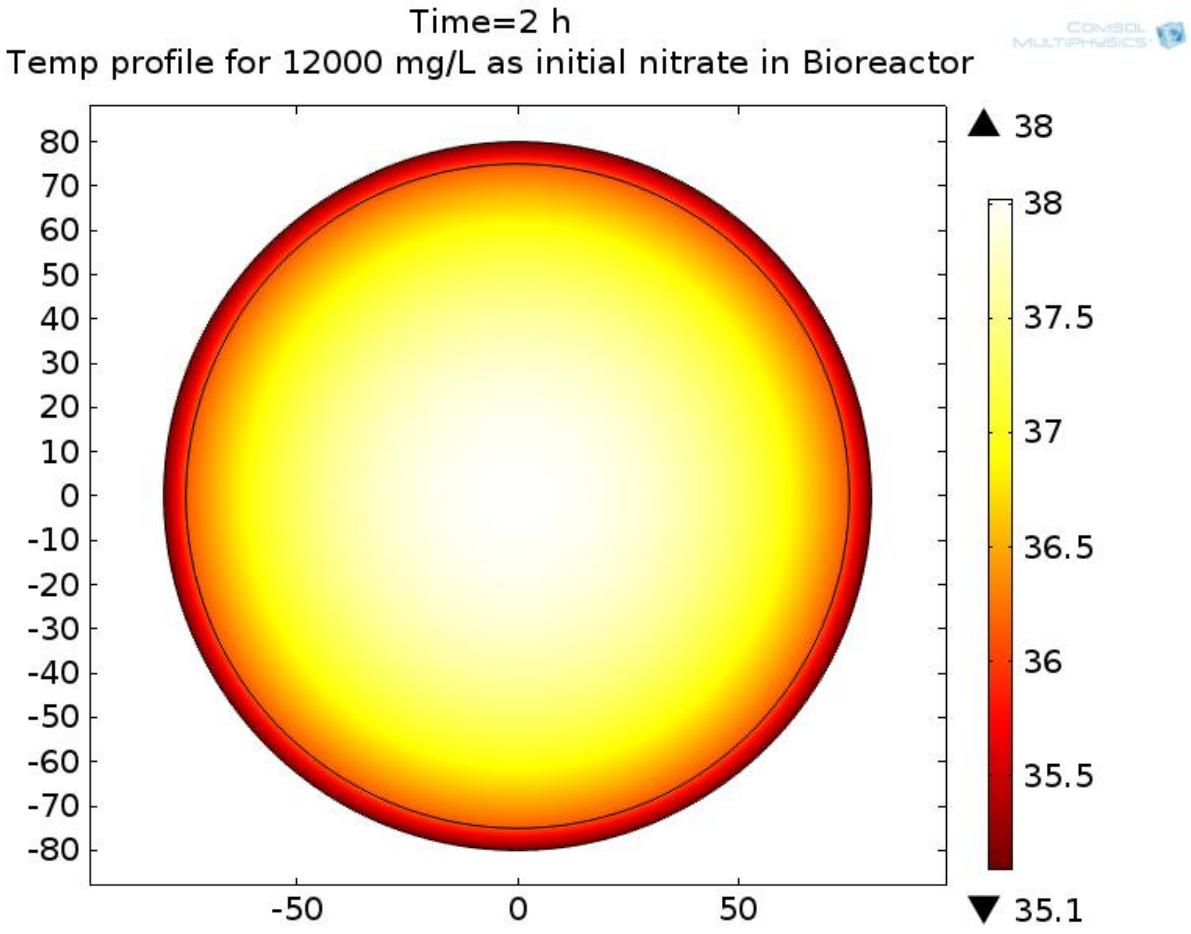

Fig. 5.18 Temperature in the bioreactor at 2 h of operation

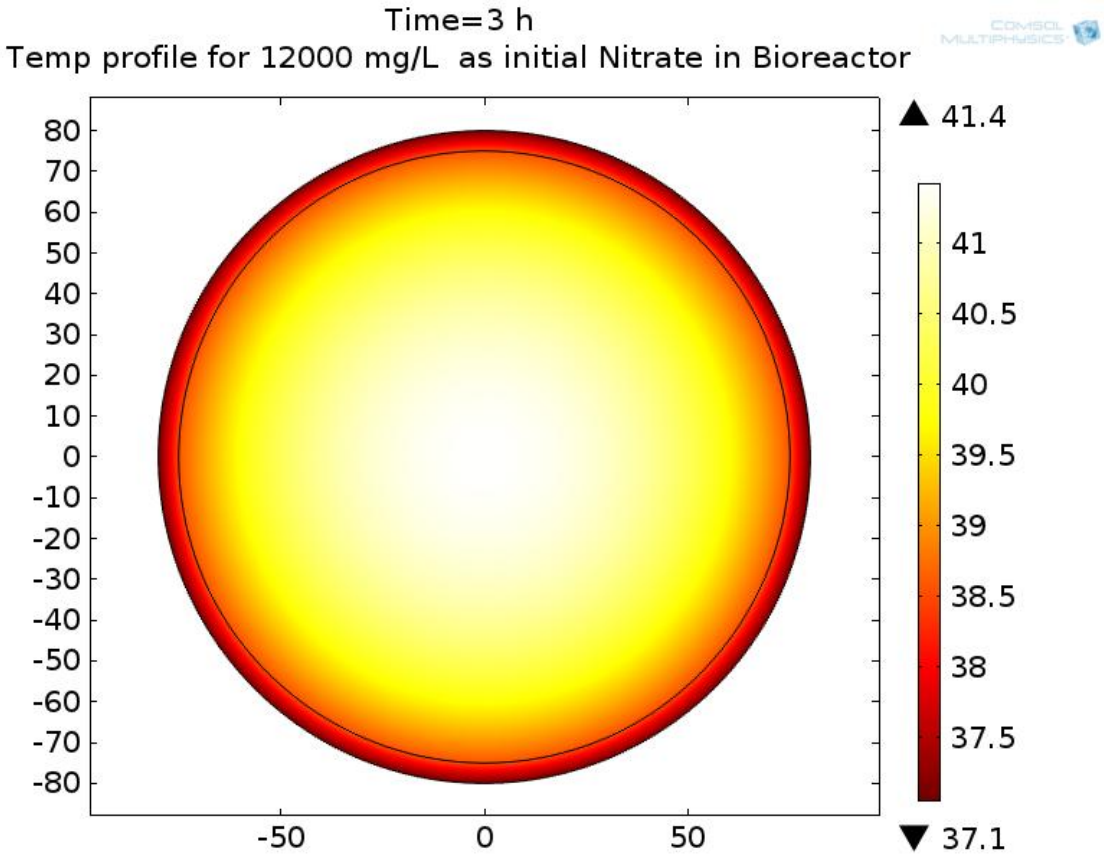

Fig. 5.19 Temperature in the bioreactor at 3 h of operation

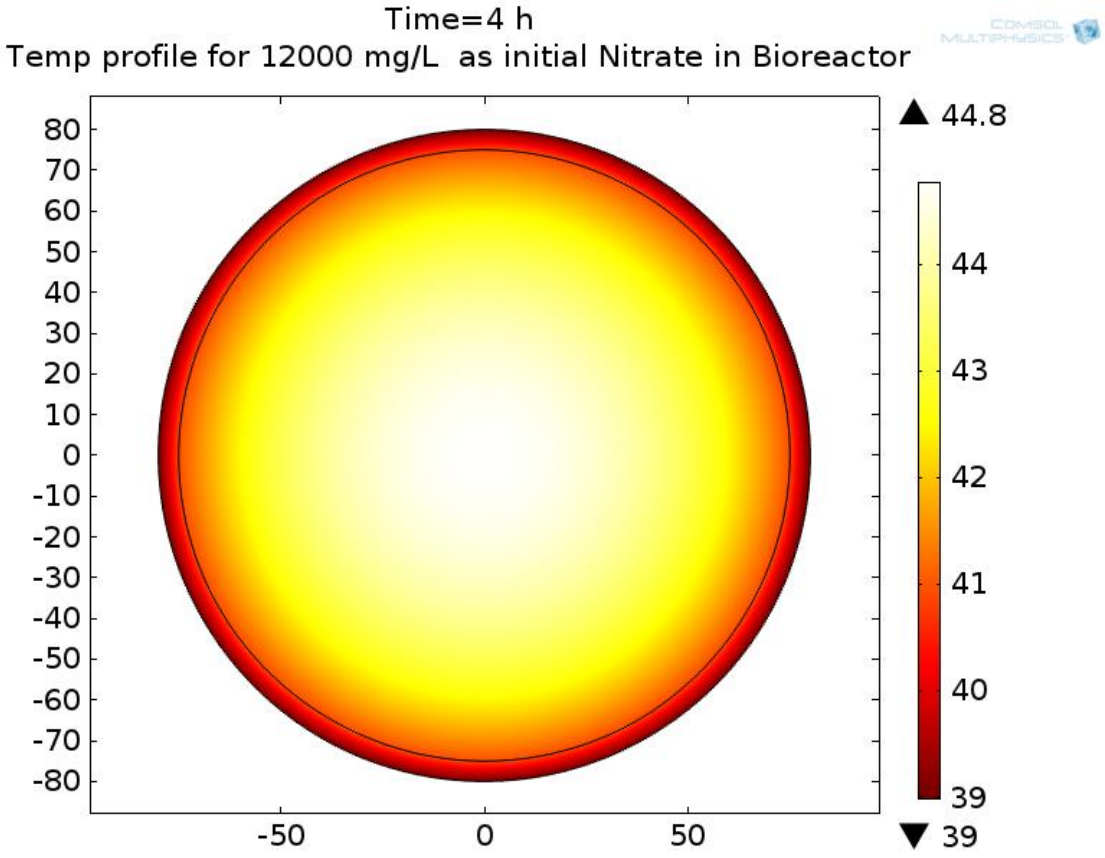

Fig. 5.20 Temperature in the bioreactor at 4 h of operation

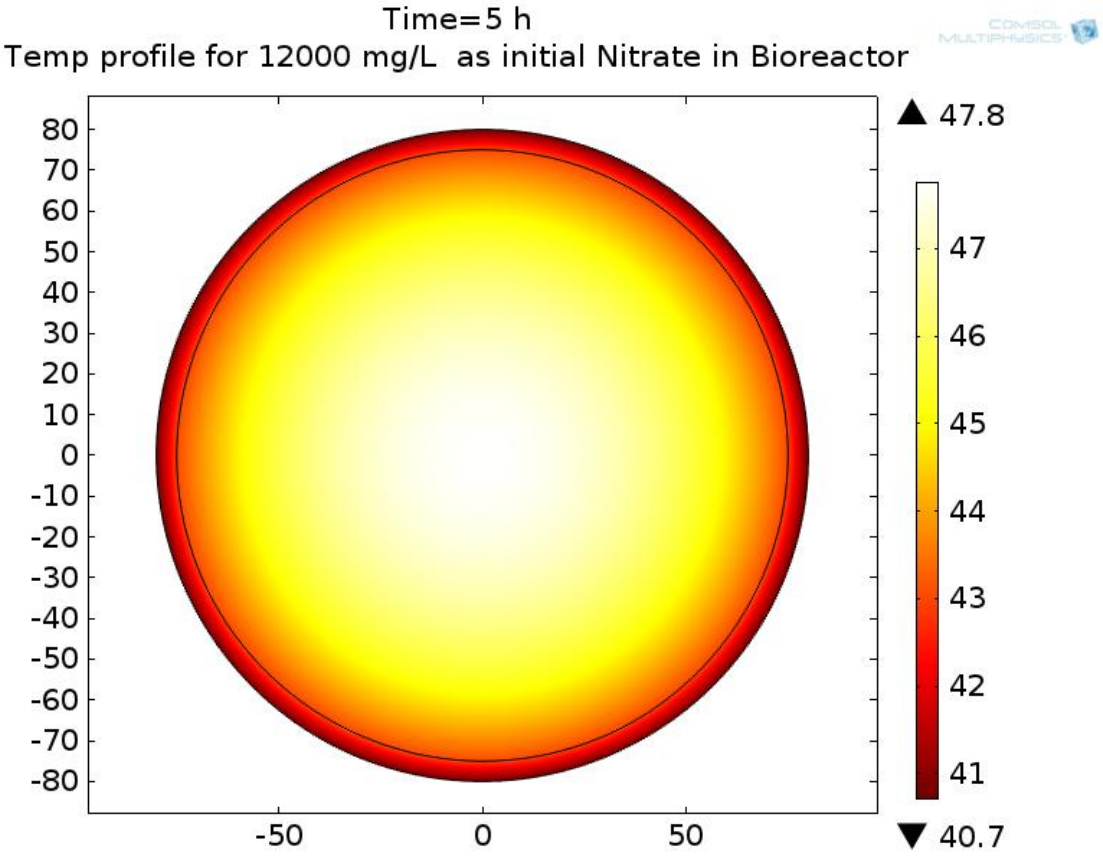

Fig. 5.21 Temperature in the bioreactor at 5 h of operation

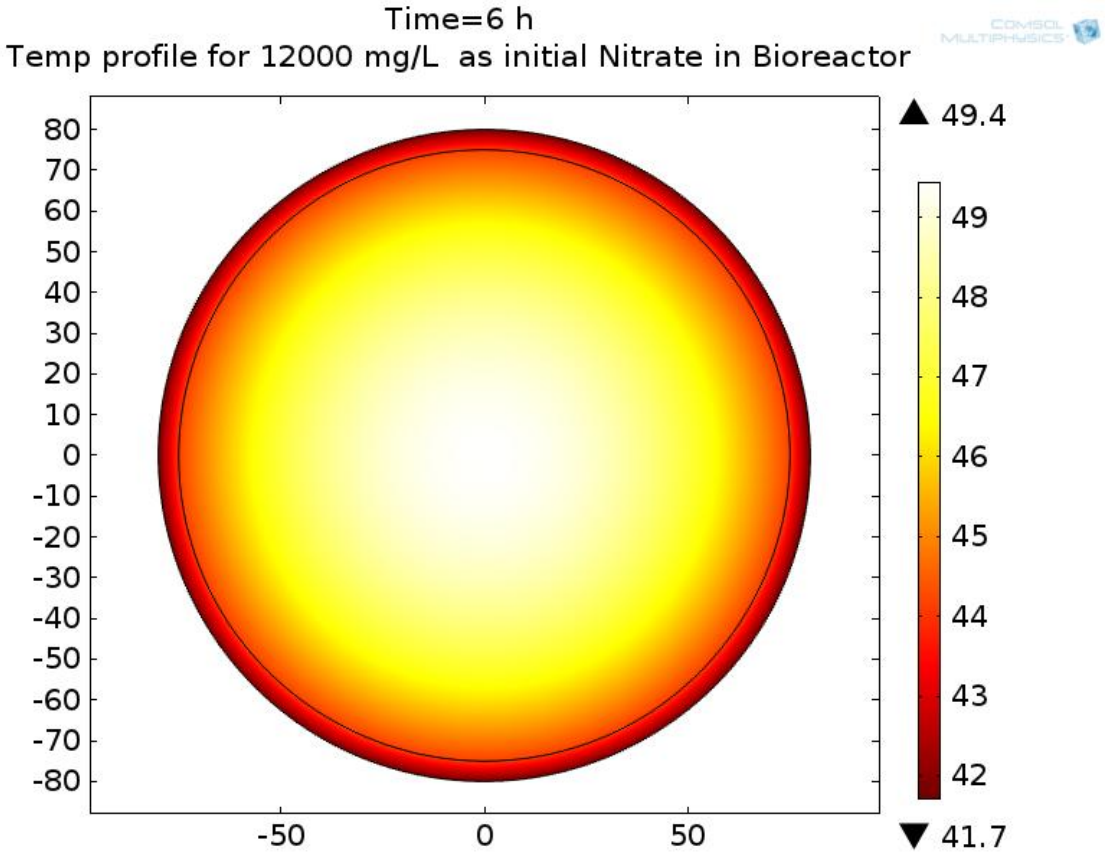

Fig. 5.22 Temperature in the bioreactor at 6 h of operation

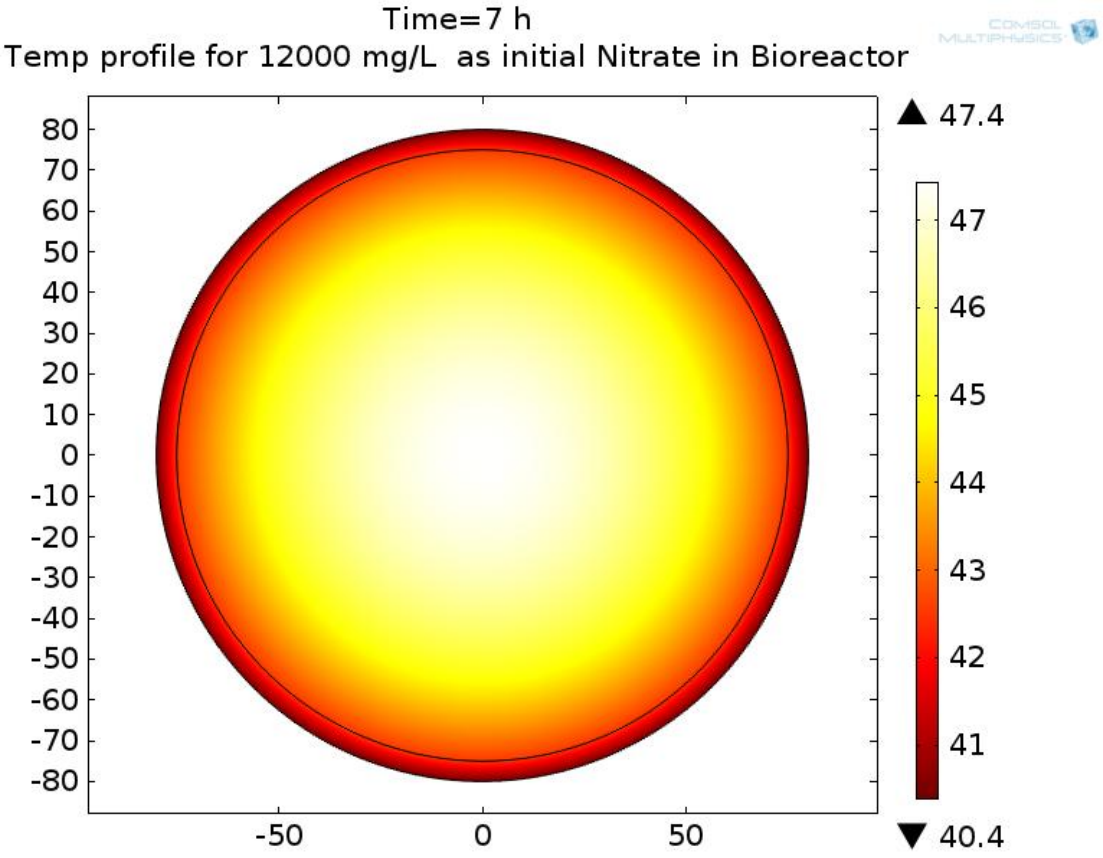

Fig. 5.23 Temperature in the bioreactor at 7 h of operation

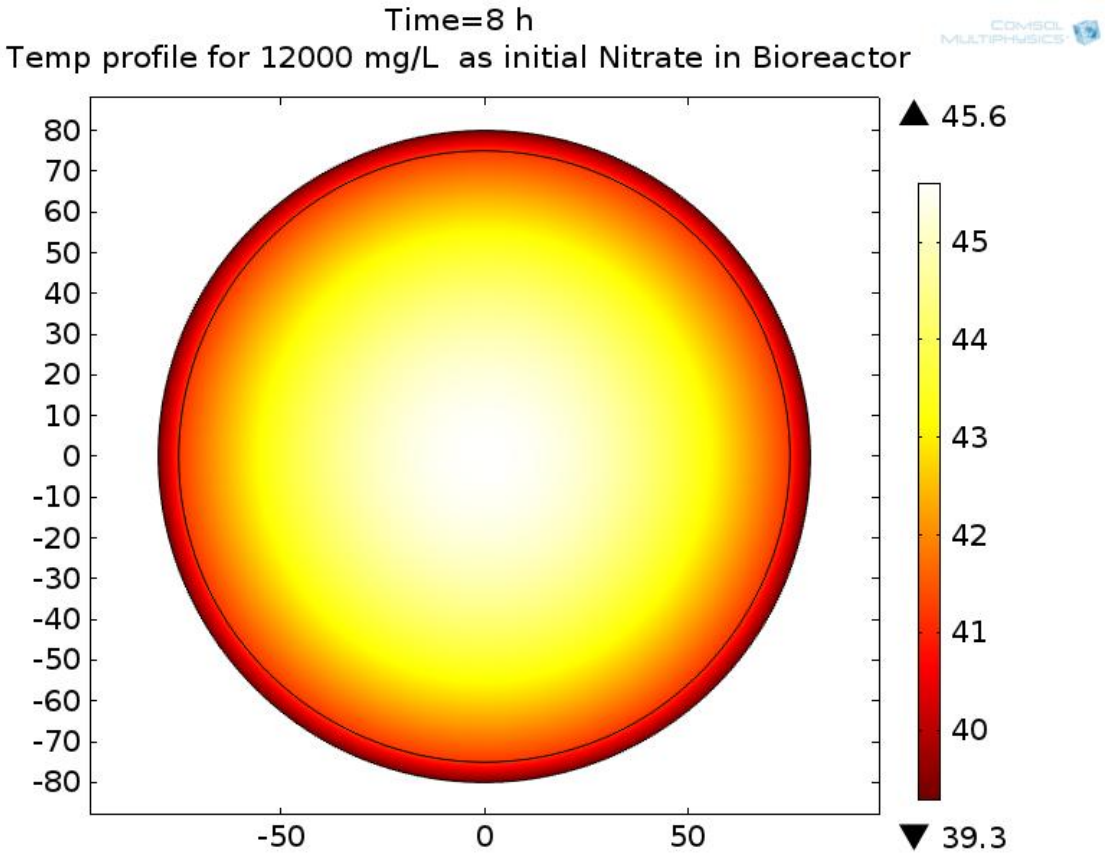

Fig. 5.24 Temperature in the bioreactor at 8 h of operation

The simulation results for the temperature distribution is shown in 2D format in Fig. 5.16 to Fig. 5.24 for 12000 mg L^{-1} in a bioreactor. There is no color change at initial condition and temperature increases with respect to time and reaches to 44.8^{o}C at 5.6 hour. Temperature in the reactor reduces after 5.6 hour and approaches to ambient condition due to heat loss modeled in the reactor.

5.16 Validation of the model with experimentally determined temperature profiles

Using the model, nitrate concentration and temperature profiles in the bioreactor were generated for initial nitrate concentrations. Model predictions and experimental results for different concentration are shown in Fig. 5.25.

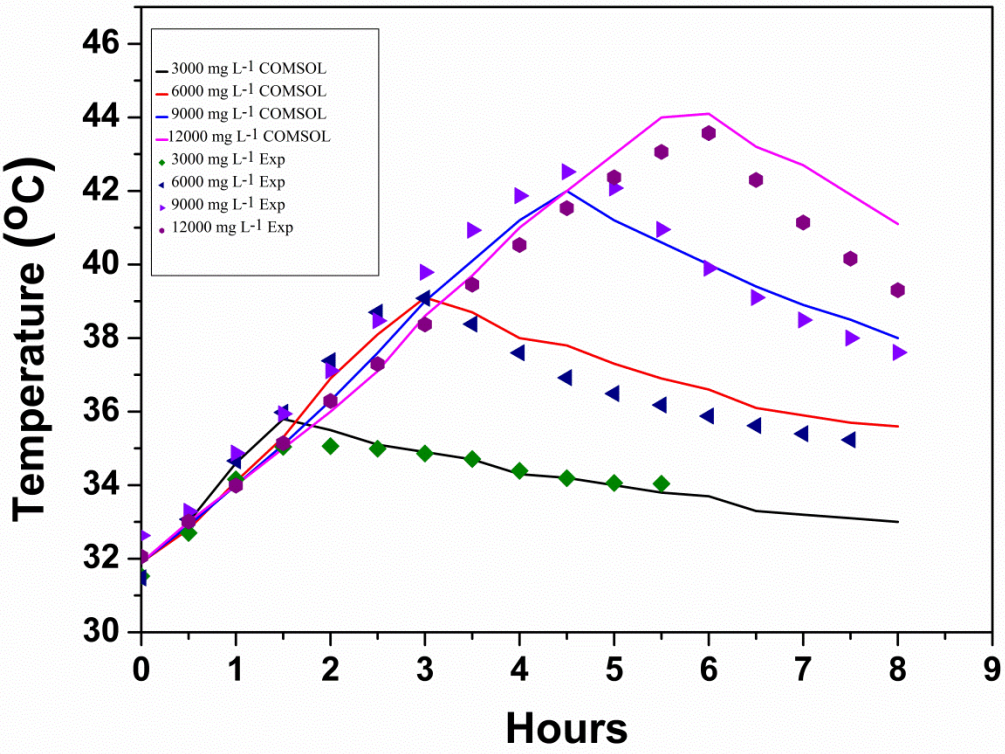

Fig. 5.25 Validation of the model for temperature profiles

It can be seen from the validation that the model could predict the temperatures for all the nitrate concentrations studied within ± 5%. The error was maximum for the initial concentration of 12,000 mg L^{-1}. For 12000 mg L^{-1}, the maximum temperature predicted by the model is 44.1 C and experimental value was 43.57 C.

The comparative results from the model and the experimental values for various concentrations are shown in Table 5.12.

Table 5.12 Comparison of Model results with experimental values

Parameter		3000 mg L^{-1}	6000 mg L^{-1}	9000 mg L^{-1}	12000 mg L^{-1}
Time for denitrification	Exp	1.2	2.8	4.4	5.5
	Model	1.2	2.6	4.3	5.7
Peak Temp ^{o}C	Exp	35.06	39.08	43.3	43.57
	Model	35.35	39.57	42.66	44.1

5.17 Estimation of Un-Measurable Parameter from the Model

The extensive parameters such as heat flux, temperature gradient and heat transfer coefficient that are not measurable, can be evaluated from the model. These are useful for scaling-up the reactor for higher strength nitrate. The heat flux variation for 3000 to 12000 mg L^{-1} as initial nitrate concentration at transient condition was computed from the model and shown in the Table 5.13 and presented in Fig. 5.26 for 6000 mg L^{-1} pictorial form.

Table 5.13 Heat flux variation for various concentrations

Time (h)	Heat Flux(W/m^2) for 3000 mg L^{-1}	Heat Flux (W/m^2) for 6000 mg L^{-1}	Heat Flux(W/m^2) for 9000 mg L^{-1}	Heat Flux (W/m^2) for 12000 mg L^{-1}
0	0.16	0.13	0.13	0.47
0.25	14.8	14.8	14.8	15.1
0.5	19	19.1	19.1	19.3
0.75	25.7	22.9	22.9	23.2
1	30.9	26.6	26.6	26.9
1.25	35.9	32.4	30.2	30.5
1.5	33.1	37.5	33.7	34
1.75	31.1	32.3	38.7	37.3

2	30.1	46.9	43.8	40.4
2.25	29.1	51.4	48.4	43.7
2.5	28.2	55.8	52.8	49.7
2.75	27.3	60	57.1	54.1
3	26.5	55.1	61.3	58.4
3.25	25.7	53	65.4	62.5
3.5	24.9	51.3	69.3	66.4
3.75	24.1	49.6	73.1	70.3
4	23.4	48.1	76.8	74.1
4.25	22.7	46.6	80.3	77.8
4.5	22	45.2	72.1	81.4
4.75	21.4	43.8	69.8	84.8
5	20.7	42.5	67.6	88.2
5.25	20.1	41.2	65.5	91.4
5.5	19.5	39.9	63.5	94.5
5.75	18.9	38.8	61.6	97.6
6	18.3	37.6	59.6	88.4
6.25	17.7	36.4	57.9	85.5
6.5	17.2	35.3	56.1	82.8
6.75	16.6	34.2	54.4	80.3
7	16.1	33.2	52.8	77.7
7.25	15.6	32.1	51.2	75.4
7.5	15.1	31.1	49.6	73.1
7.75	14.6	30.1	48.2	70.9
8	14.2	29.2	46.7	68.8

The heat flux variation for 6000 mg L^{-1} is shown in Fig. 5.26. The maximum heat flux observed is 97.6 W/m^2 @ 5.75 hour for 12000 mg L^{-1}. Heat flux varied with time and

reached a maximum when all the nitrate got consumed and it is varies with initial concentrations of the reactor.

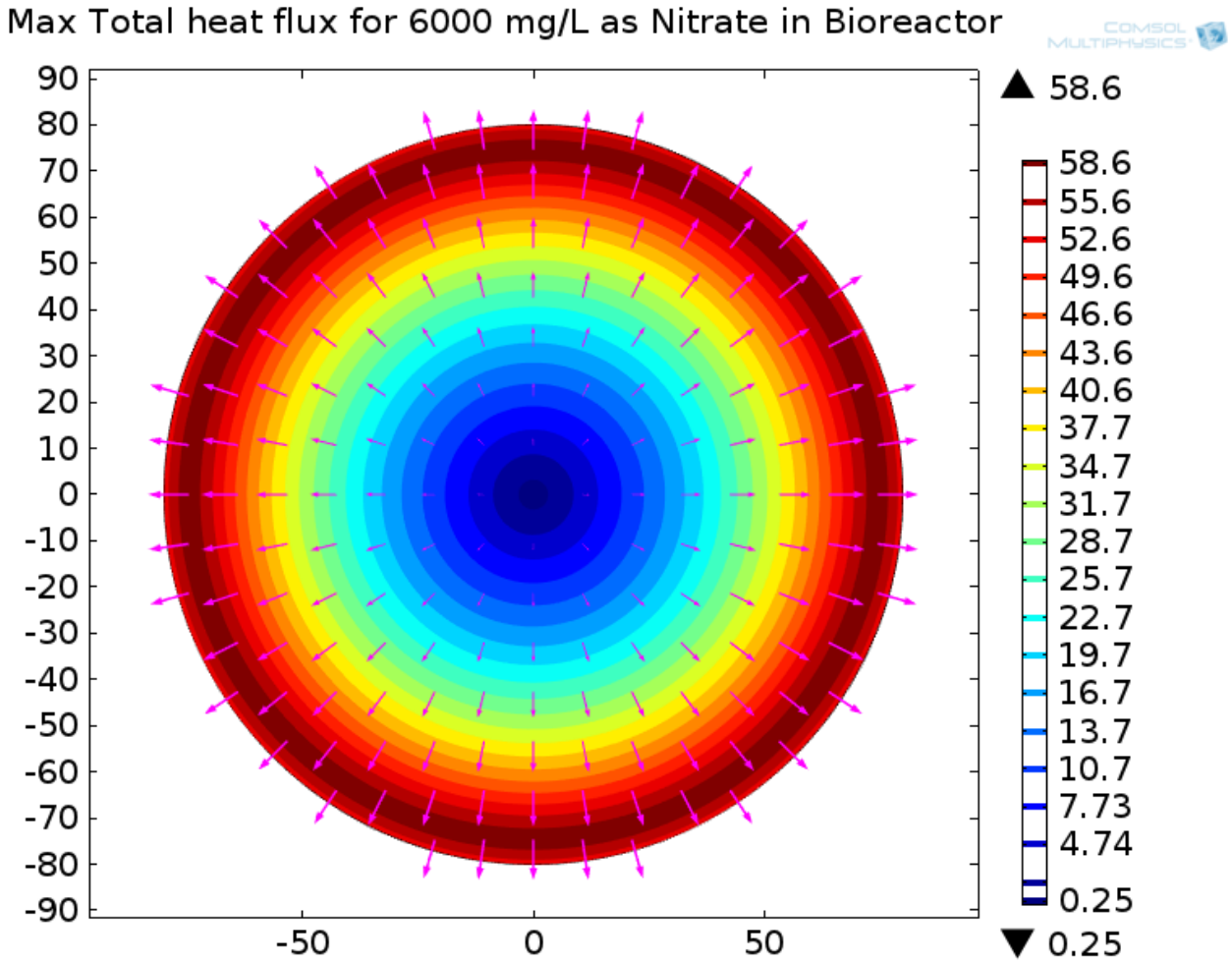

Fig. 5.26 Total Heat flux variation in X-direction for 6000 mg L^{-1} as initial nitrate

5.18 Temperature Profile in Reactor at Radial Direction

Radial temperature distribution, shown in Fig. 5.27 and Fig. 5.28 for nitrate concentrations of 3000 mg L^{-1} and 6000 mg L^{-1}, is uniform and flat at initial condition. When nitrate is added to the bioreactor, reaction starts and temperature in the reactor increases because of the exothermic reaction. Heat loss occurs from reactor to the ambient air. Reactor temperature decreases after completion of denitrification. The peak

temperature for each concentration varies depending on the initial nitrate concentration in the reactor.

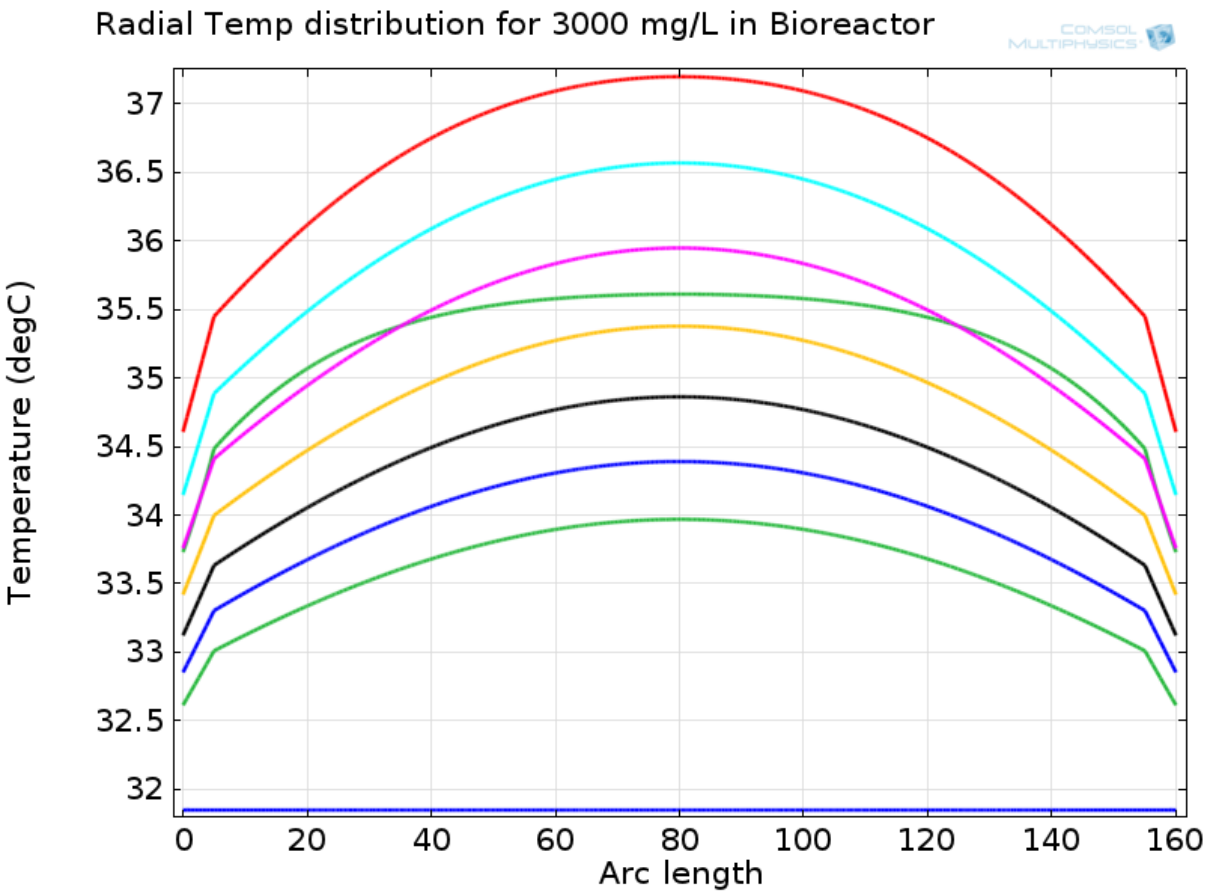

Fig. 5.27 Temperature distribution across the bioreactor for 3000 mg L^{-1} as initial nitrate

The above simulated values from the model were compared with the experimental values obtained during bio-denitrification for various nitrate concentration and results are shown in the Table 5.14.

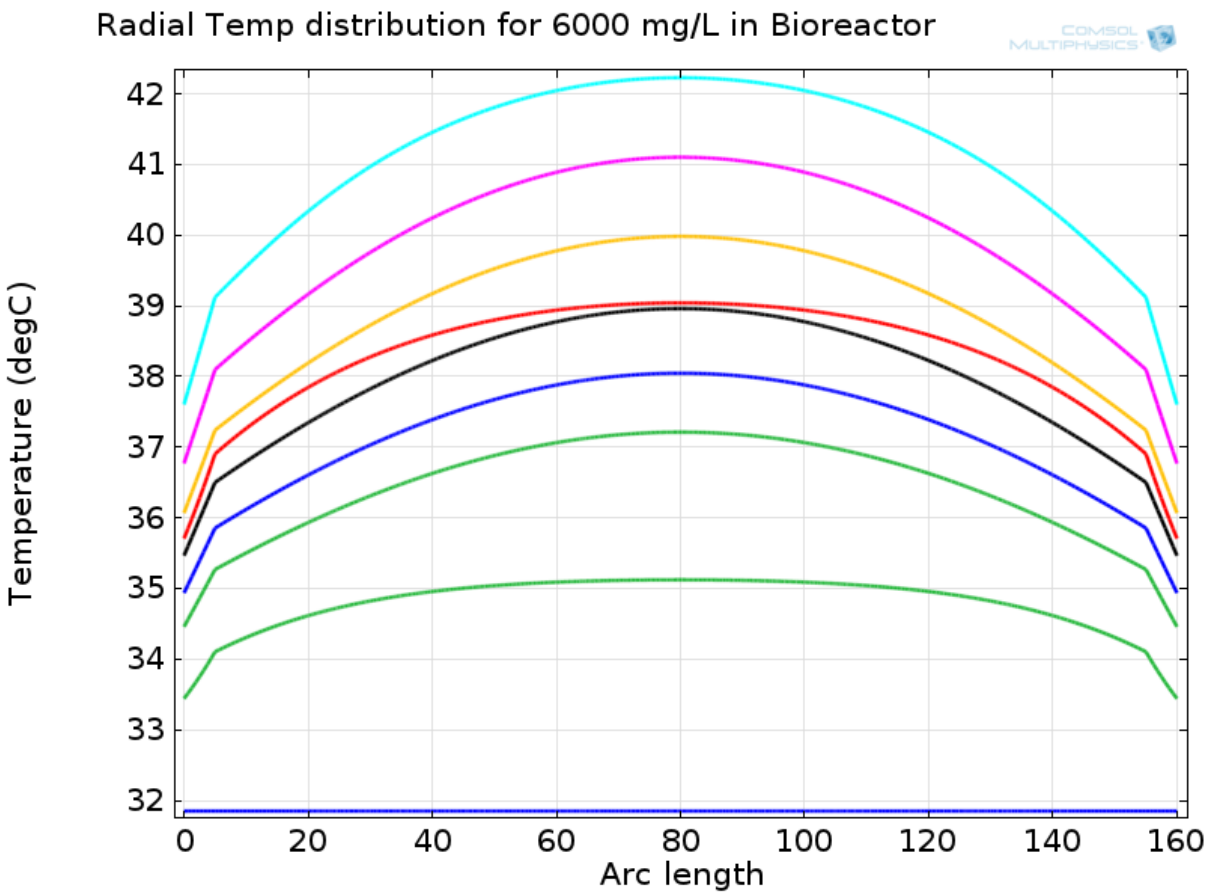

Fig. 5.28 Temperature distribution across the bioreactor for 6000 mg L^{-1} as initial nitrate

Table 5.14Temperature comparison between model and experimental values

Nitrate concentration (mg L^{-1})	Model (^{o}C)	ΔT by model	Actual (^{o}C)	ΔT from Experiment (^{o}C)
3000	31.90 to 35.5 @1.4 h	3.5	31.53to 35 @ 1.5 h	3.47
6000	31.90 to 39.1 @ 2.85 h	7.2	32.19 to 39.08 @ 2.7 h	6.89
9000	31.90 to 43.3 @ 4.3 h	11.46	33.19 to 43.3 @4.2 h	10.11
12000	31.90 to 44.59 @ 5.75 h	12.65	32.21 to 43.75 @5.85 h	11.54

Table 5.14 shows that, ΔT increases with increase in nitrate concentration. The difference between the model and experimental value is due to the certain assumptions made in the model. The predicted temperatures are in good agreement with experimental values. Denitrification follows zero order kinetics, the time required for denitrification of various initial nitrate concentrations can be estimated in lab scale and this data can be used to simulate industrial scale results.

Operation of high nitrate strength bearing wastes results in higher reactor temperatures because of large amount of heat energy evolved due to exothermic reaction. External cooling can be used for controlling the temperature in the bioreactor. Bioreactor modeling is useful to upgrade the reactor to industrial scale.

6 SUMMARY AND FUTURE DIRECTIONS

6.1 Summary

Sequencing batch reactors were used for cultivating denitrifying granular biomass to treat high strength nitrate wastewaters.

Compact denitrifying granular sludge capable of denitrification of up to 2710 mg $L^{-1}NO_3$-N at different C/N ratios was developed in sequencing batch reactor (SBR), using acetate as carbon source. Complete denitrification was observed at C/N ratios of 1.5, 2 and 3. Nitrite accumulation was observed at all three C/N ratios tested. The specific denitrification rates observed were 2 - 3 times higher than those reported for similar studies on high strength denitrification. Kinetic study revealed that nitrate and nitrite denitrification rates were of zero order. The study shows that C/N ratio of 1.5 is optimum for efficient and stable denitrification, as denitrification times and peak nitrite concentrations were lowest for this C/N ratio. As this C/N ratio 1.5 is low compared to the optimum C/N ratios reported by many other researchers, the treatment scheme investigated in the present study using granular biomass in SBRs is highly cost effective.

Denitrifying granular sludge cultivated in SBR exhibited efficient and stable denitrification during long-term operation. Complete denitrification of feed nitrate-N up to 5420 mg L^{-1} was achieved with effluent nitrate-N and nitrite-N levels below 10 mg L^{-1}. The granular sludge formed under denitrifying conditions possessed compact microstructure and diverse microbial community. When the denitrifying granular sludge, cultivated with a C/N ratio of 3, was abruptly fed with high strength nitrate at a lower C/N ratio of 2, complete denitrification could not be achieved. Acclimatization of the

granular sludge by increasing the feed nitrate concentration in steps, at a given C/N ratio, appears to be essential to achieve complete and stable denitrification of high strength nitrates. High strength denitrification involves nitrite accumulation and therefore, selection of nitrite tolerant strains through adaptation and enrichment of the denitrifying community is a prerequisite.

Denitrifying granules capable of complete denitrification of 1355 mg $L^{-1}NO_3$-N in the feed at pH 4 and pH 5 were cultivated in a 3 liter SBR. Complete denitrification of feed with pH 4 and pH 5 was successfully achieved by *in situ* neutralization caused by the biologically generated alkalinity and adaptation of microbial community. Whereas batch experiments showed that pH 4 and pH 5 were inhibitory to denitrification of high strength nitrate. Denitrifying granules were colonized by rod and coccus shaped microorganisms when fed with nitrate waste at pH 7.5 and pH 4, respectively. The denitrification performance in bench scale SBR shows the practical utility of internal recycling of biologically generated alkalinity for neutralization and treatment of acidic nitrate waters.

Compact denitrifying granular biomass capable of denitrification of up to 2710 mg L^{-1} NO_3-N at both C/N ratios was developed in a continuous stirred tank reactor. The denitrification was complete and stable during long term operation for both C/N ratios without any accumulation of nitrite. The study shows that C/N ratio of 1.5 is optimum for efficient and stable denitrification, as complete utilization of acetate was observed and further treatment of effluent for removal of excess carbon is not required. Complete denitrification up to 4742 mg L^{-1} NO_3-N was achieved in EGSBR with a hydraulic residence time of 16 h.

When experiments were conducted to see the effect of temperature on denitrification, complete denitrification was observed at all temperatures. Denitrifying granular biomass capable of denitrification of 1355 mg L^{-1} NO_3-N at different temperatures (20-40 ^oC) was developed in SBR operated with 24 h cycle period and 50% volume exchange ratio. Nitrite accumulation for the indicated C/N ratios at all temperatures (20-40 ^oC) was observed. Specific denitrification rates were found to be increasing with increase in temperature. Kinetic study revealed that nitrate and nitrite denitrification rates were found to be zero order. The experimental study showed that temperature range 35-40 ^oC is optimum for efficient denitrification.

Compact denitrifying granular biomass capable of efficient denitrification of up to 9484 mg L^{-1} NO_3-N was developed in SBR operated with 24 h cycle period and 50% volumetric exchange ratio. Microscopy showed that compact granular sludge was composed of cocci and rod shaped cells enmeshed in a matrix. PCR-DGGE revealed a major shift and formation of stable microbial community during denitrification. Nitrite accumulation of up to 85% of initial nitrate was observed. High specific denitrification rates observed were 2 - 3 times higher than those reported in the literature for activated sludge systems. The study indicated that granular sludge sequencing batch reactors could be effectively employed for treatment of high strength nitrate wastes of industrial origin, at low C/N ratios with fast kinetics and are inherently immune to the problems caused by nitrite accumulation.

Formation of denitrifying granular biomass capable of complete denitrification of up to 5420 mg L^{-1} NO_3-N was demonstrated in a 24 L volume semi pilot scale sequencing batch reactor. Microscopy showed that compact denitrifying granules were colonized by

cocci and rod shaped microorganisms. Successful denitrification of up to 5420 mg L^{-1} NO_3-N in the feed was achieved at C/N ratio of 1.5 in semi pilot reactor. The experimental data generated in this work showed possibilities for scaling up of granular sludge sequencing batch reactors for treating large quantities of high strength nitrate wastewaters.

6.2 Future directions

The current study demonstrated denitrification for initial nitrate concentrations of 9484 mg L^{-1} NO_3-N, but the effluents from nuclear industry are 4 to 5 times higher. Therefore, a set of strategies need to be developed to treat higher concentrations.

The effect of temperature on denitrification was studied up to 40 ^{o}C. Denitrification rates were found to be declining at temperatures above 40 ^{o}C. The effect of temperature on denitrification up to 50 ^{o}C can be studied.

Present study showed that acidic effluents up to pH 4 can be treated using acclimatization strategy. In view of the fact that pH of industrial effluents may be as low as 2, studies may be planned for effluents with pH lower than 4. In the current denitrification studies, C/N ratio of 1.5 was the lowest. Further reduction in C/N ratio can be studied to reduce the cost of denitrification.

Bio-augmentation strategy can be adopted to increase nitrite reductase to reduce overall denitrification time as nitrite reduction was found to be higher than that of nitrate reduction. EGSBRs were employed to denitrify the nitrate concentrations up to 4742 mg L^{-1} NO_3-N with HRT 16 h. This leaves scope for finding ways to increase nitrate concentrations and reduce HRT.

Denitrification at semi pilot scale (24 L reactor) demonstrated good results suggesting a good case for carrying out studies at Pilot scale handling larger volumes. All the denitrification studies demonstrated were with synthetic wastewaters, suggesting a need to demonstrate denitrification with actual industrial wastewaters.

References

1. Gleick, P.H., 1993. Water in Crisis: A Guide to the World's Freshwater Resources. Oxford University Press. p. 13, Table 2.1 "Water reserves on the earth".
2. Larry, W., 2006. "World Water Day: A Billion People Worldwide Lack Safe Drinking Water".
3. Ritter, K. Solomon, P. Sibley, K. Hall, P. Keen, G. Mattu, 2002. Sources, pathways, and relative risks of contaminants in surface water and groundwater: a perspective prepared for the Walkerton Inquiry, J Toxicol Environ Health A, 65, 1–142.
4. Briggs, D , 2003. Environmental pollution and the global burden of disease Br. Med. Bull. 68: 1-24.
5. Fawell J., and Nieuwenhuijsen , M.J., 2003. Contaminants in drinking water: Environmental pollution and health, Br. Med. Bull. 2003 68: 199-208.
6. Aboyeji, O.O., 2013. Freshwater Pollution in Some Nigerian Local Communities, Causes, Consequences and Probable Solutions, Academic Journal of Interdisciplinary Studie, Vol 2 No 13.
7. Chinadaily.com.cn. June 7, 2005.
8. USEPA (United States Environmental Protection Agency), 2002. Washington, DC. "The National Water Quality Inventory: Report to Congress for the 2002 Reporting Cycle – A Profile."
9. NRC (National Research Council), U.S., 1978. Panel on Nitrates US, Nitrates: An Environmental Assessment : a Report.
10. Watertechonline.com/articles/nitrate-nitrite, MARCH 05, 2011.
11. Francis, C.W., Mankin, J.B.,1977. High nitrate denitrification in continuous flow stirred reactors, Water Res. 11, 289–294.
12. Glass, C., Silverstein, J.,1998. Denitrification kinetics of high nitrate concentration water: pH effect on inhibition and nitrite accumulation, Water Res. 32, 831–839.
13. Glass, C., Silverstien, J.,1999. Denitrification of high nitrate, high salinity wastewater, Water Res. 33, 223–229.
14. Liao R., Shen K., Li A., Shi P., Li Y., Shi Q., Wang Z.,2013. High-nitrate wastewater treatment in an expanded granular sludge bed reactor and microbial diversity using 454 pyrosequencing analysis, Bioresour. Technol. 134, 190–197.
15. Viers, J.H., Liptzin, D., Rosenstock, T.S., Jensen, V.B., Hollander, A.D., McNally, A., King, A.M., Kourakos, G., Lopez, E.M., De La Mora, N., Fryjoff -Hung, A., Dzurella, K.N., Canada, H.E., Laybourne, S., McKenney, C., Darby, J., Quinn, J.F. & Harter, T., 2012 Nitrogen Sources and Loading to Groundwater. Technical Report 2 in :Addressing Nitrate in California's Drinking Water with a Focus on Tulare Lake Basin and Salinas Valley Groundwater. Report for the State Water Resources Control Board Report to the Legislature . Center for Watershed Sciences, University of California, Davis.

16. Bernet N., Habouzit F., Moletta R., 1996. Use of an industrial effluent as a carbon source for denitrification of a high-strength wastewater. Appl. Microbiol. Biotechnol. 46, 92–97.

17. Sandhya U., Banerjee D., Srinivas C., Shah J.G., Wattal P.K.,2011. Biological Process for Denitrification of High Sodium Nitrate Bearing Waste Effluents of Reprocessing Origin, BARC News Letter, 323, 33-37.

18. Taylor P.A., Kurath D.E., Guenther R.,1993. Evaluation of nitrate destruction methods Technical Report DOE/MWIP—10.

19. Hancher C. W., Taylor P. A., and Napier J. M., 1978. OPERATION OF A FLUIDIZED-BED BIOREACTOR FOR DENITRIFICATION, Symposium on biotechnology in energy production, Gatlinburg, TN, USA.

20. Weyer, P., 1999. "Should we worry about nitrate in our water?" http://www.ag.iastate.edu/centers/leopold/newsletter/99-3leoletter/99-3nitrate.html, accessed 5/8/03, 1999.

21. Shrimali M., Singh K.P.,2001. New methods of nitrate removal from water, Environ. Pollut. 112 351–359.

22. http://www.ansnuclearcafe.org

23. Rocca C.D., Belgiorno V., Meric S., 2006. Anheterotrophic/autotrophic denitrification (HAD)approach for nitrate removal from drinking water, Process Biochem., 41, 1022–1028.

24. www.physicalgeography.net

25. Hiscock, K.M., Lloyd, J.W., Lerner, D.N., 1991. Review of natural and artificial denitrification of groundwater. Water Res. 25, 1099–1111.

26. Bae, B.U., Jung, Y.H., Han, W.W., and Shin, H.S., 2002. "Improved brine recycling during nitrate removal using ion exchange." Water Research, 25, 3330-3340.

27. Clifford, D. A., Sorg, T. and Ghurye, G.. 2010. "Ion Exchange and Adsorption of Inorganic Contaminants." Chapter Twelve in Water Quality and Treatment Sixth Edition, pp. 12.1-12.97, James K. Edzwald, ed.,AWWA and McGraw Hill, Inc., New York, 2010.

28. Guter, G.A., 1982. "Removal of Nitrate from Contaminated Water Supplies for Public Use: Final Report." Cincinnati, OH: USEPA, EPA-600/2-82-042.

29. Guter, G.A,. 1995. Chapter: "Nitrate Removal from Contaminated Groundwater by Anion Exchange." In IonExchange Technology: Advances in Pollution Control. Sengupta, A.K., ed. Lancaster, PA: Technomic Publishing Company.

30. Korngold, E., 1973 Removal of Nitrates from Potable Water by Ion Exchange. Water, Air and Soil Pollution, 1, 15. http://dx.doi.org/10.1007/BF00572386

31. Kapoor A., Viraraghavan T.,1997. Nitrate removal from drinking water-review. J. Environ. Eng. 123, 371–380.

32. Van der Hoek, J.P. and Klapwijk, A. 1987 Nitrate removal from groundwater. Water

Research 21(8) 989-997.

33. Van der Hoek JP, Paul JM, Abraham K., 1988. Combined ion exchange/biological denitrification for nitrate removal from ground water under different process conditions. Water Res. 22(6):679–84.

34. Clifford, D.; Liu, X., 1993. Ion exchange for nitrate removal, Journal–American Water Works Association 1993, 85, 135–143.

35. Matosic, M.& Mijatovic, I.& Hodzic, E.. 2000. "Nitrate removal from drinking water using ion exchange – comparison of chloride and bicarbonate form of the resins", Chemical and Biochemical Engineering Quarterly, vol. 14, 4, 141-146.

36. Darbi A., Viraraghavan T., Butler R. & Corkal D., 200) Pilot-Scale Evaluation of Select Nitrate Removal Technologies, Journal of Environmental Science and Health, Part A: Toxic/Hazardous Substances and Environmental Engineering, 38:9, 1703-1715,

37. Boumediene M., and Achour D., 2004. "Denitrification of the underground waters by specific resin exchange of ion" Desalination, 168, 187-194.

38. Samatya S., Kabay N., Yuksel U., Arda M., Yuksel M.,. 2006. Removal of nitrate from aqueous solution by nitrate selective ion exchange resins, Reactive & Functional Polymers 66, 1206–1214.

39. Dördelmann, O., Panglisch, S., Klegraf, F., Hell, F., Moshiri, A., Emami, A. and Höll, W. (UNKNOWN). "Nitrate Removal from Drinking Water in Iran – An Assessment of Three Different Treatment Processes Based on Pilot-Scale Investigations."

40. Cevaal, J.N., Suratt, W.B., and Burke, J.E., 1995. "Nitrate removal and water quality improvements with reverse osmosis for Brighton, Colorado." Desalination, 103, 101-111.

41. Black, J. 2003, May 1. "Treasure from the Deep: Drinking Water." Business Week Online.

42. Howe, K.J., 2004. "Technical Challenges to Concentrate Disposal from Inland Desalination." The University of New Mexico, Department of Civil Engineering. In: Proceedings Identifying Technologies to Improve Regional Water Stewardship: A Conference Series Featuring Intersections of Technology and Water Management North – Middle Rio Grande Corridor.

43. Elyanow, D. and Persechino, J., 2005. "Advances in Nitrate Removal." GE – General Electric Company, Water & Process Technologies. Accessed June 11, 2010 via <http://www.gewater.com/pdf/Technical%20Papers_Cust/Americas/English/TP1033EN.pdf>.

44. Rautenbach R., Kopp W., van Opbergen G. and Hellekes R., 1987. Nitrate reduction of well water by reverse osmosis and electrodialysis - studies on plant performance and costs Desalination, 65, 241.

45. Bohdziewicz J., Bodzek M., Wqsik E., 1999. The application of reverse osmosis and nanofiltration to the removal of nitrates from groundwater. Desalination 121 139-147.

46. Schoeman,J.J., Steyn, 2003.A Nitrate removal with reverse osmosis in a rural area in South AfricaDesalination, 155, 15–26

47. Kneifel, K., Luhrs, G., and Wagner, H., 1988. “Nitrate Removal by Electrodialysis for Brewing Water.” Desalination, 68, 203-209.

48. Hell, F., Lahnsteiner, J., Frischherz, H. and Baumgartner, G., 1998. “Experience with full-scale electrodialysis for nitrate and hardness removal.” Desalination, 117, 173-180.

49. Koparal, A.S. and Ogutveren, U.B., 2002. “Removal of Nitrate From Aqueous Solutions By Electrodialysis.” Intern. J. Environ. Studies, 59, 323-329.

50. Midaoui, A.E., Elhannouni, F., Taky, M., Chay, L., Sahli, M.A.M., Echihabi, L., and Hafsi, M.,2002. “Optimization of nitrate removal operation from groundwater by electrodialysis.” Separation and Purification Technology, 29, 235-244.

51. Sahli, M.A.M., Annouar, S., Mountadar, M/, Soufiane, A., and Elmidaoui, A., 2008. “Nitrate removal of brackish underground water by chemical adsorption and by electrodialysis.” Desalination, 227, 327-333.

52. Banasiak, L. and Schafer, A., 2009. “Removal of boron, fluoride and nitrate by electrodialysis in the presence of organic matter.” Journal of Membrane Science, 334, 101-109.

53. Wisniewski, C., Persin, F., Cherif, T., Sandeaux, R., Grasmick, A., and Gavach, C., 2001. Denitrification of Drinking Water by the Association of an Electrodialysis Process and a Membrane Bioreactor: Feasibility and Application, Desalination, 139, 199–205.

54. Sahli, M.M.A., Tahaikt, M., Achary, I., Taky, M., Elhanouni, F., Hafsi, M., Elmghari, M., and Elmidaoui, A., 2006.Technical Optimization of Nitrate Removal for Groundwater by ED Using a Pilot Plant, Desalination, 189, 200–208.

55. Ali M.B.S., Mnif A., Hamrouni B., Dhahbi M., 2010. Denitrification of brackish water by electrodialysis: Effect of process parameters and water characteristics, Surf. Eng. Appl. Electrochem. 46(3) 253–262.

56. James C. Fanning, 2000. The chemical reduction of nitrate in aqueous solution, Coordination Chemistry Reviews, 199) 159–179.

57. Murphy, A. P., 1991. "Chemical removal of nitrate from water." Nature, 350, 223-225.

58. Sabzali A, Gholami M, Yazdanbakhsh AR, Khodadadi A, Musavi B, et al., 2006. Chemical denitrification of nitrate from groundwater via sulfamic acid and zinc metal. Iranian Journal of Environmental Health Science & Engineering 3: 141-146.

59. Lemaignen, L., Tong, C., Begon, V., Burch, R., and Chadwick, D., 2002. “Catalytic denitrification of water with palladium-based catalysts supported on activated carbons.” Catalysis Today, 75, 43-48.

60. Pintar, A., Batista, J. and Levec, J., 2001. “Catalytic denitrification: direct and indirect removal of nitrates from potable water.” Catalysis Today, 66, 503-510.

61. Jensen V. and Darby J., 2011. An Assessment of the State of Nitrate Treatment

Alternatives, The American Water Works Association.

62. Palomares A.E., Prato J.G., Márquez F., Corma A., 2003. Denitrification of natural water on supported Pd/Cu catalysts, Applied Catalysis B: Environmental, 41, 3–13

63. Meytal U.M, Sheintuch, M., 2005. Activated carbon cloth-supported Pd–Cu catalyst: Application for continuous water denitrification, Catalysis Today, 102–103, 121–127

64. Gerardi, Michael H., 2002. Nitrification and denitrification in the activated sludge process, John Wiley and Sons, Inc, New York, USA.

65. Mateju V, Cizinska S, Krejci J and Janoch T., 1992 Biological water denitrification - A review. Enzyme Microb. Technol. 14 170-183.

66. Knowles R.,1982.Denitrification, Microbiol. Rev. 43-70.

67. Rittmann, B.E., McCarty, P.L., 2001. Environmental Biotechnology: Principles and Applications, McGraw Hill, New York.

68. Porges, N.; Jasewicz; L.,and.Hoover S.R, 1956."Principles of biological oxidation." In Biological Treatment of Sewage and Industrial Wastes. Eds. J.McCabe and W.W.Eckenfelder. New York: Reinhold Publ.

69. Gaber Z.B., Josef W., 2010, Bio-removal of nitrogen from wastewaters-A review Journal of American Science, 6, 508-528

70. Mahvi, A. H., (2008). Sequencing Batch Reactor; A promising technology in wastewater treatment, Iran. J.Environm. Sci. Eng., 5, 79-90.

71. Fuzhen W., Aifeng C., Yongzhen P., Erjie Y., Baikun L., 1994. Nitrogen removal in sequencing batch reactor, Journal of Environ. Sciences, 6, 164-172.

72. Dangcong P., Yi W., Hao W., Xiaochang W., 2004 Biological denitrification in a sequencing batch reactor Water Sci Technol. 50,:67-72.

73. Obaja D., Mace S., Mata-Alvarez J. (2005) Biological nutrient removal by a sequencing batch reactor (SBR) using an internal organic carbon source in digested piggery wastewater. Bioresour. Technol. 96 7–14

74. Dhamole, P.B., Nair, R.R., D'Souza, S.F., Lele, S.S.,2007. Denitrification of high nitrate waste. Bioresour. Technol. 98, 247–252.

75. Nair, R.R., Dhamole, P.B., Lele, S.S., D'Souza, S.F., 2007. Biological denitrification of high strength nitrate waste using preadapted denitrifying sludge. Chemosphere 67, 1612–1617.

76. Fernández-Nava, Y., Marañón, E., Soons, J., Castrillón, L., 2008. Denitrification of wastewater containing high nitrate and calcium concentrations, Bioresour. Technol. 99 (2008) 7976–7981.

77. Fernández-Nava, Y., Maranón, E., Soons, J., Castrillón, L.,2010. Denitrification of high nitrate concentration wastewater using alternative carbon sources, J. Hazard. Mater. 173, 682–688.

78. Komori M, Sakakibara Y., 2008. High-rate hydrogenotrophic denitrification in a fluidized-bed biofilm reactor using solid-polymer-electrolyte membrane electrode

(SPEME). Water Sci Technol. 2008;58(7):1441-6.

79. Rabah F.K.J., Dahab M.F., 2004. Nitrate removal characteristics of high performance fluidized-bed biofilm reactors, Water Res. 38 2719–2728.

80. Kurt, M., Dunn, I. J., and Bourne, J. R., 1987. "Biological denitrification of drinking water using autotrophic organisms with H, in a fluidizedbed biofilm reactor." Biotechnol. Bioengrg., 24, 493-501.

81. Burghate S. P. and Ingole Dr. N. W., 2013. "Denitrification Potential of Fluidized Bed Biofilm Reactor", International Journal of Research in Environmental Science and Technology, Vol. 3(3), pp 78-85.

82. Shin, J. H., Sang B. I., Chung Y. C., and Choung Y. K., 2008. "A novel CSTR-type of hollow fiber membrane biofilm reactor for consecutive nitrification and denitrification," Desalination, vol. 221, no. 1–3, pp. 526–533.

83. Biradar, P.M., Dhamole, P.B., Nair, R.R., Roy, S.B., Satpati, S.K., D'Souza, S.F., Lele, S.S., Pandit, A.B.,2008. Long-term stability of biological denitrification process for high strength nitrate removal from wastewater of uranium industry, Environ Prog 27, 365–372.

84. Ruiz G, Jeison D, Rubilar O, Ciudad G, Chamy R., 2006. Nitrification-denitrification via nitrite accumulation for nitrogen removal from wastewaters. Bioresour Technol. 97(2):330-5.

85. Udert K.M., Fux C., Münster M., Larsen T.A., H. Siegrist and Gujer W., 2003, Nitrification and autotrophic denitrification of source-separated urine, Water Science & Technology Vol 48 No 1 pp 119.

86. Shen, J., He, R., Han, W., Sun, X., Li, J., Wang, L., 2009. Biological denitrification of high-nitrate wastewater in a modified anoxic/oxic-membrane bioreactor (A/OMBR). Journal of Hazardous Materials 172, 595–600.

87. Fu ZhiMin; Yang FengLin; An YingYu; Xue Yuan.2009. Simultaneous nitrification and denitrification coupled with phosphorus removal in an modified anoxic/oxic-membrane bioreactor (A/O-MBR). Biochemical Engineering Journal, 43, 191-196

88. Francis C. W. and Hatcher C. W., 1980 Biological denitrification of high-nitrate wastes generated in the nuclear industry. In Biological fuidized Bed Treatment of Water and Wastewater, eds P. F. Cooper and B. Atkinson. Ellis Horwood Ltd., Chichester.

89. Abu-Ghararah Z.H., 1996, Biological denitrification of high nitrate water: Influence of type of carbon source and nitrate loading, J. Environ. Sci. Health, A31(7), 1651-1668.

90. Foglar, L., Briski, F., Sipos, L., Vukovic, M., 2005. High nitrate removal from synthetic wastewater with the mixed bacterial culture, Bioresour. Technol. 96, 879–888.

91. Dhamole PB, Nair RR, D'Souza SF, Lele SS, 2008. Denitrification of highly alkaline nitrate waste. Appl Biochem Biotech 151:433–440.

92. Dhamole PB, Nair RR, D'Souza SF, Lele SS, 2009. Simultaneous removal of carbon

and nitrate in an airlift bioreactor. Bioresour Technol 100:1082–1086.

93. Constantin H., Fick M., 1997.. Influence of C-sources on the denitrification rate of a high-nitrate concentrated industrial wastewater, Water Res. 31, 538–589.

94. Eusebi A.L., Troiani C., Fatone F., Battistoni P., 2009. Biological nitrogen removal at high performances in platform for the treatment of industrial liquid wastes, Chem. Eng. Trans., 17, 239-244.

95. Cortez S., Teixeira P., Oliveira R ., Mota M., 2011, Denitrification of a landfill leachate with high nitrate concentration in an anoxic rotating biological contactor, Biodegradation, 22, 661-671.

96. Cyplik P., Marecik R., Piotrowska-Cyplik A., Olejnik A., Drozdzynska A., Chrzanowski L., 2012. Biological Denitrification of High Nitrate Processing Wastewaters from Explosives Production Plant, Water Air Soil Pollut. 223, 1791–1800

97. Nair R.R., D'Souza S.F., 2012. Denitrification of high nitrate wastewater in a cloth strip bioreactor with immobilized sludge. J Ind Microbiol Biotechnol , 39:1637–1643

98. Rezaee A., Godini H., Soltani R.D.C., Hossini H., Ahmadabadi A.N., 2012. Denitrification of high salinity, high nitrate wastewater using clinoptilite in a packed bed bioreactor. Journal of Environmental Research and Management Vol. 3(2). pp. 031-036.

99. Filippis P. De, Di Palma L., Scarsella M., Verdone N., 2013. Biological Denitrification of High-Nitrate Wastewaters: a Comparison Between Three Electron Donors CHEMICAL ENGINEERING TRANSACTIONS, 32, 319-324.

100. Foglar L, Bolf N, LukicM. 2010. The impact of temperature on surface water biodenitrification —kinetic modelling. Adv Biomed Res Proc:196–201.

101. Casey, T.J.,2006. Unit Treatment Processes in Water and Wastewater Engineering. John Wiley & Sons, Chichester.

102. Delwiche, C.C. and Bryan, B.A., 1976. DENITRIFICATION. Ann. Rev. MicrobiaL 30:241-62.

103. Elefsiniotis, P., Li, D., 2006. The effect of temperature and carbon source on denitrification using volatile fatty acids, Biochemical Engineering Journal, Volume 28, Issue 2, Pages 148–155.

104. Fontenot, Q., Bonvillain, C., Kilgen, M., Boopathy, R., 2007. Effects of temperature, salinity, and carbon: nitrogen ratio on sequencing batch reactor treating shrimp aquaculture wastewater. Bioresour. Technol. 98, 1700-1703.

105. Wang J., Baltzis B. and Lewandowski G., 1995. Fundamental denitrification kinetic studies with Pseudomonas denitrificans. Biotech. Bioengng 47, 26-41.

106. Lu, H., Chandran, K. & Stensel, D., 2014. Microbial ecology of denitrification in biological wastewater treatment Water Research 64, 237- 254.

107. Gómez M.A., Hontoria, E., González-López, J. 2002. Effect of dissolved oxygen concentration on nitrate removal from groundwater using a denitrifying submerged

filter, J Hazard Mater. 90(3):267-78.

108. Hochstein, L. I., Betlach, M. and Kritikos, G., 1984. The effect of oxygen on denitrification during steady-state growth of Paracoccus halodenitrificansArch. Microbiol.137, 74-78.

109. Oh, J., Silverstein J.,1999. Oxygen inhibition of activated sludge denitrification. Water Res. 33, 1925-1937.

110. Eckenfelder W.W.Jr., 1989. Industrial Water Pollution Control . Second edition, McGraw-Hill, Inc., USA.

111. Henze M., Gujer W., Mino T., Matsuo T., Wentzel M. C. and Marais G. v. R., 1995. Activated Sludge Model No. 2., IAWQ Task Group on Mathematical Modelling for Design and Operation of Biological Wastewater Treatment Processes. Scienti®c and Technical Report No.3. IAWQ, London, England.

112. Onnis-Hayden, A.; Gu, A. Z., 2008 Comparisons of Organic Sources for Denitrification: Biodegradability , Denitrification Rates, Kinetic Constants and Practical Implication for Their Application in WWTP. Proceedings of the 81st Annual Water Environment Federation Technical Exposition and Conference , Chicago, Illinois, Oct. 18–22; Water Environment Federation: Alexandria, Virginia.

113. Srinu Naik. S and Y. Pydi Setty, 2012. Biological denitrification of wastewater-A Mini Review on Carbon Source, International Conference on Chemical, Environmental Science and Engineering (ICEEBS'2012) July 28-29, Pattaya (Thailand).

114. Yang X., Wang S., and Zhou L., 2012. "Effect of carbon source, C/N ratio, nitrate and dissolved oxygen concentration on nitrite and ammonium production from denitrification process by Pseudomonas stutzeri D6," Bioresource Technology, vol. 104, pp. 65–72

115. Xie, L., Chen, J., Wang, R., & Zhou, Q., 2012. Effect of carbon source and COD/NO3 –-N ratio on anaerobic simultaneous denitrification and methanogenesis for high-strength wastewater treatment. Journal of Bioscience and Bioengineering, 113(6), 759–764

116. Akunna, J.C., Bizeau, C., Moletta, R., 1993. Nitrate and nitrite reductions with anaerobic sludge using various carbon sources–glucose, glycerol, acetic-acid, lactic-acid, and methanol. Water Res. 27, 1303–1312.

117. Wilawan Khanitchaidecha, Tatsuo Sumino and Futaba Kazama, 2010, "Influence of Carbon Sources on Biological Nitrogen Removal by Immobilized Bacteria", J. Water Resource and Protection, 2, 527-531.

118. Sunil S. Adav, Duu Jong Lee and Lai J.Y., 2010, "Enhanced biological denitrification of high concentration of nitrite with supplementary carbon source", Appl Microbiol Biotechnol,85, 773-778.

119. Savia Gavazza dos Santos, Maria Bernadete Amancio Varesche, Marcelo, Zaiat and Eugenio Foresti, 2004, "Comparison of Methanol, Ethanol and Methane as Electron Donors for Denitrification", Environmental Engineering Science, Vol.21, 313-320.

120. Gerber, A., Mostert, E. S., Winter C. T. & de Villiers, R. H., 1986. The effect of acetate and other short chain carbon compounds on the kinetics of biological nutrient removal. Water SA. , 12, 7-11.

121. Stief, P., 2001. Influence of Sediment and Pore-Water Composition on Nitrite Accumulation in a Nitrite-perfused Freshwater Sediment. Water Research 35(12):2811-2818.

122. McCarty, P. L., Beck, L. & Amant, P. St., 1969 Biological denitrification of wastewater by addition of organic materials. 24th Industrial Waste Conference. Purdue University, Lafayette, Ind.

123. Skrinde, J., Bhagat R. & Surinder, K., 1982 Industrial wastes as carbon sources in biological dentrification. Journal of the Water Pollution Control Federation, 54, 370-377.

124. Monteith, H. D., Bridle T. R. & Suthon, P. M., 1980. Industrial waste carbon sources for biological denitrification. Progress in Water Technololology, 12, 127-141.

125. Kristensen, G. H., and Jorgensen, P. E., 1990. "Preprecipitation followed by biological denitrification supported by addition of biological or thermal/chemical hydrolysis products." Proceedings of 4th Gothenburg Symposium, Madrid, Spain, pp. 313-328.

126. Saleh-Lakha S, Shannon KE, Henderson SL, Gover C, Trevors JT, Zebarth BJ, Burton DL., 2009. Effect of pH and temperature on denitrification gene expression and activity in Pseudmonas mandelii. Appl. Environ. Microbiol. 75, 3903-3911.

127. Karanasios, K. A., Vasiliadou, I. A., Pavlou, S., & Vayenas, D. V., 2010. Hydrogenotrophic denitrification of potable water: a review. Journal of Hazardous Materials, 180, 20–37.

128. Vayenas, D.V., 2011 Comprehensive Biotechnology Attached Growth Biological Systems in the Treatment of Potable Water and Wastewater, Elsevier

129. Shi, Y., Wu, G., Wei, N., Hu, Hu., 2015, Denitrification and biofilm growth in a pilot-scale biofilter packed with suspended carriers for biological nitrogen removal from secondary effluent, Journal of Environmental Sciences, 32, 35– 41

130. Kevin Westerling, 2014, Biological Treatment 101: Suspended Growth Vs. Attached Growth, Water Online, March 5, 2014.

131. Li Y., Gu G., Zhao J., Yu H., 2001. Anoxic degradation of nitrogenous heterocyclic compounds by acclimated activated sludge, Process Biochem. 37, 81–86.

132. Moore S., Schroeder E.,1971.The effect of nitrate feed rate on denitrification, Water Res. 5,445–452.

133. Timmermans P., Van Haute A.,1983. Denitrification with methanol, Water Res. 17, 1249–1255

134. Cavari, B. Z. and Phelps, G., 1977, Denitrification in Lake Kinneret in the presence of oxygen, Freshwater Biology, 7, 385–391

135. Grady, C.P.L, Daigger, G., Lim, H.C., 1999. Biological Wastewater Treatment, 2nd Edition, Marcel Dekker, New York, New York.

136. Messer, J., and Brenzonik, P.L., 1984. Laboratory evaluation of kinetic parameters for lake sediment dcnitrification models. Ecol. Model. 21: 277-286.

137. Nancharaiah, Y.V., Joshi, H.M., Mohan, T.V.K., Venugopalan, V.P., Narasimhan, S.V., 2006b. Aerobic granular biomass: a novel biomaterial for efficient uranium removal. Curr. Sci. 91, 503-509.

138. APHA,1995. Standard Methods for the Examination of Water and Wastewater, 19th ed., American Public Health Association, Washington DC, USA.

139. Tay J.H., Tay S.T.L., Liu Y., Show K.N., Ivanov, V., 2006. Biogranulation Technoligies for Wastewater Treatment, Waste Management Series, 6.

140. Nancharaiah, Y.V., Schwarzenbeck, N., Mohan, T.V.K., Narasimhan, S.V., Wilderer, P.A., Venugopalan, V.P., 2006a. Biodegradation of nitrilotriacetic acid (NTA) and ferric-NTA complex by aerobic microbial granules. Water Res. 40, 1539-1546.

141. Nancharaiah YV, Venugopalan VP., 2011. Denitrification of synthetic concentrated nitrate wastes by aerobic granular sludge under anoxic conditions. Chemosphere 85, 683-688.

142. Hocaoglu, S.M., Insel, G., Cokgor, E.U., Orhon, D.,2011. Effect of low dissolved oxygen on simultaneous nitrification and denitrification in a membrane bioreactor treating black water. Bioresour. Technol. 102, 4333–4340.

143. Ge, S., Peng, Y., Wang, S., Lu, C., Cao, X., Zhu, Y., 2012. Nitrite accumulation under constant temperature in anoxic denitrification process: the effects of carbon sources and COD/NO3–N, Bioresour. Technol., 114, 137–143,

144. Her, J.J., Huang, J.S.,1995. Influence of Carbon Source and C-N ratio on Nitrate-Nitrite denitrification and carbon breakthrough. Bioresour. Technol. 54, 45-51.

145. Khanitchaidecha, W., Sumino, T., Kazama, F., 2010. Influence of carbon source on biological nitrogen removal by immobilised bacteria, J. Water Resource & Protection. 2, 527-531

146. Carrera, J., Vicent, T., Lafuente, F.J., 2003. Influence of temperature on denitrification of an industrial high-strength nitrogen wastewater in a two-sludge system, Water SA, 29, (1) pp. 11–16.

147. Foglar, L., Briski, F., 2003. Wastewater denitrification process-the influence of methanol and kinetic analysis. Process Biochem. 39, 95–103.

148. Henze, M., Kristensen, G. H., Strube, R.,1994. Rate–capacity characterization of wastewater for nutrient removal processes, Water Sci. Technol. 29, 101–107.

149. Peyton B.M., Mormile M.R., Petersen J.N.,2001. Nitrate reduction with Halomonas Campisalis: kinetics of denitrification at pH9 and 12.5% NaCl, Water Res. 35, 4237–4242.

150. Sozen S., Orhon D.,1999. The effect of nitrite correction on the evaluation of the rate of nitrate utilization under anoxic conditions, J. Chem. Technol. Biotechnol. 74 790–800.

151. Glass, C., Silverstein, J., and Oh, J.: 1997..Inhibition of denitrification in activated

sludge by nitrite, Water Environ. Res., 69, 1086–1093

152. Dhamole, P.B., Nair, R.R., D'Souza, S.F., Pandit, A.B., and Lele, S.S., 2014: Denitrification of high strength nitrate waste from a nuclear industry using acclimatized biomass in a pilot scale reactor, Appl. Biochem. Biotechnol., 175, 748-756..

153. Pan Y, Ye L, Ni B-J, Yuan Z. 2012. Effect of pH and N2O reduction and accumulation during denitrification by methanol utilizing denitrifiers. Wat. Res. 46, 4832-4840..

154. Papirio, S., Esposito, G. and Pirozzi, F., 2013 Biological inverse fluidized-bed reactors for the treatment of low pH- and sulfphate-containing wastewaters under different COD/SO42- conditions. Environ. Technol. 34, 1141-1149.

155. Papirio S, Ylinen A, Zou G, Peltola M, Esposito G, Puhakka JA. 2014. Fluidized-bed denitrification for mine waters. Part I: low pH and temperature operation. Biodegradation 25, 425-435.

156. USEPA, 1993 Manual: EPA/625/R-93/010 Nitrogen Control. US EPA Office Tech. Transfer, Washington, DC.

157. Canion, A., Kostka, J.E., Gihring, T.M., Huettel, M., van Beusekom, J.E.E., Gao, H., Lavik, G., Kuypers, M.M.M.,2014. Temperature response of denitrification and anammox reveals the adaptation of microbial communities to in situ temperatures in permeable marine sediments that span 50o in latitude. Biogeosciences 11, 309-320.

158. Monod J.,1950. La Technique de Culture Continue, Theorie et Applications, Ann. Inst. Pasteur, 79, 390-410.

159. Adav, S.S., Lee, D.J., Lai, J.Y., 2010. Enhanced biological denitrification of high concentration of nitrite with supplementary carbon source, Appl. Microbiol. Biotechnol. 85, 773–778.

160. Marazioti, C., Kornaros, M., G. Lyberatos, G., 2003. Kinetic modelling of a mixed culture of Pseudomonas denitrificans and Bacillus subtilis under aerobic and anoxic conditions, Water Res, 37, 1239–1251.

List of Publications arising from the thesis

Journal

1. Development of mixed microbial granular biofilms for denitrification of concentrated wastes, **T.V. Krishna Mohan**, Y.V. Nancharaiah, V.P. Venugopalan, P. M. Satya Sai and S.V. Narasimhan.. Energy Procedia 7 (2011.) 507-511.

2. Nitrate removal from high strength nitrate-bearing wastes in granular sludge sequencing batch reactors, **Tulasi Venkata Krishna Mohan**, , Kadali Renu, Yarlagadda Venkata Nancharaiah, Pedapati Murali Satya Sai, Vayalam Purath Venugopalan, Journal of Bioscience and Bioengineering, DOI: 10.1016/j.jbiosc.2015.05.015.

3. Effect of C/N Ratio on Denitrification of High-Strength Nitrate Wastewater in Anoxic Granular Sludge Sequencing Batch Reactors, **T.V. Krishna Mohan**, Y.V. Nancharaiah, V.P. Venugopalan, P. M. Satya Sai, Submitted to **Ecological Engineering (under Revision)**.

4. Denitrification kinetics of high strength nitrate in a sequencing batch reactor using anoxic granular sludge, **T.V. Krishna Mohan**, Y.V. Nancharaiah, V.P. Venugopalan, P. M. Satya Sai, Submitted to **CLEAN – Soil, Air, Water (under Review)**.

Conferences

1. Development of mixed microbial granular biofilms for denitrification of concentrated wastes. **T.V. Krishna Mohan**, Y.V. Nancharaiah, V.P. Venugopalan, P.M. Satya Sai, S.V. Narasimhan, 2nd International Conference on Asian Nuclear Prospects 2010 (ANUP-2010), 11-13, October 2010, IGCAR, Kalpakkam.

2. Biological denitrification of high strength nitrate wastes by granular sludge in sequencing batch reactors. **T.V.Krishna Mohan**, Y.V. Nancharaiah, V.P. Venugopalan, P.M. Satya Sai, S.V. Narasimhan; Asian Congress on Biotechnology – 2013 15 – 19 December, 2013, New Delhi, India.

3. Biological denitrification of high strength nitrate wastewater by denitrifying granular biomass, **T.V. Krishna Mohan**, Y.V. Nancharaiah, V.P. Venugopalan, P. M. Satya Sai and S.V. Narasimhan. Separation Science and Technology (SESTEC-2014 Poster under the theme "Treatment of industrial effluents"; 25-28 February 2014; Mumbai, INDIA.

4. Biological denitrification of high strength nitrate synthetic wastewater by denitrifying granular sludge, **T.V. Krishna Mohan**, Y.V. Nancharaiah, V.P. Venugopalan, P. M. Satya Sai and S.V. Narasimhan. Chemical Engineers in Nuclear Technology (CHEMENT-2014); Presented Poster; 06-07 March 2014; Kalpakkam, INDIA.

5. Denitrification of high strength nitrate wastewater by anoxic granular sludge: importance of C:N ratio on denitrification efficiency **T.V. Krishna Mohan**, Y.V. Nancharaiah, V.P. Venugopalan, and P. M. Satya Sai. International Conference On Emerging Trends In Biotechnology (ICETB 2014); Poster November 6-9, 2014, JNU, New Delhi, India.

T.V. KRISHNA MOHAN